Processing Behavior of Thermoplastics Reinforced with Melt Processable Glasses

Robert T. Young

Dissertation submitted to the Faculty of the
Virginia Polytechnic Institute and State University
in partial fulfillment of the requirements for the degree of

Doctor of Philosophy
in
Chemical Engineering

Donald G. Baird, Chair
Richey M. Davis
Alfred C. Loos
Joseph T. Sullivan
Garth L. Wilkes

March 1, 1999
Blacksburg, Virginia

Keywords:
composites, melt processable glass, injection molding, forming behavior

Processing Behavior of Thermoplastics Reinforced with Melt Processable Glasses

Robert T. Young

(ABSTRACT)

This work was concerned with evaluating the behavior of thermoplastics reinforced with melt processable phosphate glasses processed by techniques including injection molding, compression molding, and thermoforming. Thermoplastic resins consisting of polyphenylene sulfide (PPS), polyetherimide (PEI) and polyetheretherketone (PEEK) were combined with phosphate glasses having glass transition temperatures (T_g) that ranged from 230-290°C to form composite systems where both the matrix and reinforcing phase were deformable during processing.

For the process of injection molding, several factors were examined to maximize the mechanical properties obtained with the addition of the phosphate glasses. The influence of variables such as the glass and matrix viscosity, glass loading, melt temperature, and mold fill rate were examined for a variety of composite blends consisting of the PPS, PEI, and PEEK reinforced with a lower T_g (234°C) phosphate glass and PEEK blended with a higher T_g (282°C) glass. From this work, it was determined that the best mechanical properties were generally produced by using processing temperatures and material combinations that minimized the viscosity differences between the thermoplastic resin and phosphate glass. Variations in the material combinations and processing conditions utilized were also found to result in the formation of a variety of glass phase morphologies that consisted of droplets, ribbons, and an interpenetrating network structure.

The addition of the phosphate glass to the neat thermoplastics resins was found to be an effective way to produce injection moldable composite blends. The stiffness of the composite blends increased with glass loading with composites containing up to 45 vol% phosphate glass exhibiting machine direction tensile and flexural moduli in the range of 3-5 times greater than that those of the neat thermoplastics. Additionally, these composites were found to offer moduli and strengths that ranged from 25-50% lower than conventional E-glass fiber reinforced materials of the same loading. The lower mechanical properties of the neat phosphate glasses coupled with a lack of adhesion between the matrices and the glasses helped contribute to the lower mechanical properties exhibited by the phosphate glass reinforced composites. Still, the phosphate glass reinforced blends offered certain advantages including lower mechanical anisotropy, smoother surfaces, and lower viscosities.

The processing behavior of phosphate glass reinforced thermoplastics was also examined at temperatures commonly used in forming and shaping operations such as compression molding and thermoforming. It was determined that it was possible to deform the phosphate glass reinforcing phase along with the matrix resin at temperatures only 30-50°C above the T_g of the glass. The deformable phosphate glass reinforcing phase resulted in composite blends that exhibited greater extensibility than a solid E-glass fiber reinforced material. The elongation of the phosphate glass into a higher aspect ratio reinforcing morphology was found to result in an almost 25% increase in the tensile modulus for a polyphenylene sulfide based composite.

Acknowledgments

The author would like to express his appreciation Dr. Baird for his support and guidance in the completion of this work. Also, he would like to extend his thanks to Dr. Davis, Dr. Sullivan, Dr. Loos, and Dr. Wilkes for serving on his research committee.

The author would also like to give special recognition to the following groups and individuals:

- His parents, brothers, and grandmother for helping shape the author into the person he is today.

- Dr. Mike McLeod, who was always there to offer his help and advice both as a colleague and a friend.

- The gang up in Fredricksburg, especially Tim and Donna Mason, who have provided numerous entertaining and memorable moments over the years.

- Mr. Rex Bannister and Mr. Allen Walters, who treated the author like a son and made sure he grew both as a professional and a person while co-oping at DuPont.

- All the graduate students and Post-Docs the author has had the pleasure of knowing and working alongside while at Virginia Tech. Special gratitude is extended to the following individuals for providing assistance on a number of occasions: Norman Broyles, Varun Ratta, "Watson" Srinivas, and Chris Robertson.

- Dr. Jon Geibel at Phillips Chemical Company for providing a wealth of information and material that made this work possible.

- Dr. Wilkes for use of the SEM and Dr. Norm Eiss for the surface roughness measurements.

- Mr. Wendall Brown for all the machining jobs performed, both big and small.

- Mr. Riley Chan for all the assistance provided when it came to dealing with electronics.

- All the secretaries for their help over the years.

Original Contributions

The following are considered to be the significant original contributions of this research:

- The best processing conditions for producing in situ injection molded composites consisting of polyphenylene sulfide reinforced with a melt processable phosphate glass were established.

- It was demonstrated that it was possible to develop a wide range of phosphate glass reinforcing morphologies within injection molded composites by varying the processing conditions and the material combinations utilized.

- It was determined that phosphate glass reinforced thermoplastics offered better shaping and forming behavior than solid E-glass fiber reinforced materials. The ability of the phosphate glass to undergo deformation at temperatures used to shape the thermoplastic resin resulted in composite blends that displayed enhanced performance in compression molding and thermoforming. The application of shearfree deformation at temperatures 30-50°C above the T_g of the phosphate glass was found to elongate the glass reinforcing phase leading to an enhancement in the mechanical properties of certain composite blends.

Table of Contents

1.0 Introduction....……..……1
1.1 In Situ composites...…....……..…….……..3
1.2 Phosphate Glass...……..……7
1.3 Phosphate Glass/Polymer blends...……..……..9
1.4 Advantages of P-Glass Reinforced Thermoplastics……...…….12
1.5 Disadvantages of P-Glass Reinforced Thermoplastics...…..……..……..16
1.6 Research Objectives...……..17
1.6.1 Research Objective #1…….…..18
1.6.2 Research Objective #2…...……18
1.6.3 Research Objective #3.……...……19
1.7 References.....……20
2.0 Literature Review.....……..24
2.1 Polymeric Blends (General Considerations).....……...……26
2.2 Interfacial Tension...……27
2.3 Droplet Deformation……30
2.4 Capillary Instabilities……40
2.5 Rheology of Inorganic Glasses....……45
2.5.1 Rheology of Silica Glasses.....49
2.5.2 Rheology of Phosphate Glasses.....52
2.6 Rheology of Immiscible Fluid Blends……..…….……..54
2.6.1 Rheology of Polymer-Polymer Blends……54
2.6.2 Rheology of Polymer-Phosphate Glass Blends ...……....……58
2.7 Rheology of Solid filled Polymers ...……60
2.7.1 Viscous Response of Solid Filled Polymers……61
2.7.2 Elastic Response of Solid Filled Polymers……..63
2.8 Processing of Conventional Glass filled Thermoplastics....…….64

2.8.1 Drawbacks of Conventional Short fiber Glass Reinforcement...……64
2.8.2 Properties of Short fiber reinforced Thermoplastics……..65
2.8.3 Forming of Conventional Fiber reinforced Thermoplastics.....……..68
2.9 Processing of Self-Reinforcing Composite Systems...…….71
2.9.1 Injection Molding of TLCP Reinforced Composite Systems...…..…….71
2.9.2 Post Processing of TLCP Reinforced Composite Systems...……..74
2.10 Processing of Phosphate Glass Reinforced Thermoplastics..……..…76
2.10.1 Injection Molding of Phosphate Glass Reinforced Composites.....……..76
2.10.2 Deformation of Phosphate Glass Reinforced Composite Systems .....…….80
2.11 Research Objectives...……80
2.12 References .……82
3.0 Processing Effects..……..90
(ABSTRACT) - The Influence of Processing Variables on Injection Molded In Situ Composites Based on Polyphenylene Sulfide and a Melt Processable Glass 91
3.1 Introduction.....……91
3.2 Experimental..……..95
3.2.1 Materials.. ..……95
3.2.2 Rheological Characterization..……96
3.2.3 Injection Molding...…….98
3.2.4 Mechanical Properties...…..……99
3.2.5 Morphology.....……99
3.3 Results and Discussion.....…..……99
3.3.1 Rheological Characterization...…..……..……99
3.3.2 Effects of Mixing History ……103
3.3.3 Composite Mechanical Properties ……107
3.3.4 Composite Blend Morphology ...……..113
3.4 Conclusions……119
3.5 Acknowledgments ...……..120

3.6 References ...……..120

4.0 Injection Molded Properties….……..122

(ABSTRACT) - Properties of Injection Molded In Situ Composites Based 123
on Polyphenylene Sulfide and a Melt Processable Glass

4.1 Introduction ..……123

4.2 Experimental……..126

4.2.1 Materials ..……126

4.2.2 Injection Molding……..……127

4.2.3 Mechanical Properties..……127

4.2.4 Morphology ……..……128

4.2.5 Surface Roughness……128

4.2.6 Dynamic Mechanical Analysis ..……128

4.3 Results and Discussion ……..……129

4.3.1 Mechanical Properties ..……..…..……...……129

4.3.2 Composite Morphology….……132

4.3.3 Composite Surface Roughness…..……138

4.3.4 Dynamic Mechanical Properties of Composite Blends...……..138

4.4 Conclusions……146

4.5 Acknowledgments ...……..148

4.6 References ...……..148

5.0 Processing Effects and Molded Properties ……..……..150

(ABSTRACT) - Processing and Properties of Injection Molded Thermoplastic...151
Composites Reinforced with Melt Processable Glasses

5.1 Introduction ...……151

5.2 Experimental ..……155

5.2.1 Materials ...……155

5.2.2 Rheological Characterization ……156

5.2.3 Injection Molding.……157

5.2.4 Mechanical Properties …..……158

5.2.5 Dynamic Mechanical Thermal Analysis..……158
5.2.6 Morphology ..……158
5.3 Results and Discussion ……..……159
5.3.1 Rheological Characterization..…..……..……159
5.3.2 Composite Mechanical Properties…….165
5.3.3 Composite Morphologies……..……173
5.3.4 Dynamic Mechanical Response...……..179
5.4 Conclusions……182
5.5 Acknowledgments ...……..186
5.6 References ...……..187
6.0 Forming and Shaping Behavior….……..……..……..189
(ABSTRACT) - Extensional Processing Behavior of Thermoplastics.....……..190
Reinforced with a Melt Processable Glass
6.1 Introduction……191
6.2 Experimental ...……194
6.2.1 Materials ...……194
6.2.2 Composite Blend Preparation ...……195
6.2.3 Composite Tensile Mechanical Properties ...…….……196
6.2.4 Morphology…… …..……196
6.2.5 Deformation of Composite Blends…....……197
6.2.6 Thermoforming of Composite Blends...……198
6.3 Results and Discussion ……..……198
6.3.1 Forming Properties of Composite Blends..…….……..……198
6.3.2 Uniaxial Deformation of the Composite Blends.……..…….205
6.3.3 Planar Deformation of the Composite Blends...……208
6.3.4 Thermoforming of Composite Blends.……..219
6.4 Conclusions……222
6.5 Acknowledgments ...……..223
6.6 References ...……..223

7.0 Recommendations……..226

Appendix A: Phosphate Glass Rheological Data...…….229

Appendix B: Durability of Glass Reinforced Composites.……..244

Appendix C: Effect of Processing Conditions on Mechanical Properties of PEI Reinforced with a P-glass...……250

Appendix D: Tensile Properties for Composite Blends at Elevated Temperatures.....253

Appendix E: Rheological Properties of Neat Thermoplastics and Composite Blends...…….256

Appendix F: Dynamic Mechanical Thermal Analysis Data...……..265

Appendix G: Miscellaneous PPS Data...…….272

List of Figures

Chapter 1

Figure 1.1: Comparison of shear viscosity (η) of phosphate and borosilicate glass filled polyetherketone at 405°C.....……..…13

Chapter 2

Figure 2.1: Droplet Deformation in Various flow fields. ..……32

Figure 2.2: Experimentally observed modes of droplet deformation in various flow fields..…….……36

Figure 2.3: Effect of viscosity ratio on critical Weber number for Newtonian fluids in rotational (shear) and irrotational (extensional) flow fields……..….53

Figure 2.4: Sinusoidal disturbance on a liquid cylinder.…….60

Figure 2.5: Dominant wave number (χ_m) and growth function (Ω_m) as a function of viscosity ratio (λ).....…….…62

Figure 2.6: Variation of viscosity with temperature for simple glass-forming oxides…….…68

Figure 2.7: Non-Newtonian response for silica glasses for varying conditions....…..…73

Figure 2.8: Experimentally observed rheological responses for various fluid-fluid blends of varying concentration.....……..80

Figure 2.9: Effects of temperature and composition on the viscosity and normal stress for polystyrene/high density polyethylene blends....……..….82

Figure 2.10: The effects of the addition of phosphate glass on the viscosity of various thermoplastics.……...85

Figure 2.11: Viscosity versus shear rate for polystyrene filled with carbon black...…..89

Figure 2.12: Effects of deformation on various fiber reinforced materials in thermoforming.……..……..103

Chapter 3

Figure 3.1: Evolution of complex viscosity ($|\eta^*|$) versus time for neat PPS and P-glass at 330.2 ± 0.1°C.……..101

Figure 3.2: Complex viscosity (|η*|) versus angular frequency for neat PPS and P-glass at 330.1 ± 0.1°C…….…….102

Figure 3.3: Evolution of complex viscosity (|η*|) versus time for neat PPS and P-glass at 350.2 ± 0.1°C.…….104

Figure 3.4: Complex viscosity (|η*|) versus angular frequency for neat PPS and P-glass at 350.0 ± 0.1°C……..……105

Figure 3.5: Complex viscosity (|η*|) versus temperature for PPS and phosphate glass using a cooling rate of 2.4 ± 0.1°C/min……..…….106

Figure 3.6: Scanning electron micrographs of the core region along the machine direction for molded Ryton PR09 reinforced with 60 wt% P-glass.(a) Dry blended (b) Preblended...……..109

Figure 3.7: Scanning electron micrographs of the skin region along the machine direction for Fortron 320 reinforced with 40 wt% P-glass molded at an injection rate of 19 cm^3/sec. (a) Processed at 330°C (b) Processed at 350°...……...……..116

Figure 3.8: Scanning electron micrographs along the machine direction of Ryton PR09 reinforced with 40 wt% P-glass molded at 350°C with an injection rate of 10 cm^3/sec (a) Skin region (b) Core region.……..118

Chapter 4

Figure 4.1: Scanning electron micrographs along the machine direction for PPS reinforced with 20 wt% P-glass. (a) Skin region (b) Core region.……...…134

Figure 4.2: Scanning electron micrographs along the machine direction in the core region of injection molded samples. (a) 40 wt% P-glass(b) 60 wt% P-glass.....….136

Figure 4.3: Scanning electron micrographs along the machine direction in the skin region of injection molded samples. (a) 60 wt% P-glass (b) 40 E-glass..……137

Figure 4.4: Storage modulus (G′) versus temperature of the neat PPS and various glass filled composites for a heating rate of 2.5 ± 0.1 °C/min……...…140

Figure 4.5: Loss factor (tan δ) versus temperature of the neat PPS and various glass filled composites for a heating rate of 2.5 ± 0.1 °C/min……..142

Figure 4.6: Storage Modulus (G′) and Loss Modulus (G″) versus applied strain at 10 rad/sec and 300.1 ± 0.1°C for glass filled PPS composites……..144

Figure 4.7: Complex viscosity (|η*|) versus angular frequency (ω) for neat PPS, neat P-glass, and various glass filled composites at 300.1 ± 0.1°C...……..145

Figure 4.8: Complex viscosity (|η*|) versus temperature for neat PPS and various glass filled composites for a heating rate of 4.6 ± 0.1°C/min……...…147

Chapter 5

Figure 5.1: The complex viscosity (|η*|) versus angular frequency (ω) for various materials at 370.3 ± 0.5°C..…… 160

Figure 5.2: The complex viscosity (|η*|) versus angular frequency (ω) for various materials at 410.1 ± 0.1°C……..…….162

Figure 5.3: The complex viscosity (|η*|) versus temperature for various materials, cooling from 370°C using a rate of 2.4 ± 0.1 °C/min……..……163

Figure 5.4: The complex viscosity (|η*|) versus temperature for various materials, cooling from 410°C using a rate of 2.4 ± 0.1 °C/min……..164

Figure 5.5: Scanning electron micrographs along the machine direction in the skin region of injection molded PEI composites reinforced with P-glass (T_g - 234°C). (a) 30 wt% P-glass (b) 45 wt% P-glass....……..……174

Figure 5.6: Scanning electron micrographs along the machine direction in the core region of injection molded PEI composites reinforced with P-glass (T_g - 234°C). (a) 30 wt% P-glass (b) 45 wt% P-glass……..……175

Figure 5.7: Scanning electron micrographs along the machine direction in the skin region of injection molded PEEK composites reinforced with 55 wt% P-glass (T_g- 234°C). (a) Victrex 150G (b) Victrex 450G.…….…….177

Figure 5.8: Scanning electron micrographs transverse to the flow direction in the core region of injection molded PEEK composites reinforced with 45wt% P-glass (T_g - 234°C). (a) Victrex 150G (b) Victrex 450..……..178

Figure 5.9: Scanning electron micrographs along the machine direction within the skin region of injection molded PEEK composites reinforced with 43 vol% P-glass. (a) Victrex 150G with 60 wt% P-glass (T_g - 234°C) (b) Victrex 450G with 66 wt% P-glass (T_g - 282°C)…….180

Figure 5.10: Storage modulus (G′) versus temperature of the neat PEI and various glass {E-glass & P-glass (T_g - 234°C)} filled composites using a heating rate of 2.5 ± 0.1 °C/min……181

Figure 5.11: Storage modulus (G′) versus temperature for neat PEEK and composites reinforced with 43 vol% of various phosphate glasses using a heating rate of 2.5 ± 0.1°C/min...…….……183

Figure 5.12: Loss factor (tan δ) versus temperature of the neat PEI and various glass filled composites using a heating rate of 2.5±°C/min.….……184

Figure 5.13: Loss factor (tan δ) versus temperature for PEEK reinforced with 43 vol% of various phosphate glasses using a heating rate of 2.5 ± °C/min.…….185

Chapter 6

Figure 6.1: Apparent tensile modulus versus temperature for polyetherimide reinforced with various glasses....……200

Figure 6.2: Scanning electron micrographs from the skin region of injection molded specimens along the machine direction. (a) 45 wt% P-glass (b) 30 wt% E-glass fiber.……201

Figure 6.3: Apparent tensile toughness versus temperature for polyetherimide reinforced with various glasses....……202

Figure 6.4: Stress-strain curves for polyetherimide reinforced with 45 wt% phosphate glass as function of temperature...……..204

Figure 6.5: Scanning electron micrographs of the surface of injection molded polyetherimide composites stretched uniaxially. (a) 30 wt% E-glass fiber (b) 30 wt% P-glass (T = 268°C, $\varepsilon \approx 0.75$, $\dot{\varepsilon}_0 = 0.02\ sec^{-1}$).…….207

Figure 6.6: Scanning electron micrographs parallel to the deformation direction for polyetherimide injection molded specimens stretched uniaxially. (a) 30 wt% P-glass, core region (b) 45 wt% P-glass , skin region (T = 268°C, $\varepsilon \approx 0.75$, $\dot{\varepsilon}_0 = 0.02\ sec^{-1}$)……209

Figure 6.7: Scanning electron micrographs parallel to the deformation direction for polyetherimide injection molded specimens exposed to planar deformation. (a) 30 wt% P-glass, core region (b) 45 wt% P-glass , skin region (T = 268°C, $\varepsilon \approx 0.75$)....…….212

Figure 6.8: Storage Modulus (G′) versus temperature for PPS reinforced with 60 wt% phosphate glass measured at 2.4 ± 0.1°C/min., 10ω, and 0.1% strain..……..215

Figure 6.9: Scanning electron micrographs parallel to the machine direction for polyphenylene sulfide injection molded composites. (a) 40 wt% P-glass, skin region (b) 60 wt% P-glass, core region..……..216

Figure 6.10: Scanning electron micrographs parallel to the deformation direction for polyphenylene sulfide injection molded composites reinforced with 40 wt% phosphate glass exposed to planar deformation at 282°C. (a) Core region, as molded (b) Core region, $\varepsilon \approx 0.75$...……217

Figure 6.11: Scanning electron micrographs parallel to the deformation direction for polyphenylene sulfide injection molded composites reinforced with 60 wt% phosphate glass exposed to planar deformation at 283°C. (a) Core region, $\varepsilon \approx 0.5$ (b) Core region, $\varepsilon \approx 0.75$.……..218

Figure 6.12: Thermoformed polyetherimide based composites reinforced with various glasses. (a) 30 wt% E-glass, (b) 30 wt% P-glass, (c) 45 wt% P-glass.……..221

Appendix A

Figure A.1: Complex viscosity ($|\eta^*|$) versus angular frequency (ω) with Newtonian viscosity fits for a phosphate glass (T_g - 234°C)..……...232

Figure A.2: **:** Zero shear viscosity ($|\eta^*|_0$) versus temperature with an Arrhenius fit for a phosphate glass (T_g - 234°C)..…….234

Figure A.3: Complex viscosity ($|\eta^*|$) versus angular frequency (ω) with Newtonian viscosity fits for a phosphate glass (T_g - 282°C).....…….……..239

Figure A.4: Zero shear viscosity ($|\eta^*|_0$) versus temperature with an Arrhenius fit for a phosphate glass (T_g - 282°C)....…….241

Appendix B

Figure B.1: Loss factor (tan δ) versus temperature for PEEK reinforced with 60 wt% P-glass (T_g - 234°C)...…….249

List of Tables

Chapter 1

Table 1.1: Anisotropy of TLCP reinforced in situ injection molded composites.....…..5

Table 1.2: Phosphate glass compositions commonly used for blending with polymer melts.....……..…8

Table 1.3: Injection molded properties of phosphate glass reinforced thermoplastics as compared to borosilicate (E-glass) filled composites.....……..…11

Chapter 2

Table 2.1: Activation energies for viscous flow for various simple glass forming oxides.……48

Table 2.2: Properties for a TLCP reinforced with various loadings of phosphate glass of various configurations.....……..……79

Chapter 3

Table 3.1: Machine Direction Properties of Injection Molded Neat PPS.....……97

Table 3.2: Effects of Mixing History on the Machine Direction Properties of Injection Molded PPS/Phosphate Glass Blends..……108

Table 3.3: Effects of Injection Rate and Resin on Machine Direction Properties of PPS Reinforced with 40 wt% P-glass processed at 330°C…….110

Table 3.4: Effects of Injection Rate and Resin on Transverse Direction Properties of PPS Reinforced with 40 wt% P-glass processed at 330°C....…….…….112

Table 3.5: Effects of Injection Rate and Resin on Machine Direction Properties of PPS Reinforced with 40 wt% P-glass processed at 350°C…….114

Table 3.6: Effects of Injection Rate and Resin on Transverse Direction Properties of PPS Reinforced with 40 wt% P-glass processed at 350°C.....…..……115

Chapter 4

Table 4.1: Mechanical Properties for injection molded PPS based composites reinforced with various loadings of glass..…….……..130

Table 4.2: Ratio of Machine to Transverse direction Properties for Film-gated Injection Molded PPS composites reinforced with Glass……133

Table 4.3: Surface Properties of Various Glass Reinforced PPS Injection Molded Composites……..139

Chapter 5

Table 5.1: Mechanical Properties for injection molded PEI based composites reinforced with various loadings of P-glass (T_g - 234°C) and E-glass..……..166

Table 5.2: Mechanical Properties for injection molded PEEK based composites reinforced with 45 wt% (29 vol%) P-glass (T_g - 234°C)…...……..…..169

Table 5.3: Mechanical Properties for injection molded PEEK based composites reinforced with 51 wt% (28 vol%) P-glass (Tg - 282°C).……..…..171

Table 5.4: Mechanical Properties for injection molded PEEK based composites reinforced with approximately 43 vol% P-glass.....…….……172

Chapter 6

Table 6.1: Tensile Properties for injection molded PEI composites reinforced various loadings of glass stretched uniaxially along the machine direction at 268°C and 50 mm/min (Initial strain rate = 0.02 sec^{-1}).....…….……..206

Table 6.2: Tensile Properties for injection molded PEI composites reinforced various loadings exposed to planar deformation along the machine direction at 268°C...……210

Table 6.3: Tensile Properties for injection molded PPS composites reinforced with phosphate glass exposed to planar deformation along the machine direction at 282-283°C.……..213

Appendix A

Table A.1: Complex viscosity ($|\eta^*|$) versus angular frequency (ω) for a phosphate glass (T_g - 234°C)…….230

Table A.2: Newtonian (Zero shear) viscosity versus temperature for a phosphate glass (T_g - 234°C)....…….233

Table A.3: Complex viscosity ($|\eta^*|$) at 1 radian/second versus temperature for a phosphate glass (T_g - 234°C)...……235

Table A.4: Complex viscosity (|η*|) at 1 radian/second versus time for a phosphate glass (T_g - 234°C)..……..236

Table A.5: Complex viscosity (|η*|) versus angular frequency (ω) for a phosphate glass (T_g - 282°C)...……..237

Table A.6: Newtonian (Zero shear) viscosity versus temperature for a phosphate glass (T_g - 282°C).....……240

Table A.7: Complex viscosity (|η*|) at 1 radian/second versus temperature for a phosphate glass (T_g - 282°C)...……242

Table A.8: Complex viscosity (|η*|) at 1 radian/second versus time for a phosphate glass (T_g - 282°C)...……243

Appendix B

Table B.1: Accelerated Aging of Polyphenylene Sulfide Composites Reinforced with P-glass (T_g - 234°C) and E-glass..……...246

Table B.2: Accelerated Aging of Polyetherimide and Polyetheretherketone Composites Reinforced with Phosphate glasses..……247

Appendix C

Table C.1: Effect of Injection rate on mechanical properties of PEI reinforced with 30 wt% phosphate glass (T_g -234°C) processed at 370°C..……...251

Table C.2: Effect of Injection Rate on mechanical properties of PEI reinforced with 60 wt% phosphate glass (T_g -234°C) processed at 370°C...…….252

Appendix D

Table D.1: Tensile Properties for Polyetherimide Composites reinforced with P-glass (T_g - 234°C) and E-glass evaluated at 250 mm/min (Initial strain Rate=0.10 sec^{-1})..……..….254

Table D.2: Tensile Properties for Polyphenylene Sulfide Composites reinforced with P-glass (T_g - 234°C) and E-glass evaluated at 250 mm/min (Initial strain rate of 0.10 sec^{-1})…….255

Appendix E

Table E.1: Complex viscosity (|η*|) versus angular frequency (ω) for various grades of neat PPS..…….257

Table E.2: Complex viscosity (|η*|) versus angular frequency (ω) for a various grades neat of PEEK and PEI.……258

Table E.3: Complex viscosity (|η*|) at 1 radian/second versus temperature for various grades of neat PPS, cooling from 350°C...……..259

Table E.4: Complex viscosity (|η*|) at 1 radian/second versus temperature for various neat thermoplastics, cooling from 370°C...……..260

Table E.5: Complex viscosity (|η*|) versus 1 radian/second temperature for various grades of neat PEEK, cooling from 410°C.....……261

Table E.6: Strain sweeps performed at 10 radians/second and 300°C for PPS composite blends reinforced with P-glass (T_g - 234°C) and E-glass...…….262

Table E.7: Complex viscosity (|η*|) versus angular frequency (ω) at 300°C for various PPS composite blends reinforced with P-glass (T_g - 234°C) and E-glass……263

Table E.8: Complex viscosity (|η*|) at 1 radian/second versus temperature for various PPS composite blends reinforced with P-glass (T_g - 234°C) and E-glass, heating from 300°C.…….264

Appendix F

Table F.1: Storage Modulus (G′) at 10 radians/second versus temperature for PPS composite blends reinforced with P-glass (T_g - 234°C) and E-glass...…….266

Table F.2: Storage Modulus (G′) at 10 radians/second versus temperature for PEI composite blends reinforced with P-glass (T_g - 234°C) and E-glass……268

Table F.3: Storage Modulus (G′) versus temperature at 10 radians/second for various grades of PEEK reinforced with 45 wt% P-glass (T_g - 234°C).……..270

Table F.4: Storage Modulus (G′) versus temperature at 10 radians/second for various grades of PEEK reinforced with 43 vol% P-glass...……271

Appendix G

Table G.1: Effect of Processing Temperature on Injection molded Mechanical Properties of neat PPS (Ryton PR09)....…….273

Table G.2: QCM Off-gasing values for neat PPS, P-glass (T_g-234°C) and various composite blends.……275

List of Equations

Chapter 2

Equation 2.1: Surface or Interfacial Tension....…….27
Equation 2.2: Work of adhesion....……28
Equation 2.3: Work of adhesion (All components)..……28
Equation 2.4: Work of adhesion (Harmonic mean equation)....……28
Equation 2.5: Work of adhesion (Geometric mean equation)..……29
Equation 2.6: Young's equation for contact angles.…….29
Equation 2.7: Young's equation & harmonic mean equation.....……..29
Equation 2.8: Young's equation & geometric mean equation……..29
Equation 2.9: Taylor's deformation parameter (Interfacial forces dominating)……33
Equation 2.10: Taylor's deformation parameter (Viscous forces dominating)...……..33
Equation 2.11: Chaffey and Brenner's deformation parameter .....……33
Equation 2.12: Cox's time dependent deformation parameter (Shear flow) ..……..34
Equation 2.13: Angle of droplet orientation (Cox's deformation parameter) ……..34
Equation 2.14: Critical Weber number (Shear flow) ……34
Equation 2.15: Cox's time dependent deformation parameter (Extensional flow)..…..35
Equation 2.16: Dynamic interfacial tension.…….39
Equation 2.17: Dimensions of a sinusoidally distorted fluid thread.…….41
Equation 2.18: Distortion amplitude of distorted fluid thread……..41
Equation 2.19: Growth rate of distorted fluid thread....……41
Equation 2.20: Time to burst for distorted fluid thread……44
Equation 2.21: Graetz Number...……..73

Chapter 1: Introduction

1.0 Introduction

The development of low cost materials possessing high strength, stiffness, dimensional and thermal stability has been an area of major research in the last few years. Composite systems composed of metals and ceramics can often meet requirements in areas such as stiffness, strength, and service temperature but can possess many shortcomings in regards to weight, ease of processing, cost of raw materials, and certain mechanical properties such as impact resistance and toughness. To overcome some of the problems associated with metals and ceramics, these materials are often combined with polymeric materials to form high performance composites.

Thermoplastics can be combined with reinforcing materials such as glass, graphite, carbon and aromatic polyamide (Kevlar) to create composites that offer many advantages. These composites often possess moduli and strengths that are comparable to other high performance materials such as metals and ceramics. Other advantages of these polymeric composites over metals and ceramics include the lower cost of raw materials, resistance to a variety of environments, and lighter weight for finished products.

Fiber reinforced thermoplastic and thermoset composite systems also exhibit some disadvantages in terms of processing. One of the major factors that limits the use of these composites is the difficulty of incorporating the reinforcing phase into the resin. In the case of thermosetting systems, long processing times and special equipment are required to insure impregnation of the continuous fibers and allow proper curing of the resin. For thermoplastic resins, the compounding of the filler into the resin requires special equipment that involves time and energy intensive processes. The addition of the fillers also raises the viscosity of the melt and leads to wear on processing equipment due to abrasion[1].

Besides suffering from problems dealing with the incorporation of the solid reinforcement, fiber reinforced composites often create difficulties for post-processing operations such as compression molding or thermoforming. During these forming operations, the reinforcing phase can be buckled or broken when undergoing deformation such as shaping within a mold [2-6]. These composite systems also have other problems such as rough and broken surfaces and are limited by the strains that can be applied due to the uneven stress distribution within the material.

To overcome the wetting and deformation problems seen with standard filled systems, it would be desirable to produce composites where both the reinforcing phase and matrix are deformable during various processing steps. These composites would be completely deformable during melt processing steps, such as compounding, resulting in lower viscosities and less wear on equipment when compared to solid filled systems. The reinforcing phase would be completely wetted by the matrix and the reinforcing phase

morphology could be controlled by the deformation applied during processing. Processes such as injection molding, fiber spinning, strand extrusion, and various forming operations could be used to generate the final composite morphology. Since the reinforcing phase morphology comes into existence as the composite is being formed, composites generated in this fashion are often referred to as in situ composites[7].

1.1 In Situ Composites

The addition of short fiber reinforcement is commonly used to elevate the properties (primarily stiffness) of polymeric materials, but the benefits gained by the addition of this solid reinforcement do not come without a cost. The addition of the solid phase introduces numerous difficulties in terms of processing equipment and processing behavior. One of the greatest difficulties encountered is achieving adequate dispersion of the solid fibers into the thermoplastic resin. To insure adequate dispersion, shear intensive processes are often utilized resulting in fiber breakage which reduces the effectiveness of the reinforcement. The abrasive nature of the fiber results in wear on the barrel, screws, and molds of the processing equipment. The addition of the fiber can also have a dramatic effect on the processing behavior of the resin. Reinforced resins often have high viscosities resulting in problems such as short shots, flash formation, weld lines, and premature freezing in molding operations [1,8-11].

The difficulties associated with the generation and processing of short fiber reinforced systems has led to the search for alternative methods for the manufacture of thermoplastic composites. One of the most promising methods involves the generation of the reinforcing phase during melt processing steps such as injection molding and extrusion. Because both the matrix and reinforcing phases are deformable during processing, a variety of operations such as injection molding, strand extrusion, sheet extrusion, and blow molding can be utilized to produce the composite system [12].

A large portion of the work performed with in situ composite generation has involved the use of thermotropic liquid crystalline polymers (TLCPs) as the reinforcing phase. TLCPs are organic macromolecules that possess sufficiently high chain stiffness to promote high strength and modulus while remaining readily melt processable. These TLCPs offer properties such as high use temperatures, excellent chemical resistance, low melt viscosity, and low coefficient of thermal expansion [13]. Because these materials are melt processable, TLCPs can be blended with thermoplastics in conventional processing equipment. A wide variety of processing techniques can be used to produce a range of composites that are wholly thermoplastic.

The use of TLCPs as the reinforcing phase in a thermoplastic composite matrix relies strongly on the ability of the processing technique to induce orientation of the TLCP phase. In order to obtain high mechanical properties in TLCPs, the material has to achieve

an adequate level of molecular orientation [14-16]. Oriented TLCPs often show very high properties in the direction of deformation while the transverse direction properties remain very poor. In order to obtain this high degree of molecular orientation, processes utilizing elongational flows are often preferred over shear flows because material exposed predominately to shear flows often remains unoriented. The inability to fully orient the TLCP in the blend produces composites with mechanical properties which are below theoretical expectations.

The injection molding of TLCP based in situ composites has received considerable attention in the literature. Several studies have reported significant improvement in mechanical properties based on blends of TLCPs with engineering thermoplastics [7,17-24]. A variety of thermoplastics such as polypropylene, polyethylene terephthalate, polycarbonate, and polyetherimide have been blended with a range of TLCPs. Anisotropy was found to be prevalent in these composites with the machine direction properties showing great improvement with incorporation of TLCP while the transverse direction properties remained nearly constant. Bafna et al. [23] demonstrated this phenomenon with TLCP reinforced polyetherimide blends molded with a rectangular film-gated mold (see Table 1.1). One interesting point to note is that even with the anisotropy, the machine direction mechanical properties of these TLCP blends can be comparable to glass filled systems. When PEI is reinforced with 30 wt% glass fiber, the machine direction tensile modulus is 9.2 GPa, while a 30 wt% loading of a TLCP (HX4000, a DuPont material) produces a modulus of 9.8 GPa. The PEI composite reinforced with HX4000 also yields a composite blend that has a density of 1.3 g/cm^3 as compared to the 1.5 g/cm^3 found with the E-glass filled material.

Composite fibers of TLCP filled thermoplastics often offer higher mechanical properties than injection molded composites [20,25-29]. Processes such as fiber spinning and strand extrusion offer the advantage of being able to apply high strains of purely uniaxial extensional deformation resulting in greater orientation of the TLCP with leads to higher mechanical properties. For example, a comparison can be made between blends containing PP with 20 wt% Vectra B950 (a TLCP from Hoechst Celanese) produced via injection molding and fiber spinning. For a film-gated injection molded plaque, O'Donnell, Datta, and Baird [18] found the machine direction tensile modulus to be 3.2 GPa while Robertson [30] using the same composition was able to spin strands with a tensile modulus of 13 GPa. In the case of the injection molded composite, a random planar sample would theoretically have a tensile modulus of 5.3 GPa if all the TLCP was highly oriented into fibrils with aspect ratios over 100. For the TLCP reinforced strands, the theoretical modulus for a uniaxially aligned composite under the same conditions would be on the order of 12 GPa. As can be seen here, processes imparting high degrees of extensional deformation are more effective in fully utilizing the reinforcing capability of the TLCP to produce composites with better properties.

Table 1.1: Anisotropy of TLCP reinforced in situ injection molded composites [23].

Weight Fraction (PEI/TLCP)	Ultem 1000 / HX 1000		Ultem 1000 / HX4000	
	MD Flexural Modulus (GPa)	TD Flexural Modulus (GPa)	MD Flexural Modulus (GPa)	TD Flexural Modulus (GPa)
100/0	3.00	3.05	3.00	3.05
80/20	6.20	-	5.31	3.12
70/30	7.27	3.20	7.00	3.21
50/50	12.92	3.20	12.25	2.71
30/70	15.83	2.70	14.75	2.62
0/100	15.60	2.40	14.00	2.36

Note: Ultem 1000 is a neat grade of PEI with HX1000 and HX4000 being TLCPs
Flexural tests performed on film-gated rectangular plaques

Processing techniques, such as injection molding and fiber spinning, which lead to the formation of composites on an in situ basis often fail to produce composites with the highest mechanical properties. Often a highly oriented skin is formed while the core contains material with lower orientation. By not having the core region oriented, the full reinforcing potential of the TLCP is not realized.

One method developed to overcome some of the problems associated with the formation of in situ composites is through the patented dual extruder mixing technique [31]. The processes of injection molding and standard strand extrusion rely on the breakup and deformation of TLCP droplets into reinforcing fibrils. During these processes, the TLCP and thermoplastic matrix are exposed to the same thermal history often resulting in degradation of the matrix resin. The dual extruder mixing technique allows the TLCP and thermoplastic to undergo differing thermal histories through the use of separate extruders for each resin. The dual extrusion process also creates the TLCP fibrils through the splitting of continuous TLCP streams. The effectiveness of the dual extruder system was demonstrated by Sukhadia [20]. Composite strands composed of PET with 30 weight percent of the TLCP Vectra A were prepared with a single screw extruder and the dual extruder process. For the dual extruder system, a sample having a draw ratio of 50 had a tensile modulus of 19 GPa while a sample with a similar draw ratio produced via single screw extrusion only had a modulus of 13.5 GPa.

The in situ formation of TLCP reinforced composites has been widely investigated but certain limitations do exist for these composites. One of the major factors that has limited the use of TLCPs as a reinforcing agent is the high cost of these novel materials. Neat TLCPs currently range in cost from $26/kg to $48/kg [32,33] as compared to $1.65/kg [34] for glass fiber. Because the mechanical properties of TLCP filled composites are dependent on obtaining a high level of molecular orientation, the processing methods used to generate these composites are rather limited. These composites are often anisotropic and often do not meet their potential in terms of the ultimate mechanical properties.

Besides TLCPs, another material that has potential for in situ composite generation techniques are melt processable glasses. These inorganic glasses have low glass transition temperatures (200-350°C), allowing the glass and a thermoplastic to be blended in standard melt processing equipment [35-42]. Composites reinforced with these glasses have only been investigated on a very limited basis. The influence of factors such as viscosity, interfacial tension, composition, and processing conditions on the final composite properties remains an area open to much research.

1.2 Phosphate Glass

The use of glass to reinforce thermoplastics has found wide use in many industries. The glasses most commonly combined with thermoplastics are glasses based on SiO_2. These glasses possess high glass transition temperatures so that the glass does not show significant softening behavior until temperatures above 840 °C [11] so that the glass remains as a solid when processed with thermoplastics. During plastics forming operations these glasses behave as solids, which can create numerous processing difficulties. Incorporating the glass into the resin, wear on processing equipment, altered flow characteristics of the resin, poor surface finish, and anisotropic parts are some of the problems seen with these reinforced systems.[1,8-11].

Besides silica, a number of inorganic oxides such as boron, germanium, and phosphorous can be utilized to form inorganic glasses. The limited chemical durability of boron and cost of germanium has limited the use of these materials in composite structures. The most promising melt processable glasses are composed of phosphorous pentoxide, P_2O_5. The P_2O_5 has a tendency to form isolated cyclic molecules in contrast to the three dimensional network structure found with silicate glasses. Normally these cyclic structures are connected via weak Van der Waals attraction to form sheet like structures. To increase the rigidity of these glasses alkalis and alkaline earths are added. It is believed that the ring molecules are broken by the addition of these modifier ions to form linear phosphate chains of varying length. These linear phosphate chains can easily move past one another resulting in viscous flow at temperatures in the range of 300-450°C, low enough for melt processing with some thermoplastics [36,43-44]. An example of the typical compositions of phosphate glasses blended with thermoplastics are shown in Table 1.2.

For the novel glasses, a variety of oxides are combined to give a balance between the chemical durability and glass transition temperature (T_g). The primary glass forming compound in these glasses is P_2O_5 whose concentration is a controlling factor for the durability of these novel glasses. Ultraphosphate glasses (>50 mol% P_2O_5) are generally hygroscopic and show poor durability. Between the pyrophosphate region (33 mol% P_2O_5) and the metaphosphate regions (50 mol% P_2O_5), glasses become non-hygroscopic and chemical durability improves as the phosphate concentration declines. Below the pyrophosphate composition, spontaneous crystallization and devitrification is often observed. Alkali oxides are added to control the T_g and durability of the glass. Often PbO and SnO are used as a replacement of ZnO in order to increase the refractive index, improve durability, and lower the T_g. Rare earth oxides are often added in small amounts to improve resistance to water and acid but often suffer from solubility problems and elevate the T_g to unacceptable levels. Sulfate (SO_3) is often added to glasses in order to lower the T_g without compromising the durability [37]. As can be seen here, the chemistry of these novel glasses is a complicated balance between the chemical durability, glass

Table 1.2: Phosphate glass compositions commonly used for blending with polymer melts [37].

Role	Component	Mole %
Base glass	P_2O_5	28 - 40
	Zn0	23 - 55
	Na_2O, LiO_2, K_2O	10 - 35
Alkali substitution	Cu_2O	0 - 20
Zn0 Substitution	PbO	0 - 35
	SnO	0 - 35
	CuO	0 - 20
Anion Substitution (lower T_g)	SO_3	0 - 17
Improve durability (raise T_g)	Al_2O_3	0 - 6
	CeO_2, Nd_2O_3, Pr_2O_3	0 - 3
	ZrO_2	0 - 5
	CaO, MgO, BaO, MnO, SrO	0 - 10
Stabilize blend microstructure	SiO_2	0 - 3

transition temperature, and composition that would provide interaction with polymeric matrices.

In order to lower the glass transition temperature of these glasses certain sacrifices are made in regards to mechanical properties and chemical durability. Water can attack phosphate glasses through the hydrolysis of the covalent P-O-P bonds as well as the disruption of the ionic bonds between the phosphate chains [37,44,45]. Exposure of these materials to a humid environment often results in a steady decline of mechanical properties [36,37,46-50]. Much of the present work in regards to phosphate glasses is geared toward the development of compositions possessing lower T_gs with greater chemical durability [37,46-50]. In comparison to silicate glasses, the lower T_g phosphate glasses also have mechanical properties that are rather limited. The phosphate glasses that are commonly blended with thermoplastics possess an elastic modulus on the order of 40 GPa with a tensile strength in the range of 20 MPa [36]. These values are low when compared to borosilicate glasses which have a tensile modulus on the order of 70 GPa with pristine fibers exhibiting strengths in the range of 2000-3000 MPa [11].

1.3 Phosphate Glass/Polymer Blends

Inorganic glasses and thermoplastics each offer unique properties that can be combined to form composites that possess a balance of properties. It is well known that glasses exhibit desirable properties such as high stiffness, thermal stability and abrasion resistance. Glasses can be combined with thermoplastic matrices to form composite systems that offer properties somewhere between the neat glass and polymeric resin. What distinguishes phosphate glass (P-glass) from borosilicate glass (E-glass) is its behavior at the elevated temperatures used to process thermoplastics. Due to its high T_g, borosilicate glass is a rigid solid during polymer processing operations resulting in the numerous difficulties that have been stated earlier. Meanwhile, the phosphate glass is fluid at elevated temperatures allowing the in situ generation of composites that possess the same general properties of an E-glass filled system while overcoming many of their problems. This novel behavior of P-glass filled systems allows composites with higher glass concentrations to be processed within standard equipment and has the potential to open many processing operations not available to E-glass filled systems.

The processing of phosphate glass filled thermoplastics has received limited attention in the literature. Ray and co-workers [35] were the first to process a number of low T_g lead phosphate glasses with a variety of thermoplastics such as polypropylene (PP), polyethylene terephthalate (PET), polysulfone (PS), and polycarbonate (PC). Processes such as rod extrusion, strand extrusion, sheet extrusion and injection molding were investigated. For example, polypropylene was blended with glass in a single screw extruder to form a composite blend containing 75 wt% (44 vol%) glass. The composite was extruded into a rod which had a tensile modulus of 9.7 GPa versus 1.4 GPa for pure

PP. Extruded blends composed of polysulfone and PET with 25 vol% glass had tensile moduli of 10.3 GPa and 8.8 GPa, respectively, as compared to approximately 2.8 GPa for the neat materials. Other processes such as fiber spinning, injection molding, and sheet extrusion were examined to assess the processing potential for these blends. The glasses used for these studies possessed very low transition temperatures in the range of 140 - 210 °C with tensile moduli ranging from 23 - 35 GPa. The usefulness of these composite blends was limited due to the poor durability of the glasses which showed weight losses on the order of 0.02 - 5% per minute when immersed in boiling water.

In recent years, as glasses with lower transition temperatures and improved durability have been developed, interest in these new materials for composite manufacture has grown. Bahn and co-workers [36] have recently investigated the processing of phosphate glass/thermoplastic alloys. These materials were referred to as alloys due to claimed interactions between the phosphate glass and organic polymer. These particular blends were comprised of higher transition glasses (225 °C < T_g < 350°C) blended with high performance thermoplastic resins such as polyetherimide (PEI), polyethersulfone (PES), polyetheretherketone (PEEK), polyetherketone (PEK), and thermotropic liquid crystalline polymers (TLCPs). Because the phosphate glass was deformable during processing, much higher glass loadings could be achieved when compared to E-glass filled composites. A comparison between the properties of phosphate and E-glass filled composites are shown in Table 1.3. In order to obtain phosphate glasses with lower T_gs, sacrifices were made in regards to mechanical properties. For the blends listed here, the phosphate glass utilized only had a tensile modulus of 40 GPa with a tensile strength of 20 MPa and an elongation to break of only 0.05% [36]. These properties are much lower than the typical values seen for borosilicate E-glass which has a tensile modulus of 70 GPa with a strength on the order of 3500 MPa and an elongation to break of 3 - 4%[11]. For E-glass filled systems, the volume fraction of glass is limited to approximately 30 vol% glass due to the effect of fiber on the viscosity of the resin. Due to the phosphate glasses ability to undergo deformation during processing, much higher glass concentrations (upwards of 70 vol%) can pass through standard equipment with the polymer matrix remaining as the continuous phase[37]. The higher glass loadings translate into composites that possess higher modulus, heat deflection temperatures, and better flame resistance when compared to E-glass filled materials. These composite systems suffer from lower strength and elongation to break than standard E-glass filled materials due to the inherent properties of the phosphate glasses. Because the chemical durability of phosphate glasses is an issue of concern, higher T_g glasses often have to often be utilized in the composite systems. The higher T_gs of these glasses elevates the required processing temperatures to the level of high performance thermoplastics such PEEK, PEK, PEI, and TLCPs. As the glass chemistry is developed to produce glasses with lower transition temperatures and improved chemical durability, these composites could be expanded to include lower cost commodity resins such as polypropylene.

Table 1.3: Injection molded properties of phosphate glass reinforced thermoplastics as compared to borosilicate (E-glass) filled composites.

Matrix	Matrix/Glass (wt/wt)	Matrix/Glass (vol/vol)	E[1] (GPa)	σ[2] (MPa)	% Elongation
PEK [36]	100/0	100/0	3.99	103	5.00
PEK [36]	15/85	30/70	29.9	76	0.29
PEEK [36]	100/0	100/0	1.10	100	80.0
PEEK [36]	20/80	40/60	26.9	83	0.36
PEEK [51]	60/40*	74/26	17.9	193	2.00
TLCP [36]	100/0	100/0	-	110	1.10
TLCP [36]	20/80	39/61	16.1	53	0.44
TLCP [36]	30/70	52/48	20.1	81	0.59
TLCP [52]	60/40*	73/27	21.4	172	1.40

TLCP - Xydar, (*) Commercial Borosilicate (Type E) glass filled material

[1] E = Tensile Modulus

[2] σ = Tensile Strength

1.4 Advantages of P-Glass Reinforced Thermoplastics

Phosphate glass filled materials offer several advantages when compared to borosilicate glass filled materials In the previous section it was shown that phosphate reinforced blends can achieve moduli which match or exceed those of E-glass reinforced thermoplastics. Phosphate glasses offer the greatest advantage over silicate glasses in terms of their processing behavior.

Due to the low glass transition temperatures of phosphate glasses, the equipment requirements for these materials are not as a complex as borosilicate glass filled materials. Phosphate glasses are easily processable within standard melt processing equipment at conditions comparable to commercial thermoplastics. These glasses can display viscosities of the same order of magnitude as a polymeric melt (< 10,000 Pa·s) [53], allowing glass loadings as high as 70 volume percent to be processed within standard equipment. For E-glass filled resins, special compounding equipment has to be utilized in order to introduce the reinforcing filler into the resin. During this compounding step, fiber breakage occurs reducing the reinforcing potential of the glass. These compounded resins then have to be processed in a certain manner to minimize any further degradation of the fiber aspect ratio. The solid filled systems will also shorten the life of processing equipment by wearing and abrading the screws, barrels, and molds while phosphate glasses will not produce this wearing effect.

The rheology of these neat glasses and thermoplastic/glass blends may offer the greatest processing advantage when compared to standard filled systems. Neat zinc phosphate glasses appear to display Newtonian behavior over a wide range of temperatures with the viscosity changing an order of magnitude for every 15-25°C [37,53]. Through the use small amplitude oscillatory strain measurements, Sammler et al. [53] studied the rheological behavior of two zinc phosphate glasses. From this work it was found that phosphate glasses display viscosities comparable to engineering thermoplastics (< 10,000 Pa·s) in the range of 100°C above the T_g of the glass . The lower viscosities of the glasses allows these materials to be blended with a thermoplastic within conventional polymer processing equipment. Due to the fluid-like nature of the phosphate glass, these materials can display lower viscosities at higher glass loadings when compared to E-glass filled materials. Figure 1.1 shows the viscosity of polyetherketone reinforced with phosphate glass and E-glass. As can seen by the figure, at equivalent volume fractions of P-glass and E-glass (30 vol%), the phosphate glass filled material has a viscosity almost an order of magnitude lower than the E-glass filled resin. Even increasing the phosphate glass loading to 62 vol%, the blend only shows only a slight increase in viscosity and is still much lower than the E-glass blend containing 30 vol% glass.

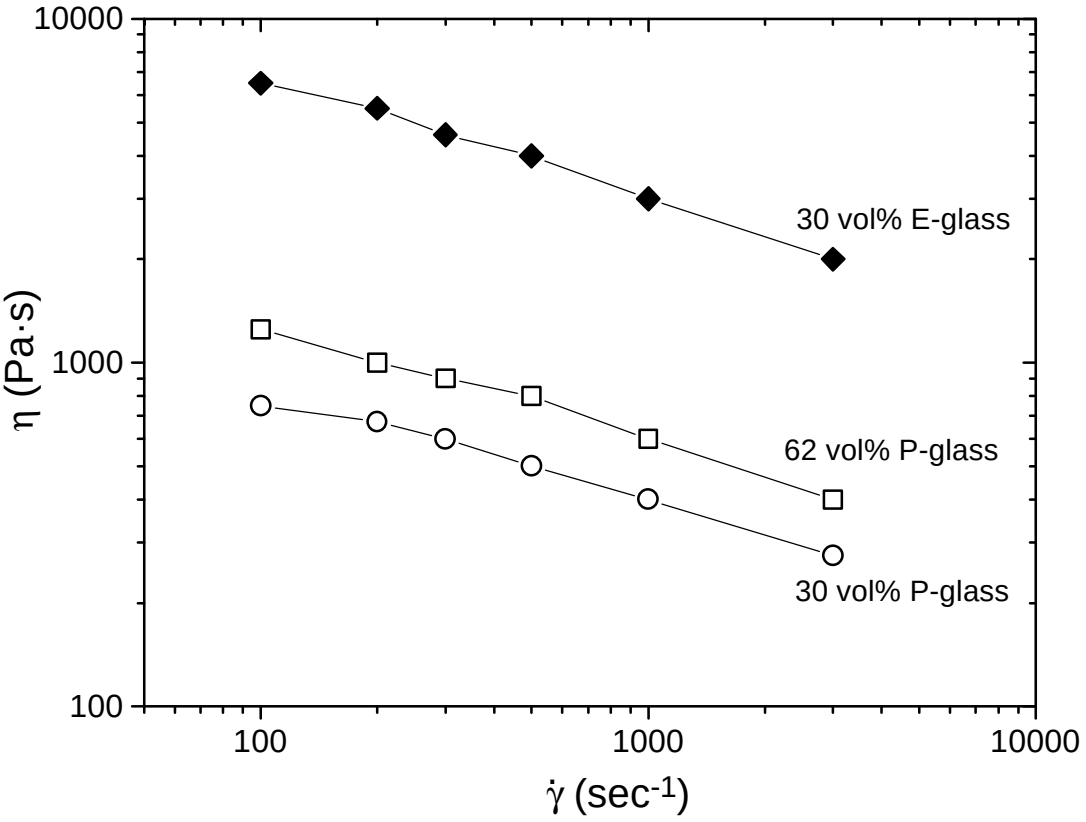

Figure 1.1: Comparison of shear viscosity (η) of phosphate and borosilicate glass filled polyetherketone at 405°C [37].

Due to the lower viscosity of the phosphate glass, composite blends possessing high glass loadings can easily be processed while E-glass filled systems do not have this luxury. Injection molded composites can contain up to 70 volume percent phosphate glass [36] while borosilicate filled composites are limited to 20-30 volume percent reinforcement [11]. The concentration of E-glass fiber reinforcement that can be added to a thermoplastic resin is limited due to the effect of the fibers on the processing behavior of the resin. The addition of fiber reinforcement elevates the viscosity of resin (especially at lower shear rates), alters the flow characteristics of the resin and increases the required injection pressures and temperatures [1,8]. Besides changing the processing behavior of the resin, solid glass reinforcement can have a dramatic effect on the final product properties such as surface finish and anisotropy in terms of both fiber orientation and stress distribution.[1,8] As the glass fiber concentration is increased the aforementioned problems would be magnified resulting in processing difficulties and composites with undesirable properties. For phosphate glass filled materials, the glass is dispersed as smaller domains usually in the form of droplets or slightly elongated regions. This morphology has a tendency to produce parts that have much finer molding tolerances, smoother surfaces, and are less anisotropic than E-glass filled systems.[37,38]

The higher phosphate glass loadings have a significant effect on the thermal characteristics of the composites such as heat deflection temperature and flame resistance. For example, pure PEEK exhibits a heat deflection temperature of 160°C while a PEEK/phosphate glass blend (75 wt% glass) possesses a heat deflection temperature in the range of 267 - 285°C [36]. One of the most marked improvements of phosphate glass filled composites is the flame resistance of these materials. One way to measure the flammability of a material is the limiting oxygen index which reports the level of flowing oxygen at which sample becomes self-extinguishing. Pure PEK has a limiting oxygen index of 40, while commercially available PEK with a level of filler of 20 volume % has an index of 45. A phosphate glass filled blend with 60 volume % glass has a limiting oxygen index of 100 [41]. The dramatic improvement in the flame resistance of phosphate glass filled composites can be attributed to three major mechanisms. First, phosphate compounds are commonly used as flame retardants. Secondly, the higher glass loadings leave less polymer to burn. Finally, once a sample is burning the phosphate glass can flow forming a barrier to oxygen thus preventing further combustion.

An additional area that the low T_g of phosphate glasses may offer an advantage over short glass fiber is in forming operations. E-glass fiber reinforced thermoplastics are difficult to form due to the material's lack of melt strength and pliability. During the forming operation, especially around the corners of the mold, fiber breakage and/or buckling often occurs [2-6]. Phosphate glass filled blends may be able to withstand a variety of forming operations that require large scale deformation due to the fluidity of the glass. An example of such a process is the fiber spinning or strand extrusion of the P-glass blends. Ray and coworkers [35] produced a variety of thermoplastic/phosphate glass blend strands via extrusion. Blends containing up to 30 wt% glass were extruded into

strands using take-up rates ranging from 0.5 - 7.5 meters/second. The resulting composite strands contained glass fibrils with diameters ranging 1- 5 μm and aspects ratios on the order of 30 - 200. The forming potential of these materials was also demonstrated with processes such as thermoforming and vacuum forming of glass sheets laminated with polypropylene and polyvinyl chloride [35]. These composite sheets could easily be formed and bent at angles greater than 90° without breaking the glass reinforcement.

Another advantage that phosphate glass filled blends may offer is in the area of recycling. Because the glass domains are deformable during processing, there is the potential that the reinforcing morphology could be regenerated by replasticating the material. For short fiber reinforced materials, there is a continuous reduction of the glass fibers aspect ratio due to grinding and fiber breakage within the equipment. Graham et al. [54] showed that injection molded polypropylene reinforced with 30 wt% E-glass contains glass fibers with an initial aspect ratio of 36 with a tensile modulus of 6.7 GPa and a strength of 80 MPa. After being granulated and re-injection molded 4 times, the glass aspect ratio had fallen to 27 with the composite possessing a modulus of 5.3 GPa and a strength of only 52 MPa. This continual loss in the glass' reinforcing capability can be partially offset by the addition of new glass fiber. In the same study, it was shown that the tensile modulus of once recycled PP containing 30 wt% glass could be elevated to values comparable to the control sample through the addition of 2.5-5 wt% virgin glass. Because the reinforcing morphology of phosphate glass filled blends are generated by a different mechanism, it might be possible to recycle these materials using methods not available to E-glass reinforced thermoplastics. For example, these blends could be granulated and directly reprocessed in an effort to regenerate the reinforcing morphology.

Because phosphate glasses can possess a variety of compositions, it may be possible to tailor the chemistry in order to interact with specific polymers. In order to obtain the optimal properties in short fiber reinforced composites, the addition of materials referred to as sizing agents are often utilized [1,11,55,56]. These sizings are used to promote adhesion between the polymer and glass resulting in higher mechanical properties. With short fiber composites, the glass fiber has to be sized for use with a resin and must be able to withstand the temperatures used during processing. It may be possible to adjust the composition of phosphate glasses to promote specific interactions with the desired thermoplastic in order to increase mechanical properties. Hersch and co-workers [57], through the use of methods such as Diffuse Reflectance Fourier Transform Infrared Spectra (DRIFT) and X-ray photoelectron spectroscopy (XPS), showed that the surfaces of zinc phosphate glasses are reactive toward ammonia and substituted amines. It was found that the amines and substituted amines were reactive with the zinc phosphate groups (Bronsted acid sites) and the zinc ions (Lewis acid sites) on the glass surface. It was also found that nitridation reactions can occur forming both bonding and non-bonding P-N groups which could be used as a possible structure to attach polymer structures. It has also been determined that acid sensitive polymers, such as polyamides, are reactive with these glasses often resulting in degradation of the thermoplastic [36]. It appears that

systems containing polyester linkages (such as TLCPs) may also be compatible with these glasses [36,37]. The TLCP Xydar was blended with a zinc phosphate glass and the properties compared to a composite containing unsized E-glass beads. The phosphate glass blend containing 54 vol% glass had a tensile strength of 72 MPa while the E-glass blend with 56 vol% glass only had a strength of 46 MPa [37]. Optical micrographs of the fracture surface for the phosphate glass/TLCP blends revealed substantial polymer/glass adhesion with very little glass pull out. As the chemistry of these novel glasses becomes better understood, there is a potential to develop high temperature composite systems that do not rely on the addition of a third component such as a sizing agent in order to obtain good adhesion between the polymer and reinforcement.

1.5 Disadvantages of P-Glass Reinforced Thermoplastics

Even though phosphate glasses offer many advantages in terms of processing behavior, there are some drawbacks to consider as well. Limitations of these materials extends to areas such as service environments and ultimate mechanical properties.

As mentioned earlier, the phosphate glasses are susceptible to the effects of moisture. At low glass concentrations, the polymer matrix may encapsulate the glass enough to protect it from the effects of moisture. As the glass concentration increases, the blend will become more sensitive to the water. For example, a TLCP/phosphate glass blend comprised of 80 wt% glass displayed an initial tensile strength of 53 MPa and after being immersed in boiling water for 24 hours the composite strength fell to approximately 32 GPa [36] . These composite materials also readily absorb moisture which results in swelling of the composite. Aitken et al. [58], placed a phosphate glass/PEK composite (55/45 wt%) in boiling water for 5 days where the sample displayed a 4.75 percent weight gain. The swelling and loss of mechanical properties of the glass blends can be limited by the addition of materials such as $CaCO_3$ or ZnO. By adding 20 wt% zinc oxide to the aforementioned PEK composite, the weight gain under these conditions was reduced to less than 0.5 %. The addition of the ZnO stabilizer also helped the blend retain its strength. The unstabilized sample possessed an initial flexural strength or modulus of rupture (MOR) of 106 MPa while after exposure to boiling water for 5 days the MOR fell to 43 MPa. For the zinc oxide stabilized material the initial MOR only fell from 105 MPa to 94 MPa. The stability of these composites are constantly being improved with the development on new and better glass compositions as well as additives to help improve the blend durability.

The phosphate glasses used for blending with thermoplastics are often at a disadvantage in areas such as mechanical properties and density when compared to other reinforcing materials. The lower T_g phosphate glasses display a tensile modulus in the range 20-40 GPa [36] as compared to 70-80 GPa for borosilicate glass fiber [11], 207-630 GPa for carbon fiber [8], 125 GPa for Aramid fiber [59], and 40 -100 GPa for TLCPs

[12]. The strength of these phosphate glasses are also much lower than standard reinforcing material with the tensile strength only falling in the range of 20-30 MPa [36]. The density of phosphate glass is often in the range 2.4 - 3.5 g/cm^3 [37] which is comparable to 2.1 - 2.7 g/cm^3 for reinforcing fiberglass (E-glass) [11] but is still higher than the other reinforcing materials. The higher density and lower mechanical properties of phosphate glasses usually means that higher glass loadings have to be used to obtain mechanical properties comparable to other reinforcing materials.

One of the complexities that arises with the processing of phosphate glasses are changes in the glass structure that can occur due to processing. Because the glasses are usually passed through equipment between the materials' glass transition temperature and melting point, events such as crystallization or devitrification (phase separation) could occur. Crowder and co-workers [60] performed a study on the crystallization of zinc alkali phosphate glasses under both quiescent and shearing conditions. The crystallization of the glasses was monitored using both differential scanning calorimetry (DSC) and X-ray diffraction (XRD). At a temperature of 400 °C, a glass possessing a T_g of 272°C displayed the formation of crystalline order under quiescent conditions in a period of 4 hours. At the same temperature, a sample sheared in a batch style mixer showed the formation of crystalline regions in less than an hour. As the mixer speeds were increased, the glass crystallized at accelerated rates, producing higher torques which eventually shut down the mixer. Because it appears these glasses can undergo shear induced crystallization during processing, great care has to be used when processing the material. For composites of high glass loadings, crystallization could occur as the material is conveyed in a screw resulting in the plugging of equipment. The high stresses generated during processes such as injection molding could also lead to the crystallization of the glass resulting in variations of the reinforcing morphology obtained.

1.6 Research Objectives

The manufacture of in situ composites with melt processable materials has widely been investigated mainly using TLCPs as the reinforcing agent. The use of phosphate glasses in these types of composites has been studied only on a limited basis. The literature available only presents a general database in order to evaluate the potential of these novel composites. Because these melt processable glass blends are intended to replace other fiber reinforced composites, it would be interesting to compare these novel blends to well established composite systems. It has been shown that phosphate glass filled systems offer certain processing advantages with limitations in areas such as chemical durability and ultimate mechanical properties. The processing advantages and limits of these novel composites as compared to conventional E-glass filled materials have not fully been determined. With this in mind, the overall objectives for this research are to compare phosphate and E-glass filled blends in terms of processing behavior evaluated

through injection molding, rheological testing, and post processing techniques such as thermoforming and compression molding.

1.6.1 Research Objective #1

For other in situ reinforced systems, such as TLCPs, the final mechanical properties are strongly dependent on material variables as well the processing conditions utilized. Variables such as concentration, viscosity ratio between the phases, and interfacial tension play large roles in the composite final morphology. Other variables that effect the composite final morphology are processing related including the stress field and flow kinematics. A fundamental understanding of the formation of the blend morphology is paramount in obtaining composites with the best possible properties. With this in mind, the first research objective is:

> **Evaluate the injection molding of phosphate glass filled composites. The effects of variables such as glass concentration, interfacial tension, and viscosity ratio on the composites final mechanical properties will be determined. The sensitivity of the composite's mechanical properties to various injection molding conditions will also be evaluated.**

1.6.2 Research Objective #2

Almost all the work concerned with phosphate glasses has involved the use of injection molding as the method to generate the composite morphology. Factors such as the flow kinematics, rapid changes in viscosity, and premature solidification of the glass phase often limits the mechanical properties of composites generated by this method. One possible way to develop a more favorable reinforcing morphology would involve the deformation of the polymer/glass blends at lower temperatures (slightly above the glass T_g). The use of E-glass in processes such as thermoforming and compression molding is limited due to problems such as low melt strength, fiber breakage, and rough surface appearance. The phosphate glass/thermoplastic composites may display attributes that are more suited to these processes. Since the potential of these composites in these type of processes has not been investigated, the second research objective is:

> **Evaluate the feasibility of processing phosphate glass filled thermoplastics in thermoforming and compression molding. The effects of deformation on the morphology and mechanical properties of these blends will also be determined.**

1.6.3 Research Objective #3

One of the major factors that limits the use of short fiber filled composites in many commercial applications are the changes in the rheological behavior of the resin with the addition of the filler. The addition of solid fillers usually result in an increase of the viscosity which is more pronounced at lower shear rates[61,62]. The elastic nature of these materials, as evaluated through the first normal stress difference and storage modulus (G′), is also effected by the addition of solid reinforcement. It is typically found that the addition of solid fiber results in an increase in the first normal stress difference (N_1) while particulate fillers tend to reduce N_1[61]. The factors that control the behavior of these systems include the type of filler and suspending fluid, the size and aspect ratio of the reinforcement, volume fraction of the filler, and surface treatments on the reinforcement[61]. The changes in the viscous and elastic response of these materials plays a large role in the processing of these filled systems. In the case of phosphate glass filled systems, at lower temperatures the glass can behave as solid reinforcement while at elevated temperatures the blend would contain two materials that are fluid. The rheology of neat phosphate glasses as well as phosphate glass/thermoplastic blends is an area open to much research. Considering the importance of rheology in the processing of the melt processable composites, the third objective is:

> **Determine if phosphate glass filled polymer blends possess any unique rheological behavior when compared to common short fiber reinforced systems. Through the use of dynamic mechanical testing the viscoelastic properties of the neat glasses and composite blends will be evaluated and compared to conventional short fiber reinforced materials.**

A brief introduction to melt processable composites was presented with an emphasis on TLCP and phosphate glass reinforced systems. The findings of the literature in regards to phosphate glass filled thermoplastics were outlined and the main objectives of this research given. In the following chapter, a review of the literature pertinent to the completion of the objectives will be presented.

1.7 References

1 A.M. Shibley, in *Handbook of Composites* (Chapter 7), ed. G. Lubin, Van Nostrand Reinhold, New York 1982.

2 J.D. Muzzy, X. Wu, and J.S. Colton, *Polym. Comp*., 11 (5), 280 (1990).

3 J.E. Manson, T.L. Schnieder, and J.C. Seferis, *Polym. Comp*., 11 (2), 114 (1990).

4 A. Dutta, M, Niemeyer, and M. Cakmak, *Polym. Comp*., 12 (4), 257 (1991).

5 D.M. Bigg and J.R. Preston, *Polym. Comp*., 10 (4), 261 (1989).

6 S. Di Pede and R.T. Woodhams, *Polym. Eng. Sci.*, 30 (19), 1185 (1990).

7 G. Kiss, *Polym. Eng. Sci*., 27 (6), 410 (1987).

8 Schweizer and Winterman, *Thermoplastic Polymer Additives: Theory and Practice*, ed. J.T. Lutz Jr., Marcel Dekker, New York 1989.

9 B. Frazén, C. Klason, J. Kubát, and T. Kitano, *Composites*, 20 (1), 65 (1989).

10 S.H. Collins, *Plastics Compounding*, 5 (3), 113 (1982).

11 S. Kessler, in *Plastics Additives and Modifiers Handbook* (Chapter 48), ed. J. Edenbaum, Van Nostrand Reinhold, New York 1992.

12 D.G. Baird, in *Polymeric Materials Encyclopedia* (vol. 5), ed. J. Salemore, 3207 (1996).

13 W. Huh, R. A. Weiss, and L. Nicolais, SPE ANTEC Tech. Papers, 32, 306 (1986).

14 Y. Ide and Z. Ophir, *Polym. Eng. Sci*., 23 (5), 261 (1983).

15 S. Kenig, *Polym. Eng. Sci*., 27 (12), 887 (1987).

16 D.J. Blundell, R.A. Chivers, A.D. Curson, J.C. Love, and W.A. MacDonald, *Polymer*, 29, 1459 (1988).

17 A. Datta, H.H. Chen, and D.G Baird, *Polymer*, 34 (4), 759 (1993).

18 H.J. O'Donnell, A. Datta, and D.G. Baird, *SPE ANTEC Tech. Paper*, 38, 2248, (1992).

19 J. Seppälä, M. Heino, and C. Kapanen, *J. Appl. Polym. Sci*., 44, 1051 (1992).

20 A.M. Sukhadia, *Ph.D. Dissertation*, Virginia Polytechnic Institute & State University (1991).

21 G. Crevecoeur, *Ph.D. Dissertation*, Katholiede Universiteit Leuven (1991).

22 A.I. Isayev and M.J. Modic, *Polym. Comp*., 8 (3), 158 (1987).

23 S.S. Bafna, J.P. de Souza, T. Sun, and D.G. Baird, *Polym. Eng. Sci*., 33 (13), 808 (1993).

24 J.P. de Souza and D.G. Baird, *Polymer*, 37 (10), 1985 (1996).

25 P. Zhuang, T. Kyu, and J.L. White, *Polym. Eng. Sci*., 28 (17), 1095 (1988).

26 K.G. Blizard, C. Federici, O. Federico, and L.L. Chapoy, *Polym. Eng. Sci*., 30 (22), 1442 (1990).

27 S. Mehta and B. Deopura, *J. Appl. Polym. Sci*., 56, 169 (1995).

28 M.T. Heino and J.V. Seppälä, *J. Appl. Polym. Sci*., 44, 2185 (1992).

29 E.A. Sabol, A.A. Handlos, and D.G Baird, *Polym. Comp*., 16 (4), 330 (1995).

30 C.R. Robertson, *Master Thesis*, Virginia Polytechnic Institute and State University (1995).

31 A.M. Sukhadia and D.G. Baird, U.S. Patent 5,225,488 (1993).

32 A. Roggero, *Thermotropic Liquid Crystalline Polymers Blends*, ed. F.P. La Mantia, Technomic, Lancaster (PA), 1993.

33 D.J. Williams, *Adv. Polym. Tech*., 10(3), 173 (1991).

34 *Modern Plastics Encyclopedia '92*, McGraw-Hill, New York (1992).

35 N.H. Ray and F.R. Sherliker, U.S. Patent 3,732,181 (1973).

36 W.A. Bahn, G.H. Beall, J. Ference, B.C. Monahan, C.J. Quinn, and P.S. Roussel, U.S. Patent 5,043,369 (1991)

37 C.J. Quinn, P. Frayer, and G.H. Beall, in *Polymeric Materials Encyclopedia* (vol. 4), ed. J. Salemore, 2766 (1996).

38 W.A. Bahn and C.J. Quinn, *SPE ANTEC Tech. Paper*, 2370 (1991).

39 C.J. Quinn and G.H. Beall, *ACS Polymer Preprints*, 32 (2) , 205 (1990).

40 G.H. Beall and C.J. Quinn, *Ceram. Trans*., (33), 321 (1993).

41 C.J. Quinn and G.H. Beall, in *Chem. Process Adv. Mater*., ed. L. Hench, 799 (1992).

42 C.J. Quinn, G.H. Beall, J. Dickinson, *Int. Cong. Glass*, 16 (4), 79 (1992).

43 S. W. Martin, *Eur. J. Solid State Inorg. Chem*., 28, 163 (1991).

44 A. Varshneya, *Fundamentals of Inorganic Glasses*, Academic Press, New York 1994.

45 B.C. Bunker, G.W. Arnold, M. Rajaram, and D.E. Day, *Proceedings of American Ceramic Society*, (87), 425, (1986).

46 G.H. Beall and J.E. Pierson, U.S. Patent 5,328,874 (1994).

47 G.H. Beall and C.J. Quinn, U.S. Patent 4,940,667 (1990).

48 G.H. Beall, J.E. Dickinson, C.J. Quinn, U.S. Patent 4,996,172 (1991).

49 B.G. Aitken, G.H. Beall, and J.E. Dickinson, U.S. Patent 5,529,960 (1996).

50 B.G. Aitken, G.H. Beall, and J.E. Dickinson, U.S. Patent 5,529,961 (1996).

51 *Plastics Digest*, 17 (2), D.A.T.A. Business Publishing, Englewood, CO (1996).

52 Amoco Product literature, Xydar G-630, (1997).

53 R.L. Sammler, J.U. Otaigbe, M.L. Lapham, N.L. Bradley, B.C. Monahan, and C.J. Quinn, *J. Rheol*., 40 (2), 285 (1996).

54 W.D. Graham, R.B. Jutte, and D.L. Ship, Proceedings of the 48th Annual Conference, SPI, Inc, (1993).

55 E.P. Plueddemann, *Silane Coupling Agents*, Plenum Press, New York 1991.

56 S. Wu, *Polymer Interface and Adhesion* (Chapter 11), Marcel Dekker, Inc., New York 1982.

57 L.S. Hersh, E.C. Onyiriuka, and W. Hertl, *J. Mater. Res*., 10 (8), 2120 (1995).

58 B.G. Aitken, D.C. Bookbinder, J.E. Dickinson, and B.M. Wedding, U.S. Patent 5,367,012 (1994).

59 J.J. Pigliacampi, in *Modern Plastics Encyclopedia* , McGraw Hill, New York (1992).

60 C.E. Crowder, J.U. Otaigbe, M.A. Barger, R.L. Sammler, B.C. Monahan, and C.J. Quinn, J. Non-Cryst. Solids, 210, 209 (1997).

61 H.M. Laun, *Colloid Polym. Sci*., 262, 257 (1984).

62 J.M. Deally and K.F. Wissbrun, *Melt Rheology and its Role in Plastic Processing: Theory and Applications*, Van Nostrand Reinhold, New York (1990).

Chapter 2: Literature Review

2.0 Literature Review

The development of higher performance polymeric matrices has lead to their use in many areas such as polymer blends and composite materials. Polymers can be blended with a wide variety of materials ranging from organic and inorganic solids as well as other polymeric materials to form mixtures that offer many advantages over the neat substituents. The search for composite materials based on polymeric matrices has led to the development of many novel processes to generate composite systems rapidly and inexpensively. One such process entails the generation of self-reinforcing blends through a variety of processing techniques. Much of the work concerning these self-reinforcing composite systems has concentrated on thermotropic liquid crystalline polymer (TLCP) reinforced thermoplastics, but the development of new melt processable reinforcing materials (such as phosphate glasses) offer an opportunity to further investigate the potential of those processing techniques. Melt processable glass reinforced composite systems may offer several advantages as compared to conventional solid reinforced systems.

The properties of self-generating composite systems, such as thermoplastics reinforced with melt processable glasses, are strongly dependent on the reinforcing phase morphology that is generated during processing. The interactions between the glass and polymer matrix when exposed to varying processing conditions will control the ultimate morphology that can be developed. A fundamental understanding of the deformation of multiphase blends will be paramount in evaluating the processing behavior of these melt processable glass filled blends. With this in mind, a brief discussion of multiphase blends will be presented in sections 2.1- 2.4. Emphasis will be placed on evaluating the factors that control deformation of the various materials in multiphase blends.

As will be revealed in the sections discussing deformation in fluid blends, the rheological behavior of the materials utilized will have a large effect on the morphologies that could be generated. Due to the large role of rheology in the formation of the blend microstructure as well as the overall processing behavior of the materials, sections 2.5-2.7 will concentrate on the rheological behavior of inorganic glasses as well as multiphase polymeric systems. The rheological responses typically seen in fluid-fluid systems will be presented and compared to solid filled systems to help ascertain the possible benefits of using melt processable reinforcing materials over conventional solid reinforcement.

The processing behavior and properties of conventional solid reinforced materials as well as melt processable composite blends will then be presented in sections 2.8 through 2.10. The effects of material as well as processing parameters on the properties of the composites will be discussed. The limitations of conventional glass filled materials will be presented and a brief discussion of some of the processing benefits of self reinforcing materials highlighted.

The formation of the reinforcing phase morphology in melt processable glass composites is directly related to the deformation of the fluid glass droplets suspended in a polymeric matrix. There are several factors that control the final glass phase morphology in these composite mixtures. Some of these factors include glass concentration, viscosity of the substituents, interfacial tension between the phases, and the flow field experienced during processing. In order to generate composites with the desired mechanical properties, the variables critical to the formation of these blends has to be established.

2.1 Polymeric Blends (General Considerations)

When two or more materials are passed through some common processing step, the resulting blend can take on several forms. Depending on the interactions between the materials that are blended together, the resulting mixture can display the characteristics of either a single-phase or multiphase mixture. The characteristics of these blend systems can be examined with many different methods that include rheological, optical, thermal, and mechanical testing. Blends of materials can be considered either miscible, partially miscible, or immiscible. In the case of a miscible system, strong interaction between the materials results in a blend that behaves as a single phase resulting in characteristics such as a single glass transition temperature. For partially miscible systems, the material interactions are less pronounced and the blend displays the characteristics of a multiphase system. A partially miscible system displays multiple glass transition temperatures that are shifted slightly from the transition temperatures of the neat blend components' values. In the case of miscible and partially miscible blends, the interactions between the phases often results in blends that possess properties that offer some advantage over the neat materials. Unfortunately, many polymeric blends do not display these types of behaviors and an immiscible system is the result [1,2].

Most often blends of polymeric materials result in the formation of an immiscible mixture. These blends often display very distinct glass transition temperatures that are indicative of the blend neat constituents. In the case of immiscible systems, numerous phases with distinct boundaries are formed which can lead to complications for these systems. The interactions between the distinct phases occur at the interface between the components, so that items such as the mechanical properties of these systems are strongly dependent on the structure attained during processing [3,4]. Often the resulting phase morphology is a function of variables such as processing history and dispersed phase concentration which means great care has to be taken when processing these systems in order to obtain the desired phase morphology [3-6].

When trying to deform the phases in a multi-component blend, the interfacial energy between the substituents is one of the vital parameters in determining the final phase morphology. The interfacial energy between the components has a direct effect on the morphology, dispersion, and ultimate mechanical properties of the blend. The

elongation and breakup of the reinforcing phase under both flow and quiescent conditions will be partially controlled by the interfacial energy between the substituents. A knowledge of the surface energy between the substituents in an immiscible blend is useful in predicting the composite blend phase morphology as well as the ultimate mechanical properties as controlled by the adhesion between the various phases.

2.2 Interfacial Tension

When dealing with multiphase systems, the interactions between the various phases are controlled to a large extent by the interfacial or surface energy between the substituents. This surface or interfacial tension can generally be thought of as the surface free energy per unit area with a simple example of this parameter being seen by considering the behavior of a liquid droplet placed on a solid planar surface. After the droplet is initially placed on the solid, the surface area of the droplet increases due to the spreading of the liquid. As liquid molecules migrate to form the new surface, they will move against unbalanced molecular forces. The molecules in the liquid surface layer now possess additional energy due to the work performed to bring them to the surface [7]. In essence, the reversible work required to create the interfacial (surface) area is the interfacial or surface tension (γ) and can be represented by the following expression [7]:

$$\gamma = \left(\frac{\partial G}{\partial A} \right)_{T,P,n} \qquad (2.1)$$

where G is the Gibbs free energy of the total system, A is the interfacial area, with T, P, and n representing the temperature, pressure, and number of moles of matter in the system, respectively. Basically, the surface tension is a parameter that characterizes the ability of the material to form greater surface area.

Materials are commonly classified into two broad categories based on the characteristics of their surfaces. Materials can either possess what is known as a high-energy or low-energy surface. High-energy materials are often hard, refractory, and dense and often possess surface tensions in the range of 200-5000 dynes/cm [7]. High energy materials include metals, metal oxides, and inorganic materials such as glasses. Materials such as melt processable glasses based on phosphates and borosilicate glasses such as E-glass generally fall into this category. Often these high-energy substances are easily wetted by the other general class of materials known as low-energy materials. Low-energy materials are usually soft, low-melting and of light weight and include substances such as organic compounds and organic polymers. These low-energy materials usually have surface tensions below 100 dynes/cm [8].

When two distinct materials are placed in contact with one another, an interface is formed that is dependent on the surface properties of the materials themselves. The materials could interact with one another in a favorable manner, resulting in a greater interfacial attraction. There would be a certain amount of work that would be required to separate the interface between the bulk phases which is generally regarded as the work of adhesion. This work of adhesion can be thought of as the decrease in the Gibbs free energy per unit area when an interface is formed from the two individual surfaces. The work of adhesion (W_a) can be related to the interfacial tension between the two phases (γ_{12}) and the surface tension of the individual phases, γ_1 and γ_2, by the following equation [8]:

$$\gamma_{12} = \gamma_1 + \gamma_2 - W_a \qquad (2.2)$$

From this relationship, it can be seen that a greater interfacial attraction between the phases, represented by W_a, results in a lower the interfacial tension between the two materials.

When two materials are brought into contact, there are numerous intermolecular forces that exist between the materials. These forces or interaction parameters include dispersive (nonpolar) forces, dipole (dipole-dipole) forces, inductive (dipole-induced dipole) forces, and hydrogen bonding. It has been assumed that surface tension and the work of adhesion are additively composed of the contributions from the various interaction potentials. The surface tension and work of adhesion are assumed to be composed of two main components consisting of a dispersive (nonpolar) and a polar (dipole-dipole, dipole-induced dipole, and hydrogen bonding) component. By assuming the work of adhesion can be split into various components, equation 2.2 can be rewritten as:

$$\gamma_{12} = \gamma_1 + \gamma_2 - W_a^{\,d} - W_a^{\,P} \qquad (2.3)$$

According to Wu [8], the dispersive work of adhesion ($W_a^{\,d}$) and polar work of adhesion ($W_a^{\,p}$) can be estimated by two different methods. For the combination of two low-energy materials, the harmonic mean equation is often utilized which yields the following expression [8]:

$$W_a^d = \frac{4\gamma_1^d\gamma_2^d}{\gamma_1^d + \gamma_2^d} \quad \text{and} \quad W_a^P = \frac{4\gamma_1^P\gamma_2^P}{\gamma_1^P + \gamma_2^P} \qquad (2.4)$$

where γ_i^d and γ_i^p are dispersive and polar components of the surface tension for the various materials. In the case of the combination of a high-energy surface and low-energy surface material, the dispersive and polar terms of the work of adhesion can be represented by the following terms:

$$W_a^d = 2(\gamma_1^d \gamma_2^d)^{1/2} \quad \text{and} \quad W_a^P = 2(\gamma_1^P \gamma_2^P)^{1/2} \qquad (2.5)$$

Through the use of thermodynamics, many relationships have been developed describing the interactions of multiphase systems. One of the relationships that has been developed addresses the behavior of a fluid drop placed on a solid surface. When a liquid drop is placed on solid planar surface and allowed to equilibrate, the following relationship was developed by Young [9]. At equilibrium, the interfacial tensions between the three phases, i.e. γ_{LV} , γ_{LS} , γ_{SV} (where L - liquid, S- solid, V- vapor), must balance and can be related to the observable angle (Θ) of the liquid on the solid surface through Young's equation:

$$\gamma_{SV} = \gamma_{SL} + \gamma_{LV} \cos \Theta \qquad (2.6)$$

The equation developed by Young allows interfacial tension to be related to an easily measurable variable consisting of the contact angle. This contact angle for a liquid on a solid surface can be determined by a variety of methods. These methods include the use of devices such as a goniometer, where the contact angle can be measured directly. Other methods, such as tensiometric measurements, relate the changes in force as a solid sample is immersed into a liquid to the contact angle. By combining the experimentally determined contact angle in Young's equation with the harmonic and geometric mean equations, it is possible to experimentally determine the polar and dispersive components of the surface tension of an unknown solid and quantify the surface characteristics of the material.

Through the combination of Young's equation and the geometric and harmonic mean equations, the surface tension of an unknown solid can easily be determined. By placing low energy fluids in contact with a low energy solid surface and applying the harmonic mean equation, the following relationship can be utilized [6]:

$$(1+\cos\Theta_i)\gamma_i = 4\left(\frac{\gamma_i^d \gamma_s^d}{\gamma_i^d + \gamma_s^d} + \frac{\gamma_i^p \gamma_s^p}{\gamma_i^p + \gamma_s^p}\right) \qquad (2.7)$$

Where γ_i refers to the testing liquids and γ_s is the unknown solid. By taking two liquids with known polar and dispersive components of the surface tension, two simultaneous quadratic equations can be solved to find the value for γ_s^d and γ_s^p. For high energy surfaces a similar method can be utilized by applying the geometric mean equation which yields [6]:

$$(1+\cos\Theta_i)\gamma_i = 2\left[(\gamma_i^d \gamma_s^d)^{1/2} + (\gamma_i^p \gamma_s^p)^{1/2}\right] \qquad (2.8)$$

Through the use of the aforementioned techniques, the adhesion and interfacial tension between two materials can easily be estimated. These techniques have been applied to study the interaction between phases in a wide variety of polymer blends. De Souza and Baird [10] utilized contact angle measurements to estimate the work of adhesion and interfacial tension between various thermotropic liquid crystalline polymers (TLCPs) and polyetherimide (PEI). From this data, it was determined that the interfacial tension between PEI and the TLCP, Vectra A (made by Hoechst Celanese) was 20.8 dynes/cm while the interfacial tension between PEI and the DuPont TLCP, HX1000, was only 7.2 dynes/cm. Due to the low interfacial tension between the HX1000 and PEI, the work of adhesion for this blend was found to be 81.7 dynes/cm as compared to 64.1 dynes/cm for the Vectra A blend and 105.6 dynes/cm for the neat PEI. The blends containing the HX1000 displayed higher mechanical properties which is reflected in the lower interfacial tension and higher work of adhesion for these particular blends. The lower interfacial tension between the PEI and HX1000 coupled with favorable viscosity ratios led to a composite blend offering higher properties than other comparable TLCP filled systems.

These measurements can also be used to quantify the role of compatibilizers in the generation of composite blends. O'Donnell and Baird [11] demonstrated the effects of adding maleic anhydride grafted polypropylene (MAP) to polypropylene/TLCP blends. With the addition of the maleated polypropylene, the interfacial tension between the substituents was decreased and an increase in the work of adhesion was also observed. The lowering of the interfacial tension and elevation in the work of adhesion resulted in composite systems possessing higher mechanical properties. For example, an injection molded blend containing polypropylene (PP) reinforced with 30 wt% of the TLCP Vectra B (VB) had a machine direction tensile modulus and strength of 3.7 GPa and 23 MPa, respectively. By adding 10 wt% MAP to the polypropylene, the machine direction modulus was increased to 4.2 GPa with the strength increasing to 28 MPa. Contact angle measurements showed that by adding the MAP, the interfacial tension between the PP and VB decreased from 5.1 dynes/cm to 1.7 dynes/cm.

2.3 Droplet Deformation

Many polymer processing operations are performed to promote the dispersion of some minor phase into a matrix material. In order to disperse a material, processes such as compounding in the screws of extruders or injection molders are utilized in an attempt to generate a uniform blend system. For mixing operations, it is desirable to subject the blend to high shear conditions in order to help disperse the materials. In the case of solid additives, these high shear conditions can lead to problems such as fiber breakage and abrasive wear on equipment. For systems containing two or more deformable fluids, the factors that control dispersion become more complicated when compared to solid additives. During mixing, fluid particles are deformed to a certain extent until surface

tension driven disturbances lead to the breakup of the material into a series of droplets. This process is repeated until the dispersed material obtains its equilibrium size due to a balance between the applied shear stress and the interfacial tension between the two components [12]. The deformation and breakup of the suspended phase is dependent on a complex relationship between many material variables, such as interfacial tension and viscosity as well as processing variables such as flow kinematics.

The material variables such as interfacial tension and viscosity are often outside the control of the processing engineer, but the one important variable that can be varied is the flow field experienced by the blend during processing. During polymer processing operations, fluid materials can be exposed to two basic types of flows. The most common flow is simple shear flow, where the velocity gradient is perpendicular to the flow direction which allows the fluid element to rotate during deformation. This type of flow is most commonly seen in polymer processing operations such flow in the screw of an extruder or injection molder. The other type of flow involves what is known as shearfree flow, where the velocity gradient is parallel to the flow direction allowing the fluid elements to be exposed to tension or compression. Processes that utilize this type of flow include the advancing front seen in the mold filling step of injection molding and free surface operations such as fiber spinning, blow molding, and film blowing. By applying the various types of flow fields during processing, the phases could undergo a wide range of deformations resulting in a variety of morphologies.

The first effort to study the deformation of liquid drops suspended in a viscous media was undertaken by G.I. Taylor [13-15]. Taylor investigated the deformation of a Newtonian drop with a viscosity of μ_d suspended in a viscous media with the viscosity (μ_m), for both a uniform shearing and plane hyperbolic (shearfree) flow field (see Figure 2.1). In the case of steady uniform small shear deformation, Taylor approximated the geometry of the deformed droplet as being nearly ellipsoidal so that the droplet shape could be related to the viscosity ratio ($\lambda = \mu_d / \mu_m$) between the droplet and suspending medium, the local shear stress ($\mu_m \dot{\gamma}$), the droplet radius (a), and the interfacial tension (σ) between the phases. Taylor's analysis focused on relating the role of viscous forces and interfacial forces on the deformation of a suspended droplet. The viscous forces would have a tendency to elongate the droplet while the interfacial forces would have a tendency to restore the droplet to its most stable state. The ratio of the viscous forces/interfacial forces i.e. $\mu_m \dot{\gamma} a / \sigma$ is often quantified through the dimensionless group known as the Weber (We) or capillary (Ca) number.

Taylor's analysis for droplet deformation under simple shear was limited to the extreme cases where either the interfacial tension is dominant over the viscous effects or the viscous effects are greater than the surface tension effects. For the case where the interfacial forces dominate (i.e. λ=O(1) & We << 1), Taylor's analysis reduces to the following form:

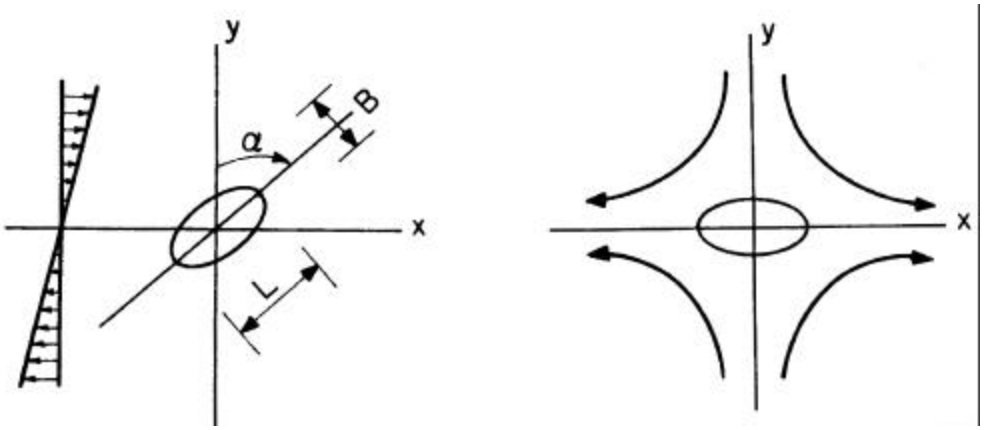

Uniform shear flow Plane hyperbolic flow

Figure 2.1: Droplet Deformation in various flow fields [12].

$$D = \frac{L - B}{L + B} = \left(\frac{\mu_m \dot{\gamma} a}{\sigma}\right)\left(\frac{19\lambda + 16}{16\lambda + 16}\right) \quad \text{with } \alpha = \pi/4 \text{ or } 45° \quad (2.9)$$

where D characterizes the overall deformation of the droplet, with L being the major drop axis dimension (length) and B the minor drop axis dimension (breadth). The angle α relates the orientation of the deformed droplet in respect to the principal shearing direction. For other extreme case where viscous effects dominate interfacial tension effects (i.e. $\lambda >> 1$ & We =O(1)) , the equation simplifies even further to the following:

$$\frac{L - B}{L + B} = \frac{5}{4}\lambda \qquad \text{with } \alpha = 0° \qquad (2.10)$$

For the first case (interfacial forces >> viscous the forces), the group containing the viscosity ratio (λ) only varies from 1 to 1.187 as the viscosity ratio varies from zero to infinity and the deformation can be directly related to the Weber number. For the other extreme case, (viscous forces >> interfacial forces), the deformation scales directly with the viscosity ratio.

Taylor verified his predictions by studying the deformation of fluid drops in shear flow in a specially built parallel band mill apparatus [13]. Taylor examined the two extreme cases where the suspended drop has a much lower viscosity than the suspending media and the case where the droplet was much more viscous than the surrounding material. For the first case where $\mu_d << \mu_m$ (i.e. $\lambda << 1$), the drops would distort and align at an angle of 45° to the shearing direction at low deformation rates. As the shear rate in the apparatus increased (increasing We), the droplets would deform into a long slender shape with pointed tips. For the other extreme where $\mu_d >> \mu_m$ (i.e. $\lambda >> 1$), the viscous drops only assumed a slightly deformed shape that was oriented at 45° to the shearing direction for low Weber numbers and as shear rate increased the droplet became oriented in the flow direction.

In order to theoretically analyze the deformation of a droplet in a medium, Taylor's original work had assumed the drop to be nearly spherical in shape for small deformations. Taylor's solution can be considered as a first order perturbation solution for the deformation parameter D. Chaffey and Brenner [16] obtained a second-order solution in terms of a deformation parameter (E) which yielded the following result:

$$E = \frac{L - B}{L + B} = \left(\frac{\mu_m \dot{\gamma} a}{\sigma}\right)\left(\frac{19\lambda + 16}{16\lambda + 16}\right) \qquad (2.11)$$

By comparing the equation above with experimental results, Turner and Chaffey [17]

determined that the second order theory showed no significant improvement when compared to Taylor's original first order theory.

Another theory was developed by Cox [18], where a series expansion of the velocity field in terms of the perturbation parameter was utilized. This theory considered the time dependence of the deformation parameter and reduces to the following form for equilibrium conditions (long time periods):

$$D = \frac{L - B}{L + B} = \frac{5(19\lambda + 16)}{4(1+\lambda)\sqrt{(19\lambda)^2 + (20/We)^2}} \qquad (2.12)$$

$$\text{with} \quad \alpha = \frac{\pi}{4} + \frac{1}{2}\tan^{-1}\left(\frac{19\lambda We}{20}\right) \qquad (2.13)$$

For the extreme cases where either viscous forces or interfacial forces dominate, it can be seen that Cox's theory reduces back to Taylor's original equation. Torza et. al. [19] experimentally verified Cox's equation and found that it produced greater agreement with experimental data as compared to Taylor's or Chaffey and Brenner's theories.

Experimental results showed that under shear flow, droplets can elongate to a certain extent until the viscous forces surpass the interfacial forces resulting in rupture and breakup of the droplet. Various equations have been developed in an effort to determine the point where these droplets would burst. Taylor was the first to estimate the conditions where this may occur through the use of equation 2.9. Taylor equated the maximum pressure difference in the matrix fluid at the interface to the Laplace equation for the capillary pressure, $2\sigma/a$. By doing this, it was determined theoretically that droplet rupture should occur when the deformation parameter D has a value of 0.5. This assumption was verified experimentally and it was determined that the critical Weber number for droplet rupture under shear flow is:

$$We_c = \left(\frac{1}{2}\right)\left(\frac{19\lambda + 16}{16\lambda + 16}\right) \qquad (2.14)$$

The initial droplet deformation theories developed by Taylor and Cox were also extended to situations dealing with shearfree flow such as planar extensional flow. Taylor [13] concluded that his theory developed for simple shear flow could be applied to planar extensional flow by substituting the shear rate, $\dot{\gamma}$, in equation 2.9 with $\dot{\varepsilon}/2$ where $\dot{\varepsilon}$ is the elongational rate. In a similar fashion, the theory of Cox was expanded to consider the time dependent behavior of a drop exposed to planar elongational flow to yield [18]:

$$D(t) = 2We\left(\frac{19\lambda + 16}{16\lambda + 16}\right)\left(1 - e^{\left(\frac{19\lambda t}{20We\dot{\varepsilon}}\right)}\right) \qquad (2.15)$$

The validity of the equations developed for both shear and shearfree flow have been confirmed by many authors [13,19-23] with Taylor's equation generally holding true when considering viscosity ratios between 0.1 and 1.

The early theoretical and experimental work of Taylor and Cox lead to many other studies on the deformation of fluid-fluid blends. A comprehensive study on drop deformation and breakup for various viscosity ratios and interfacial tensions was performed by Rumsheidt and Mason [23]. A representation of their findings can be seen in Figure 2.2. In shear flows for viscosity ratios, $\lambda < 0.1$, it was found that drops orient 45° to the flow direction with the loss of material from the ends in what is known as tip streaming. For the viscosity ratios in the range of $0.1 < \lambda < 1.0$, the greatest droplet deformation was observed. At the critical Weber number, the droplet deformed until it formed two equal pieces while at higher Weber numbers, the droplet elongated into a thread followed by breakup. For higher viscosity ratios, $\lambda > 4$, the droplets do not break up but oriented parallel to the flow direction. In the case of elongational flows, it was found that for viscosity ratios less that 0.1, tip streaming could occur and at viscosity ratios greater than one deformation could not occur.

Another detailed evaluation of droplet deformation and breakup was undertaken by Grace [21]. In this work, systems with components exhibiting viscosity ratios from 10^{-6} to 1000 and interfacial tensions on the order of a fraction of a dyne/cm to 25 dynes/cm were investigated under both shear and planar elongational flow. The effects of viscosity ratio and flow type on the critical Weber number can easily be seen by looking at Figure 2.3. In the case of shear flows, the conditions most favorable for droplet breakup (minimum in the We_c versus viscosity ratio, λ) occurs at viscosity ratios on the order of 0.1 to 1 with the critical Weber number being on the order of 0.5-0.6. For elongational flows, it was found the critical Weber number can drop as low as 0.2 with the conditions required for droplet breakup displaying far less sensitivity with viscosity ratio. Based on these results, it appears that irrotational flows produce more effective breakup and dispersion than simple shear flow for a wider range of viscosity ratios at similar deformation rates.

Since previous work had established that there was a difference in droplet deformation behavior under simple shear and extensional flow, Bentley and Leal [24,25] investigated droplet deformation under a variety of intermediate conditions. A modified four-mill roll device, similar to the one utilized by Taylor [13], was built. This modified system allowed the speed of each roller to be controlled individually so that a wide range

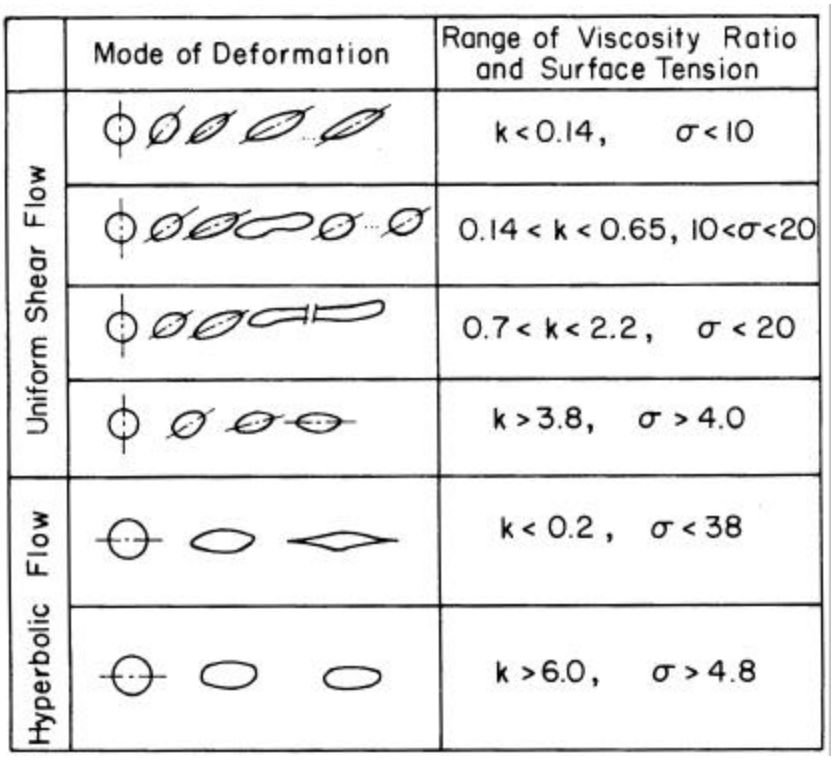

Figure 2.2: Experimentally observed modes of droplet deformation in various flow fields [23].

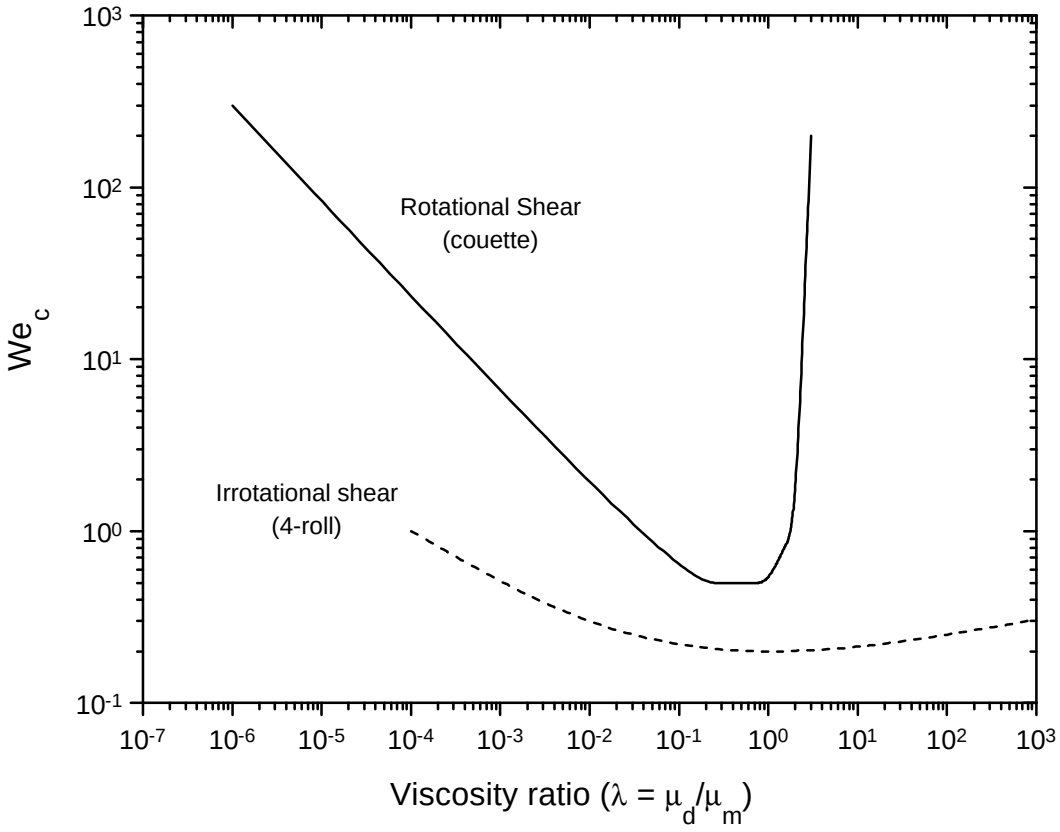

Figure 2.3: Effect of viscosity ratio on critical Weber number for Newtonian fluids in rotational (shear) and irrotational (extensional) flow fields [21].

of flow conditions could be obtained. By adjusting the speeds of the rolls, flows ranging from simple shear to hyperbolic flows as well as intermediate flows could easily be obtained. From this work it was determined that for flows dominated by a rotational component and viscosity ratios less than one ($\lambda < 1$), the Weber number for rupture decreased as the viscosity ratio increased. It was also observed for simple shear flows, that the critical Weber number achieves a minimum at a viscosity ratio of one and there exists an upper limit in the viscosity ratio beyond which no droplet rupture is possible. For flows dominated by an irrotational component, such as extensional flow, the critical value of the Weber number reached a constant value that remain unchanged as the viscosity ratio increased. For these elongational dominated flows, the droplets could be ruptured at lower Weber numbers and displayed far less sensitivity to the viscosity ratio.

The findings discussed up to this point have been limited to ideal situations where the flow field is assumed to be uniform and both the suspending and droplet fluids behave as Newtonian materials. In many polymer processing operations, such as extrusion and injection molding, the deformation seen by the material is non-uniform resulting in drastic changes in the final dispersed phase morphology. Another factor that complicates droplet deformation and dispersion in polymeric materials is the tendency of these materials to exhibit non-Newtonian behavior. Often the materials used in polymer processing operations have viscosities that are dependent on the rate of the deformation. These polymeric materials are often viscoelastic as compared to the perfectly viscous fluids that have been used in many of the fundamental studies.

In order to extend the fundamental studies of droplet deformation into areas more applicable to polymer processing, one has to consider the deformation of droplets in non-uniform shear flows such as Poiseuille flow (seen in process such as the flow through extrusion dies and injection molder nozzles). In Poiseuille flow, the velocity gradient varies with position with the shear rates being highest near the wall. For flow of Newtonian fluids in a tube, Goldsmith and Mason [26] reported that droplets had a tendency to migrate toward the tube axis. A similar study was performed by Gauthier and coworkers [27] where Newtonian droplets were suspended in a either a pseudoplastic or viscoelastic media. In the case of a pseudoplastic media, the drops located initially at the tube axis migrated toward the walls while the drops initially located at the tube wall moved toward the tube axis and attained an equilibrium position between the axis and wall. When a viscoelastic medium was used, the droplets had a tendency to migrate toward the tube center. Theoretical studies were also carried out by Chaffey et. al. [28] and Hetsroni and coworkers [29]. Chaffey showed that deformed droplets migrate away from the tube wall in the direction perpendicular to the wall. The studies by Hetsroni showed that a neutrally buoyant drop has a tendency to move toward the tube wall. As shown by the results previously listed, the uniformity of the flow field as the nature of the suspending media can have a large effect of the droplet deformation that is difficult to control for standard processing operations.

One of the other factors that complicates the understanding of droplet deformation and breakup in polymer blends is that the medium and/or droplets can display viscoelastic behavior. Newtonian fluids, such as the ones utilized by Taylor, dissipate deformation by undergoing viscous flow. Polymeric fluids often do not display this simple response and the resulting response is a combination of viscous and elastic behavior. The elasticity can be thought of as the ability of material to store deformational energy and is responsible for phenomena such as die swell and the generation of normal forces seen with many polymeric fluids. One of the studies concerned with the deformation and breakup of Newtonian and viscoelastic fluids in simple shear flow was performed by Tavgac [22]. As the Deborah number (material's characteristic time/characteristic flow time) increased for a viscoelastic fluid, the critical Weber number increased to values higher than a Newtonian fluid. At lower Deborah numbers, the critical Weber number was found to be lower than the Newtonian limit. For high viscosity ratios ($\eta_{droplet} >> \eta_{matrix}$), the matrix elasticity had a tendency to promote easier breakup of the droplets. For low viscosity ratios, it was found that the matrix elasticity has a tendency to stabilize the droplet. Similar results were obtained by Elmendorp and Maalcke [30], who determined for various Newtonian and non-Newtonian fluids that higher elasticity of the droplet led to a more stable droplet while elasticity of the matrix led to easier droplet breakup.

The effects of elasticity were considered by Van Oene [31], who developed an expression for what is known as the dynamic interfacial tension. This modified surface tension has the following form:

$$\sigma = \sigma^{o} + \frac{r}{6}[N_{2,d} - N_{2,m}] \qquad (2.16)$$

where σ^{o} is the quiescent interfacial tension between the matrix and droplet, $N_{2,d}$ and $N_{2,m}$ are the second normal stress difference of the dispersed phase and matrix phase, respectively, and r is the radius of the droplet. From this relation Van Oene predicted that when the dispersed phase has greater elasticity than the matrix, the droplet would obtain a more stable form at the same deformation rates when compared to the Newtonian case. Similar studies were performed by Milliken and Leal [32,33] who utilized a wide variety of fluids in their work ranging from purely viscous to viscoelastic fluids. In planar extensional flow, it was found that the critical Weber number versus the viscosity ratio was not sensitive to the rheological properties of the drop. In the case of shear flows, it was determined that larger Weber numbers were required to breakup viscoelastic drops and that the fluid elasticity within the drop limits the deformation of the droplet.

The effects of viscoelastic fluids on droplet dispersion and breakup in polymeric materials has been addressed by many authors [34-36]. Wu [34], studied the effects of using viscoelastic materials by blending rubber particles with both PET and nylon. From a blend compounded in a twin-screw extruder, the dispersed droplet size was determined which allowed an approximation between the critical Weber number and viscosity ratio to

be determined. For rubber particles dispersed in both nylon and PET, a V-shaped curve, centered around a viscosity ratio of one, was obtained for the critical Weber number versus the viscosity ratio. In the case of Newtonian fluids, it had been determined that it would be difficult to breakup droplets in shear flows for viscosity ratios greater than 4 or less than 0.003. Due to the viscoelastic (fluid/solid) nature of the materials and the complex flow fields utilized, droplet breakup could be achieved at viscosity ratios well above four, a feat not possible for Newtonian fluids.

Similar experiments were also performed by Ghodgaonkar and Sundararaj [35] with the blending of various viscoelastic polymers. An expression was developed that related the size of the dispersed phase to the shear rates seen during processing. This equation was developed from a force balance based on the assumption that the sum of the shear forces and matrix elasticity should be proportional to the sum of the interfacial forces and droplet elasticity. The elasticity of the various media was characterized by the first normal stress difference, N_1, which was approximated by $2G'$ where G' is the elastic or storage modulus . For certain blends, a minimum in the particle diameter was found at some critical shear rate while for other systems a minimum in the drop diameter as a function of shear rate could not be observed. It was generally found that when the elasticity ($2G'$) of the dispersed phase was high, it was difficult to deform the droplet so that droplet size remained constant at higher shear rates. A similar study was undertaken by Levitt [36], where the elasticity of the matrix and dispersed phase (as measured by the storage modulus) was related to the interfacial tension and the droplet dimensions. The second normal stress difference (N_2) was estimated to be a fraction of the first normal stress difference ($N_1 \approx 2G'$) from theory developed by Doi and Edwards [37]. From these results, it was determined that as the elasticity between the drop and matrix increased, the droplet became more flattened with the droplet characteristic dimension being directly proportional to the second normal stress difference.

2.4 Capillary Instabilities

The deformation of droplets suspended in various media has been studied under a variety of conditions. The effects of the viscosity, interfacial tension, elasticity, and flow field have been analyzed for a wide range of well controlled conditions. Another aspect of droplet deformation that is important when considering the generation of composite systems is the stability of the deformed droplets. When trying to generate self-reinforcing composite blends, it is desirable to create a reinforcing morphology that has the greatest aspect ratio in order to obtain the optimum mechanical properties. When these highly elongated reinforcing domains are generated due to flow, they must be frozen in quickly before they break up into droplets in an effort to lower the interfacial area. The relationship between this break-up time and the solidification time becomes another important consideration when trying to generate these self reinforced composites.

It had been observed that fluid threads can possess periodic distortions that become amplified resulting in the breakup of the fluid element. The formation of these surface distortions was first addressed by Lord Rayleigh when considering the breakup of water jets in air [38]. In his analysis, Raleigh ignored the effects of viscosity and considered this breakup to be a surface driven phenomena.

An extension of Rayleigh's work was undertaken by Tomotika [39] in which the behavior of a Newtonian thread imbedded in a Newtonian matrix was addressed. Tomotika considered the stability of a thread exposed to small axisymmetric sinusoidal distortions as shown in Figure 2.4 :

$$R(z) = \overline{R} + \xi \sin\left(\frac{2\pi z}{\Lambda}\right) \qquad (2.17)$$

where: $\overline{R}$ is the average thread radius: $\left(R_o^2 - \xi^2/2\right)^{1/2}$

R_o is the initial thread radius

ξ is the distortion amplitude

Λ is the distortion wavelength

z is the coordinate along the thread

From experimental observations, it was determined that when the wavelength of the distortion (Λ) becomes larger than the circumference of the thread ($2\pi R_o$), the interfacial area decreases as the distortion amplitude (ξ) increases. From Tomotika's theory, when the condition of $\Lambda > 2\pi R_o$ is met, the distortion amplitude would increase exponentially with time following the relationship:

$$\xi = \xi_o e^{(qt)} \qquad (2.18)$$

with the growth rate: $$q = \frac{\sigma}{2\eta_m R_o}\Omega(\xi,\lambda) \qquad (2.19)$$

where σ is the interfacial tension, λ is the viscosity ratio, R_o is the thread radius, and the matrix viscosity is η_m. Tomotika determined that the function for the growth rate of the disturbance, $\Omega(\xi,\lambda)$, showed a maximum for a certain wavelength and displayed a strong dependence on the viscosity ratio. From this it was determined that the distortion wavelength (Λ), where the function Ω showed a maximum, was expected to induce thread breakup. The conditions required for breakup of a thread at this dominant wavelength (Λ_m) is often characterized by the dominant wavenumber, $\chi_m = 2\pi R_o/\Lambda_m$, and the dominant growth rate, Ω_m. Figure 2.5 shows the dominant wave number (χ_m) and the corresponding maximum growth rate (Ω_m) as a function of viscosity ratio between the thread and surrounding media. As can be seen in the figure, the maximum dominant

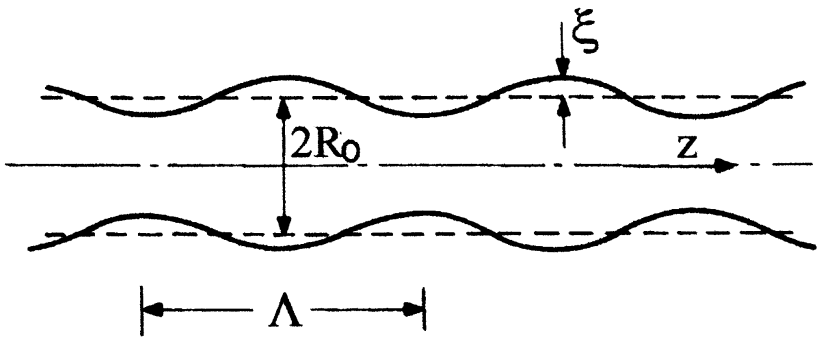

Figure 2.4: Sinusoidal disturbance on a liquid cylinder [40].

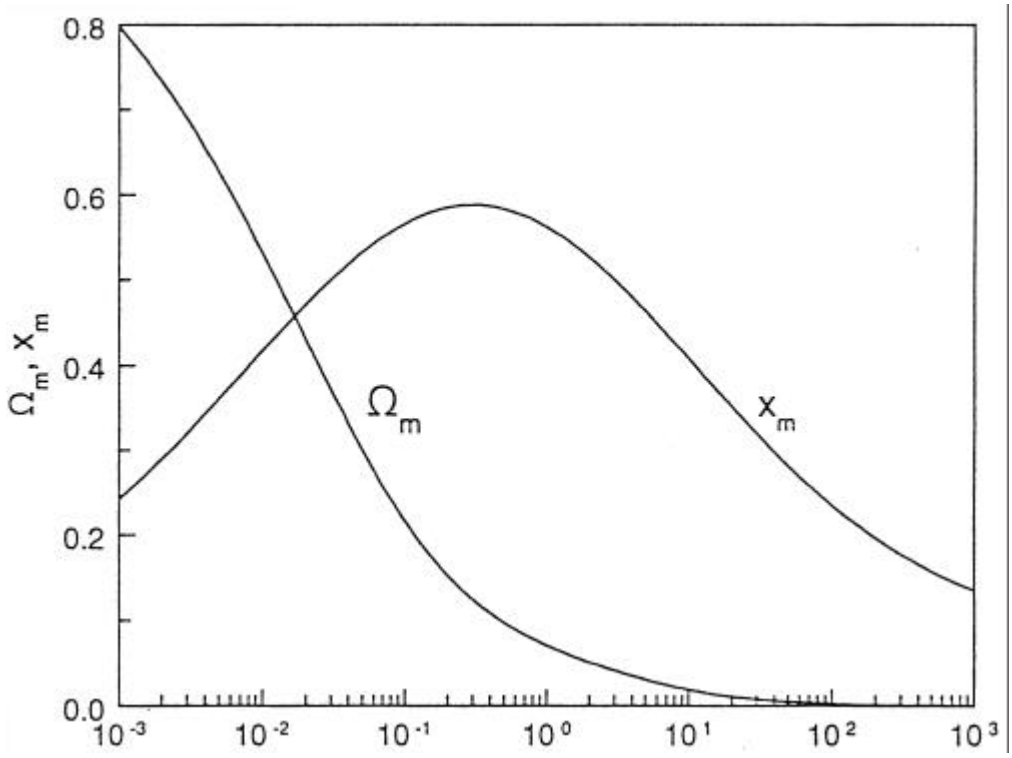

Figure 2.5: Dominant wave number (χ_m) and growth function (Ω_m) as a function of viscosity ratio (λ) [40].

wavenumber occurs between the viscosity ratios of 0.1 and 1.0. At these conditions thread breakup is more readily observed for either larger diameter threads or smaller wavelength disturbances.

From the basic theories developed on capillary instabilities, the time required for the distortions to reach the conditions leading to breakup could easily be determined. The breakup of a thread would be complete when the amplitude equals the average radius, i.e. $\bar{R} = \xi$, which would occur when $\xi = 0.82\ R_o$. Substituting these conditions into equation 2.18, yields the derived time to breakup (t_b) to be:

$$t_b = \frac{1}{q} \ln\left(\frac{0.82 R_o}{\xi_o} \right) \qquad (2.20)$$

From this it can be pointed out that when trying to process self reinforcing composite systems, the conditions utilized must allow for the proper deformation of the reinforcing phase as well allow the preservation of the desired morphology before it is destroyed by these capillary instabilities.

Tomotika's initial work was further expanded by Elmendorp [40], who studied the breakup of both Newtonian and viscoelastic threads suspended in a Newtonian matrix. In the case of a Newtonian fluid suspended in the Newtonian matrix, the experimental data matched Tomotiko's theory with the time to breakup decreasing with increasing magnitude of the initial distortions. In the case of a viscoelastic thread suspended in a Newtonian matrix, the time dependence of the relative distortion showed deviation from Tomotiko's theory. In the initial stages of the thread thinning, the process was predicted well by Tomotiko's theory. As time increased, the distortions grew at faster rate than the predicted value and then eventually at slower rate. These deviations from theory were attributed to factors such as shear thinning of the fluid with the eventual strain hardening of the thread at high degrees of elongation. Threads consisting of materials that displayed a yield stress also showed deviation from Tomotiko's theory, and this was attributed to a correlation between the yield stress and the pressure difference within the thread. It was determined that the pressure difference within the thread must be greater than the yield stress for the droplet to breakup. When Elmendorp utilized polymer melts, the deformation behavior generally followed Tomotiko's theory, and this was attributed to the observed Newtonian viscosity for the low shear rates that were utilized during the experiments.

In a similar study, Chin and Han [41] looked at the stability of deformed droplets in non-steady shear flow. By using Poiseuille flow, long pointed ellipsoids or threads could be created that formed droplets of different configurations depending on conditions such as the initial drop size, type of fluids, and the type of flow. A pertubation analysis was used to analyze the conditions under which the elongated threads would be the most

stable. The analysis took into account the viscosity and elasticity differences between the phases. The elasticity of the phases was characterized by using relaxation times obtained from fits for a linear Maxwell model. For long wavelength disturbances, it was found that matrix viscosity and elasticity had a tendency to enhance the thread stability while higher interfacial tension led to easier breakup. When the analysis was extended to short wave disturbances, it was found that the growth rate of the disturbances increased with an increase in elasticity (both matrix & droplet) and an increase in interfacial tension. It was found that greater matrix elasticity resulted in smaller broken drops while greater droplet elasticity had a tendency to produce large droplets. The effects of viscosity ratio were also analyzed with lower viscosity ratios showing the maximum growth rate of disturbances occurred at long wavelengths resulting in the formation large droplets after breakup of the thread. As the viscosity ratio increased, the growth rate of disturbances occurred at shorter wavelengths resulting in smaller droplets after breakup.

As shown in the previous sections, the deformation of a suspended droplet is dependent on many variables such as viscosity, elasticity, and interfacial tension. When manufacturing in-situ composites, droplet deformation and breakup plays a major role in two main aspects of the processing. The first area where droplet deformation and breakup plays an important role is the dispersion of the materials within the screw of an extruder (single or twin). The other area where droplet deformation and break up is important is in the generation of the reinforcing morphology through processes such as strand or film extrusion or injection molding.

From the work performed on droplet deformation, it becomes evident that the rheological behavior of the blend constituents is important in controlling the formation of the reinforcing phase morphology. In the next section, a review of the rheological behavior of inorganic glasses will be presented. As will be indicated in the section, the literature available concerning the rheology of neat melt processable glasses as well glass/thermoplastic blends is very limited. In order to help contrast the behavior of these novel organic/inorganic fluid blends, a brief discussion of the rheological behavior of the polymer-polymer blends will be discussed as well as the rheological response of solid filled systems will be presented.

2.5 Rheology of Inorganic Glasses

The rheological response of phosphate glasses will be an important controlling factor in the final morphology obtained for these novel thermoplastic/glass composites. As with polymeric materials, an understanding of the response of the glasses to deformation at various temperatures is important in processing these materials. In this section, various aspects of the rheology of various types of glasses will be addressed. Due to the lack of available rheological data on phosphate glasses, the response of silica

based glasses will be briefly discussed under the assumption that other inorganic glasses should show similar behavior.

Because viscosity plays a large role in many commercial glass manufacturing processes, it would be useful to point out some of the common viscosity reference points used when considering inorganic glasses. There are four common references points which include the working point, softening point, annealing point, and strain point [42]. The working point is the temperature where the large scale deformation used in processing occurs and corresponds to a viscosity of around 1000 Pa·s. The softening point corresponds to a temperature where the viscosity has value of $10^{6.65}$ Pa·s and is generally regarded as the minimum viscosity where the glass will not deform under its own weight. The annealing point and strain points are utilized when considering post processing operations to relieve stresses generated in the glass during forming steps. The annealing point corresponds to a viscosity of 10^{12} Pa·s and can be thought of the point where the glass would release the majority of the residual stress within a matter of minutes. At the strain point (viscosity = $10^{13.5}$ Pa·s), the release of the stress occurs over a time period of hours. When using inorganic glasses, knowing the conditions where these processing points occur is important in obtaining products with desired properties. For example, many glass manufacturing processes involve rapid temperature changes that have a tendency to lock in excessive stress within the glass. These residual stresses can cause the glass to fracture easily when external stress is applied or display nonuniform properties such as refractive index or thermal expansion coefficient. By exposing the glass to temperatures in the range of the annealing and strain point, the glass properties can be homogenized, resulting in a material with more desirable properties. Because the viscosity is a strong function of temperature, understanding the response of these materials to temperature is paramount in achieving the desired processing behavior.

Many of the glasses used in manufacturing processes are based on the Zachariasen glass forming oxides that can show a wide range of responses with temperature. The four most common glass forming oxides are composed of SiO_2, GeO_2, P_2O_5, and B_2O_3 [42]. Due to the different connectivity of these various oxides, the sensitivity of the glass viscosity to temperature can be quite varied. The variation in viscosity with temperature for the various glass forming oxides is shown in Figure 2.6 Also included in Table 2.1 are the activation energies for these common glass forming oxides at temperatures where the materials are fluid. In the case of SiO_2 and GeO_2, the silica and germanium are fully connected in a tetrahedral network making it difficult for the material to flow except at elevated temperatures. Silica based glasses are commonly used as a reinforcing material for thermoplastic resins and the material behaves as a solid at the temperatures commonly used to process thermoplastic resins (i.e. less than 400°C).

As shown by Figure 2.6 and Table 2.1, glasses based on P_2O_5 and B_2O_3 are fluid at lower temperatures (< 600°C) making these materials possible candidates for the manufacture of in situ composite blends. In the case of boron and phosphorous based

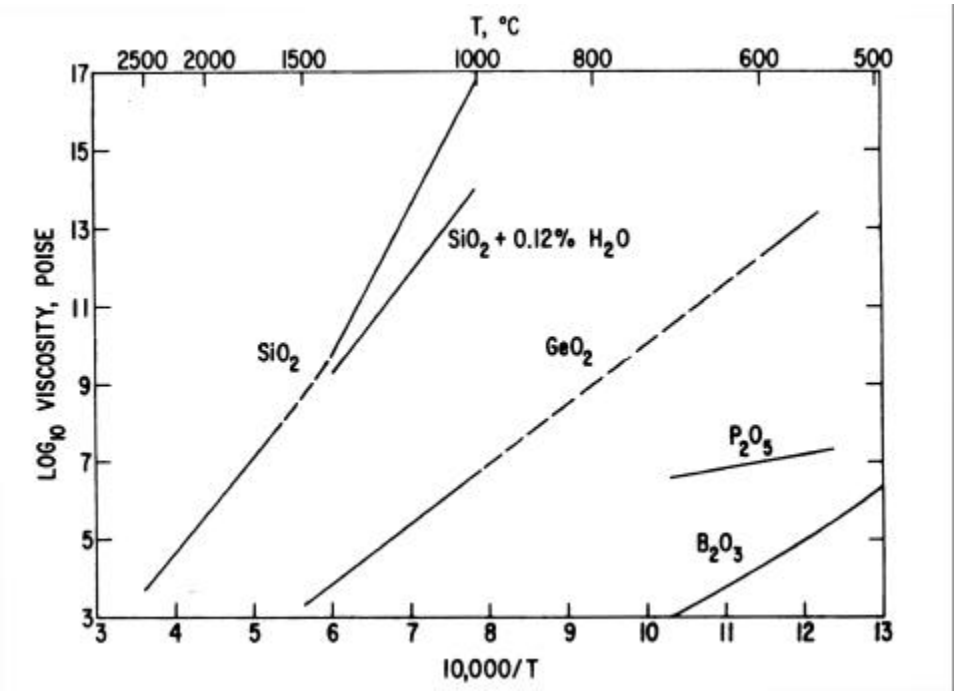

Figure 2.6: Variation of viscosity with temperature for simple glass-forming oxides [43].

Table 2.1: Activation energies for viscous flow for various simple glass forming oxides [42].

Glass	Activation Energy (kcal/mol)	Temperature Range (°C)
Vitreous SiO_2	170 123	1,100-1,400 1,600-2,500
Vitreous GeO_2	75	540-1,500
Vitreous P_2O_5	41.5	545-655
Vitreous B_2O_3	83-12	26-1300

glasses, the connections are made only at three corners making the materials far more fluid than silica based glasses. The activation energy for viscous flow for these various inorganic glasses generally range from 50-200 kcal/mol, showing that the viscosity of these materials is extremely sensitive to changes in temperature. In contrast, higher melting temperature thermoplastics such as polyphenylene sulfide (PPS) and polyetheretherketone (PEEK) exhibit activation energies only in the range of 12.6 kcal/mol and 9.9 kcal/mol, respectively [44]. When trying to process melt processable glasses with a thermoplastic matrix, the large variations in activation energies could lead to some processing difficulties. As blends consisting of thermoplastics and melt processable glass are cooled while deformation is being applied (mold filling or fiber spinning), the viscosity of the glass could rise to levels much greater than the thermoplastics, resulting in unfavorable viscosity ratios. The rapid formation of these unfavorable viscosity ratios could limit the morphologies and properties that could be generated during certain processing steps.

2.5.1 Rheology of Silica Glasses

As shown in the previous section, the viscosity of inorganic glasses can easily be changed by varying the temperature. One possible method of changing the viscosity of a glass is to vary the rate and type of deformation applied to the material. The response of the glass to deformation will be one of the important factors in determining how the glass will disperse and elongate when trying to generate self-reinforcing composites. Because limited data is available on the rheological response of low melting phosphate glasses, the rheology of silica glasses will be presented briefly in anticipation that phosphate glasses should display similar behavior.

The flow behavior of silica glasses has been investigated by a large number of researchers using a wide variety of techniques [45-49]. One of the most significant difficulties associated with testing these materials is the extremely high temperatures required. Methods such as the uniaxial stretching of glass fibers under a constant load or constant elongational strain rate have often been utilized. The behavior of these glasses has also been examined using both small amplitude oscillatory and steady shear tests with cone and plate fixtures attached to custom built instruments. Through the use of a wide variety of techniques, the response of silica based glasses have been investigated over a wide range of temperatures and deformation rates.

One of the most commonly used techniques to quantify the rheological response of an inorganic glass involves the uniaxial deformation of glass fibers. Simmon [46] utilized this method to examine the deformation of silica glass fibers at elevated temperatures for various elongational rates. At low deformation rates, the glass exhibited Newtonian behavior by displaying a linear relationship between the steady-state stress and the applied strain rate. At higher deformation rates, the steady state stress dropped below the

Newtonian value indicating pseudoplastic behavior at the higher strain rates. By also examining the transient response of the glasses for a variety of strain rates and temperatures, the non-linear behavior of the glasses was also established. At the lower strain rates, the apparent viscosity slowly rose to the Newtonian value indicating the presence of shear relaxation within the melt. As the strain rate was increased, the apparent viscosity approached steady-state over longer period of times with the steady-state values being lower than the Newtonian values. It was also observed that a short-time overshoot of the steady-state value existed during the shear relaxation period. The lowering of the apparent viscosity with increasing deformation rate was attributed to the breakdown of the glass structure at higher deformation rates resulting in faster relaxation of the stresses. By raising the temperature of the glass, the onset of this non-linear behavior was observed for higher deformation rates. From this it was determined that there was a limit on the stress that could be applied to the glass before the material would undergo catastrophic failure. At stresses below this limit, the material is able to undergo plastic deformation as the glass structure rearranges itself to accommodate the stress. At higher stresses, the material can initially undergo plastic flow but as the structure changes to adapt to the stressed condition, the glass undergoes fracture. In a similar study performed by Li and Uhlmann [48], the silica glass exhibited Newtonian behavior at low stress levels with viscosity decreasing with increasing stress above some critical stress. The critical stress level for 10% deviation from Newtonian behavior was found to be generally independent of temperature with the viscosity showing decreases on the order of 1 to 2 orders of magnitude for the shear thinning region.

Besides the uniaxial stretching of fibers, methods commonly used for polymeric melts such as torsional rheometry under both steady shear and small amplitude oscillatory strains have been used to study the behavior of high melting glasses. Simmons [47] examined the steady shear behavior of silica glasses under a variety of conditions and compared this to previous data obtained from the stretching of glass fibers [46]. Stress growth experiments were performed for shear rates ranging from 1.6 - 80 hertz for temperatures in the range of 710°C to 810°C. At low shear rates, the stress increased with time to a constant Newtonian value that remained proportional to the strain rate. At higher shear rates, the stress exhibited an overshoot that was still only half of the corresponding Newtonian stress. It was demonstrated that the glass was unable to sustain large stresses at the higher strain rates, similar to the results obtained from the fiber stretching studies. An example of this non-Newtonian behavior for a wide range of temperatures for the various techniques can readily be seen in Figure 2.7. By combining the results from the cone and plate measurements and fiber tensile testing, it was determined that the glass structure begins to break down in the shear thinning region when the applied stress exceeds some limit resulting in the catastrophic failure of the glass under rapidly applied loads.

The correlation between tensile viscosity data and dynamic oscillatory measurements on a Rhyolite melt was considered by Webb [49]. Dynamic oscillatory

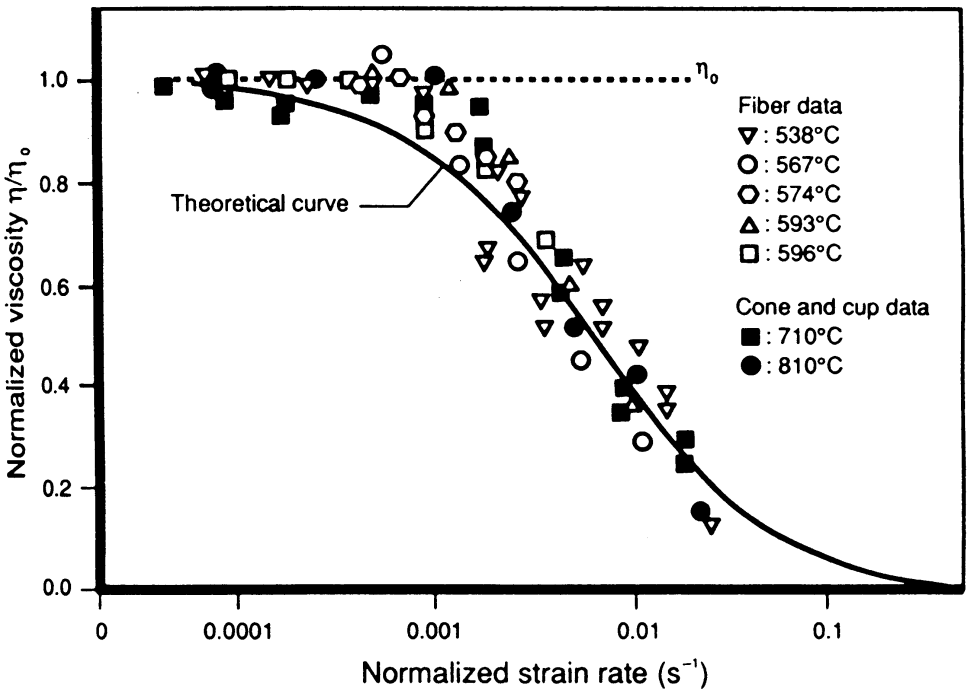

Figure 2.7: Non-Newtonian response for silica glasses for varying conditions [47].

experiments were performed in a temperature range of 700-900°C for angular frequencies ranging from 0.03-63 radians/sec. The glass displayed non-Newtonian behavior at the higher frequencies, with the complex viscosity displaying values in the range of 5 orders of magnitude lower than the Newtonian viscosity. Webb determined that the shear relaxation that occurs at the higher viscosities can best be described by a distribution of relaxation times with the cutoff occurring at relaxation times slightly longer than the Maxwell relaxation time. It was also determined that the regions where silica glasses can behave as either a relaxed, unrelaxed, or viscoelastic liquid are dependent on the viscosity and the relaxation time. For high viscosity melts, a range of relaxation times should exist that will eventually collapse to one relaxation time for lower viscosities. This more theoretical work offered support to the observed non-Newtonian behavior of glass melts.

2.5.2 Rheology of Phosphate Glasses

The bulk of the studies involving the rheological behavior of glasses has focused on silica glasses. These glasses exhibit viscosities that are too high for the generation of self-reinforcing polymeric composite systems through the deformation of the glass phase. In order for these glasses to achieve viscosities in the ranges where deformation of the glass may be possible, temperatures well above the normal processing ranges of polymers (> 400°C) would have to be utilized resulting in degradation of the polymeric matrix. Glasses that may possess viscosities in the desired range (< 100,000 Pa·s) at temperatures less than 400°C, could include materials based on phosphorous oxides. These materials appear to offer viscosities that are comparable to polymeric materials at temperatures suitable for processing thermoplastics.

The rheology of phosphate glasses exhibiting viscosities suitable for co-processing with thermoplastics has only been studied on a limited basis. One of the first studies on the rheology of these novel glasses was performed by Ray and coworkers [50,51]. The steady shear rheological behavior of low T_g glasses consisting of lead phosphate and zinc phosphate was investigated. Using a cone and plate fixture on a torsional rheometer, the viscosity of various phosphate glasses was determined for shear rates in the range of 1 to 10 hertz. The zero shear viscosity for the various glass melts was determined for a wide range of temperatures in order to ascertain the conditions required for processing the glasses with thermoplastics. In order to obtain viscosities in the range of 2500 Pa·s, the glasses had to be heated to temperatures ranging from 275-400°C. The activation energy for viscous flow for both glasses was determined to be approximately 45 kcal/mol which corresponds to the value of 41.5 kcal/mol for vitreous phosphate as shown in Table 2.1.

A similar study was also performed on zinc phosphate glasses of varying composition [51]. In this study, the conditions used to manufacture the glass were varied in an effort to gauge the effects on the ultimate properties of the glass. The refining or annealing time of the molten glass was varied in order to gauge the effects of residual

water in the glass. As the glass was annealed, the water content decreased resulting in a higher crosslink density (fraction of triply connected phosphorous atoms/water content) within the glass. The larger number of crosslinks increased the rigidity of the glass and resulted in substantially higher viscosities at temperatures 100°C above the glass T_g. As the crosslink density increased, the viscosity increased but the activation energy for viscous flow remained fairly constant at 49 kcal/mol. By controlling the manufacturing conditions, it was determined that it was possible to modify the rheological behavior of these novel glasses to facilitate their processing.

The initial work performed by Ray and co-workers [50,51] was rather cursory and involved phosphate glasses that displayed limited chemical durability. The rheology of more suitable phosphate glasses for thermoplastic composites has most recently been investigated by Sammler et al.[52]. Through the use of small amplitude oscillatory experiments, the rheological behavior of zinc alkali phosphate glasses was investigated. A nondurable glass (degraded by hot water) possessing a glass transition temperature of approximately 272°C and durable glass with a T_g of approximately 331°C were investigated. At the lower temperatures (300-360°C), the nondurable glass complex viscosity displayed non-Newtonian behavior at higher frequencies (5-100 rad/sec) very similar to the responses seen for silica glasses [45-49]. At temperatures of 370°C and higher, the glass displayed Newtonian behavior with the complex viscosity at levels acceptable for processing with thermoplastics ($|\eta^*| < 10{,}000$ Pa·s). The durable glass complex viscosity displayed a dependence on frequency over the entire temperature range investigated (330 - 420°C) with the viscosity never falling below 2×10^5 Pa·s. The activation energy for these glasses were found to be higher than the values reported by Ray [50,51] and ranged from 67-86 kcal/mol.

The melt stability of these zinc alkali phosphate glasses was also investigated under a wide variety conditions. The glasses were subjected to continuous sinusoidal shear flows for a variety of frequencies and applied strains. In the case of the nondurable glass, the sample was exposed to strains ranging from 0.35% to 30% at a temperature of 400°C. For all conditions considered, the viscosity increased with time with the higher strains causing a more rapid rise in viscosity. The increase in viscosity was attributed to the shear-accelerated crystallization of the melt. In the case of the durable glass, as the temperature was increased in an effort to lower the viscosity, the viscosity began to rise offering no improvement in the glass processability. These results just show some of the complications that may arise when processing these glasses. In an effort to lower the glass viscosity by raising the temperature, conditions may be created that accelerate the crystallization of the glass which could cause numerous processing difficulties.

In summary, the effects of deformation and temperature on the rheological behavior of melt processable glasses has only been investigated on a limited basis. As with silica glasses, phosphate glasses appear to exhibit non-Newtonian behavior at temperatures close to the glass transition temperature but at higher temperatures, the

glasses begin to display Newtonian behavior. The zero shear viscosities for phosphate glasses show rapid changes with temperature displaying activation energies for flow on the range of 45 - 90 kcal/mol. Depending on temperature and amount of applied deformation, these glasses can undergo a phase separation (crystallization) resulting in rapid rises in viscosity which could lead to processing complications, such as plugging of equipment. In conclusion, the rheology of these neat phosphate glasses and their role in the formation of the composite morphology is a complex area open to much research.

2.6 Rheology of Immiscible Fluid Blends

When two immiscible materials are brought into contact to form a mixture, a wide variety of rheological responses can be obtained. The blends can display viscosities that are higher, lower, or between the viscosities of the neat substituents. The response of these blends can vary greatly depending on the type and rate of deformation applied. Some of the factors that can control the rheology of these blend systems include the shape and size of the fluid domains, the viscosity of the phases, and the interfacial tension between the phases. Self-reinforcing composite systems, where all the phases are fluid during processing, may exhibit rheological behavior that is noticeably different than conventional solid reinforced composite systems. In the next section, a general survey of the rheological response of fluid-fluid polymeric blends will be presented.

2.6.1 Rheology of Polymer-Polymer Blends

The rheological behavior of polymer blends can show many deviations from the rheological response of the neat substituents. The addition of a second phase can serve to increase or lower the viscosity depending of factors such as concentration, temperature, and applied deformation. Surface properties such as the interfacial tension can also have a marked effect on the response of these blend systems.

When examining the rheological response of blends it is important to consider the basis of comparison for the behavior of these materials. In immiscible blends, the materials usually exist as discrete phases where the shear rate would be discontinuous across the interface because of the differences in the materials' viscosity. However, the shear stress at the interface between the phases should be continuous, making comparisons of blends based on the imposed stress more meaningful [12].

The response of immiscible blends, in terms of the observed viscosity, can be quite varied and depend on a wide range of factors such as the applied deformation, concentration, the phase morphology, and temperature. The viscosity of immiscible blends of varying compositions at some applied stress, generally display one of four blend viscosity curves as shown in Figure 2.8. The large range of responses can be attributed

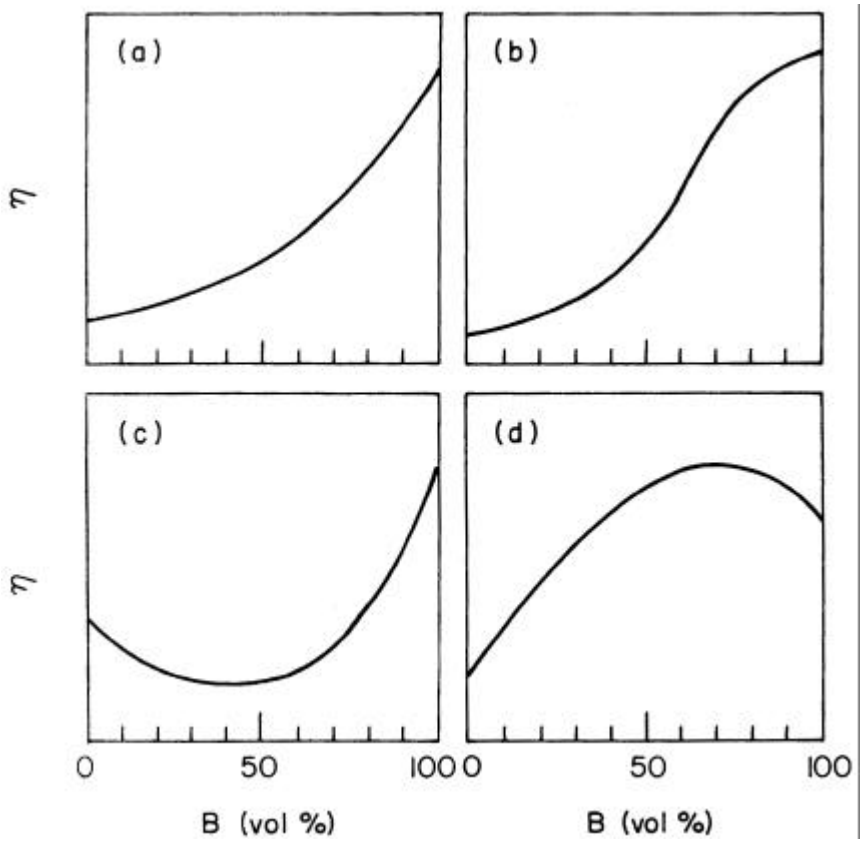

Figure 2.8: Experimentally observed rheological responses for various fluid-fluid blends of varying concentration [12]

a) Viscosity monotonically increases with composition
b) Viscosity exhibits an S-shaped curve with varying composition
c) Viscosity displays a relative minima with composition (- Deviation)
d) Viscosity displays a relative maxima with composition (+ Deviation)

mainly to the morphological state of the blend, which depends strongly on the blending ratio, the applied deformation, and thermal histories [12]. The monotonically increasing viscosity curve seen in Figure 2.8.a is generally found for blends containing dispersed droplets where there is little interaction between the phases. Often the size of the dispersed droplets can have a marked effect on the viscosity of the blend. Small droplets undergo less deformation than large droplets when exposed to an imposed stress, resulting in a higher viscosity for blends containing smaller droplets. The S-shaped curve shown in Figure 2.8.b is indicative of blends where there is phase inversion at some concentration with little interaction between the phases. For most polymer blends, the rheological responses displayed by Figures 2.8.c and 2.8.d is indicative of what is commonly observed. In the case of curve 2.8.c, the minima in the viscosity can be attributed to the deformation of one of the phases into sufficiently elongated threadlike fibrils that align in the flow direction thus reducing the resistance to flow. The behavior seen in Figure 2.8.d can be observed in systems where there may be strong interactions between droplets at low shear stresses or when the blend possesses an interlocked morphology resulting in a greater resistance to flow. The blend viscosity curves discussed above reveal the wide range of behavior that can be seen with immiscible polymer blends [12].

The representative composition blend viscosity curves presented previously have been observed for a wide range of polymeric blends that contained polystyrene (PS) as one of the components. Van Oene [53] studied the rheological behavior of blends consisting of polystyrene (PS) and polyethylene (PE) for a variety of temperatures and applied stresses. At a temperature of 170°C, the viscosity of the blend fell between the values of the neat constituents for all the stresses considered displaying a monotonic change in viscosity with composition similar to Figure 2.8.a. When the temperature of the blend was increased to 210 °C, a minimum in the viscosity versus composition curve was obtained with the viscosity at certain compositions falling below the values of the neat substituents. A more extensive study was performed by Han and Kim [54] who considered polystyrene blended with high density polyethylene (HDPE). For a given applied shear stress, the viscosity of the blends was seen to go through both a minimum and maximum as the composition was varied for a range of temperatures and applied stresses (Figure 2.9). For a blend containing 75 wt% polyethylene, the viscosity of the blend showed a maximum where it was difficult to distinguish between the separate phases due to the formation of an interlocking morphology. At a lower composition ratio (< 50 wt% PE), the blend consisted of dispersed droplets that had a tendency to lower the viscosity of the blend. Han and coworkers [55] also considered polystyrene blended with polymethylmethacrylate (PMMA). At low shear stresses, the viscosity of the blends decreased monotonically with increasing concentration of the lower viscosity PS. The minimum viscosity for the blend was found to occur at a concentration of 75 wt% PS where the formation of dispersed fibrils was observed.

Besides viscosity, immiscible polymer blends can display a wide variety of responses in terms of the elastic behavior. Often the effects on the elastic behavior of

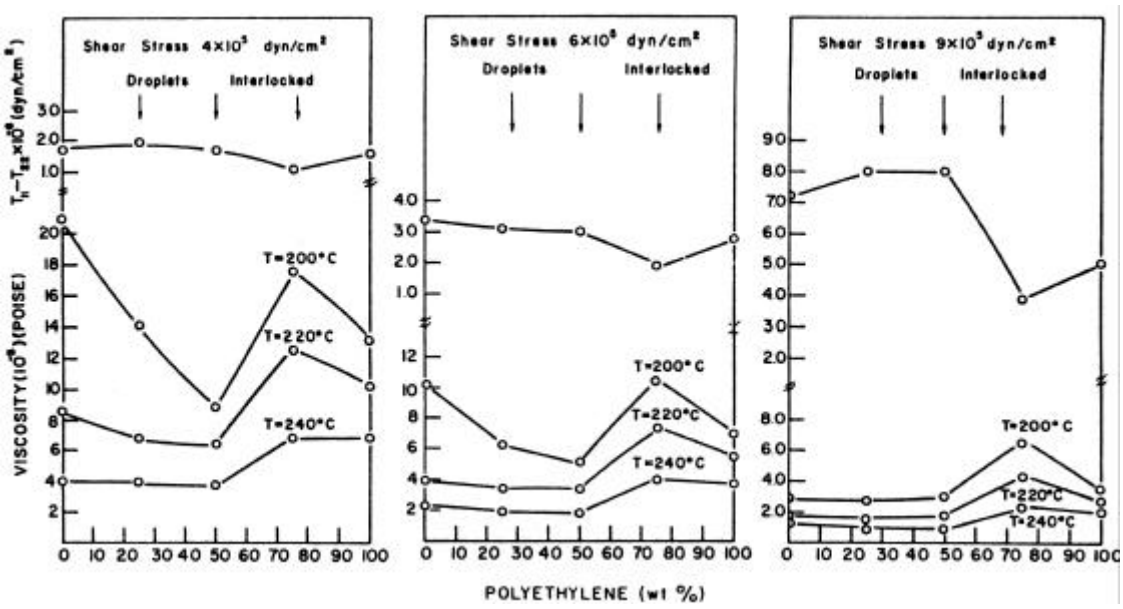

Figure 2.9: Effects of temperature and composition on the viscosity and normal stress for polystyrene/high density polyethylene blends [54].

these blends can be quantified in terms of the first normal stress difference ($\tau_{11} - \tau_{22}$), the recoverable shear strain (S_R), and the shear compliance (J_e). As with the viscosity, the first normal stress difference can often display a relative maxima or minima depending on the test conditions utilized. For numerous immiscible blends [53-55], it has been observed that at the conditions where the normal stress displays a maximum or minimum, the viscosity often displays the opposite trend. An example of this can be seen in Figure 2.8, where the viscosity of a polystyrene/high density polyethylene blend showed a maximum, the normal stress displayed a minimum. In the case of a polystyrene / polymethylmethacralate blends [55] and polystyrene/styrene-methacrylic acid copolymer blends [56], the trends in the viscosity were almost the opposite of the trends seen in the normal stress. At the conditions where a maximum in the viscosity was seen, the normal stress displayed a minimum. A morphology consisting of dispersed viscoelastic drops often display normal stresses that are greater than what are observed with a morphology consisting of interlocked phases. The exact effects of factors such as the interfacial tension and phase morphology on the elastic response of immiscible blends is an area open to much study.

2.6.2 Rheology of Polymer/Phosphate Glass Blends

Self-reinforcing blends containing materials such as melt processable glasses could offer some advantages in terms of rheological behavior when compared to standard solid filled composite materials. As with polymer-polymer blends, a wide range of rheological responses could be observed depending on factors such as concentration, morphology, interfacial interactions, and applied deformation. Since both materials are fluid during processing, the addition of the reinforcing phase may lead to more favorable viscous and elastic behavior when compared to solid filled systems. Properties of the glass such as the Newtonian viscosity, high surface tension, and large activation energy for flow could create blends that possess many unique properties when compared to other common reinforced materials.

The rheological response of thermoplastics reinforced with melt processable glasses has only been addressed on a very limited basis. The viscosity of phosphate glass reinforced thermoplastics has mainly been investigated through the use of capillary rheometry [57,58]. Due to the fluid nature of the glass, blends containing up to 80 wt% glass often show only limited increases in viscosity when compared to the neat resins. An example representative of the viscosity of phosphate glass filled blends is shown in Figure 2.10. Due to the lower viscosity of phosphate glass filled systems, higher glass loadings could be utilized in common processing equipment as compared to the conventional solid filled systems. The fluidity of the glass should minimize wear on processing equipment and allow more flexibility in regards to processing.

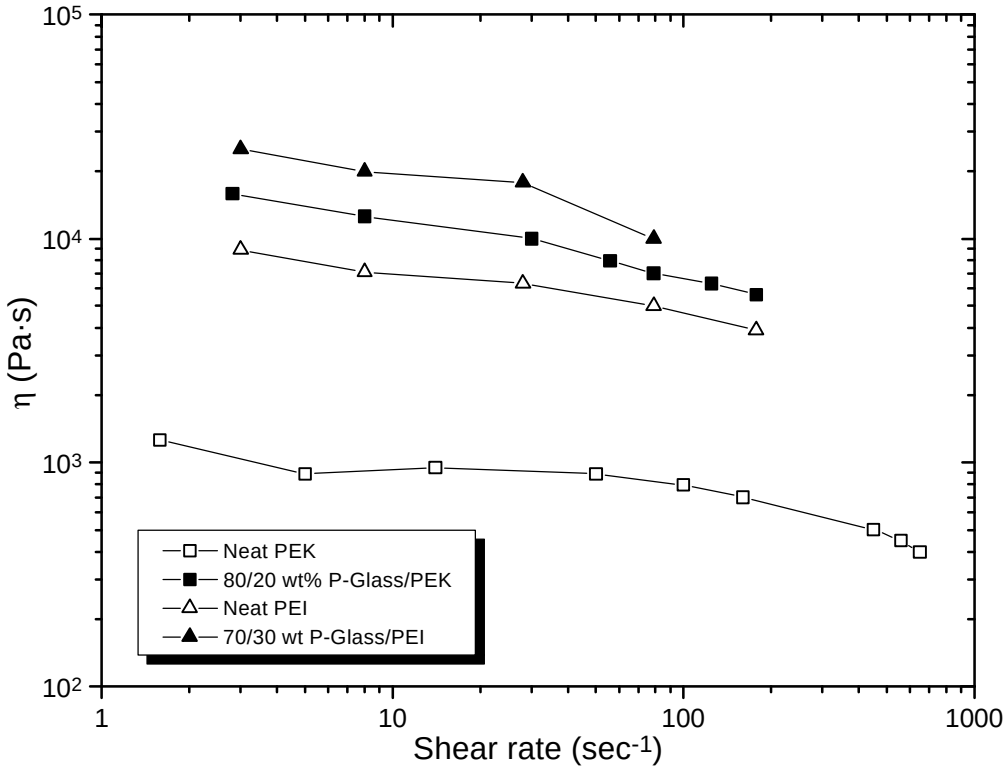

Figure 2.10: The effects of the addition of phosphate glass on the viscosity of various thermoplastics [57].

The rheological behavior of these novel blends has also been investigated through the use of small amplitude oscillatory experiments. Otaigbe et. al. [59] investigated the behavior of polyetheretherketone (PEEK) and a thermotropic liquid crystalline polymer (TLCP) filled with a phosphate glass. For blends containing 55 vol% glass, the effects of thermal history and deformation were investigated for a variety of conditions. Dynamic frequency sweeps were performed at low strains and the response of the various blends related back to factors such as interaction between the glass and polymer and the morphology of the glass. In order to understand the processing behavior of these materials, the thermal stability and solidification behavior of the blends was also investigated. The thermal stability was investigated by monitoring the evolution of the viscosity with time for a variety of temperatures. The viscosity of the PEEK blend remained constant for extended periods of time at 400°C while the TLCP blend showed an increase in the viscosity that was attributed to factors such as the crystallization or transesterification of the TLCP and chemical interactions between the glass and TLCP. The solidification of the blends was also investigated in order to ascertain the behavior of these blends during processes such as mold filling during injection molding. For an initial melt temperature of 400°C and a cooling rate of 10°C, the TLCP blend displayed solidification behavior at temperature of approximately 370°C while the PEEK blend did not show a rapid increase in viscosity until 290°C. These tests evaluating the solidification behavior of the blends were perceived as a way to determine certain key processing conditions such as the mold temperature, mold filling times, or mold holding times. Even though an understanding of the rheological behavior of these novel blends is paramount in processing these materials, a rather limited amount of work has performed in this area.

In the case of composite systems reinforced with melt processable materials such as phosphate glasses or thermotropic liquid crystalline polymers, there exists the potential for the display of a wide range of behavior. At higher temperatures the reinforcing phase can become fluid, resulting in blends that could display behavior similar to a fluid polymer-polymer mixture. As the temperature is decreased near the transition temperature of the glass, the reinforcing phase could behave as a solid resulting in behavior very similar to standard solid filled systems. In the next section, the rheological behavior of solid filled polymers will be discussed to help offer a basis of comparison of the rheological differences that may be seen with the various blends.

2.7 Rheology of Solid filled Polymers

The effects of the addition of a solid phase to a polymeric melt is an area that has received considerable attention. Commonly, solid material is added to polymers to enhance the properties and/or lower the cost of the blend. Solid additives can generally be grouped into two broad categories: particulates and fibers. Particulates are generally of small size and aspect ratio (length/diameter) and include materials such as talc, calcium carbonate, titanium dioxide, and carbon black. Fibers are generally of a larger size

(diameters of 10-13 microns) and often possess higher aspect ratios on the order of 50-100. The addition of these solid materials can often have a profound effect on both the viscous and elastic behavior of a polymeric melt [60].

2.7.1 Viscous Response of Solid filled Polymer melts

The addition of solid particulates can produce a wide range of changes in the shear behavior of a polymeric melt. The rheological response of these systems can show a dependence on a large range of variables including concentration, particle size and shape, surface treatments, and the rate of deformation.

The effects that particulates and fibers have on the viscosity of filled polymer melts have been widely studied [60-72]. Typically, it has been found that the addition of particles or fibers increases the shear viscosity of the mixture over the neat resin at an equivalent shear rate or stress. Usually, as the concentration of the particles are increased, the effects of the particles on the blend viscosity becomes more pronounced. At low additive concentrations (< 5 vol%), the filler results in a viscosity higher than the neat resin but a Newtonian viscosity plateau at low deformation rates is still often observed.. At higher concentrations, systems incorporating small particulates commonly exhibit a monotonic increase in viscosity with decreasing shear rate indicative of the formation of a yield stress. An example of this behavior for a particulate filled materials is shown in Figure 2.11. The typical unbounded viscosity curve has been observed at low shear rates for systems incorporating materials such as $CaCO_3$, carbon black, and titanium dioxide [61,65] while for other materials, such as glass beads, a Newtonian plateau can be observed to concentrations as high as 40 volume % [68,69]. The rheological response of these systems at the low shear rates can be attributed to the structure which is determined by the dynamic balance between the shear and restoring forces. In the case of high shear rates, the effects of the particles on the shear viscosity is decreased due to breakdown of the structure by shear forces. For various systems [63,64] it has been observed that the pseudoplasticity of the suspension is usually increased by increasing the concentration of the particles.

Besides concentration, factors such as the particle shape and the base resin can also influence the response of the system. For the same filler incorporated into various polymer melts, Minagawa and White [61] found that the extent of increase in the viscosity at low shear rates was approximately inversely related to the viscosity of the neat polymer. For small particles, the size and surface area have a direct effect on the restoring forces such as van der Waals forces and Brownian forces. For smaller particles and/or particles with larger surface areas, the restoring forces are larger resulting in higher viscosities at the same shear stress. It has been observed experimentally [62,69] that increasing particle size and decreasing surface area usually results in mixtures with a lower viscosity.

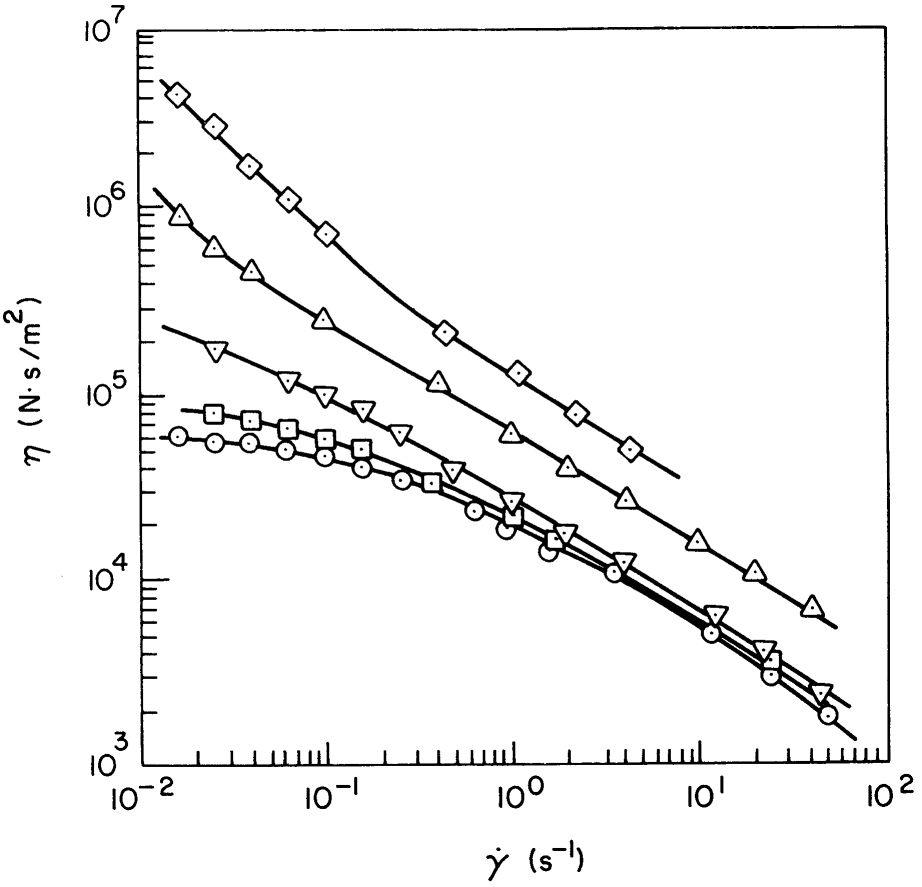

Figure 2.11: Viscosity versus shear rate for polystyrene filled with carbon black. Volume fraction of carbon black are, from top to bottom, 25%, 20%, 10%,5%, 0% [77]

Often for particulate filled systems, the solids are coated with surface treatments in order to alter the interactions between the polymer and the solids. It has been observed that the addition of surface treatments can promote a large range of behaviors. For certain systems, it has been observed that the addition of these coupling agents tends to decrease the viscosity of the blend as compared to the untreated material [70-72]. The effects of the surface treatments are most readily seen at the lower shear rates and is attributed to the reduction in the strength of the structure formed by the particles. For other systems [73], it has been seen that the addition of coupling agents can increase the viscosity of the mixtures and this has been attributed to the increased adhesion between the polymer and filler.

For the manufacture of polymeric composites in operations such as injection molding, the reinforcing phase in often in the form of fibers which can result in a wide variety of viscous responses under shear. As with small particulate filled materials, the shear viscosity of fiber filled systems shows a strong dependence on filler concentration. The fibers serve to increase the viscosity over that of the neat resin at low shear rates while the viscosity of the blend approaches that of the neat resin at higher deformation rates [63,64,66-68]. The higher viscosity at the lower shear rates can be attributed to the formation of loose structure of the fibers which is easily broken by the flow at higher shear rates. The higher shear rates promote the orientation of the fibers with flow and results in a lower disturbance of the flow field which is manifested as a lower viscosity.

As with particulate fillers, the size of the reinforcing fibers can have a marked effect on the flow behavior of the filled resin. The reinforcing fibers aspect ratio (length/diameter) can have a dramatic effect on the viscosity of a filled system. Smaller diameter fibers have a tendency to produce a higher viscosity when compared to larger diameter fibers of the same aspect ratio [74]. It has also been observed that larger aspect ratio fibers have a tendency to increase the viscosity due to increased particle interactions [74,75].

Sizing or coupling agents are added to fiber filled systems to increase the mechanical properties of these glass filled materials. These additives can also have a large effect on the rheological behavior of the blend. Generally surface treatments serve to lower the viscosity of the mixture as compared to the untreated fibers [61,72,73]. The lowering of the viscosity can be attributed to factors such as the lowering of the interfacial tension between the phases and the reduction in the interaction between the reinforcing fibers.

2.7.2 Elastic Response of Solid filled Polymer Melts

Besides altering the viscous response of a polymeric material, suspensions of viscoelastic fluids containing fibrous and non-fibrous material can show a wide range of elastic responses. It has generally been observed that the addition of small non-fibrous

particulates results in an increase in the first normal stress difference (N_1) for a wide range of shear rates [61,76,77]. As the concentration of particulates is increased, N_1 increases for all shear rates. If a comparison is made on the basis of shear stress, the normal stress decreases for increasing concentration. As with the viscosity, the treatment of the surface of the particulates can result in either an increase or decrease in the normal stress depending on the materials used [73,76]. In the case of fiber filled systems, the addition of fibers tends to increase the normal stress difference when comparisons are made on a basis of either the applied shear stress or shear rate [67,75,76].

2.8 Processing of Conventional Glass filled Thermoplastics

The focus of this work is to examine various aspects of the processing behavior of low melting glass filled thermoplastics. In order to ascertain what advantages these new composite systems offer, it is necessary to examine the characteristics of conventional E-glass filled composite materials.

2.8.1 Drawbacks of Conventional Short fiber Glass Reinforcement

Melt processable glass filled materials have the potential to replace conventional glass filled materials for processes such as injection molding or extrusion. As pointed out earlier, the addition of fibers can have a large effect on the rheological behavior of the polymeric melt that subsequently alters the processing behavior of the resin. The addition of the fibers can serve to enhance the mechanical properties of the resin but often numerous processing difficulties arise.

The addition of glass fibers to a resin can create conditions that can adversely change the processing behavior of the resin for applications such as injection molding. As pointed out earlier, the addition of solid particles has a tendency to increase the viscosity of resin and alter the elastic characteristics of the blend. At the fiber levels utilized for composite manufacture (20-40 wt%), the viscosity of the resin increases enough to significantly change the flow behavior of the resin. In order to overcome this increase in viscosity, the processing temperatures are often increased which can lead to problems such as degradation of the matrix [78,79]. The structure created by the interaction of the glass fibers often requires the use of higher pressures in order to fill out the mold properly [78,79]. The addition of the solid fibers creates a mixture that can interact with the processing equipment in a detrimental manner resulting in wear on various parts of the equipment such as the screw, barrel, and mold [79-81].

Solid fibers are often added to elevate the properties of the neat resin, but there are some detrimental effects in the terms of final properties of the molded parts. The complex interactions between the flow field and the fibers often results in parts that are anisotropic in terms of both the fiber orientation and stress distribution [78,79,82,83]. This anisotropy

in properties can lead to problems in areas such as mechanical and thermal performance. The glass fibers used for composite manufacture in injection molding often have typical diameters ranging from 10-13 μm with aspect ratios ranging anywhere from 10 - 100 [84-86]. Due to the large size of the glass fibers, a product containing glass fibers often has a poorer surface appearance than a product made from the neat resin. The presence of the glass often leads to problems such as surface waviness, sink marks, and loss of the high gloss finish [79,83]. When molding glass filled materials, great care has to be used in order minimize the formation of weld lines [82,83]. The presence of the glass fibers hinders the blending of melt streams resulting in the formation of weld lines which could serve to weaken the completed part. Even with the aforementioned problems, fiber reinforced composites are still widely used due to the benefits gained in terms of mechanical properties.

2.8.2 Properties of Short Fiber Reinforced Thermoplastics

In the previous section, it was shown that fiber filled systems possess some disadvantages but the benefits gained in terms of mechanical properties often outweigh these problems. As with the rheology of fiber filled systems, a wide range of variables can alter the properties of the composite blend. Factors such as fiber loading, fiber dimensions, fiber orientation, and surface treatment will have a large impact on the ultimate mechanical properties of a fiber filled material.

Typically, the mechanical properties of short fiber reinforced blends are controlled by varying the concentration of the fiber reinforcement. Commercially available material for molding operations usually contains 20-40 wt% reinforcement where higher loadings offer no significant enhancement of properties but may lead to processing difficulties. It has generally been found that the mechanical properties of a fiber reinforced material will increase with increasing reinforcement concentration. As the reinforcement concentration reaches a certain level, the gain in properties are often minimized due to the increased fiber interactions. Xavier and Misra [87] examined the effects various loadings of glass fiber on the mechanical properties of injection molded polypropylene. The tensile modulus for the blend rose from 1.59 to 3.41 GPa for a glass concentrations of 10 and 35 wt%. It was also determined that the average fiber length decreased from 0.55 to 0.35 mm due to fiber breakage from increased particle interactions. At higher glass concentrations, a larger number of glass fibers are present whose ends could serve as stress concentrators which may lead to premature failure of the composite. A similar study was performed by Hiscock and Bigg [88] for nylon reinforced with glass fibers of various loadings. At a loading of 10 wt%, the composite blend had a tensile modulus of 5.10 GPa with a tensile strength of 101 MPa. By increasing the loading to 35 wt%, the modulus rose to 11.1 GPa while the strength increased to 169 MPa. The properties of a reinforced system can be increased through the addition of fiber reinforcement but as the level of reinforcement is increased particle interactions can lead to lower reinforcing efficiency and premature failure of the system.

One of the other important variables in the properties of fiber reinforced systems is the size (diameter and length) of the reinforcing phase. Various theories for the properties of composite systems have proposed reinforcement with higher aspect ratios have a tendency to produce composites with better mechanical properties [89-91]. One way to increase the aspect ratio of the fibers is to incorporate and retain fibers of a longer length into the matrix. Through the development of manufacturing techniques and processing technology, it has become possible to incorporate long fibers for injection molding operations. A comparison between the properties of short fiber and long fiber filled systems was made by Cianelli and coworkers [92,93]. Using a specially modified injection molding unit, polyamide 6,6 containing 50 wt% glass in the form of either long or short fibers was processed. The processed short fiber composite contained fibers that had an average length of 0.013 inches with a flexural modulus and strength of 12.3 GPa and 323 MPa, respectively. The processed long fiber composite contained fibers with a length of 0.114 inches and had a flexural modulus of 14.1 GPa with a flexural strength of 351 MPa. For all the systems considered, the long fiber filled materials showed enhanced properties over the short fiber filled materials. The one area where the long fiber filled material offered superior performance was in the impact properties. In the case of the nylon 6,6 with 50 wt% glass, the long fiber filled material had a notched impact strength of 261 (J/m) while the short fiber filled composite only had impact strength of 131 (J/m).

Another characteristic dimension of the reinforcing fiber that can have a large impact on the properties of a composite is the diameter of the fiber. The effects of fiber diameter on the ultimate mechanical properties of composites has been investigated by a large number of individuals [94-96]. The effect of fiber diameter on the tensile and impact strength for a variety thermoplastics was examined by Watkins et. al. [95]. A variety of amorphous and semi-crystalline thermoplastics were blended with glass fibers to produce mixtures containing 20 to 40 wt % glass. For all the composites considered, both the tensile and impact strength increased as the fiber diameter decreased. However, work performed by Sato and co-workers [96] revealed that there may be an optimum fiber size that yields the highest properties. In this study, glass fibers with diameters of 0.5, 4, 7, and 13 microns were blended with a polyamide 6,6 matrix. The composites containing the 7 micron fibers yielded the highest tensile and flexural strength, with the composites containing 13 μm and 4 μm fibers having equivalent properties. The composites containing the 0.5 microns fibers displayed properties that were substantially lower than the other sizes investigated. It was speculated that the smaller diameter fibers results in a larger number of fibers being present when comparing systems based on the weight fraction of glass. This larger number of fibers results in an overall larger surface area between the fibers and matrix, increasing the potential for better stress transfer between the matrix and filler. A competing effect may arise from increased number of fiber ends that could serve as stress concentrators that may lead to the premature failure of the composite. From this it appears, that there could be a critical fiber diameter that balances the benefits gained from the increased surface area and the harmful effects of the increased number of fiber ends.

One of the most important factors controlling the properties of polymer materials reinforced with inorganic fibers is the effectiveness of the bond between the resin and the fiber. The effectiveness of the bond between the resin and reinforcement in transferring stress across the interface will play a large role in the determining the mechanical properties which could be achieved. Often small amounts of a material referred to as a coupling agent has to be added to enhance the bond between the resin and the reinforcement and elevate the properties of the composite. In the case of borosilicate glass filled materials, organofunctional silicones are often utilized due to their specific interactions with both the glass and polymeric matrix. Besides increasing the adhesion between the phases, these coupling agents often help preserve the properties of the composites when exposed to certain environments. Often when neat glass/polymeric blends are placed in a moist environment, a loss in strength is observed due to the debonding of the resin from the hydrophilic glass due to the intrusion of water. The increased adhesion between the polymer and glass from the coupling agent is thought to reduce the infiltration of the moisture leading to the preservation of the polymer/glass bond [97].

The addition of coupling agents to injection moldable short fiber glass reinforced thermoplastics has generally lead to composites with increased properties and greater durability. Richards and Sims [98] investigated the effects of various glass coupling agents on the properties of injection molded samples consisting of polypropylene and nylon-6. For the polypropylene composites, it was generally found that the addition of silane coupling agents lead to an increase in properties with a better retention of strength after being immersed in water. For example, a composite reinforced with 30 wt% glass only had a tensile strength of 35.8 MPa while various coupling agents produced composites with strengths ranging from 44.2 to 48.5 GPa. In the case of the nylon blends, the addition of the same silane agents improved the strength composites but after immersion in water these benefits were quickly lost. A similar study of the effects of coupling agents on the properties of glass filled nylon composites was performed by Bader and Collins [99]. In this study it was found that depending on the silane coupling agent utilized, increases in the dry strength on the range of 20% could be achieved over the unsized fibers. The main benefits of the silanes could be seen after the composites were immersed in water, where the silane coated materials displayed properties far superior to the unsized glass filled composites. The benefits gained through the addition of coupling agents can be varied depending on the complex interactions between the glass and polymeric material.

Besides factors such as fiber concentration, size, and adhesion, the orientation of the glass fibers during processing can affect the overall properties of the composite. The flow kinematics generated during processing will play a large role in determining the ultimate mechanical properties of the composite. In injection molding, the effects of process parameters such as the mold dimensions, gate location, and processing temperatures determine how the fibers will be oriented in the molded part. Often

processes such as injection molding, result in composites that contain varying degrees of fiber orientation which is reflected in the mechanical properties. How fiber orientation is developed can be attributed to the flow kinematics in the mold which is dependent of factors such as the gate type and location and mold dimensions. A study was performed by Darlington and co-workers [100] which examined the influence of flow kinematics on the mechanical properties of an end-gated circular disk. Changes in the flow kinematics were achieved by varying the diameter and thickness of the mold. It was found that the mechanical anisotropy could be reduced by utilizing a thinner mold or mold with a larger diameter. During the mold filling it was determined that a skin formed oriented predominately in the flow direction while the core was oriented mainly transverse to the flow direction. By reducing the mold thickness or increasing the mold diameter, the orientation in the skin and core could be modified to achieve the desired properties.

The location and type of gate used in the processing fiber filled materials can also influence the orientation of the fibers which can be reflected in the mechanical properties. The effects of end-gates of various configurations on the orientation of fibers has been widely investigated [101-104]. For end-gated plaques, it was found that the addition of a runner served to reduce the orientation of the fibers perpendicular to the flow direction for shorter distances down the length of the plaque. Goettler [104] found that orientation produced by fan gates was more sensitive to injection speeds with more transverse fiber orientation occurring in this gate design when compared to an edge-gate. By locating the gate in the center of the sample, the orientation in the skin and core regions can be varied. In the skin region the fibers are commonly oriented along the flow direction while the fibers in the core region are often oriented perpendicular to the flow direction reducing, the anisotropy of the sample.

2.8.3 Forming of Conventional Fiber Reinforced Thermoplastics

Often the objective of blending reinforcing fibers with a polymeric material is to create a composite blend that can be easily shaped or formed into some desired configuration. Processes such as injection molding allow the rapid fabrication of discontinuous fiber filled material into a finished product but there are limitations for this process. Problems such a weld lines, anisotropy, and residual stress can limit the shapes that can be produced. The reinforcement gained in these composites is also limited due to the aspect ratio of the fibers that can be retained for this type of process. Alternative shaping techniques such as compression molding, thermoforming, and hot stamping have been implemented for a variety of fiber filled materials.

The addition of fiber reinforcement serves to increase the properties of the neat resin but the addition of these fibers can adversely effect the dynamic performance of the system. The solid reinforcement serves to lower the extensibility of the composite system. For the composite blend, the polymeric material can undergo affine deformation while the reinforcing fiber behaves as rigid solid over the temperature ranges considered. Factors

such as the number of fiber ends and distance between them can have large impact on the dynamic response of the blend. It has been shown, that in short fiber composites the fiber ends can be considered as potential weak points due to the formation of small voids and missing interfacial bonding in these areas [106]. This lack of deformability of the reinforcing fibers and lack of interfacial adhesion between the reinforcement and matrix can result in problems such as fiber buckling or breakage, formation of cracks or voids, and uneven deformation within the sample often resulting in finished products with undesirable appearances or properties [105-109].

Composites systems consisting of thermoplastics reinforced with continuous fibers have offered the most promise as replacement over traditional thermosetting composite systems. Continuous fiber systems can be loaded with up to 60 vol% reinforcement and with the almost infinite aspect ratio of the reinforcing fiber, these systems can provide significant improvements in properties over the neat matrix. One of the major drawbacks of continuous fiber filled systems is the behavior of the material under deformation which can create many processing issues. These issues include fiber placement control, lower molding cycle times and the formation of wrinkle free complex shapes [106]. In these composite systems, the inextensibility of the continuous fibers in the laminates results in the build up of stresses which can result in defects. To overcome this problem, time consuming processes that rely on interply and intraply slip mechanisms have to be utilized [105-107,109]. Processing conditions such as consolidation temperature, pressure, and speed have to be controlled to minimize these problems. A thorough study on the role of processing variables on the forming behavior of various continuous fiber reinforced thermoplastics was performed by Hou et. al. [108]. It was found that at low consolidation speeds (< 200 mm/min) and pressures, the fibers have a tendency to buckle and break in regions of curvature. For high consolidation speeds (> 500 mm/min) or excessive pressures, intensive thinning in regions of curvature and resin migration perpendicular to the fiber direction often occurs. Care has to be taken to utilize processing conditions that allows interply and intraply shear to occur, allowing more accurate deformation of the composite blend.

Composites containing long discontinuous fibers (LDF) have been investigated to alleviate the aforementioned problems with continuous fiber reinforced systems. The LDF composite systems contain fibers on the order of 5 cm and provide mechanical properties that are comparable to the continuous fiber reinforced systems. Since the fibers are discontinuous with the matrix material, elastic deformation can occur between the fiber ends resulting in more uniform deformation. A schematic comparison of the deformation seen for processes such as thermoforming for continuous fiber and long discontinuous fiber filled material is shown in Figure 2.12. Studies involving the deformation and forming behavior of these LDF composites have been performed by a number of individuals [106,109]. Okine and coworkers [109] found that long discontinuous fiber reinforced materials formed better shapes with lower degree of fiber bucking of breakage. Schuster and Friedrich [106] compared the properties of undeformed continuous and long

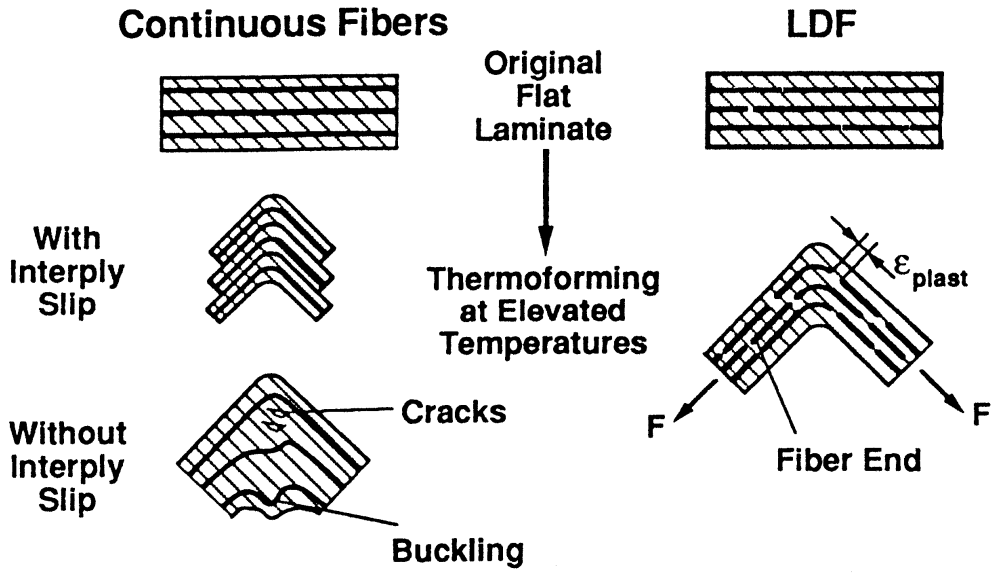

Figure 2.12: Effects of deformation on various fiber reinforced materials in thermoforming [106].

continuous fiber reinforced materials to the properties of LDF filled materials elongated from 3-12%. By deforming the LDF materials uniaxially to 3% elongation, a tensile strength could be obtained that was higher than the undeformed continuous or LDF reinforced materials. At higher elongations, the LDF reinforced materials showed a loss of strength that was attributed to local decreases in the fiber volume fraction. Even though LDF filled materials offer higher extensibility than conventional continuous filled materials, the processing difficulties associated with these composites still limits the use of these materials.

2.9 Processing of Self-Reinforcing Composite Systems

In order to overcome some of the problems of solid reinforced composites, the development of composite systems where the reinforcing morphology is generated during processing have been considered as a possible alternative. The ability to generate the reinforcing morphology relies on the phenomena of droplet deformation and stability which is controlled by factors such a interfacial tension, rheology, and the flow kinematics used during processing.

2.9.1 Injection Molding of TLCP Reinforced Composite Systems

The most widely studied self-generating composite systems, have involved thermoplastics blended with thermotropic liquid crystalline polymers (TLCPs). TLCPs are polymeric materials that can offer mechanical properties on the order of other reinforcing media when processed under the proper conditions. These TLCPs are thermoplastic in nature allowing the material to be blended and processed with other thermoplastics in conventional processing equipment. One process often implemented to generate the reinforcing morphology involves injection molding.

The injection molding of TLCP reinforced thermoplastics has been investigated for a number of systems under a wide range of processing conditions [110-122]. For almost all the systems considered, the addition of the TLCP serves to enhance the mechanical properties of the blend to values exceeding that of the neat resin. Even with the increase in properties, TLCP filled systems still fall short in achieving the desired level of reinforcement. Samples are often anisotropic in terms of their mechanical properties [115-120] with properties in the direction transverse to flow often in the range of the neat resin. For example, Bafna et. al. [120] examined the anisotropy of end-gated injection molded blends of polyetherimide (PEI) reinforced with varying concentrations of TLCPs. For a blend containing 50 wt% of the TLCP HX1000, the machine direction flexural modulus was 12.9 GPa while the transverse direction flexural modulus was only 3.2 GPa, a value comparable to the neat PEI transverse modulus of 3.1 GPa. Besides being anisotropic, the maximum stiffness of these blends are often lower than the theoretical maximum that could be achieved with the addition of the TLCP [123]. A blend containing polypropylene

reinforced with 30 wt% of the TLCP Vectra A that was injection molded into a tensile bar only had a modulus of 2.16 GPa. By using the modulus of pure Vectra A molded at the same conditions, the predicted modulus of the blend from composite theory should have been upwards of 4.24 GPa [124].

The complex flow field seen during the mold filling step contributes to the anisotropy and lower mechanical properties seen in these blends. As the blend is injected into the mold, only the material at the leading edge of the advancing front is elongated by the fountain flow kinematics. This highly stretched and elongated material is laid against the wall where it begins to solidify. This surface layer (skin) often contains TLCP fibrils with the highest aspect ratio and molecular orientation. The material in the center region following the advancing front is often only exposed to shear flow or a mixture of shear and elongational flow depending of the mold configuration [125,126]. This core region is less effective in inducing orientation in the TLCP resulting in a lower properties. The complex flow field generated during the mold filling step usually results in an anisotropic composite that possesses a skin that is highly oriented in the flow direction with an unoriented core that does not fully utilize the TLCP [127-129].

Other processing factors such as the injection speed, mold temperature, and mold thickness can play a large role in the properties of injection molded TLCP reinforced composite systems. By adjusting any of the aforementioned processing parameters, the heat transfer during the mold filling step can be varied which can have a profound effect on the formation of the reinforcing morphology. The temperatures used during processing have to be high enough to allow fibrillation of the TLCP but cool enough to allow the rapid solidification of TLCP to prevent any molecular relaxation or fiber breakup due to capillary instabilities.

The effects of varying processing conditions on the mechanical properties of TLCP reinforced thermoplastics was analyzed by O'Donnell [115-117]. In these studies polypropylene (PP) mixed with maleic anhydride grafted polypropylene (MAP) in a 90/10 weight ratio was blended with various TLCPs to form a composite blend containing 30 wt% TLCP. The mold temperature, mold thickness, mold fill time, and initial melt temperature were varied to ascertain the conditions that would lead to the greatest level of reinforcement.

One of the variables that was found to have a profound influence on the mechanical properties of the blend was the mold thickness. For pure TLCPs, it had been generally found that thinner molds are more effective in orienting the TLCP due to reduction of the unoriented core region. In the case of PP reinforced with various TLCPs, the effects of mold thickness varied depending on the conditions and blends utilized. For example, a blend of PP/MAP/Vectra B (63/7/30 wt%) injected into a 1.5 mm mold had a maximum flexural modulus of 5.10 GPa with a flexural strength of 60.5 MPa. The same blend injected into molds with a thickness of 1.0 mm and 2.3 mm under similar conditions

was only able to produce composites with flexural moduli ranging from 3.7-3.9 GPa and flexural strengths ranging from 51-54 MPa. For a blend containing polypropylene with MAP and the same loading of the TLCP LC3000, a different trend was observed. For the LC3000 blend, the highest properties were achieved with the thinnest mold (1.0 mm) with the flexural modulus being on the order of 5.14 GPa with the strength being approximately 65 MPa. For the 1.5 and 2.3 mm molds, the highest flexural modulus and strength that could be achieved under similar conditions was only on the order of 3 GPa and 60 MPa, respectively.

The influence of injection speed or mold filling time on the mechanical properties of the PP/TLCP blends was also analyzed. As with the mold thickness, the results varied depending of the conditions and blends utilized. In the case of the PP/MAP/Vectra B blends, the highest flexural properties were obtained for the faster injection times (0.5-3 seconds) for all the mold thickness considered. Even though the faster injection speeds resulted in higher machine direction properties, the anisotropy within the samples had a tendency to increase. For the 1 mm thick mold, a sample injected in 0.5 seconds displayed an anisotropy ratio (MD flexural modulus/TD flexural modulus) of 2.64 while a sample with a filling time of 2.8 seconds only had an anisotropy ratio of only 2.18. For blends of PP and MAP with the TLCP LC3000, the trends were not as defined. For the thin mold (1 mm), the maximum properties were achieved for a mold filling time of approximately one second. For the thicker molds (1.5 & 2.3 mm), the maximum properties were achieved for much longer filling times on the order of 6-8 seconds.

The variations in mechanical properties with mold thickness and injection speeds were attributed to the solidification behavior of the various TLCPs which was controlled by the heat transfer during the mold filling. The dimensionless group known as the Graetz number was used to quantify the heat transfer occurring during the mold filling step. The Graetz number relates the amount of heat convected in flow channel to the heat conducted in the transverse direction and can be represented by the following:

$$N_{GR} = \frac{U \cdot H^2}{\alpha \cdot L} \qquad (2.21)$$

where H is half the mold thickness, U is the fluid average velocity, L is the mold length, and α is thermal diffusivity which is the thermal conductivity divided by the density and heat capacity of the blend. In the case of a system reinforced with the TLCP Vectra B950, it was determined that the modulus of the blends increased at a Graetz number of 10 independent of the mold thickness. At Graetz numbers less than 10, the modulus displayed a significant drop that was attributed to the premature solidification of the TLCP, making it difficult to deform the material into reinforcing fibrils. In the case of the LC3000 filled blend, the flexural modulus transitioned from low to high values for a Graetz number of 5. For the thin mold (1mm) it was found the flexural modulus increased

for increasing Graetz number revealing that the higher injection speeds allowed the TLCP to remain fluid enough that imposed stress could elongate the TLCP domains. In the case of the thicker molds (1.5 & 2.3 mm), the properties were at a maximum for Graetz number of only 5 indicating that solidification of the TLCP phase may occur rapidly minimizing the orientation that could obtained. From these studies, it was determined that the solidification behavior of the reinforcing phase plays an important role in the ultimate mechanical properties of the composite blend. The temperatures and conditions utilized must allow adequate deformation of the reinforcing phase into the desired morphology that can be locked in as the sample is cooled.

2.9.2 Post Processing of TLCP Reinforced Composite Systems

Even though TLCPs can be utilized to make self reinforcing composites for processes such as injection molding, limitations for these systems do exist. The composites manufactured via this method are often anisotropic and often incompletely utilize the full reinforcing of the TLCPs. In order to overcome these problems, alternative processing techniques have been utilized in order to generate more favorable properties. A variety of processes that impart shear free deformation on the TLCP phase in various blends have been investigated [130-133].

One such process involves the compression molding of the TLCP reinforced blends at conditions where the reinforcing phase would be deformable. In one such study, Isayev and Viswanathan [132] examined the compression molding of a polyphenylene oxide/polystyrene alloy blended with various concentrations of TLCP. Uniaxially oriented prepreg laminates of varying degree of draw and TLCP concentration were compression molded in two basic configurations. One configuration consisted of stacking all the prepreg laminates parallel to one another along the machine direction to form a uniaxial composite. The other configuration involved stacking the subsequent layers at 45° to one another in order to form a quasi-isotropic samples. The final consolidated composites were compressed to varying reduction ratios (sum of the thickness of all the prepreg laminate sheets/final consolidated composite thickness). It was found that the uniaxially consolidated samples with high draw and reduction ratios produced composites with higher machine direction properties than an injection molded sample. The quasi-isotropic laminated composites possessed mechanical properties that were either equal to or exceeded those obtained for injection molded samples. The mechanical properties of the quasi-isotropic laminates at the highest reduction ratio were found to be much higher than values predicted based on the properties of the original uniaxial laminate. These increases in properties were attributed to the inducement of orientation during the consolidation process.

A similar study was performed by de Souza [131], where various types of deformation were applied to injection molded blends in order to reduce the anisotropy of the composite blend. Various types of shearfree deformation including uniaxial, planar,

and biaxial deformation were applied to blends consisting of polyetherimide (PEI) and various TLCPs. The various types of deformation were applied at a wide range of temperatures and rates for a number of blends of varying concentration.

In order to investigate the effects of uniaxial deformation, tensile stretching at elevated temperatures was performed under a variety of conditions. Uniaxial deformation applied along injection molded machine direction resulted in the formation of higher aspect ratio fibers accompanied by an increase in properties in the stretching direction. An injection molded blend containing PEI and 20 wt% of the TLCP HX1000 had an initial machine direction tensile modulus and strength of 5.13 GPa and 105 MPa, respectively. When this blend was stretched uniaxially to 0.75 strain units (112% elongation), the modulus and strength rose to 10.4 GPa and 199 MPa, respectively. Even though the machine direction properties were increased, the problems of anisotropy became magnified. For the aforementioned blend, stretching elevated the anisotropy ratio (MD modulus/TD modulus) from 1.8 to 4.2. When the uniaxial deformation was applied transverse to the molding direction, it became possible to elevate the properties in this direction resulting in more isotropic composite blends. With the elevation of the transverse direction properties often the flow direction properties suffered a decline due to the realignment of the reinforcing fibers. This often resulted in composite blends with properties only slightly greater than neat PEI. When a blend consisting of PEI reinforced with 20 wt% of the TLCP Vectra A was stretched 0.5 strain units in the transverse direction, the sample was isotropic with a tensile modulus of 3.2 GPa, a value slightly greater than the 3.0 GPa found for neat PEI.

Since it was found that uniaxial deformation offered limited improvements in the mechanical properties and anisotropy of the injection molded blends, de Souza [131] investigated the effects of planar deformation on the properties of these blends. Hot tensile stretching and constrained compression molding were utilized to impart planar deformation of varying degrees to the blends. It was generally found that the planar deformation lead to the spreading of the TLCP domains into the plane of deformation resulting in a ribbon-like morphology. The extent of the fiber spreading was dependent on the relative direction of the applied deformation, with transverse planar compression having more of a tendency to spread the TLCP phase. For example, PEI reinforced with 20 wt% of the TLCP HX1000 was stretched to 0.75 strain units in the transverse direction. Under these conditions, the machine direction tensile modulus remained unchanged at approximately 5.1 GPa while the transverse direction modulus was elevated from 2.8 GPa to 5.1 GPa. It was also determined that constrained planar compression molding had a tendency to produce blends with better properties as compared to planar stretching. With compression molding, the PEI and TLCP were kept in intimate contact during deformation while for the planar stretching it was observed that excessive fiber pull out and void formation occurred, minimizing the reinforcing potential of the TLCP.

In a further effort to examine the effects of flow kinematics on the mechanical properties of TLCP filled materials, biaxial deformation of varying degrees was applied to the samples [131]. Processes such a biaxial stretching and lubricated squeezing flow were implemented in an effort to generate composites with more uniform properties. Depending on the TLCP blended with the PEI, morphologies consisting of droplets or flake-like structures could be obtained. The formation of a droplet morphology was attributed to exceeding some critical stress resulting in the breakup of the TLCP fibrils into droplets. The reinforcing morphology could be modified to yield more isotropic samples, but the complex interactions between the matrix and TLCP resulted in varying reinforcing morphologies.

Since it was determined that deformation applied to thermoplastic/TLCP blends could result in large changes in properties, it was envisioned that processes such as thermoforming might be able to induce the desired changes in morphology. The thermoforming of TLCP reinforced PEI was examined by de Souza [131] for various forming conditions. It was found that the TLCP reinforcement became elongated in the corners of the mold where the material was exposed to the highest strains. In the case of solid glass filled materials, these high strains led to fiber breakage resulting in a part of poor quality. From this work, it appears that these self-reinforcing blends could offer some large processing advantages over conventional solid filled materials. Since the reinforcing phase is deformable during processing, shaping the blend may result in an enhancement of composite properties instead of the reductions normally seen with solid filled blends.

2.10 Processing of P-Glass Reinforced Thermoplastics

From the work performed with TLCPs, it appears that self-reinforcing composite blends composed of melt processable materials may offer some significant processing advantages over conventional solid reinforced systems. By imparting deformation of the composite blend at conditions where both phases are fluid, the reinforcing phase morphology may be controlled by the processing conditions utilized. Besides TLCPs, another material that might offer some similar advantages and warrants further investigation are melt processable glasses.

2.10.1 Injection Molding of P-Glass Reinforced Composites

Melt processable materials such as phosphate glass may be able overcome some of the processing difficulties associated with solid fiber reinforcement. Due to the fluidity of the glass at the conditions used to process many thermoplastics, a wide range of processing alternatives not available to normal solid reinforced materials may be possible. Higher glass loadings could be processed without detrimental effects to equipment, so composite blends with greater mechanical properties and thermal stability could be

produced. Processes such as injection molding may allow the rapid fabrication of these highly loaded blends into a final product without all of the difficulties associated with solid filled systems.

Surprisingly, the injection molding potential of these novel phosphate glass filled thermoplastics has been investigated only on a limited basis [134-139]. One of the first studies on the injection molding capability of these novel blends was performed by Ray and coworkers [134]. In this study phosphate glasses with transition temperatures ranging from 140-210 °C were molded with a variety of thermoplastics including polypropylene (PP), polycarbonate (PC), and polysulfone (PS). The glass/polymer mixtures were pre-blended in a single screw extruder, pellitized, and then fed into an injection molding unit operating at a temperature range of 260-310°C. The melt from the injection molder was then shot into an end-gated mold at room temperature to produce bars with the dimensions 50 mm x 9 mm x 3 mm. For the molded composites, the glass was in the form of small fibrils with aspect ratios of over 50 leading to significant reinforcement of the thermoplastics. For example, the addition of 30 wt% of a phosphate glass to polysulfone elevated the flexural modulus from 2.2 GPa to 4.8 GPa. It was also shown that high glass loadings (up to 92 vol%) could easily be processed via injection molding. This initial work was limited to a few representative samples due to the limited chemical durability of the phosphate glasses utilized.

The development of more durable phosphate glasses offered further opportunities to investigate the injection molding of the novel melt processable glass filled blends [58,135-139]. The glass transitions temperatures for the glasses used in these studies ranged from 225-350 °C, limiting the thermoplastic matrices to materials such as polyetherimide (PEI), polyethersulfone (PES), polyetheretherketone (PEEK), polyetherketone (PEK), and thermotropic liquid crystalline polymers (TLCPs). Composite blends containing up to 70 vol% glass were prepared by first mixing the thermoplastic and glass in a twin screw extruder operating at temperatures upwards of 430°C. The blends were subsequently pelletized and re-plasticated in an injection molding unit operating at 345-430°C. The glass/polymer melt blends were next injected into a heated mold (175 °C - 285°C) of an unspecified configuration. Due to the lower tensile properties of these glasses as compared to borosilicate glasses, higher glass loadings (> 50 wt%) were investigated in anticipation these loadings would provide properties of the desired level.

For these particular studies, a variety of glasses and thermoplastics were blended for a range of concentrations to ascertain the extent of reinforcement that could be achieved with the various glasses. For all the injection molded blends considered, it was found that the tensile modulus increased with glass concentration while the tensile strength had a tendency to decline. For example, neat PES had a reported tensile modulus of 2.4 GPa with a strength of 84 MPa. With the addition of 50 wt% phosphate glass the modulus rose to 11.4 GPa with the strength falling to 71 MPa. Increasing the glass

concentration to 70 wt%, increased the modulus even higher to a value of 22.1 GPa while the strength suffered a substantial loss falling to 46 MPa. The loss in strength with the addition of glass is not surprising considering the strengths of the neat phosphate glasses are much lower than the thermoplastics often falling in the range of only 20 MPa [135]. It is interesting to note that it was possible to obtain injection moldable composites with tensile moduli on the order of 20-30 GPa for glass loadings as high as 80 wt%. Conventional E-glass filled resins can usually accommodate only 40-50wt% glass and offer tensile moduli on the order of 10-15 GPa [140].

As with TLCP reinforced thermoplastics, the phosphate glass phase morphology should have a significant impact on the overall mechanical properties of the blends. By varying the processing conditions, Quinn and coworkers [58] were able to vary the reinforcing glass phase morphology for various blends. For composite blends containing 54 and 62 vol% phosphate glass with a TLCP, morphologies consisting of small beads, bead and fibers, or ribbons were achieved. The effects of the morphologies on the properties of the composite blends are shown in Table 2.2. The glass phase morphology of small glass beads offered the lowest aspect ratio resulting in composite blends that possessed the lowest properties. By deforming these droplets or beads into either fibers or ribbons, the aspect ratio was increased significantly which led to a dramatic rise in the mechanical properties. A blend containing 62 vol% P-glass with a TLCP only had a tensile modulus of 17 GPa with a strength of 52 GPa when glass was present as droplets. By generating ribbons and increasing the aspect ratio, the modulus and strength was elevated to 28 GPa and 72 GPa, respectively. It should be pointed out that the exact processing conditions used to obtain the phase morphologies was not specified. Due to the fact that a TLCP was used as the matrix material, the conditions used to elongate the glass phase may have led to orientation of the TLCP leading to the increase in mechanical properties.

It has been established that high loadings of phosphate glass can be injection molded using a wide variety of thermoplastics. At higher glass loadings, the moduli for these novel glass blends can exceed the values obtained for conventional borosilicate glass filled materials. As with other self reinforcing systems, a knowledge of the effects of the processing conditions on the ultimate mechanical properties of these blends is paramount in achieving composites with the best possible properties. The few studies on the processing of these novel blends have often failed to address the role of the materials and processing conditions on the final properties of the composites. A great deal of knowledge could be gained by systematically analyzing the role of material variables (viscosity & interfacial tension) and processing variables (deformation and temperature) on the formation of the reinforcing morphology in these novel glass filled composites.

Table 2.2: Properties for a TLCP reinforced with various loadings of phosphate glass of various configurations [58].

Properties		Glass Microstructures					
		54 vol% P-glass			62 vol% P-glass		
		Small Beads	Beads & Fibers	Ribbons	Small Beads	Beads & Fibers	Ribbons
Tensile Modulus	**GPa**	14	17	21	17	21	28
Tensile Strength	**MPa**	62	72	83	52	62	72
Elongation at Break	**%**	0.8	0.6	0.6	0.6	0.4	0.4
Flexural Modulus	**GPa**	13	16	19	16	19	24
Flexural Strength	**MPa**	100	125	150	75	100	125
HDT at 264 psi	**°C**	267	275	288	275	288	300

(HDT - Heat Deflection Temperature)

2.10.2 Deformation of P-Glass Reinforced Composite Systems

Due to the low glass transition temperatures of phosphate glasses, these materials may offer certain advantages for processes requiring large scale deformation such as compression molding or thermoforming. The fluidity of the glass at elevated temperatures makes it possible to generate a reinforcing morphology in processes such as injection molding but the rapid temperature changes in injection molding coupled with complex flow kinematics may not allow the full reinforcing potential of these novel glasses to be realized.

Since injection molding may not allow the full reinforcing potential of these novel blends to be realized, other processes imparting large scale deformation may be suited for these composite systems. Processes imparting extensional deformation such as fiber spinning, sheet extrusion, thermoforming, or lubricated compression molding may offer opportunities to generate glass morphologies that allow adequate utilization of the reinforcing capability of the glasses.

The evaluation of the behavior of these melt processable glass blends in processes other than injection molding is rather limited. A cursory evaluation of other processing alternatives for these blends was performed by Ray and coworkers [134]. Processes such as sheet extrusion, fiber spinning, and sandwich thermoforming were evaluated for a number of glass/polymer blends. From this work, it was determined that extensional deformation such as that seen in fiber spinning can deform the dispersed glass phase into reinforcing fibrils. For example, PET blended with 10 wt% glass was extruded from a capillary rheometer to produce a composite strands containing glass fibers with diameters in the range of 1-2 μm with aspect ratios over 200. For PP reinforced with 33 wt% glass, it was possible extrude the blend into a sheet that contained glass platelets oriented in the plane of the sheet. The formability of the composite blends was examined by considering the processing behavior of sandwich laminated blends. Continuous glass sheets laminated between sheets of polypropylene and polyvinylchloride were heated to temperatures in the range of 175-200 °C where the composite blend was formed into various configurations. The potential of these blends in other processing techniques was briefly addressed by Bahn and coworkers [135]. Bahn reported that an extrudate comprised of a perfluoroalkoxy resin (Teflon) with 87 wt% phosphate glass was pliable and exhibited exceptional melt strength indicating the material may be viable for processes such as sheet extrusion or thermoforming. Even though the potential of these blends for other processing techniques was mentioned, no experimental investigations for those processes were attempted.

2.11 Research Objectives

The topics covered in the previous sections address some of areas that are concerned with various aspects on the processing thermoplastic composites reinforced

with melt processable glasses. These self-reinforcing composite systems appear to offer many advantages over conventional inorganic filled composites. Many of these advantages are a result of the lower transition temperatures displayed by phosphate glasses. These lower transition temperatures appear to open many processing opportunities not available to conventional solid reinforced systems. Solid reinforcement can be used elevate the properties of the polymeric matrices, but the addition of these materials lead to many processing difficulties such as elevated viscosities, abrasive wearing on equipment, and limited deformability. Melt processable phosphate glasses can offer many of the benefits seen with conventional inorganic reinforcement but with the processing capabilities of thermoplastics.

As with any composite system, the reinforcing phase morphology will play a large role in the properties that can be obtained. In order to obtain composites with the ultimate mechanical properties, an understanding of the mechanisms responsible for the formation of the reinforcing morphology is of the utmost importance. The generation of the morphology rests on the phenomena of droplet deformation and breakup, which is dependent on many variables including the applied flow field, interfacial tension between the phases, and the viscous and elastic nature of the phases. Variables such as the flow field and viscosity ratio between the respective phases can readily be altered by exposing the composite blends to a variety of processing conditions and techniques.

The initial work performed on thermoplastics reinforced with melt processable glasses has shown that composites of high glass loadings can be facilitated by processes such as injection molding. These initial studies have been limited mainly to higher performance thermoplastics and have concentrated on blends containing high glass loadings. These rather limited studies have failed to reveal if the processing conditions utilized have any appreciable effects on the properties of the composites. Also, the potential for these blends in processes requiring deformation at lower temperatures (forming and shaping operations) has only been addressed on a very limited basis. It has been revealed that these novel blends may offer certain advantages over conventional fiber reinforced composites for forming operations, but the limitations and effects of deformation on these composites has yet to be determined. Due to the fluid nature of the glass at the conditions used to co-process the glasses with thermoplastics, it has been generally determined that these glass filled blends can offer lower viscosities than conventional solid reinforced materials. The effects of this fluid filler on other rheological properties such as transient response has yet to be determined.

Since a large number of questions remain about the processing behavior of thermoplastics reinforced with these melt processable glasses, the research to be performed will investigate the following areas:

1. **Evaluate the injection molding of various phosphate glass filled thermoplastics, paying attention to the role of variables such as processing conditions, glass**

concentration, interfacial tension, and viscosity ratio on the properties of the composites.

2. **Evaluate the processing performance of phosphate glass filled thermoplastics for lower temperature forming operations such as compression molding or thermoforming. It will be determined if deformation applied at these conditions leads to an enhancement of the properties of the composite.**

3. **Determine if phosphate glass filled polymer blends offer any unique viscoelastic behavior over conventional short fiber reinforced resins.**

A review of the literature relevant to various aspects of the processing of self-reinforcing melt processable blends was presented this chapter. An emphasis was placed on the factors controlling the formation of the reinforcing morphology with a brief synopsis of the work performed utilizing melt processable glasses. In the following chapter, a detailed account of the experimental procedures to be used to meet the aforementioned objectives will be presented.

2.12 References

1 D. Vesely, in *Polymer Blends and Alloys (Chapt. 5)*, ed. M.J. Folkes and P.S. Hope, Chapman and Hall, New York, 1993.

2 O. Olabisi, L.M. Roberson, and T.M. Shaw, *Polymer-Polymer Miscibility*, Academic Press, New York, 1979).

3 F. Ghuam and J.L. White, *Polym. Eng. Sci.*, 31 (2), 76 (1991).

4 C.D. Han, K.U. Kim, J. Parker, N. Siskovic, and C.R. Huang, *Appl. Polym. Symp.*, 20, 91 (1973).

5 W.J. Ho and R. Salovey, *Polym. Eng. Sci.*, 21, 839 (1981).

6 K. Min, J.L. White, and J.F. Fellers, *J. Appl. Polym. Sci.*, 29, 2117 (1984).

7 Z. Tadmor and C.G. Gogos, *Principles of Polymer Processing*, John Wiley and Sons, New York 1979.

8 S. Wu, *Polymer Interface and Adhesion* Marcel Dekker, Inc., New York 1982.

9 T. Young, *Phil. Trans.*, 95 (65), 84 (1805).

10 J.P. de Souza and D.G. Baird, *Polymer*, 36 (2), 259 (1995).

11 H.J. O'Donnell and D.G. Baird, *Polymer*, 36 (16), 3113 (1995).

12 C.D. Han, *Multiphase Flow in Polymer Processing*, Academic Press, New York 1981.

13 G.I. Taylor, *Proc. Roy. Soc*., A146, 501 (1934).

14 G.I. Taylor, *Proc. Roy. Soc*., A138, 31 (1932).

15 G.I. Taylor, *Proc. Roy. Soc*., A226, 289 (1954).

16 C.E. Chaffey and H. Brenner, *J. Coll. Interf. Sci*., 24, 258 (1967).

17 B.M. Turner and C.E. Chaffey, *Trans. Soc. Rheol*., 12, 411 (1969).

18 R.G. Cox, *J. Fluid Mech*., 37 (3), 601 (1969).

19 S. Torza, R.G. Cox, and S.G. Mason, *J. Coll. Sci*., 38 (2), 395 (1970).

20 H.J. Karam and J.C. Bellinger, *Ind. Chem. Eng. Fundam*., 11 (3), 321 (1972).

21 H.P. Grace, *Chem. Eng. Commun*., 14, 225 (1982).

22 T. Tavgac, *PhD Dissertation*, University of Houston, Texas (1972).

23 F.D. Rumsheidt and S. Mason, *J. Coll. Interf, Sci*., 16, 238 (1961).

24 B.J. Bentley and L.G. Leal, *J. Fluid. Mech*., 167, 219 (1986).

25 B.J. Bentley and L.G. Leal, *J. Fluid. Mech*., 167, 241 (1986).

26 H.L. Goldsmith and S.G. Mason, *J. Coll. Sci*., 17, 448 (1962).

27 F. Gauthier, H.L. Goldsmith, and S.G. Mason, *Trans. Soc. Rheol*., 15, 297 (1971).

28 C.E. Chaffe, H. Brenner, and S.G. Mason, *Rheol. Acta*., 4, 56 (1965).

29 G. Hetsroni, S. Haber, H. Brenner, and T. Greenstien, *Progress in Heat and Mass Transfer*, (6) 591, Pergamon, London, 1971.

30 J.J. Elmendorp and R.J. Maalcke, *Polym. Eng. Sci*., 25(16), 1041 (1985).

31 H.J. Van Oene, *J. Coll. Interf, Sci*., 40, 448 (1972).

32 W.J. Milliken and L.G. Leal, *J. Non. Newt. Fluid Mech*., 40, 335 (1991).

33 W.J. Milliken and L.G. Leal, *J. Non. Newt. Fluid Mech*., 42, 231 (1992).

34 S. Wu, *Polym. Eng. Sci*., 27 (5), 335 (1987).

35 P.G. Ghodgaonkar and U. Sundararaj, *Polym. Eng. Sci*., 36 (12), 1656 (1996).

36 L. Levitt and C. Macosko, *Polym. Eng. Sci*., 36 (12), 1647 (1996).

37 M. Doi and S.F. Edwards, *The Theory of Polymer Dynamics, Oxford Science* Publications, 1986.

38 J.W.S. Rayleigh, *Philosp. Mag*., 34, 145 (1892).

39 S. Tomotika, *Proc. Roy. Soc*., A150, 332 (1935).

40 J.J. Elmendorp, *Polym. Eng. Sci*., 26, 418 (1986).

41 H.B. Chin and C.D. Han, *J. Rheol*., 24 (1), 1 (1980).

42 A.K. Varshneya, *Fundamentals of Inorganic Glasses*, Academic Press, New York 1994.

43 R.H. Doremus, *Glass Science*, Wiley & Sons, New York 1973.

44 D.G. Baird and D.I. Collias, *Polymer Processing: Principles and Design*, Butterworth-Heinemann, Newton, Ma 1995.

45 H. Hessenkemper and R. Brückner, *Glastech. Ber*., 61, 312 (1988).

46 J.H. Simmons, R.K. Mohr, and C.J. Montrose, *J. Appl. Phys*., 53 (6), 4075 (1988).

47 J.H. Simmons, R.Ochoa, and K.D. Simmons, *J. Non-Cryst. Solids*, 105, 313 (1988).

48 J.H. Li and D.R. Uhlmann, *J. Non-Cryst Solids*, 3, 127 (1970).

49 S.J. Webb, *Phys. Chem. Minerals*, 19, 240 (1992).

50 N.H. Ray, C.J. Lewis, J.N.C. Laycock, and W.D. Robinson, *Glass Tech.*, 14 (2), 50 (1973).

51 N.H. Ray, C.J. Lewis, J.N.C. Laycock, and W.D. Robinson, *Glass Tech.*, 14 (2), 55 (1973).

52 R.L. Sammler, J.U. Otaigbe, M.L. Lapham, N.L. Bradley, B.C. Monahan, and C.J. Quinn, *J. Rheol*., 40 (2), 285 (1996).

53 H. Van Oene, *Polymer blends*, Vol. 1., ed. Paul and Newman, Acad. Press., New York 1978.

54 C.D. Han and Y.W. Kim, *Trans. Soc. Rheol*., 19, 245 (1975).

55 C.D. Han, Y.W. Kim, J. Parker, N. Siskovic, and C.R. Haung, *Appl. Polym. Symp*., 21, 191 (1973).

56 K. Iwakura and T. Fujimura, *J. Appl. Polym. Sci*., 19, 1427 (1975).

57 C.J. Quinn and G.H. Beall, in *Chem. Process. Adv. Mater*., ed. L. Hench, 799 (*1992*).

58 C.J. Quinn. P. Frayer, and G.H. Beall, in *Polymeric Materials Encyclopedia* (vol. 4), ed. J.C. Salamone, 2766 (1996).

59 J.U. Otaigbe, B.C. Monahan, C.J. Quinn, and G.H. Beall, *Polym. Comp*., 19(1), 18 (1998).

60 M.R. Kamal and A. Mutel, *J. Polym. Eng*., 5 (4), 293 (1985).

61 N. Minagawa and J.L. White, *J. Appl. Polym. Sci*., 20, 501 (1976).

62 J.L. White and J.W. Crowder, *J. Appl. Polym. Sci.*, 18, 1013 (1974).

63 T. Kataoka, T. Kitano, M. Sasahara, and K. Nishijima, *Rheol. Acta*, 17, 149 (1978).

64 T. Kataoka, T. Kitano, Y. Oyanagi, and M. Sasahara, *Rheol. Acta*, 18, 635 (1979).

65 B. Fisa and L.A. Utracki, *NRCC-IMRI Symposium on Rheology of Polymers*, 65th CIC Chem. Conf., Toronto, May 1982.

66 R.J. Crowson, M.J. Folkes, and P.F. Bright, *Polym. Eng. Sci*., 20, 925 (1980).

67 Y. Chan, J.L. White, and Y.J. Oyanagi, *J. Rheol*., 22, 507 (1978).

68 D.W. Sundstrom, *Rheol. Acta*, 22, 420 (1983).

69 F. Nazem and C.T. Hill, *Trans. Soc. Rheol*., 18 (1), 87 (1974).

70 F.M. Chapman and T.S. Lee, *SPE J*., 26 (1), 37 (1990).

71 C.D. Han, C. Sandford and H.J. Yoo, *Polym. Eng. Sci*., 18 (11), 849 (1978).

72 C.D. Han, *J. Appl. Polym. Sci*., 18, 821 (1974).

73 C.D. Han, T.V.D. Weghe, P. Shete, and J.R. Haw, *Polym. Eng. Sci*, 20, 925 (1980).

74 H.M. Laun, *Coll. Polym. Sci*., 262, 257 (1984).

75 T. Kitano, T. Kataoka, and Y. Nagatsuka, *Rheol. Acta*, 23, 20 (1984).

76 H. Tanaka and J.L. White, *Polym. Eng. Sci*., 20 (14), 949 (1980).

77 W.M. Lobe and J.L. White, *Polym. Eng. Sci.*, 19 (9), 617 (1979).

78 A.M. Shibley, *Handbook of Composites (Chap. 7)*, ed. G. Lubin, Van Nostrand Reinhold, New York 1982.

79 Schweizer and Winterman, *Thermoplastic Polymer Additives: Theory and Practice*, ed. J.T. Lutz, Jr., Marcxel Dekker, New York 1989.

80 B. Franzen, C. Klason, J. Kubat, and T. Kitano, *Composites*, 20 (1) 65 (1989).

81 S.H. Collins, *Plastics Compounding*, 5 (3), 113 (1982).

82 L.A. Utracki, *Rubber Chem. Tech*., 57, 507 (1984).

83 S.G. Advani, *International Encyclopedia of Composites (Vol. 3)*, ed. S.M. Lee. VCH New York 1990.

84 S. Kessler, *Plastics Additives and Modifiers Hanbook (Chap. 48)*, Ed. J. Edenbaum, Van Nostrand Reinhold, New York 1992.

85 P.K. Mallick, *Fiber-Reinforced Composites*, Marcel Dekker, New York 1988.

86 W.R. Graner, *Handbook of Composites*, ed. G. Ludin, Van Nostrand Reinhold, New York 1982.

87 S.F. Xavier and A. Misra, *Polym. Compos*., 6 (2), 93 (1985).

88 D.F. Hiscock and D.M. Bigg, *Polym. Compos*., 10 (3), 145 (1989).

89 J.C. Halpin and J.L. Kardos, *Polym. Eng. Sci*., 16 (5), 344 (1976).

90 D. McNally, *Polym. Plast. Tech. Eng*., 8 (2), 101 (1977).

91 T.S. Chow, *J. of Mat. Sci*., 15, 1873 (1980).

92 D.A. Cianelli, J.E. Travis, and R.S. Bailey, *43rd Ann. Cong., Composites Inc., The Society of the Plastics Industry*, Session 3-B, 1988.

93 D.A. Cianelli, J.E. Travis, and R.S. Bailey, *Plastics Tech*., 34 (4), 83 (1988).

94 R.W. Richards and D. Sims, *Composites*, 214 (1971).

95 J. Watkins, P. Gaa, and R. Swisher, *SPE ANTEC Tech. Papers*, 34, 258 (1988).

96 N. Sato, T. Kurauchi, S. Sato, and O. Kamigaio, *J. Compsite Mat*., 22 (9), 850 (1988).

97 E.P. Plueddemann, in *Silane Coupling Agents*, Plenum Press, New York, 1991.

98 R.W. Richards and D. Sims, *Composites*, Dec., 214 (1971).

99 M.G. Bader and J.F. Collins, *Fibre. Sci. Tech*., 18, 217 (1983).

100 M.W. Darlington, P.L. McGinley, and G.R. Smith, *J. Mat. Sci*., 11, 877 (1976).

101 M. Vincent and J.F. Agassant, *Two Phase Polymer Systems (Chap. 11)*, ed. L.A. Utracki, Hanser, New York 1991.

102 S.H. Lim, T. Kikutani, J.L. White, and T. Kyu, *Adv. Poym. Tech*., 8 (3), 325 (1988).

103 S.H. Lim and J.L. White, *J. Rheol*. , 34 (3), 343 (1990).

104 L.A. Goettler, *Mod. Plast*., 48, 140 (1970).

105 H.F. Giles and D.L. Reinhard, *Comp. Polym*., 5 (2), 90 (1991).

106 J. Schuster and K. Friedrich, *Appl. Comp. Mat.*, 1, 55 (1994).

107 A. Dutta, M. Niemeyer, and M. Cakmak, *Polym. Comp*., 12 (4), 257 (1991).

108 M. Hou, K. Friedrich, R. Scherer, *Comp. Struct*., 27 , 157 (1994).

109 R.K. Okine, D.H. Edison, and N.K. Little, *32nd International SAMPE Symposium*, 1417 (1987).

110 A.I. Isayev and P.R. Subramanian, *Polym. Eng. Sci*., 32 (2), 85 (1992).

111 J. Seppala, M. Heino, and C. Kapanen, *J. Appl. Polym. Sci*., 44 , 1051 (1992).

112 M. Heino and J. Seppala, *J. Appl. Polym. Sci*., 44 , 1531(1992).

113 D. Berry, S. Kenig, and A. Sigmann, *Polym. Eng. Sci*., 31 (6), 451 (1991).

114 D. Berry, S. Kenig, and A. Sigmann, *Polym. Eng. Sci*., 31 (6), 459 (1991).

115 H.J. O'Donnell and D.G. Baird, *Polym. Eng. Sci,* 36 (7) , 963 (1996).

116 H.J. O'Donnell and D.G. Baird, *Intl. Polym. Proc.*, 11 (3), 257 (1996).

117 H.J. O'Donnell and D.G. Baird, *Polymer*, 36 (2)

118 A. Datta and D.G. Baird, *Polymer*, 36(3), 505 (1995).

119 L.M. Smartt and D.G. Baird, *SPE ANTEC Tech. Papers*, 41 (II), 1428 (1995).

120 S.S. Bafna, J.P. de Souza, T. Sun, and D.G. Baird, *Polym. Eng. Sci.*, 33 (13), 808 (1993).

121 M.S. Silverstein, A. Hiltner, and E. Baer, *J. Appl. Polym. Sci.*, 43, 157 (1991).

122 D.G Baird, in *Polymeric Materials Encyclopedia* (vol. 5), ed. J.C. Salamone, 3207 (1996).

123 A.A. Handlos, *PhD Dissertation*, Virginia Polytechic Institute and State University, Blacksburg, VA (1994).

124 H.J. O'Donnell , A. Datta, and D.G. Baird, SPE ANTEC Tech. Paper, 38, 2248 (1992).

125 S.K. Karg and S. Kenig, *High Modulus Polymers*, ed. A.E. Zachariades and R.S. Porter, Marcel Dekker, New York 1988.

126 Z. Tadmor, *J. Appl. Polym. Sci*., 18, 1753 (1974).

127 A. Siegmann, A. Dagan, and S. Kenig, *Polymer*, 26, 1325 (1985).

128 G. Crevecouer and G. Broeninkx, *Polym. Eng. Sci.*, 30 (9), 532 (1990).

129 T. Limtasiri and A.I. Isayev, *J. Appl. Polym. Sci*., 42, 2923 (1991).

130 M.J. Folkes, Multicomponent Polymer Systems (Chap. 8), ed. I.S, Miles, John Wiley and Sons, New York (1992).

131 J.P. de Souza, *PhD Dissertation*, Virginia Polytechic Institute and State University, Blacksburg, VA (1994).

132 A.I. Asayev and R. Viswanathan, *Polymer*, 36 (8), 1585 (1995).

133 R. Ding and A.I. Isayev, *J. Therm. Comp. Mat*., 8, (1995).

134 N.H. Ray and F.R. Sherliker, U.S. Patent 3,732,191 (1973).

135 W.A. Bahn, G.H. Beall, J. Ference, B.C. Monahan, C.J. Quinn, and P.S. Roussel, U.S. Patent 5,043,369 (1991).

136 C.J. Quinn and G.H. Beall, *ACS Polymer Preprints*, 32 (2), 205 (1990).

137 G.H. Beall and C.J. Quinn, *Ceram. Trans*., (33), 321 (1993).

138 C.J. Quinn and G.H. Beall, in *Chem. Process. Adv. Mater*., ed L. Hench, 799 (1992).

139 C.J. Quinn, G.H. Beall, J. Dickenson, *Int. Cong. Glass*, 16 (4), 79 (1992).

140 Plastics Digest, 17 (2), D.A.T.A. Business Publishing, Englewood, CO (1996).

Chapter 3: Processing Effects

Preface

This chapter addresses the first objective of the research. Specifically, the effects of processing variables on the mechanical properties of injection molded composites consisting of polyphenylene sulfide reinforced with a melt processable phosphate glass were examined. The influence of variables such as resin viscosity, melt temperature, and mold filling rate were evaluated to maximize the amount of reinforcement attained with the addition of the phosphate glass. This chapter is organized as a manuscript for future publication.

The Influence of Processing Variables on Injection Molded In Situ Composites Based on Polyphenylene Sulfide and a Melt Processable Glass

R.T. Young and D.G. Baird

Department of Chemical Engineering and
NSF Science and Technology Center for High Performance
Polymeric Adhesives and Composites

Virginia Polytechnic Institute and State University
Blacksburg, VA 24061-0211

(ABSTRACT)

This work was concerned with addressing how processing variables such as resin viscosity, melt temperature and mold filling rate influenced the mechanical properties of injection molded composites consisting of polyphenylene sulfide (PPS) reinforced with a melt processable phosphate glass. During injection molding, both the PPS and melt processable glass were deformable allowing the reinforcing phase morphology to be developed during the filling of the mold. Processing variables such as resin viscosity, mixing history, melt temperature, and mold filling rate were investigated to help maximize the reinforcing contribution of the melt processable glass. It was determined that a higher viscosity resin preblended and molded at melt temperatures greater than 330°C led to the formation of composites with the highest mechanical properties. For a composite blend containing 40 wt% (26 vol%) investigated, the utilization of the optimum processing conditions led to the formation of composites that offered machine direction moduli 2-3 times greater than that of the neat PPS.

3.1 Introduction

The addition of high aspect ratio inorganic reinforcement, such as glass fiber, has allowed the production of composite systems that possess moduli and strengths significantly greater than that of neat thermoplastics. While the addition of solid reinforcement often results in significant enhancements in mechanical properties, it can also lead to numerous problems in injection molding. During injection molding the presence of solid fibers can result in wear on various parts such as the screw, barrel, and mold. The complex interactions between the fibers and flow field seen during molding can

lead to molded products that suffer from a variety of problems such as anisotropy in properties, weld line formation, and poor surface appearance [1,2].

Due to the processing difficulties created by the addition of solid reinforcement, work has been performed on the development of alternative composite systems that overcome many of the problems associated with conventional short fiber reinforced thermoplastics. One such method referred to as in situ composite manufacturing relies on the formation of the reinforcing phase morphology during processing [3]. During processing operations, both the thermoplastic matrix and reinforcing phase are fluid, thereby alleviating many of the problems seen with conventional solid reinforced systems. The final reinforcing phase morphology can be developed from deformation applied through a variety of processing techniques such as injection molding, fiber spinning, and film casting.

One material that has shown great promise for in situ composite generation techniques are melt processable glasses [4-7]. These inorganic glasses have low glass transition temperatures (200-350°C) allowing them to be combined with thermoplastic resins for use in conventional polymer processing techniques. The lower thermal transition temperatures for these materials are obtained by utilizing P_2O_5 instead of SiO_2 as the primary glass former. Additional materials such as alkali and alkaline earth oxides are added in order to help control the thermal transitions and chemical durability of the glasses [6]. Due to their structure, phosphate based glasses typically display lower mechanical properties than borosilicate glasses commonly utilized in the reinforcement of thermoplastics. The utilization of phosphate glasses in engineering applications has been limited due to poor chemical durability of the glass. Present research is being focused on formulating melt processable glasses with lower transition temperatures and improved chemical durability [8-10]. The development of more durable glasses with lower transition temperatures could make these materials a viable alternative reinforcing phase for a variety of composite fabrication techniques.

Investigations of phosphate glass as a reinforcement for thermoplastics have mainly concentrated on injection molding applications[4-7]. Much of the work has involved the blending of a variety of thermoplastics with a number of glasses in order to ascertain the properties that could be achieved. In recent years, the development of glasses with lower transition temperatures and increased chemical durability have shown great promise for injection molding applications. For example Bahn, Quinn, and co-workers [5-7] injection molded composites consisting of higher transition glasses (225°C $< T_g <$ 350°C) blended with higher performance thermoplastics such as polyetherimide (PEI), polyethersulfone (PES), polyetheretherketone (PEEK), polyetherketone (PEK), and thermotropic liquid crystalline polymers (TLCPs). Much of the work performed concentrated on higher glass loadings (50-70 vol%) because P-glass composites manufactured with conventional glass loadings (up to 40 vol%) appeared to offer only modest increases in mechanical properties relative to those obtained with E-glass.

Composites reinforced with high loadings of phosphate glass had tensile moduli 4-10 times greater than those of the neat resins. For example, an injection molded PEK composite containing 70 vol% phosphate glass had a tensile modulus of approximately 30 GPa while the neat thermoplastic resin only had a modulus of 4 GPa. In addition to greater stiffness, phosphate glass reinforced composites were shown to offer other advantages such as low anisotropy, finer molding tolerances, greater resistance to creep and stress relaxation, and lower thermal expansion coefficients [6,7]. One of the drawbacks found with utilizing such high inorganic loadings was that the tensile strengths of the composite blends were found to fall below that of the neat resins.

While a number of thermoplastics reinforced with phosphate glasses have been investigated under injection molding, limited studies have been conducted on the effects of processing parameters on the morphology and properties of P-glass reinforced composites. Work performed by Bahn and Quinn [11] investigated the role of parameters such as glass concentration and material viscosities on the morphology of extruded composites consisting of polyaryletherketones (PAEK) reinforced with a phosphate glass. At low glass loadings (10-40 vol%), limited dispersion of the glass was obtained within a twin screw extruder resulting in a glass microstructure consisting of large glass particles (>100 μm) interdispersed with fine glass spheres on the order of 2-3 μm. Increasing the glass loading to 40-65 vol% resulted in a glass microstructure consisting of well dispersed spherical particles (2-3 μm). The formation of the well dispersed morphology was attributed to increased glass particle interactions which led to the elongation of the glass phase into strands which eventually reached a critical diameter and broke into spherical particles. It was also found that lower viscosity ratios between the polymer and glass resulted in smaller dispersed glass phases. The lower viscosity ratios between the glass and polymer matrices were achieved through a variety of techniques including the utilization of higher processing temperatures and higher viscosity thermoplastic resins. Composite blends containing high glass loadings (>65 vol%) were found to undergo phase inversion with the polymer resin being present as dispersed droplets. The phase inversion also appeared to be linked to factors such as the glass loading and the viscosity differences between the glass and thermoplastic resin.

Variations in composite morphologies through injection molding were investigated by Quinn and coworkers [6] for a thermotropic liquid crystalline polymer (Xydar) reinforced with a zinc alkali phosphate glass. A variety of reinforcing morphologies consisting of small glass beads, fibers, and ribbons were produced using a high speed injection molding unit capable of screw forward speeds up to approximately 1000 mm/s. High speed injection molding was utilized due to the high thermal conductivity and rapid solidification of the composite blends which contained up to 62 vol% phosphate glass. The transition of the glass morphology from beads to elongated ribbons was found to result in significant increases in the composite's mechanical properties. For a blend containing 62 vol% glass, a morphology consisting of small glass beads yielded a tensile modulus of 17 GPa while a morphology consisting of glass ribbons resulted in tensile modulus of 28 GPa.

Similar enhancements in the strength were observed with the transition in morphology elevating the tensile strength from 52 MPa to 72 MPa. Even though a variety of data was presented on the effects of the various morphologies on the properties of the composites, no correlations were made between the formation of the composite morphology and processing conditions utilized.

For other in situ composite systems, the formation of the reinforcing phase morphology during molding has been shown to be dependent on a complex interaction between both material and processing parameters [12-17]. Material parameters such as the viscosity ratio and interfacial tension between the various phases have been shown to play key roles in the formation of the reinforcing phase morphology [14-17]. Factors such as the stress fields and heat transfer have also been found to affect the mechanical properties of in situ composites which used TLCPs as the reinforcing phase [13,14]. For example, O'Donnell [14] studied the effects of mold thickness, viscosity ratio, melt temperature and mold fill rate on the properties of a polypropylene/maleic anhydride grafted polypropylene blend reinforced with 30 wt% of a TLCP (LC3000, a copolyester of polyethylene terephthalate and hydrobenzoic acid). The highest mechanical properties were obtained when a fibrillar reinforcing morphology was generated within the skin regions of the molded samples. This was promoted when the PP/TLCP viscosity ratio was approximately one and the storage and loss moduli of the TLCP melt were approximately equal. It was also found that variations in the stresses and heat transfer obtained by varying the mold thickness and injection rate could lead to composites displaying a wide range of properties. Processing conditions which generated higher stresses and prolonged the deformation of the reinforcing phase during mold filling were generally found to produce composites with the highest level of reinforcement. It was also believed that processing conditions which allowed the elongated TLCP fibrils to solidify before they had a chance to breakup due to interfacial instabilities maximized the reinforcement attained with the addition of the TLCP.

The formation of the reinforcing phase morphology within in situ composites has often been analyzed in terms of the theories developed for droplet deformation and breakup for Newtonian fluids. Work performed with Newtonian fluids established that a dispersed droplet can be elongated into a higher aspect ratio thread when exposed to either shear or elongational flow under certain conditions [18-23]. Deformation of the suspended droplet typically occurs when the disruptive hydrodynamic force is great enough to overcome the cohesive interfacial force between the components. The magnitude of the hydrodynamic force (stress) will depend strongly on the applied deformation rates as well as the rheological properties of the components. The viscosity ratio between the components (ratio of droplet to matrix viscosity) has also been found to have a large effect on the ability of the suspended phase to undergo deformation. Within simple shear flow, viscosity ratios between 0.1 and 3.5 have been shown to lead to conditions favorable to the deformation and eventual breakup of suspended droplets. Meanwhile, shearfree or extensional flows provide conditions favorable to the deformation

of the suspended phase over a much wider range of viscosity ratios. Trends similar to those seen with Newtonian fluids have been qualitatively observed in regards to the formation of the reinforcing morphology within in situ injection molded composites [12-17]. The extensional flow field generated from the advancing front during mold filling has been found to lead to the formation of elongated fibrillar morphologies over a broad range of viscosity ratios. Regions within the molded injection specimens where shear flow was predominant often contained lower aspect ratio domains due to the inability of the flow field to adequately deform the reinforcing phase.

The purpose of this paper is to determine if the mechanical properties of injection molded blends of polyphenylene sulfide reinforced with a melt processable glass are sensitive to injection molding conditions. By investigating a range of processing variables, it will then be possible to obtain the maximum deformation of the glass reinforcing phase resulting in composites with the highest possible mechanical properties. In particular, the effects of processing variables including mixing history, melt temperature, mold fill rate, and resin viscosity on the composite ultimate mechanical properties are investigated.

3.2 Experimental

3.2.1 Materials

The melt processable phosphate glass used in this study was an experimental material supplied by Corning, Inc. (Corning, NY). This particular phosphate glass is composed of P_2O_5 (33 mol%), $ZnCl_2$ (26 mol%), B_2O_3 (4 mol%) and M_2O (37 mol%) where M consists of various alkali metals. The glass utilized is considered non-durable in that the material suffers from a loss in weight and mechanical properties when exposed to hot water. The glass samples were received as large shards that were crushed and sorted to yield particles ranging from 1-2 mm for use in injection molding. For rheological studies, the glass shards were ground to yield disks with thicknesses ranging from 1-2 mm. The glass transition temperature for the glass was found to be 233.7 ± 2.2°C based on differential scanning calorimetry (DSC) measurements performed at a heating rate of 10°C/min. The density of the glass was determined to be 2.62 ± 0.01 g/cm^3 from measurements made on as received glass samples utilizing a pyconometer (Micrometrics Accupyc, Model 1330).

Polyphenylene sulfide (PPS) was utilized as the matrix resin for the injection molding studies. Polyphenylene sulfide is a semi-crystalline engineering thermoplastic that has good mechanical properties, excellent chemical resistance, high temperature thermal stability, and inherent flame resistance[24]. Two grades of PPS consisting of Ryton PR09 supplied by Phillips Chemical Company and Fortron 0320 provided by Hoechst Celanese were investigated. The Ryton PR09 is an extrusion grade of PPS possessing a glass transition temperature of 91°C, a melting point of 279°C, and a density of 1.40 g/cm^3.

The Fortron 0320 is also an extrusion grade of resin having a glass transition temperature of 93°C, a melting temperature 283°C, and a density of 1.40 g/cm^3. The Ryton is a high molecular weight material possessing long chain branching and ionic endgroups while the Forton is a linear, fractionated material where the ionic groups have been neutralized by acid washing [25]. The mechanical properties of injection molded neat samples of the various grades of PPS are presented in Table 3.1. As shown by the table, the various grades of PPS show no significant differences in mechanical properties with both neat resins offering a balance of properties in terms of stiffness and strength.

3.2.2 Rheological Characterization

Rheological characterization of the neat thermoplastics and glass samples was performed using parallel plate fixtures attached to a Rheometrics Mechanical Spectrometer (Model RMS-800). Dynamic oscillatory measurements were carried out under a variety of conditions depending on the materials being investigated. The complex viscosity ($|\eta^*|$) of the PPS was determined from test specimens consisting of pellets of the neat resin loaded between 25 mm diameter plates. For the glass samples, test specimens consisted of pre-ground disks having thicknesses ranging from 1-2 mm and a diameter of either 7.9 or 25 mm. Smaller diameter plates (7.9 mm) were utilized with the glass under certain conditions in order to generate lower strains and help insure measurements did not exceed the compliance of the instrument. Each sample was brought to the desired temperature and allowed to equilibrate for a least three minutes before the start of testing. The sample temperature was monitored by a thermocouple in contact with the lower plate fixture. The temperature was maintained by blanketing the sample with heated nitrogen in order to minimize degradation. Before rheological testing, samples were dried for a least 24 hours in a vacuum oven maintained at 150°C.

The thermal stability of the phosphate glass and the two grades of PPS was analyzed by monitoring the complex viscosity with time under isothermal conditions. Samples were loaded between the parallel plates with the initiation of data collection occurring once the desired temperature was achieved. Complex viscosity data were obtained at an angular frequency (ω) of 1 radian/second (rad/sec) using strains ranging from 5-10% for PPS and 0.1-0.5% for the phosphate glass. Time sweeps were performed for a period of ten minutes to help establish the stability of the materials during further rheological testing and injection molding.

The complex viscosity of the various materials was also determined by varying the angular frequency while holding the sample temperature constant. For the PPS samples, angular frequency sweeps were performed at strain rates ranging from 10-30%. For the neat glass samples, angular frequency sweeps were performed at the lowest possible strains (0.1-1%) that allowed adequate resolution of the transducer torque signal (≥ 0.2 gm·cm). The lowest possible strains were utilized in anticipation the glass would show the

Table 3.1: Machine Direction Properties of Injection Molded Neat PPS

Resin	Tensile Properties			Flexural Properties	
	Modulus (GPa)	**Strength (MPa)**	**% Elong.**	**Modulus (GPa)**	**Strength (MPa)**
Ryton PR09	3.14 (0.17)	76.9 (1.33)	3.62 (0.45)	4.05 (0.11)	113.0 (3.3)
Fortron 0320	3.06 (0.10)	76.4 (1.21)	3.52 (0.33)	3.70 (0.06)	108.5 (2.2)

Note: % Elong. = Elongation to yield; Standard deviations given in parentheses

lowest strain dependence at these conditions allowing testing to occur in the linear viscoelastic region.

In order to study the processing behavior of the materials under the nonisothermal conditions similar to those seen during mold filling, the complex viscosity of the samples was monitored as the samples were cooled from a specified temperature. Samples were held at the desired temperature for a brief period (≈ 3 minutes) and then cooled at a rate of approximately 2.5°C/min while the complex viscosity was monitored at an angular frequency of 1 rad/sec. The strain applied during testing was reduced as the sample viscosity rose to insure the measurements stayed within the linear viscoelastic region. The neat PPS sample measurements were performed with 25 mm diameter plates while 7.9 mm plates were utilized for the glass in order to generate lower strains.

3.2.3 Injection Molding

Composite blends were produced using an Arburg Allrounder, model 221-55-250, injection molding unit. The molder has a 22 mm screw with a check ring non-return valve and was fitted with a general purpose nozzle having a 2 mm exit diameter. For this study, the injection molding unit was used for two main processing steps including preblending and actual composite manufacture. All materials used during processing were dried for at least 24 hrs at 150°C under vacuum before being plasticated.

The first processing step involved utilizing the injection molding unit as an extruder to preblend the glass with the PPS. Due to the variety of blends to be studied and the limited availability of the phosphate glass, the molding unit was seen as an effective way to preblend small batches of composite material. The initial dispersion of the glass within the thermoplastic matrix could be achieved rapidly while minimizing thermal degradation of the matrix resin at the higher processing temperatures.

For preblending, the barrel assembly frame was released from the mold assembly and modified to run as an extruder by adjusting the back pressure so the material would flow freely from the nozzle. A dry blend of the glass and PPS was passed through the screw operating at 200 rpm with the extrudate being collected, quenched, and granulated using a Cumberland Granulator (Model 6x8). This granulated material was then subsequently used as feed stock for the injection molding studies. Two different barrel temperature profiles were investigated as possible blending conditions for the melt processable glass/PPS composites. The first temperature profile, progressing from the solids conveying zone to the nozzle was: 330°C, 330°C, 330°C, and 330°C. The second temperature profile investigated involved maintaining the solid conveying zone temperature at 330°C while elevating all other zone temperatures to 350°C.

The second main processing step involved the fabrication of the composite blend into test specimens by injection molding. Composite plaques were produced by injecting the plasticated blend into a film-gated mold having dimensions of 75 mm by 80 mm by 1.6 mm. During molding operations the injection pressure (5 MPa), holding pressure (10 MPa), screw speed (200 rpm), and mold temperature (140°C) were held constant. A mold temperature of 140°C was utilized to help insure the PPS developed an adequate degree of crystallinity [24]. The barrel temperature profiles investigated were the same as those used in preblending step. The effect of processing conditions on the properties of the injection molded composites was also investigated by varying the volumetric flowrate of material into the mold. The volumetric flowrates investigated varied in a range from approximately 7 to 33 cm^3/sec. The volumetric flowrate into the mold was estimated from the total volume of the mold cavity including the plaque, gate, runner and sprue (13.9 cm^3) divided by the time taken to advance the screw from the retracted to the fully forward position.

3.2.4 Mechanical Properties

The tensile and flexural properties of the various composite blends were measured using an Instron Mechanical Tester (Model 4204). Test specimens approximately 75 mm long by 8 mm wide were cut from the injection molded plaques along both the machine (flow) and transverse directions. Tensile properties were measured using a 5 kN load cell following ASTM standard B 638-87B. The crosshead speed was kept constant at 1.27 mm/min with the strain imposed on the sample measured using an extensionmeter (Instron Model 2630-25). Flexural properties were measured using a three-point bending test following ASTM standard D 790M 86. All the mechanical properties reported are the average of at least five test samples.

3.2.5 Morphology

The morphology of the composite injection molded plaques was examined using a Stereoscan S200 scanning electron microscope with an accelerating voltage of 20 kV. The surfaces examined were prepared by immersing the sample in liquid nitrogen for approximately 5 minutes before fracturing. The samples were subsequently attached to mounting studs and coated with a layer of gold using a sputter coater (Bal-Tec Model SCD 005) to enhance conductivity.

3.3 Results and Discussion

3.3.1 Rheological Characterization

Rheological characterization was performed on the neat resins as well as the phosphate glass to help ascertain the effects of various thermal and deformation histories

on the response of the materials. The rheological testing was seen as an effective way to determine the processing conditions that would facilitate the dispersion and deformation of the phosphate glass phase during processing.

During processing, it desirable to utilize temperatures that would minimize the degradation of the components which could have a detrimental effect on the overall properties of the finished composite. For PPS, processing temperatures no greater than 330°C are often utilized to help minimize the complex chain scission and crosslinking reactions that are known to occur in the melt [24]. The thermal stability of both the PPS and phosphate glass at this temperature was investigated by monitoring the evolution of the material's complex viscosity with time. At a temperature of 330°C, both the Phillips (Ryton PR09) and Celanese (Fortron 0320) materials appeared stable showing only a 5-10% loss in complex viscosity over a 10 minute time period (Figure 3.1). In the case of the phosphate glass, the complex viscosity rose slightly during testing indicating the possible formation of crystalline regions. The formation of crystalline regions in phosphate glasses above the glass T_g has been seen by several investigators [26-28]. The formation of these crystalline regions has been found to be dependent on a number of variables including the glass composition, temperature and the applied strain and is an area open to much investigation. It is desirable to avoid processing conditions that could lead to a rapid rise in the glass viscosity which would serve to limit the deformation of the glass phase within the composite blend and possibly result in fouling of the equipment.

Because both materials appeared thermally stable at 330°C, the viscosity ratios between the various materials was estimated using dynamic angular frequency sweeps. The complex viscosity as a function of angular frequency for PPS and phosphate glass is shown in Figure 3.2. For the angular frequencies investigated, the phosphate glass showed predominately Newtonian behavior with the complex viscosity being on the order of 30,000 Pa·s. The thermoplastic resins displayed much lower complex viscosities with the Ryton and Fortron displaying varied responses with angular frequency. The Fortron 0320 exhibited predominately Newtonian behavior with the complex viscosity falling almost two orders of magnitude lower than the phosphate glass. The Ryton displayed a zero shear viscosity almost twice that of the Forton, with the complex viscosity approaching that of the Fortron at the highest angular frequencies analyzed (100 rad/sec). Assuming the Cox-Merz rule [i.e. $|\eta^*(\omega)| \approx \eta(\dot{\gamma})$] applies for the materials investigated, the viscosity ratios (η_{glass}/η_{PPS}) for both grades of PPS were on the order of 50-100. Even though both materials were stable at 330°C, it appeared that the high viscosity of the phosphate glass coupled with the unfavorable viscosity ratios between the PPS and glass (i.e. $\eta_{glass}/\eta_{PPS} >> 1$) may limit the deformation and dispersion of the suspended glass.

Because it appeared that processing at 330°C would lead to unfavorable viscosity ratios, the response of the materials was analyzed at higher temperatures. The thermal stability for both the PPS and phosphate glass was investigated for a temperature of 350°C

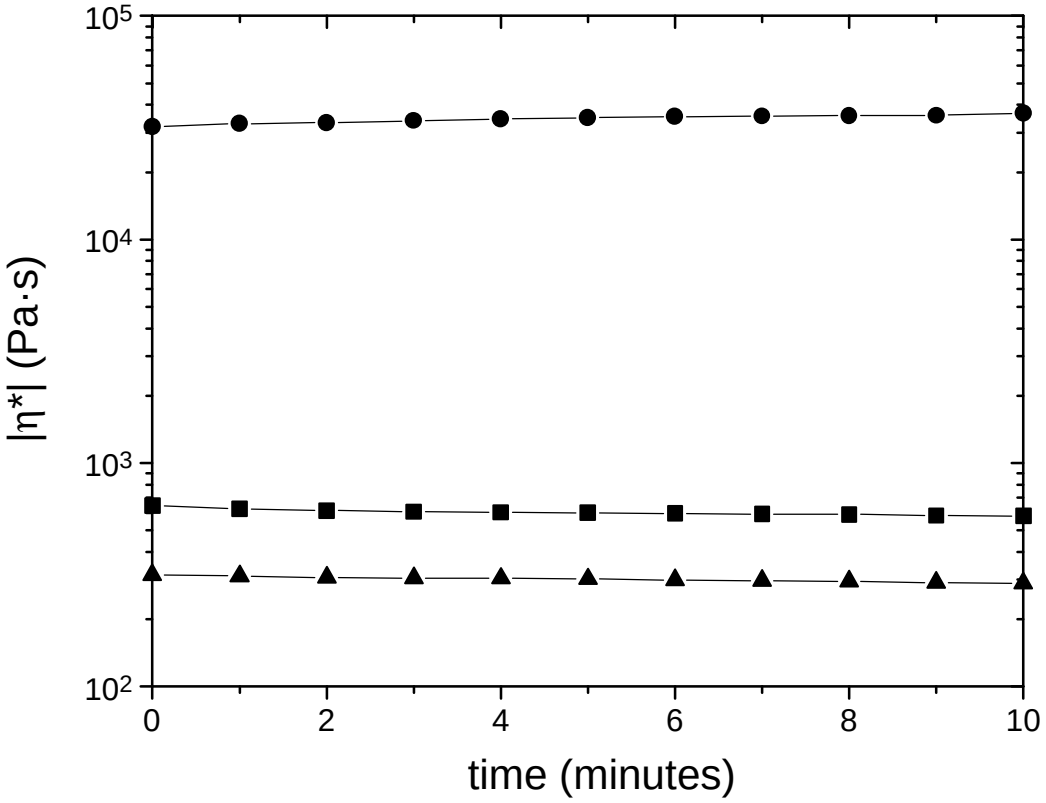

Figure 3.1: Evolution of complex viscosity (|η*|) versus time for neat PPS and P-glass at 330.2 ± 0.1°C. (●) P-glass, (■) Ryton PR09, and (▲) Fortron 0320.

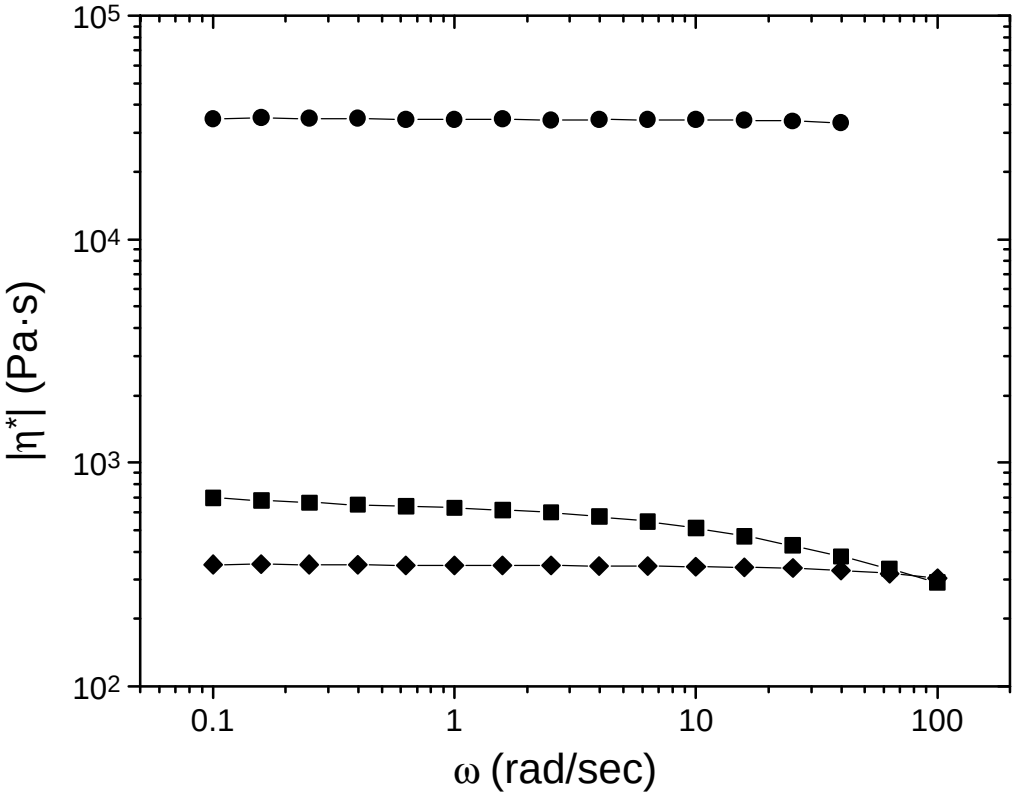

Figure 3.2: Complex viscosity (|η*|) versus angular frequency for neat PPS and P-glass at 330.1 ± 0.1°C. (●) P-glass, (■) Ryton PR09, and (▲) Fortron 0320.

(Figure 3.3). At these conditions, the glass appeared stable while the two grades of PPS showed significant losses in complex viscosity (25-30%) over a ten minute time period. Even though it appeared that PPS undergoes some degradation at 350°C, the increase in temperature significantly lowered the viscosity of the P-glass resulting in more favorable viscosity ratios with the PPS. As can be seen in Figure 3.4, increasing the temperature to 350°C lowered the viscosity ratios between the glass and PPS to approximately 10 over the range of angular frequencies investigated. Therefore, a higher processing temperature on the range of 350°C would appear to possibly lead to slight degradation of the PPS but would result in substantially lower viscosity ratios between the phosphate glass and PPS. These lower viscosity ratios in turn would possibly result in conditions more favorable to deformation of the glass phase.

In an effort to gauge the effects of temperature on the viscosity ratios seen between the phosphate glass and PPS during processing, samples were cooled within the rheometer at rate of approximately 2.5°C/min while monitoring the evolution of the complex viscosity. The complex viscosities of the phosphate glass and both grades of PPS as function of temperature are presented in Figure 3.5. The phosphate glass showed a rapid rise in viscosity with temperature indicative of the large activation energies found with inorganic glasses of this type[27]. Both the Fortron and Ryton displayed a much lower viscosity over the temperature ranges investigated with both showing the onset of crystallization at a temperature of approximately 235°C, almost 50°C below the melting point of PPS. From the starting temperature of 350°C, the viscosity ratios between the P-glass and PPS were unfavorable with a rapid divergence in the complex viscosity as the materials were cooled.

3.3.2 Effects of Mixing History

In order to determine if mixing history had an effect on the properties of the phosphate glass reinforced systems, a limited injection molding study was performed for a few select blends. From rheological testing, it appeared that the Phillips Ryton PR09 processed with the phosphate glass at temperature of 350°C would provide the most favorable conditions for obtaining dispersion and deformation of the phosphate glass. Composite blends consisting of Ryton reinforced with 40 and 60 wt% P-glass were prepared by two different methods. The first method involved tumbling the PPS and glass together to form a dry blend that was fed directly into the injection molder to form the composite plaques. The second method involved preblending the PPS and glass by running the material through the molding unit operating as an extruder. The blended extrudate was collected, quenched, and granulated for the subsequent injection molding step. For each processing operation (i.e. blending and injection molding), the temperature profiles within the molding unit were kept constant with the maximum barrel temperatures being set to 350°C. The composite samples were all molded under the same conditions using a mold temperature of 140°C with a mold fill rate of approximately 10 cm^3/sec.

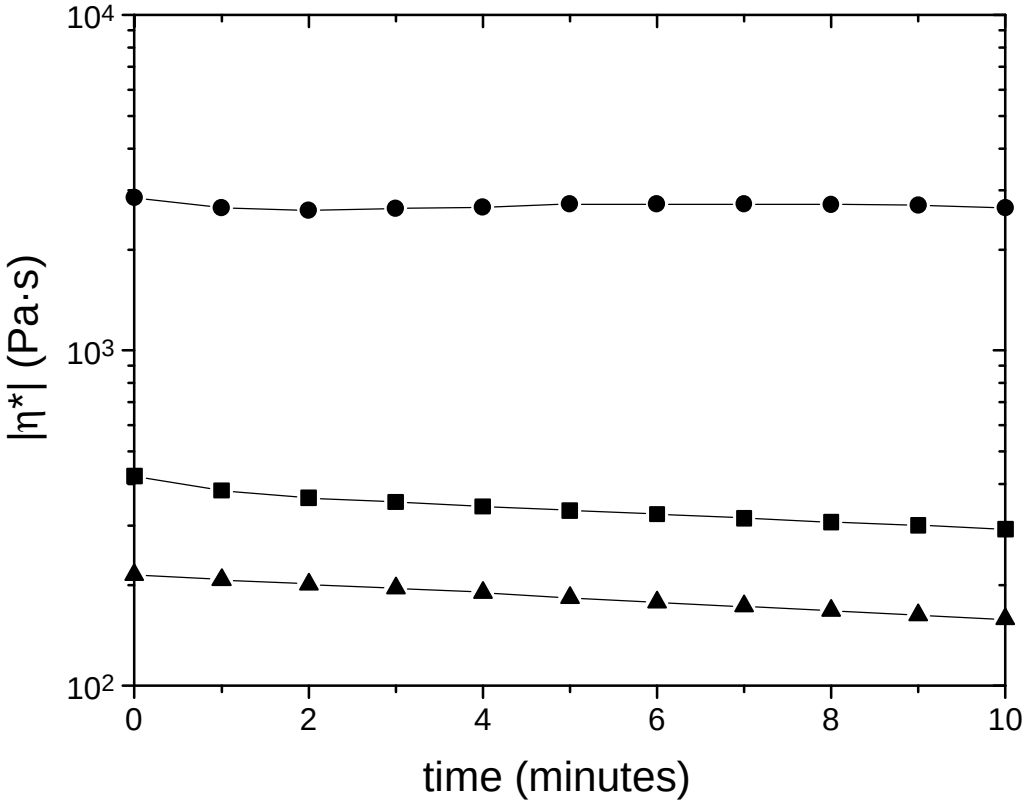

Figure 3.3: Evolution of complex viscosity (|η*|) versus time for neat PPS and P-glass at 350.2 ± 0.1°C. (●) P-glass, (■) Ryton PR09, and (▲) Fortron 0320.

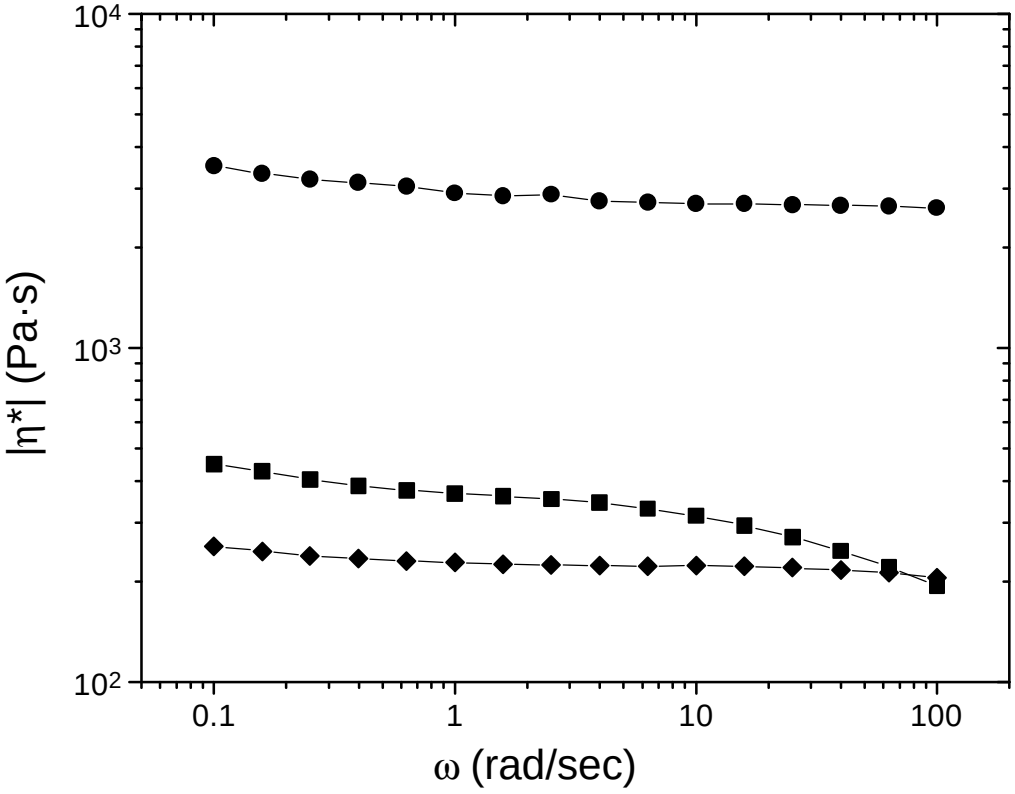

Figure 3.4: Complex viscosity (|η*|) versus angular frequency for neat PPS and P-glass at 350.0 ± 0.1°C. (●) P-glass, (■) Ryton PR09, and (▲) Fortron 0320.

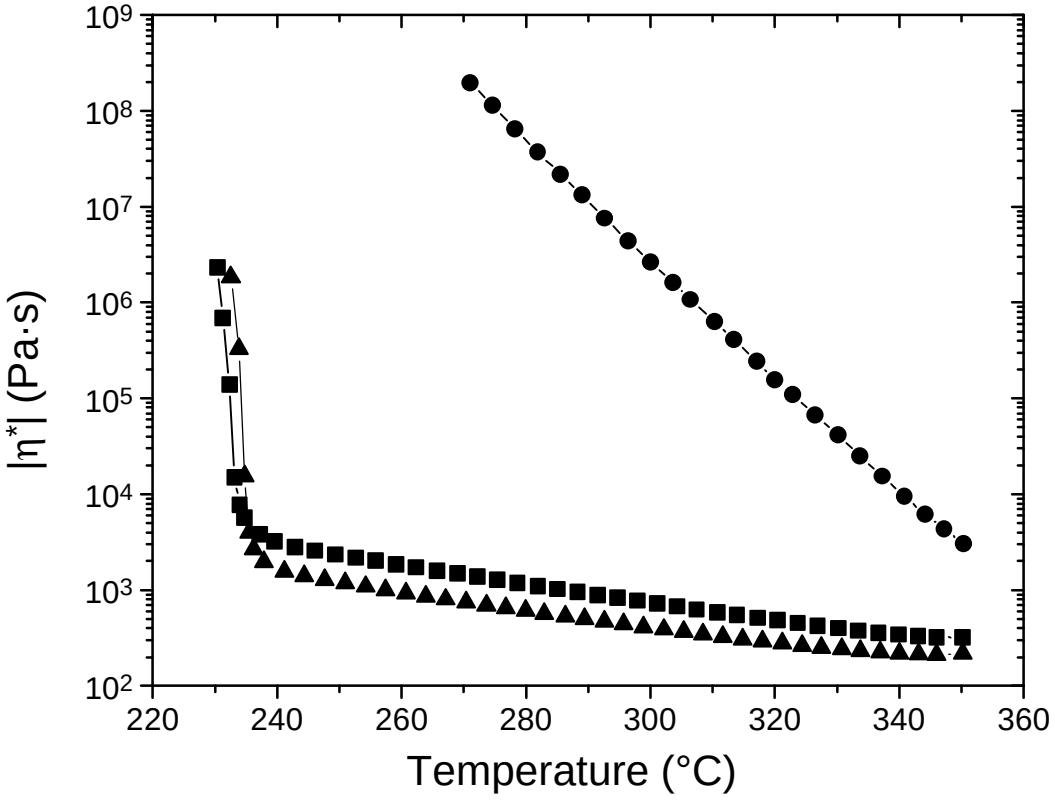

Figure 3.5: Complex viscosity (|η*|) versus temperature for PPS and phosphate glass using a cooling rate of 2.4 ± 0.1°C/min. (●) P-glass, (■) Ryton PR09, and (▲) Fortron 0320.

The effects of varying the mixing history on the properties of the composite blends can be seen in Table 3.2. For the composite blends investigated, preblending did not appear to lead to any significant improvement in the machine direction tensile properties. The largest impact of preblending was found in the flexural properties of the various blends. For both glass loadings investigated, the flexural modulus and strength showed a significant improvement with preblending. For both the 40 wt% and 60 wt% P-glass filled blends, the additional mixing led to an improvement in the flexural modulus on the order of 1.4 GPa. The flexural strength of both blends also showed improvement with mixing with the blend containing 60 wt% P-glass showing the greatest enhancement with a 30% increase in the strength. The effects of preblending on the composite morphology of the injection molded samples containing 60 wt% glass were examined by scanning electron microscopy (Figure 3.6). The micrographs revealed that the additional mixing led to enhanced dispersion of the glass phase within the thermoplastic matrix. The pre-blended composite possessed a more uniform distribution of smaller glass domains than the comparable composite manufactured by just dry blending the polymer and glass. It is believed that the presence of these smaller domains facilitated the formation of a reinforcing morphology that resulted in an enhancement of the composite's machine direction properties.

3.3.3 Composite Mechanical Properties

In an effort to obtain composites with the optimum mechanical properties, the two grades of PPS blended with 40 wt% (≈ 26 vol%) phosphate glass were processed under a variety conditions. Processing temperatures of 330°C and 350°C as well as a variety of mold fill rates were investigated. The PPS and glass were preblended using a maximum processing temperature of either 330°C or 350°C with the subsequent injection molding being performed using the same temperature profile. The rate at which material was injected into the mold was varied to determine if deviations in the stress fields and heat transfer seen during processing had an impact on the final composite mechanical properties. Other processing variables such as mold temperature (140°C), cooling time (45 seconds), injection pressure (5 MPa), and holding pressure (10 MPa) were held constant.

In an attempt to minimize the degradation of the PPS during processing, a maximum processing temperature of 330°C was first investigated. Both the Ryton PR09 and Fortron 320 were preblended with the glass and subsequently injected into the mold at a variety of injection rates ranging from approximately 7 to 33 cm^3/second. The effects of varying the injection rate on the machine direction properties of the composite blends processed at 330°C are shown in Table 3.3. For both the Fortron and Ryton based blends, the variations in injection rate had the greatest impact on the flexural properties along the machine direction. For the Ryton based blend, utilizing the lowest injection rate yielded a composite that had a flexural modulus of 7.39 GPa (± 0.17 GPa) with a flexural strength of 104.6 MPa (± 3.6 MPa). Increasing the injection rate to the maximum value allowed

Table 3.2: Effects of Mixing History on the Machine Direction Properties of Injection Molded PPS/Phosphate Glass Blends

Ryton PR09 with 40 wt% P-glass					
	Tensile Properties			**Flexural Properties**	
Mixing History	**Modulus (GPa)**	**Strength (MPa)**	**% Elong.**	**Modulus (GPa)**	**Strength (MPa)**
Dry blended	7.70 (0.25)	50.9 (7.47)	0.75 (0.16)	7.82 (0.48)	111.5 (5.0)
Preblended	7.87 (0.38)	58.3 (3.56)	0.71 (0.08)	9.28 (0.33)	126.8 (5.2)
Ryton PR09 with 60 wt% P-glass					
	Tensile Properties			**Flexural Properties**	
Mixing History	**Modulus (GPa)**	**Strength (MPa)**	**% Elong.**	**Modulus (GPa)**	**Strength (MPa)**
Dry blended	11.0 (0.40)	44.6 (4.24)	0.48 (0.06)	13.6 (0.76)	90.8 (5.7)
Preblended	12.4 (0.57)	47.1 (5.96)	0.38 (0.06)	15.0 (0.41)	120.9 (2.5)

Note: % Elong. = Elongation to break; Standard deviations given in parentheses

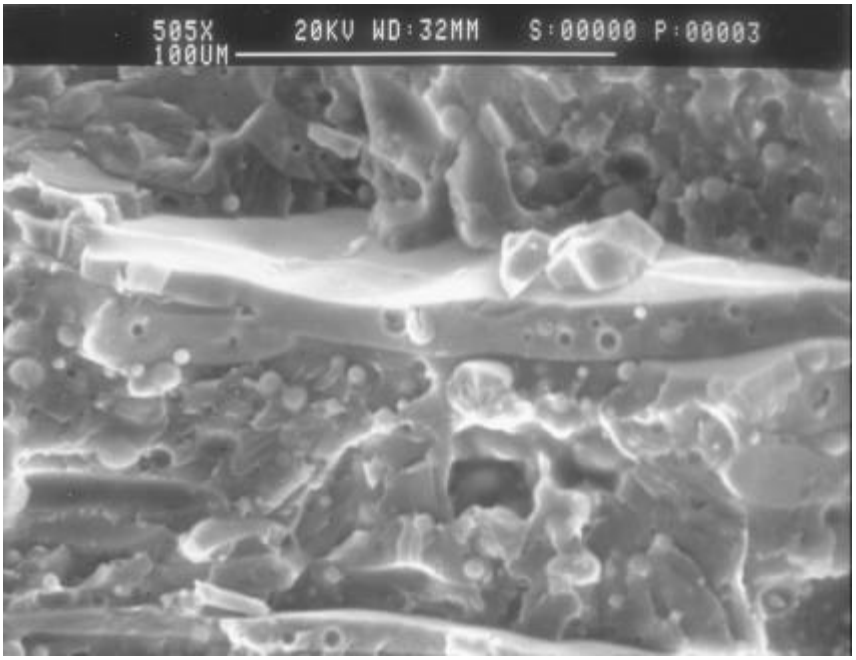

(a)

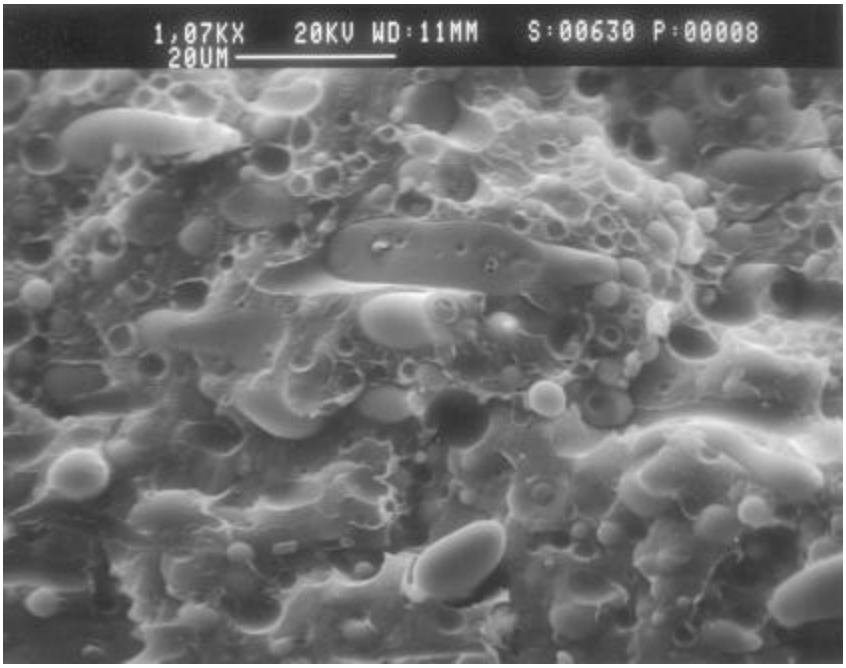

(b)

Figure 3.6: Scanning electron micrographs of the core region along the machine direction for molded Ryton PR09 reinforced with 60 wt% P-glass. (a) Dry blended (b) Preblended. Also note the magnification of (b) is approximately twice that of (a).

Table 3.3: Effects of Injection Rate and Resin on Machine Direction Properties of PPS Reinforced with 40 wt% P-glass processed at 330°C

Ryton PR09					
Injection Rate (cm^3/sec)	**Tensile Properties**			**Flexural Properties**	
	Modulus (GPa)	**Strength (MPa)**	**% Elong.**	**Modulus (GPa)**	**Strength (MPa)**
7	7.19 (0.34)	57.7 (2.36)	0.85 (0.07)	7.39 (0.17)	104.6 (3.7)
10	7.05 (0.49)	49.7 (5.54)	0.73 (0.09)	8.20 (0.24)	114.5 (6.0)
19	7.46 (0.45)	55.6 (2.68)	0.77 (0.07)	8.96 (0.11)	121.1 (2.0)
33	7.35 (0.32)	53.1 (4.76)	0.77 (0.08)	9.16 (0.12)	120.9 (2.9)
Fortron 0320					
Injection Rate (cm^3/sec)	**Tensile Properties**			**Flexural Properties**	
	Modulus (GPa)	**Strength (MPa)**	**% Elong.**	**Modulus (GPa)**	**Strength (MPa)**
7	5.48 (0.10)	44.0 (1.18)	0.92 (0.05)	5.86 (0.10)	96.0 (2.4)
10	5.19 (0.26)	37.5 (3.65)	0.86 (0.10)	6.26 (0.13)	96.7 (1.2)
19	6.62 (0.32)	50.2 (0.56)	0.86 (0.05)	6.59 (0.16)	99.4 (3.8)
33	6.32 (0.34)	47.6 (2.87)	0.94 (0.11)	6.97 (0.23)	98.5 (2.9)

Note: % Elong. = Elongation to break; Standard deviations given in parentheses

by the injection molding unit (screw forward speed of ≈ 100 mm/s) resulted in a composite blend with a flexural modulus and strength of 9.16 GPa (± 0.12 GPa) and 120.9 MPa (±2.9 MPa), respectively. Similar trends were seen for the Fortron based composites with the flexural modulus increasing from 5.86 GPa (± 0.10 GPa) to 6.97 GPa (± 0.23 GPa) with increasing injection rate with the flexural strength showing little variation around a value of approximately 98 MPa. For both grades of PPS investigated, the transverse flexural properties as well as the machine and transverse direction tensile properties were largely unaffected by the variations in the injection rates (Tables 3.3 and 3.4). The large variations seen in the machine direction flexural properties while tensile properties remained constant were an indication that the changes in the glass reinforcing phase morphology were concentrated mainly in the skin region of the molded plaque. It is believed that the use of higher injection rates led to greater extensional stresses at the advancing front resulting in greater deformation of the glass phase as the material fills the mold. It is also believed that due to the large activation energy (87.9 ± 1.1 kCal/mol) [29] and initial high viscosity of the phosphate glass (≈ 30,000 Pa·s), higher injection rates allowed the glass phase to remain deformable for a longer period as the composite blend filled out the mold.

The two grades of PPS were utilized to determine if any one resin offered a substantial advantage in regards to the mechanical properties that could be obtained. The most noticeable differences in the mechanical properties for composites produced with the two resins were seen in the machine direction flexural properties (Table 3.3). For all the conditions evaluated, the Ryton based composites consistently offered statistically significant increases in the machine direction flexural properties. For example, the highest flexural properties for both the Ryton and Fortron were achieved at the maximum injection rate of approximately 33 cm^3/sec. At these conditions, the Ryton based blend possessed a machine direction flexural modulus of 9.16 GPa (± 0.12 GPa) with the Fortron blend exhibiting a flexural modulus of only 6.97 GPa (± 0.23 GPa). Similar trends were seen in flexural strength with the Fortron blend possessing a flexural strength of 98.5 MPa (± 2.9 MPa) while the Ryton yielded a strength of 120.9 MPa (± 2.9 MPa). In the case of the composite tensile properties (Tables 3.3 and 3.4), the use of the Ryton offered no statistical improvement in properties over the Fortron.

Even though it was possible to obtain reinforcement from the phosphate glass while processing at 330°C, it was believed that the use of higher processing temperatures (350°C) may lead to conditions more favorable to deforming the glass phase. For a processing temperature of 330°C, the highest injection speed allowed by the processing equipment had to be utilized to produce composites with the highest properties. For composites with higher glass loadings, the high viscosity of the phosphate glass at 330°C may lead to numerous processing problems such as premature solidification of the material as it fills the mold. Rheological testing performed on the neat phosphate glass revealed that raising the processing temperature from 330°C to 350°C served to lower the complex

Table 3.4: Effects of Injection Rate and Resin on Transverse Direction Properties of PPS Reinforced with 40 wt% P-glass processed at 330°C

Ryton PR09					
Injection Rate (cm^3/sec)	**Tensile Properties**			**Flexural Properties**	
	Modulus (GPa)	**Strength (MPa)**	**% Elong.**	**Modulus (GPa)**	**Strength (MPa)**
7	5.46 (0.19)	35.2 (4.10)	0.73 (0.07)	6.73 (0.03)	93.4 (3.0)
10	5.82 (0.24)	42.0 (5.25)	0.75 (0.11)	6.87 (0.14)	94.3 (4.1)
19	5.49 (0.05)	40.7 (3.22)	0.76 (0.06)	7.00 (0.16)	94.1 (5.4)
33	5.35 (0.22)	40.7 (2.73)	0.78 (0.06)	- -	- -
Fortron 0320					
Injection Rate (cm^3/sec)	**Tensile Properties**			**Flexural Properties**	
	Modulus (GPa)	**Strength (MPa)**	**% Elong.**	**Modulus (GPa)**	**Strength (MPa)**
7	4.91 (0.13)	38.1 (2.83)	0.85 (0.11)	6.00 (0.30)	89.8 (3.8)
10	5.48 (0.28)	40.6 (2.86)	0.89 (0.09)	5.97 (0.23)	85.5 (3.4)
19	5.06 (0.29)	40.6 (1.01)	0.92 (0.09)	6.04 (0.30)	88.7 (5.1)
33	5.49 (0.38)	42.4 (2.93)	0.90 (0.08)	- -	- -

Note: % Elong. = Elongation to break; Standard deviations given in parentheses

viscosity of the glass almost an order of magnitude. The lower glass viscosity gained by using the higher temperature leads to more favorable viscosity ratios with the PPS, but the higher temperature may also lead to thermal degradation of the PPS resulting in a loss of properties.

The effects of utilizing a higher processing temperature of 350°C coupled with the various injection rates were determined by injection molding composite blends using the two grades of PPS. The mechanical properties of the various composites preblended and processed at 350°C are presented Tables 3.5 and 3.6. Varying the injection rate had the greatest impact on the machine direction flexural properties of the Fortron based composites. Increasing the injection speed from 7 to 33 cm^3/sec elevated the machine direction flexural modulus from 7.12 GPa (± 0.28 GPa) to 8.12 GPa (± 0.15 GPa) while the flexural strength only showed a slight improvement from 105.1 MPa (± 2.6 MPa) to 111.6 MPa (± 2.4 MPa). For the Ryton based composites, the variation in injection speed appeared to have little influence on the composite machine direction flexural properties. Ryton composites processed at a variety of injection speeds all possessed flexural moduli on the order of 9.2 GPa with a flexural strength of approximately 125 MPa. The tensile properties of both the Ryton and Fortron based composites were insensitive to the injection conditions with the higher processing temperature offering no significant enhancement in the tensile properties. In the case of the Ryton composites, the use of a higher processing temperature (350°C) appeared to lead to a slight decline in the transverse direction properties possibly indicating some slight degradation of the PPS.

3.3.4 Composite Blend Morphology

Processing variables such as resin, temperature, and injection rate were found to have the largest influence on the flexural properties of the PPS composites reinforced with a melt processable glass. The insensitivity of tensile properties to the variations in processing conditions coupled with the trends seen in flexural properties indicated that the composite morphology within the skin region of the injection molded samples would show the largest deviations due to the variations in the processing conditions. With this in mind, the morphology of the composite blends was investigated using scanning electron microscopy.

For the Fortron based composites, the utilization of higher temperatures and injection rates led to significant shifts in the flexural properties. For a composite blend processed at an injection speed of 19 cm^3/sec and a melt temperature of 330°C, the glass phase in the skin region consisted mainly of large droplets (Figure 3.7). The presence of the large droplets indicated limited dispersion and deformation of the glass phase resulting in composites that were nearly isotropic (1.09 ± 0.06) with respect to the (machine/transverse direction) flexural modulus. At the same injection rate, increasing the temperature to 350°C resulted in a 1.23 GPa (± 0.30 GPa) increase in the machine direction flexural modulus due to the elongation of glass phase in the skin region of the

Table 3.5: Effects of Injection Rate and Resin on Machine Direction Properties of PPS Reinforced with 40 wt% P-glass processed at 350°C

Ryton PR09					
Injection Rate (cm^3/sec)	**Tensile Properties**			**Flexural Properties**	
	Modulus (GPa)	**Strength (MPa)**	**% Elong.**	**Modulus (GPa)**	**Strength (MPa)**
7	7.50 (0.18)	57.5 (3.27)	0.78 (0.05)	9.04 (0.15)	130.8 (4.0)
10	7.87 (0.38)	58.3 (3.56)	0.76 (0.07)	9.28 (0.33)	126.8 (5.2)
19	7.22 (0.50)	55.6 (4.55)	0.81 (0.07)	9.17 (0.43)	116.9 (2.6)
33	6.50 (0.20)	50.8 (1.75)	0.79 (0.04)	9.34 (0.21)	121.3 (4.3)
Fortron 0320					
Injection Rate (cm^3/sec)	**Tensile Properties**			**Flexural Properties**	
	Modulus (GPa)	**Strength (MPa)**	**% Elong.**	**Modulus (GPa)**	**Strength (MPa)**
7	6.41 (0.21)	48.2 (3.18)	0.78 (0.05)	7.12 (0.28)	105.1 (2.6)
10	6.44 (0.48)	47.5 (3.88)	0.78 (0.06)	7.39 (0.20)	106.6 (2.5)
19	5.94 (0.40)	49.4 (0.96)	0.88 (0.03)	7.82 (0.25)	111.5 (5.6)
33	6.05 (0.41)	47.0 (2.35)	0.81 (0.04)	8.12 (0.15)	111.6 (2.4)

Note: % Elong. = Elongation to break; Standard deviations given in parentheses

Table 3.6: Effects of Injection Rate and Resin on Transverse Direction Properties of PPS Reinforced with 40 wt% P-glass processed at 350°C

Ryton PR09					
Injection Rate (cm^3/sec)	**Tensile Properties**			**Flexural Properties**	
	Modulus (GPa)	**Strength (MPa)**	**% Elong.**	**Modulus (GPa)**	**Strength (MPa)**
7	5.11 (0.26)	32.9 (1.92)	0.69 (0.06)	6.47 (0.25)	86.2 (5.4)
10	5.26 (0.21)	35.8 (2.79)	0.71 (0.08)	6.29 (0.40)	86.0 (6.9)
19	5.28 (0.31)	31.5 (1.59)	0.62 (0.05)	6.34 (0.44)	86.2 (6.6)
33	4.97 (0.36)	32.6 (2.93)	0.68 (0.05)	6.13 (0.31)	83.4 (4.7)
Fortron 0320					
Injection Rate (cm^3/sec)	**Tensile Properties**			**Flexural Properties**	
	Modulus (GPa)	**Strength (MPa)**	**% Elong.**	**Modulus (GPa)**	**Strength (MPa)**
7	5.13 (0.27)	42.9 (1.32)	0.89 (0.01)	6.17 (0.10)	89.7 (3.6)
10	4.98 (0.14)	43.3 (3.96)	0.92 (0.09)	6.09 (0.20)	87.8 (3.4)
19	5.00 (0.18)	41.9 (3.00)	0.87 (0.07)	6.18 (0.27)	88.5 (4.0)
33	4.82 (0.20)	37.0 (5.27)	0.81 (0.15)	- -	- -

Note: % Elong. = Elongation to break; Standard deviations given in parentheses

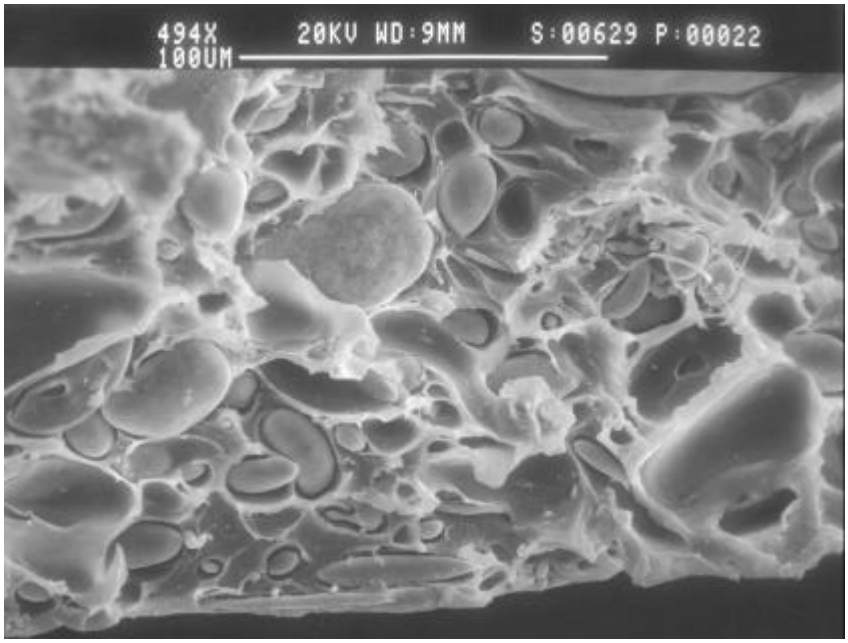

(a)

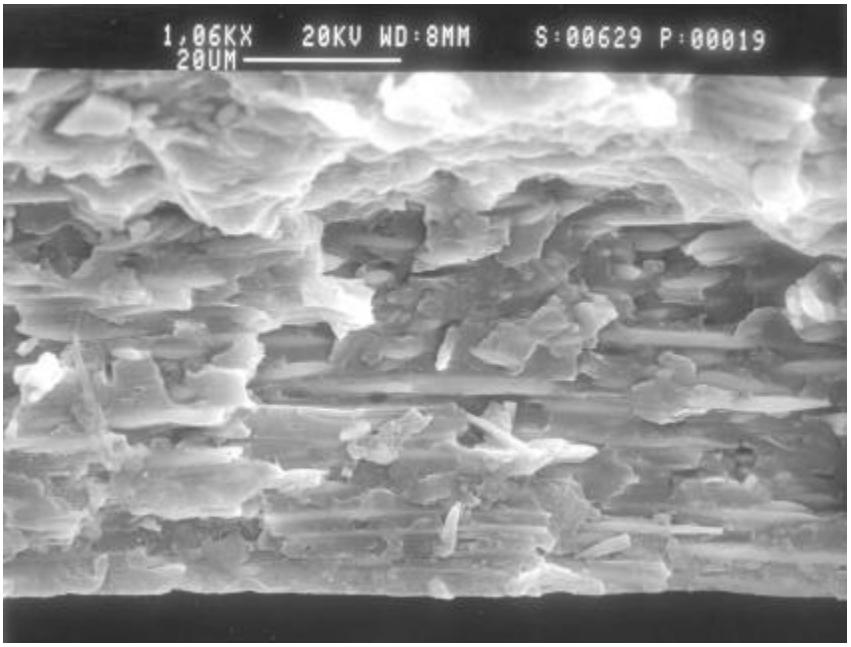

(b)

Figure 3.7: Scanning electron micrographs of the skin region along the machine direction for Fortron 320 reinforced with 40 wt% P-glass molded at an injection rate of 19 cm^3/sec. (a) Processed at 330°C (b) Processed at 350°C.

injection molded sample (Figure 3.7). From both the mechanical testing and scanning electron microscopy, it was determined that the highest processing temperatures and injection rates investigated created conditions most favorable to deforming the phosphate glass within the Fortron resin.

While the skin region morphology and flexural properties of the Fortron based composites were found to be sensitive to the processing conditions utilized, composites manufactured with Ryton displayed a weaker dependence on processing conditions. Elongated glass particles similar to those shown in Figure 3.8 were found in the skin region for all Ryton composites manufactured at 350°C and for injection rates of 19 cm^3/sec or greater for a processing temperature of 330°C. For all the conditions investigated, the core regions for both the Fortron and Ryton composite samples contained glass droplets similar to those shown in Figure 3.8. It is believed that the shear flow field found in the core region coupled with the unfavorable viscosity ratios between the phosphate glass and PPS resulted in only limited deformation of the phosphate glass in these regions.

The utilization of a variety of processing conditions and two grades of PPS led to significant shifts in the flexural properties which may be explained by certain processing parameters. The use of the various processing temperatures and injection rates led to significant shifts in the stress fields and heat transfer seen during mold filling. These deviations in thermal history coupled with the rheological characteristics of the various grades of PPS resulted in shifts in the stresses generated as well as the viscosity ratios between the P-glass and thermoplastic resin. During the filling of the mold, extensional stresses generated at the advancing front served to impart deformation to the composite blend in the skin regions near the mold wall. The formation of these extensional stresses was directly related to the extensional viscosity (η_e) of the various grades of PPS which may be approximated by the Trouton ratio ($\eta_e/\eta_o = 3$) . For both a temperature of 330°C and 350°C, the zero shear viscosity (η_o) of the Ryton was almost double that of the Fortron (Figures 3.2 & 3.4). It is believed that the formation of the higher extensional stresses coupled with lower viscosity ratios between the Ryton and P-glass led to conditions more favorable to the deformation of the glass.

Besides offering different rheological responses, the two grades PPS possess slightly different chemistries which could possibly contribute to the discrepancies seen in the mechanical properties. The grade of Ryton investigated possessed ionic endgroups while the Forton utilized had the ionic endgroups neutralized through acid washing [25]. The discrepancies in the chemical structure for the grades of PPS could lead to variations in the interactions between the phosphate glass and PPS. A more favorable interaction between the phosphate glass and the PPS may result in lower interfacial tension between the phases in the melt. From Taylor's theory [20-22], lower interfacial tension between the phases would allow deformation of the minor phase to occur at lower stresses.

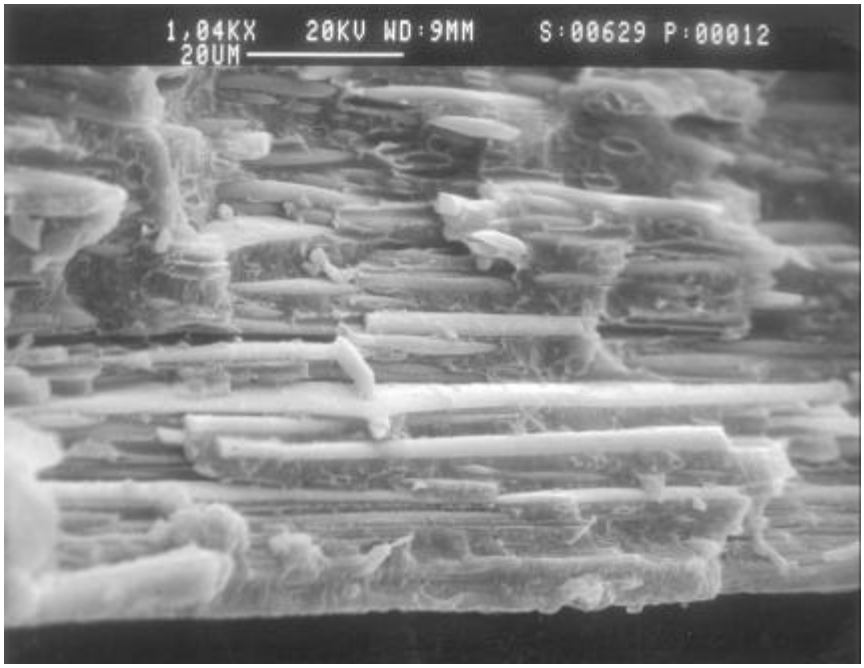

(a)

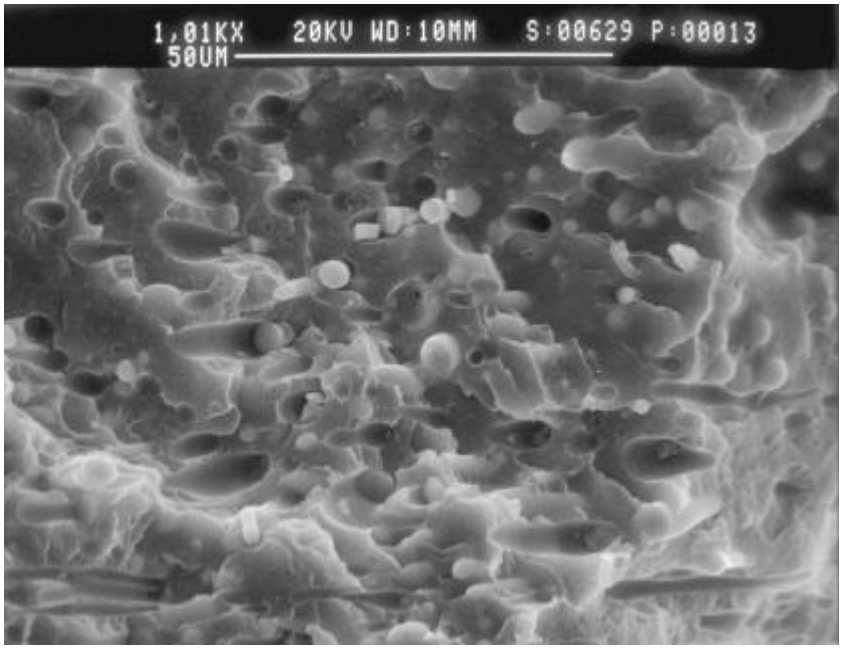

(b)

Figure 3.8: Scanning electron micrographs along the machine direction of Ryton PR09 reinforced with 40 wt% P-glass molded at 350°C with an injection rate of 10 cm^3/sec. (a) Skin region (b) Core region.

3.4 Conclusions

Melt temperature was found to have a large affect on the properties of the in situ injection molded composites, with melt temperatures greater than 330°C producing composites with the highest modulus. It was possible to obtain reinforcement from the phosphate glass while processing at 330°C. However, in the case of the lower viscosity PPS (Fortron), increasing the temperature to 350°C led to the formation of a higher aspect ratio reinforcing morphology leading to an enhancement in the composite's modulus.

The viscosity of the neat resins was also found to have a major effect on the mechanical properties of the in situ composites. For the two resins investigated, the higher viscosity resin consistently produced composites with the highest machine direction properties under all the conditions investigated. In particular, composites manufactured with the higher viscosity resin possessed enhanced machine direction flexural properties while the tensile properties showed no statistical difference with resin.

Mold fill rate was found to influence the mechanical properties of the composites depending of the melt temperature and resin utilized. At lower melt temperatures (330°C), the flexural properties increased with mold fill rate for the two resins investigated. For the higher melt temperature (350°C), the flexural properties increased with mold fill rate for the lower viscosity resin while the properties of the composites manufactured with the higher viscosity resin were insensitive to the filling rate.

For the composites investigated, the mixing history seen during processing was shown to play a large role in the mechanical properties that could be achieved through injection molding. An additional blending step before injection molding was found to lead to enhanced dispersion of the glass phase within the composite blend. The enhanced dispersion of the glass within the PPS resulted in composites with higher mechanical properties which was attributed to the formation of higher aspect ratio glass domains within molded sample.

When manufactured under the optimum processing conditions, in situ composites reinforced with 40 wt% phosphate glass offered certain enhancements in mechanical properties when compared to the neat PPS. The moduli of the in situ composite were approximately 2-3 times greater than the neat resin, proving that in situ injection molding is viable method for reinforcing lower cost engineering thermoplastics such as PPS. In particular, it was shown that the properties of the injection molded composites were sensitive to a variety of processing variables. These results serve to emphasis the importance of establishing the key processing/property relationships required to obtain composites that maximize the reinforcing potential of the phosphate glass.

3.5 Acknowledgments

The authors would like to gratefully recognize the financial support of the NSF Science and Technology Center for High Performance Polymeric Adhesives and Composites at Virginia Tech (Grant No. DMR-8809174 AMD 1) and the Army Research Office (Grant No. DAAHA04-94-G-0171). Also, we would like to thank Phillips Chemical Company and Hoechst Celanese for supplying the PPS and Corning Inc. for producing the phosphate glass utilized in this study. Appreciation is also extended to Dr. Garth Wilkes for allowing use of the scanning electron microscope and to Dr. Mike McLeod for his assistance in obtaining the SEM images.

3.6 References

1 Schweizer and Winterman, *Thermoplastic Polymer Additives: Theory and Practice*, ed. J.T. Lutz Jr., Marcel Dekker, New York 1989.

2 S. Kessler, in *Plastics Additives and Modifiers Handbook* (Chapter 48), ed. J. Edenbaum, Van Nostrand Reinhold, New York 1992.

3 G. Kiss, *Polym. Eng, Sci.*, 27, 410 (1987)

4 N.H. Ray and F.R. Sherliker, U.S. Patent 3,732,191 (1973).

5 W.A. Bahn, G.H. Beall, J. Ference, B.C. Monahan, C.J. Quinn, and P.S. Roussel, U.S. Patent 5,043,369 (1991).

6 C.J. Quinn, P. Frayer, and G.H. Beall, in *Polymeric Materials Encyclopedia* (vol. 4), ed. J.C. Salamone, 2766 (1996).

7 C.J. Quinn and G.H. Beall, in *Chem. Process. Adv. Mater*., ed L. Hench, 799 (1992).

8 G.H. Beall and C.J. Quinn, U.S. Patent 4,940,677 (1990).

9 G.H. Beall and J.E. Pierson, U.S. Patent 5,328,874 (1994).

10 B.G. Aitken, G.H. Beall, and J.E. Dickenson, Jr., U.S. Patent 5,529,961 (1996).

11 W.A. Bahn and C.J. Quinn, *SPE ANTEC Proc*., 2370 (1991).

12 A.I. Isayev and M. Modic, *Polym. Comp*., 8 (3), 158 (1987)

13 H.J. O'Donnell and D.G. Baird, *Intl. Polym. Proc*., 11 (3), 257 (1996).

14 H.J. O'Donnell and D.G. Baird, *Polym. Eng. Sci.*, 36 (7), 963 (1996).

15 H.J. O'Donnell and D.G. Baird, *Polymer*, 36 (2), 259 (1995).

16 J.P. de Souza and D.G. Baird, *Polymer*, 37 (10), 1985 (1996).

17 R.J. Krishnaswamy, S.E. Bin Wadud, and D.G. Baird, Polymer, 40, 701 (1998).

18 G. Crevecoeur, *PhD Dissertation*, Catholic University of Leuven (1991).

19 F.D. Rumsheidt and S. Mason, *J. Coll. Interf. Sci*., 16, 238 (1961).

20 G.I. Taylor, *Proc. Roy. Soc*., A138, 41 (1932).

21 G.I. Taylor, *Proc. Roy. Soc*., A146, 501 (1932).

22 G.I. Taylor, *Proc. Roy. Soc*., A226, 289 (1954).

23 H.P. Grace, *Chem. Eng. Commun*., 14, 225 (1982).

24 J. Geibel and J. Leland, in *Encyclopedia of Chemical Technology*, 4 (19), 904 (1996).

25 Private correspondence, Phillips Chemical Company, Bartlesville, OK.

26 C.E. Crowder, J.U. Otaigbe, M.A. Barger, R.L. Sammler, B.C. Monahan, and C.J. Quinn, *J. Non-Cryst. Solids*, 210, 209 (1997).

27 R.L. Sammler, J.U. Otaigbe, M.L. Lapham, N.L. Bradley, B.C. Monahan, and C.J. Quinn, *J. Rheo*., 40 (2), 285 (1996)

28 J.U. Otaigbe and G.H. Beall, *Trends in Polymer Science*, 5 (11), 369 (1997)

29 R.T. Young, *Ph.D. Dissertation*, Virginia Polytechnic Institute & State University, (1999).

Chapter 4: Injection Molded Properties

Preface

This chapter is focused on the first and third objectives of the research. Specifically, the properties of in situ injection molded composites consisting of polyphenylene sulfide reinforced with various loadings of a phosphate glass were examined. The properties of the composites both in the melt and solid state were evaluated and compared to an E-glass fiber reinforced material. This chapter is organized as a manuscript for future publication.

Properties of Injection Molded In Situ Composites Based on Polyphenylene Sulfide and a Melt Processable Glass

R.T. Young and D.G. Baird

Department of Chemical Engineering and
NSF Science and Technology Center for High Performance
Polymeric Adhesives and Composites
Virginia Polytechnic Institute and State University
Blacksburg, VA 24061-0211

(ABSTRACT)

This work was concerned with evaluating the properties of injection molded composites consisting of polyphenylene sulfide (PPS) reinforced with various loadings of a melt processable phosphate glass. During injection molding, both the PPS and melt processable glass were deformable, facilitating the processing of higher glass loadings than are possible in conventional solid glass fiber reinforced materials. The stiffness of the composite blends was found to increase with glass concentration with a composite containing 60 wt% (44 vol%) phosphate glass showing moduli over 4 times greater than that of the neat PPS. Composites possessing stiffness comparable to a conventional E-glass reinforced material (40 wt% fiber) could be produced utilizing higher phosphate glass loadings on the order of 60 wt%. While the addition of the phosphate glass led to significant enhancements in the stiffness of the composites, the strength of the blends often fell to values below that of the neat resin. Although the use of phosphate glass typically resulted in strengths 2-3 times lower than those found for the E-glass filled material, these composites offered several advantages including lower anisotropy in mechanical properties, lower viscosities, and smoother surfaces.

4.1 Introduction

The addition of high aspect ratio inorganic reinforcement, such as glass fiber, has allowed the production of composite systems that possess moduli and strengths significantly greater than those of neat thermoplastics. While the addition of the solid reinforcement often results in significant enhancements in mechanical properties it can also lead to numerous problems in a process such as injection molding. During injection molding the presence of solid fibers can result in wear on various molder parts such as the screw, barrel, and mold. The complex interactions between the fibers and flow field seen

during molding can result in molded products that suffer from a variety of problems such as anisotropy in properties, weld line formation, and poor surface appearance [1,2].

Due to the processing difficulties created by the addition of solid reinforcement, work has been performed on the development of alternative composite systems that overcome many of the problems associated with conventional short fiber reinforced thermoplastics. One such method referred to as in situ composite manufacturing relies on the formation of the reinforcing phase morphology during processing [3]. During processing operations, both the thermoplastic matrix and reinforcing phase are fluid, thereby alleviating many of the problems seen with conventional solid reinforced systems. The final reinforcing phase morphology can be developed from deformation applied through a variety of processing techniques such as injection molding, fiber spinning, and film casting.

One of the materials that has shown great promise for in situ composite generation techniques are melt processable glass [4-7]. These inorganic glasses have low glass transition temperatures (200-350°C) allowing them to be combined with thermoplastic resins for use in conventional polymer processing techniques. The lower thermal transition temperatures for these materials are obtained by utilizing P_2O_5 instead of SiO_2 as the primary glass former. Additional materials such as alkali and alkaline earth oxides are added in order to help control the thermal transitions and chemical durability of the glasses [6]. Due to their structure, phosphate based glasses typically display lower mechanical properties than the conventional borosilicate glasses commonly utilized in the reinforcement of thermoplastics. The use of phosphate glasses in engineering applications has been limited due to the poor chemical durability of the glass. Present research is being focused on formulating melt processable glasses with lower transition temperatures and improved chemical durability [8-10]. The development of more durable glasses with lower transition temperatures could make these materials a viable alternative reinforcing phase for a variety of composite fabrication techniques.

The injection molding of thermoplastics reinforced with phosphate glasses has only been investigated on a limited basis [4-7]. Much of the work performed has involved the blending of a variety of thermoplastics with a number of glasses in order to ascertain the properties that could be achieved. In recent years, the development of glasses with lower transition temperatures and increased chemical durability have shown great promise for injection molding applications. For example Bahn, Quinn, and co-workers [5-7] injection molded composites consisting of higher transition glasses ($225°C < T_g < 350°C$) blended with higher performance thermoplastics such as polyetherimide (PEI), polyethersulfone (PES), polyetheretherketone (PEEK), polyetherketone (PEK), and thermotropic liquid crystalline polymers (TLCPs). Much of the work performed concentrated on higher glass loadings (50-70 vol%) because P-glass composites manufactured with conventional glass loadings (up to 40 vol%) appeared to offer only modest increases in mechanical properties relative to those obtained with E-glass. Composites reinforced with high loadings of

phosphate glass typically had tensile moduli 4-10 times greater than those of the neat resins. For example, an injection molded PEK composite containing 70 vol% phosphate glass had a tensile modulus of approximately 30 GPa while the neat thermoplastic resin only had a modulus of 4 GPa. In addition to greater stiffness, phosphate glass reinforced composites were shown to offer other advantages such as low mechanical anisotropy, finer molding tolerances, greater resistance to creep and stress relaxation, and lower thermal expansion coefficients [6,7]. One of the drawbacks found with utilizing such high inorganic loadings was that the tensile strength of the composite blends were found to fall below that of the neat resins.

In previous work performed with phosphate glass reinforced thermoplastics, the glass concentration was determined to play a large role in the glass phase morphology that was developed during processing [5-7,11]. Bahn and Quinn [11] investigated the role of glass concentration on the morphology of extruded composites consisting of polyaryletherketones (PAEK) reinforced with a phosphate glass. At low glass loadings (10-40 vol%), limited dispersion of the glass was obtained within a twin screw extruder resulting in a glass microstructure consisting of large glass particles (>100 μm) interdispersed with fine glass spheres on the order of 2-3 μm. Increasing the glass loading to 40-65 vol% resulted in a glass microstructure consisting of well dispersed spherical particles (2-3 μm). The formation of the well dispersed morphology was attributed to increased glass particle interactions leading to the elongation of the glass phase into strands which eventually reached a critical diameter breaking into spherical particles. Depending on the viscosity differences between the glass and thermoplastic resin, composite blends containing high glass loadings (>65 vol%) were found to undergo phase inversion at a variety of conditions with the polymer resin being present as dispersed droplets within a continuous glass phase.

Because the glass phase morphology is developed during processing, a wide range of reinforcing morphologies can be generated during a process such as injection molding leading to composites possessing a variety of mechanical properties. For example, Quinn and coworkers [6] examined the properties of a thermotropic liquid crystalline polymer (Xydar) reinforced with a zinc alkali phosphate glass. A variety of reinforcing morphologies consisting of small glass beads, fibers, and ribbons were produced by varying the processing conditions. The transition of the glass morphology from low aspect ratio beads to elongated ribbons was found to result in significant increases in the composite's mechanical properties. For a blend containing 62 vol% glass, a morphology consisting of small glass beads yielded a tensile modulus of 17 GPa while a morphology consisting of glass ribbons resulted in tensile modulus of 28 GPa. Similar enhancements in the strength were observed with the transition in morphology elevating the tensile strength from 52 MPa to 72 MPa.

The lower transition temperatures of the phosphate glasses also allows the production of composite systems that offer certain advantages over a wide range of

temperatures. At the higher temperatures required for melt processing operations, the phosphate glass is fluid in nature allowing the viscosity of highly loaded composite blends to fall within acceptable limits for conventional processes such as extrusion and injection molding [6,7,12]. High phosphate glass loadings can then be incorporated into the thermoplastic resins resulting in composites that typically possess very high heat deflection temperatures and maintain a high modulus over a wide range of temperatures as indicated by dynamic mechanical thermal analysis (DMTA) [6,7,12]. The higher phosphate glass loadings also serve to reduce the flammability of the composites and lead to lower thermal expansion coefficients [6,7].

The purpose of this paper is to evaluate the effects of glass loading on various properties of injection molded composites consisting of polyphenylene sulfide reinforced with a melt processable phosphate glass. In particular, the influence of glass concentration on the reinforcing phase morphology, mechanical properties, surface roughness, and viscoelastic properties of the composites was examined. The properties of these phosphate glass filled composites were also compared to a conventional E-glass fiber reinforced material to help ascertain some of the benefits gained by utilizing a melt processable glass as the reinforcing phase.

4.2 Experimental

4.2.1 Materials

The melt processable phosphate glass used in this study was an experimental material supplied by Corning, Inc. (Corning, NY). This particular phosphate glass is composed of P_2O_5 (33 mol%), $ZnCl_2$ (26 mol%), B_2O_3 (4 mol%), and M_2O (37 mol%) where M consists of various alkali metals. The glass utilized is considered non-durable in that the material suffers from a loss in weight and mechanical properties when exposed to hot water. The glass samples were received as large shards that were crushed and sorted to yield particles ranging from 1-2 mm for use in injection molding. For rheological studies, the glass shards were ground to yield disks with thicknesses ranging from 1-2 mm. The glass transition temperature for the glass was found to be 233.7 ± 2.2°C from differential scanning calorimetry (DSC) measurements performed at a heating rate of 10°C/min. The density of the glass was determined to be 2.62 ± 0.01 g/cm^3 from measurements made on as received glass samples utilizing a pyconometer (Micrometrics Accupyc, Model 1330).

Polyphenylene sulfide (PPS) was utilized as the matrix resin for the injection molding studies. Polyphenylene sulfide is a semi-crystalline engineering thermoplastic that has good mechanical properties, excellent chemical resistance, high temperature thermal stability, and inherent flame resistance[13]. For the phosphate glass composite manufacture, a grade of PPS supplied by Phillips Chemical Company designated as Ryton

PR09 was utilized. The Ryton PR09 is an extrusion grade of PPS possessing a glass transition temperature of 91°C, a melting point of 279°C, and a density of 1.40 g/cm^3. A 40 wt% E-glass filled grade of PPS designated as Fortron 1140 supplied by Hoechst Celanese was also injection molded to facilitate comparisons between E-glass and P-glass filled composites.

4.2.2 Injection Molding

Composite blends were produced using an Arburg Allrounder, model 221-55-250, injection molding unit. The molder has a 22 mm screw with a check ring non-return valve and was fitted with a general purpose nozzle having a 2 mm exit diameter. For this study, the injection molding unit was used for two main processing steps including the preblending of the materials and actual composite manufacture. All materials used during processing were dried for at least 24 hrs at 150°C under vacuum before being plasticated.

The first processing step involved utilizing the injection molding unit as an extruder to preblend the glass with the PPS. Due to the variety of blends to be studied and the limited availability of the phosphate glass, the molding unit was seen as an effective way to preblend small batches of composite material. The initial dispersion of the glass within the thermoplastic matrix could be achieved rapidly while minimizing thermal degradation of the matrix resin at the higher processing temperatures.

For preblending, the barrel assembly frame was released from the mold assembly and modified to run as an extruder by adjusting the back pressure so the material would flow freely from the nozzle. A dry blend of the glass and PPS was passed through the screw operating at 200 rpm with the extrudate being collected, quenched, and granulated using a Cumberland Granulator (Model 6x8). The same barrel temperature profile was utilized for both the initial blending and injection molding process. The temperature profile, progressing from the solids conveying zone to the nozzle was: 330°C, 350°C, 350°C, and 350°C.

The second main processing step involved the fabrication of the composite blend into test specimens by injection molding. Composite plaques were produced by injecting the plasticated blend into a film-gated mold having dimensions of 75 mm by 80 mm by 1.6 mm. During molding operations the mold fill rate (10 cm^3/sec), injection pressure (5 MPa), holding pressure (10 MPa), screw speed (200 rpm), and mold temperature (140°C) were held constant. A mold temperature of 140°C was utilized to help insure the PPS developed an adequate degree of crystallinity [13].

4.2.3 Mechanical Properties

The tensile and flexural properties of the various composite blends were measured

using an Instron Mechanical Tester (Model 4204). Test specimens approximately 75 mm long by 8 mm wide were cut from the injection molded plaques along both the machine (flow) and transverse directions. Tensile properties were measured using a 5 kN load cell following ASTM standard B 638-87B. The crosshead speed was kept constant at 1.27 mm/min with the strain imposed on the sample measured using an extensionmeter (Instron Model 2630-25). Flexural properties were measured using a three-point bending test following ASTM standard D 790M 86. All the mechanical properties reported are the average of at least five test samples.

4.2.4 Morphology

The morphology of the composite injection molded plaques was examined using a Stereoscan S200 scanning electron microscope with an accelerating voltage of 20 kV. The surfaces examined were prepared by immersing the sample in liquid nitrogen for approximately 5 minutes before fracturing. The samples were subsequently attached to mounting studs and coated with a layer of gold using a sputter coater (Bal-Tec Model SCD 005) to enhance conductivity.

4.2.5 Surface Roughness

A Tencar Alpha-Step 500 surface profiler was used to obtain surface roughness measurements of the various materials. Measurements were made at 50 μm/second over a scan length of 500 μm utilizing a stylus having a 12.5 μm radius tip. All the injection molded samples were scanned transverse to the flow direction within the same region of each plaque. The reported values are the averages of a least ten measurements.

4.2.6 Dynamic Mechanical Analysis

Rheological characterization of the various materials was performed using parallel plate fixtures attached to a Rheometrics Mechanical Spectrometer (Model RMS-800). Dynamic oscillatory measurements were carried out under a variety of conditions depending on the materials being investigated. The complex viscosity ($|\eta^*|$) of the neat PPS and composite blends was determined using 25 mm diameter test specimens cut from injection molded plaques. For the glass samples, test specimens consisted of pre-ground disks having thicknesses ranging from 1-2 mm and a diameter of 7.9 mm. The smaller diameter plates were utilized with the glass in order to generate lower strains and help insure that measurements did not exceed the compliance of the instrument. Each sample was brought to the desired temperature and allowed to equilibrate for a least three minutes before the start of testing. The sample temperature was monitored by a thermocouple in contact with the lower plate fixture. The temperature was maintained by blanketing the sample with heated nitrogen in order to minimize degradation. Before rheological testing, samples were dried for at least 24 hours in a vacuum oven maintained at 150°C.

The strain and angular frequency dependence of the complex viscosity for the various materials was examined by varying either the strain or angular frequency while holding the other parameter and sample temperature constant. The strain dependence of the dynamic response of the various materials was investigated by varying the applied strain between 0.1-10 % while monitoring the viscoelastic properties at an angular frequency of 10 rad/sec. Angular frequency sweeps were subsequently performed at strains that would allow adequate resolution of the transducer torque signal ($\geq$ 0.2 gm·cm) and facilitate measurements within the linear viscoelastic region.

In order to study how the addition of the various glasses affected the mechanical response of the composite blends, the dynamic shear response of the materials both in the solid and melt state was examined over a wide range of temperatures. Dynamic mechanical thermal analysis (DMTA) was performed in torsion using a Rheometrics RMS-800. Rectangular strips cut along the machine direction of the injection molded plaques were heated in nitrogen at a rate of approximately 2.5°C/min. while the viscoelastic properties of the materials were probed at an angular frequency (ω) of 10 rad/sec and a strain of 0.1%. The response of the composite blends in the melt state was also examined by heating the materials from 300°C at a rate of approximately 5°C/min while the complex viscosity was monitored at an angular frequency of 1 rad/sec.

4.3 Results and Discussion

4.3.1 Mechanical Properties

Injection molded composites consisting of PPS reinforced with various loadings of glass were produced to determine the effects of glass concentration on the mechanical properties of the blends. The phosphate glass reinforced composite blends were produced under previously established processing conditions that were found to lead to the greatest enhancement in stiffness with the addition of the P-glass [14]. Highly loaded (40 wt%) commercial borosilicate (Type E) glass reinforced PPS was also injection molded to facilitate comparisons between the two composites systems.

The addition of the phosphate glass was found to be an effective way to produce composites offering greater stiffness than the neat PPS. The effects of the addition of phosphate glass on the both the tensile and flexural moduli of injection molded composites are presented in Table 4.1. Both the tensile and flexural modulus rose with increasing glass concentration with the stiffest composites being obtained at the highest glass loading investigated. For example, neat PPS processed at the same conditions as the composite blend had a machine direction tensile and flexural modulus of 3.20 GPa (± 0.21 GPa) and 3.61 GPa (± 0.10 GPa), respectively. The addition of 60 wt% (44 vol%) phosphate glass elevated the machine direction tensile modulus to 12.4 GPa (± 0.57 GPa) while the flexural modulus rose to 15.0 GPa (± 0.28 GPa). The addition of the phosphate glass (20-

Table 4.1: Mechanical Properties for injection molded PPS based composites reinforced with various loadings of glass

Machine Direction					
Glass Loading (weight %)	**Tensile Properties**			**Flexural Properties**	
	Modulus (GPa)	**Strength (MPa)**	**% Elong.**	**Modulus (GPa)**	**Strength (MPa)**
Neat PPS	3.20 (0.21)	71.9 (2.34)	3.26 (0.36)	3.61 (0.10)	106.8 (2.3)
20% P-glass	4.65 (0.28)	61.5 (3.11)	1.42 (0.14)	5.87 (0.15)	121.3 (3.0)
40% P-glass	7.87 (0.38)	58.3 (3.56)	0.76 (0.07)	9.28 (0.33)	126.8 (5.2)
60% P-glass	12.4 (0.57)	47.1 (5.96)	0.38 (0.06)	15.0 (0.41)	120.9 (2.5)
40% E-glass	13.2 (0.91)	140.5 (5.3)	1.30 (0.05)	15.1 (0.28)	259.3 (4.3)
Transverse Direction					
Glass Loading (weight %)	**Tensile Properties**			**Flexural Properties**	
	Modulus (GPa)	**Strength (MPa)**	**% Elong.**	**Modulus (GPa)**	**Strength (MPa)**
Neat PPS	3.02 (0.05)	70.5 (4.38)	2.88 (0.35)	3.75 (0.03)	109.5 (2.2)
20% P-glass	3.49 (0.12)	42.8 (3.17)	1.29 (0.14)	4.61 (0.17)	103.1 (6.4)
40% P-glass	5.26 (0.21)	35.8 (2.79)	0.71 (0.08)	6.29 (0.40)	86.0 (6.9)
60% P-glass	7.71 (0.23)	20.0 (3.56)	0.27 (0.05)	9.81 (0.25)	71.2 (3.6)
40% E-glass	6.79 (0.38)	67.9 (3.31)	1.11 (0.08)	7.12 (0.41)	115.1 (12.0)

Note: % Elong. = Elongation to break; Standard deviations given in parentheses
P-glass Composites (Ryton PR09) & E-glass Composites (Fortron 1140)

60 wt%) also served to enhance the transverse direction stiffness of the composites leading to moduli 1- 6 GPa greater than that of the neat PPS. For a composite reinforced with 60 wt% P- glass, both the tensile and flexural transverse direction moduli were found to be almost 2.5 times greater than those of the neat PPS.

While the addition of the phosphate glass resulted in composites with moduli greater than the neat resin, the strength of the composite blends often fell below that of the pure PPS (Table 4.1). The loss in strength with the addition of the phosphate glass was most pronounced in the tensile properties. For example, neat PPS had a tensile strength of approximately 70 MPa while a blend containing 60 wt% phosphate glass had a machine direction strength of MPa (± 5.96 MPa) and a transverse direction strength of only 20.0 MPa (± 3.56 MPa). The lowering of the strengths of the composite blends to values below those of the neat PPS was partially attributed to the addition of the lower strength phosphate glass. The tensile strength of phosphate glasses used to reinforce thermoplastics has been reported to be as low as approximately 20 MPa, a value well below the 70 MPa for neat PPS [5]. Another factor that was believed to contribute to the loss in strength for the composites was the lack of adhesion between the PPS and glass phase. With the glass phase showing preferential orientation along the machine direction, tensile testing along the transverse direction would place more of a load on the polymer/glass interface. For all the phosphate glass concentrations investigated, the transverse direction strength fell well below that of the neat resin giving a good indication of poor adhesion between the phases. It should be noted that the flexural strengths of the composite blends appeared far less sensitive to the addition of the phosphate glass. For all the glass concentrations investigated, the machine direction flexural strength exceeded that of the neat resin. For example, neat PPS had a machine direction flexural strength of 106.8 MPa (± 2.3 MPa) while at 60 wt% P-glass the composite blend had a flexural strength of 120.9 MPa (± 2.5 MPa). In regards to the transverse direction, the addition of the phosphate glass had a lesser effect on the flexural strength as compared to the tensile strength. At the highest glass loading investigated (60 wt%), the transverse direction flexural strength only fell approximately 35% when compared to the neat resin while the transverse direction tensile strength fell by almost 70%.

The mechanical properties of the phosphate glass filled thermoplastics were also compared to a commercially available E-glass fiber filled resin. The tensile and flexural properties of both glass filled materials are presented in Table 4.1. Since both the phosphate glass and borosilicate (Type E) glass have the same approximate density (≈ 2.6 g/cm^3), composites manufactured at similar glass loadings would contain the same volume fraction of glass. At 40 wt% glass, the E-glass filled PPS offered both higher tensile and flexural moduli and strengths when compared to a phosphate glass filled composite of the same loading. By utilizing higher phosphate glass loadings of 60 wt%, composites possessing stiffness comparable or greater than the composites reinforced with 40 wt% E-glass could be produced. While the higher phosphate glass loadings led to composites

with comparable stiffness, the strength of these composites often fell 2-3 times lower than the E-glass filled material.

The lower mechanical properties obtained with the phosphate glass versus the E-glass can be partially attributed to certain properties of the glasses utilized. One factor that contributes to the differences in properties are the mechanical properties of the neat glasses themselves. Borosilicate glasses commonly used for reinforcing thermoplastics have tensile moduli in the range of 70-80 GPa with the strength often falling around 1500-2000 MPa [15,16]. The tensile properties of phosphate glasses have been reported to be much lower often falling in the range of 20-40 GPa for the modulus with the strength having been reported to be as low as 20 MPa [4,5]. Besides supplying much higher mechanical properties than the phosphate glasses, the E-glass fibers have been treated with a sizing agent to promote adhesion between the glass fibers and the PPS. The enhanced adhesion between the E-glass and polymer matrix coupled with the higher properties of the glass would result in composites displaying much higher strengths than the phosphate glass reinforced materials.

Another area where the E-glass and phosphate glass reinforced composites were found to show significant differences was in the distribution of the mechanical properties. By utilizing a film-gated mold, a flow field was generated that facilitated a higher degree of orientation along the flow (machine) direction when compared to the transverse direction. The mechanical anisotropy for the various composites were determined by taking the ratio between the machine and transverse direction mechanical properties. The anisotropy ratios for the glass filled blends for both the flexural and tensile properties are presented in Table 4.2. In the case of the E-glass filled material, the mechanical properties along the machine direction were consistently almost twice those of the transverse direction due to the preferential orientation of the glass fibers along the flow direction. Due to the reinforcing morphology developed during processing, all the phosphate glass reinforced blends investigated displayed much lower mechanical anisotropy than the E-glass filled material. For example, a composite blend containing 60 wt% P-glass had an anisotropy ratio of only 1.53 (± 0.06) in terms of flexural modulus as compared to 2.12 (± 0.13) that was obtained for a composite containing 40 wt% E-glass fiber.

4.3.2 Composite Morphology

The composite blends were examined with scanning electron microscopy in an effort to understand the reinforcing morphology developed during injection molding. An examination of the reinforcing morphology generated in a composite reinforced with 20 wt% phosphate glass revealed the formation of numerous, high aspect ratio, thin (<5 μm) glass domains within the skin region of the injection molded sample (Figure 4.1). The formation of the high aspect ratio glass reinforcing morphology was attributed to a combination of the elongational flow from the advancing front and strong shear gradients

Table 4.2: Ratio of Machine to Transverse direction Properties for Film-gated Injection Molded PPS composites reinforced with Glass

	Tensile Properties		Flexural Properties	
Composition	**Modulus**	**Strength**	**Modulus**	**Strength**
20 wt% P-glass	1.33 (0.09)	1.44 (0.13)	1.27 (0.06)	1.18 (0.08)
40 wt% P-glass	1.50 (0.09)	1.63 (0.16)	1.48 (0.11)	1.47 (0.13)
60 wt% P-glass	1.61 (0.09)	2.36 (0.51)	1.53 (0.06)	1.70 (0.09)
40 wt% E-glass	1.94 (0.17)	2.07 (0.13)	2.12 (0.13)	2.25 (0.24)

Note: Standard deviations given in parentheses
P-glass Composites (Ryton PR09) & E-glass Composite (Fortron 1140)

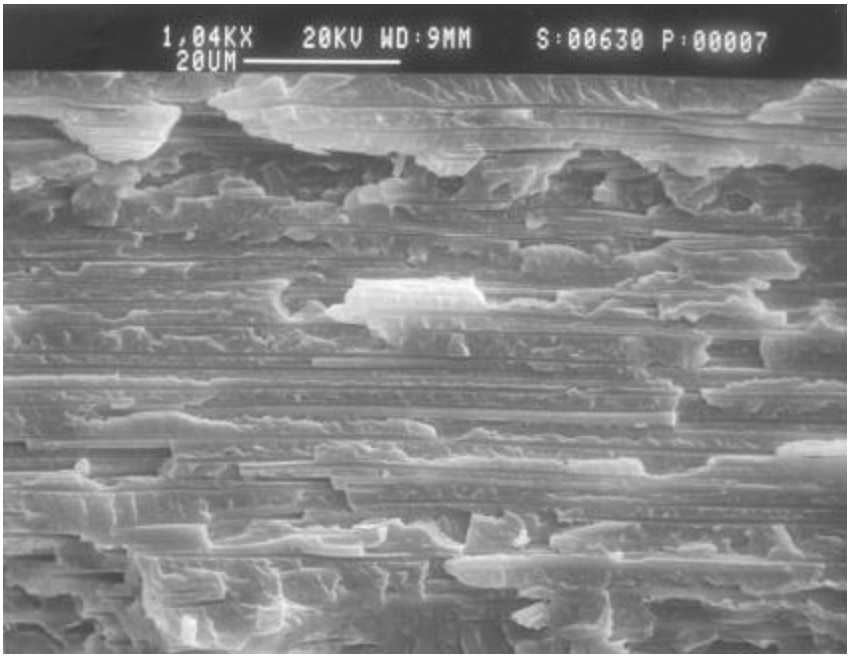

(a)

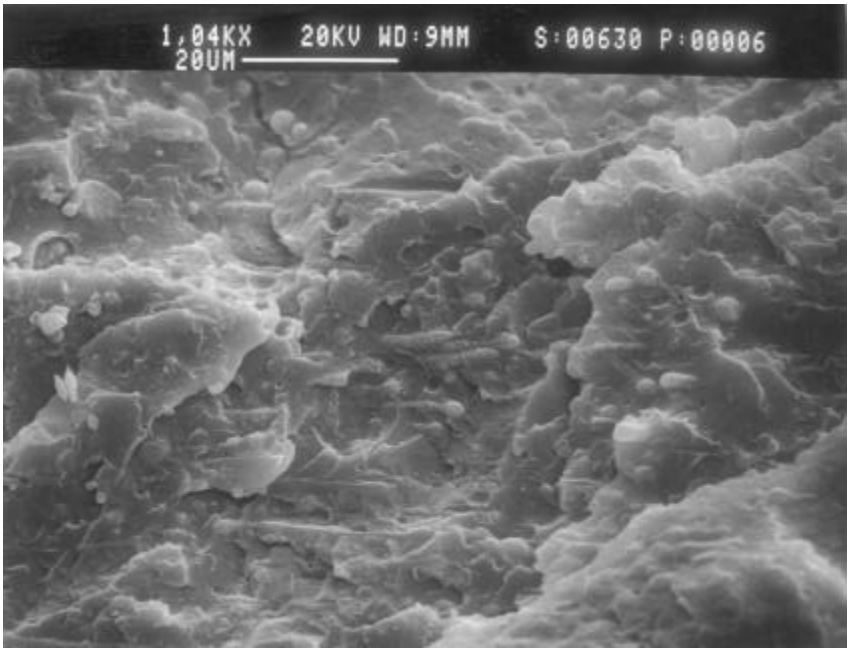

(b)

Figure 4.1: Scanning electron micrographs along the machine direction for PPS reinforced with 20 wt% P-glass. (a) Skin region (b) Core region

found close to the mold wall. The formation of these high aspect ratio glass phases oriented along the flow direction was responsible for the preferential enhancement in stiffness along the machine direction. Within the core region of the molded sample, the glass was present mainly as small, slightly elongated droplets. The limited deformation of the glass phase in the core was believed to be due to the generation of lower shear stresses in this region. The full reinforcing potential gained from the addition of the phosphate was not realized due to the formation of these lower aspect ratio glass phases within the core region. It is interesting to note that even at such low glass concentrations (≈ 12 vol%), it was possible to obtain good dispersion of the glass within the thermoplastic matrix. Previous studies performed by Bahn and Quinn [11] found that only limited dispersion of a phosphate glass at lower loadings (10-40 vol%) could be achieved within an extruded blend resulting in a glass microstructure consisting of large particles (>100 μm) interdispersed with fine glass spheres on the order of 2-3 μm.

The addition of higher phosphate glass loadings was found to lead to significant changes in the morphology within the core region of the injection molded composites. Scanning electron micrographs of the core region of composites containing 40 wt% (26 vol%) and 60 wt% (44 vol%) are shown in Figure 4.2. Like the composites containing 20 wt% phosphate glass, the core region of these composites contained glass mainly in the form of lower aspect ratio droplets. When comparing the morphologies in the core region with increasing glass concentration (Figures 4.1b, 4.2a, and 4.2b), the use of higher glass concentrations resulted in larger glass domains within this region. The presence of the larger glass domains in the core region indicated limited dispersion at the higher concentrations possibly due to increased glass-glass particle interactions which led to coalescence. The formation of these larger glass domains was believed to contribute to the lower tensile strength seen at the higher glass loadings. Glass pullout was also commonly observed for the fracture surfaces, indicating a lack of adhesion between the phases which would also serve to lower the strengths that could be attained with the addition of the phosphate glass.

While the glass phase in the core regions of the injection molded samples consisted mainly of low aspect ratio glass droplets, the skin regions were found to contain higher aspect ratio glass domains. For the phosphate glass reinforced composites, the skin region contained small, high aspect ratio glass domains (Figures 4.1b & 4.3a). With increasing glass concentration, the number of these high aspect ratio glass particles generated in the skin region was found to increase leading to the significant enhancements in the stiffness of the composites. The phosphate glass domains found in the skin regions of the injection molded plaques were found to be much smaller than the E-glass fibers typically used to reinforce thermoplastics (Figure 4.3). The phosphate glass ribbons found within the skin region of injection molded samples. (a) 60 wt% P-glass (b) 40 wt% E-glass composites typically displayed a thickness less than 5 μm while the E-glass fibers had diameters on the order of 12 μm. It was believed the formation of these smaller P-glass domains within the skin region may lead to composites that possess smoother surfaces

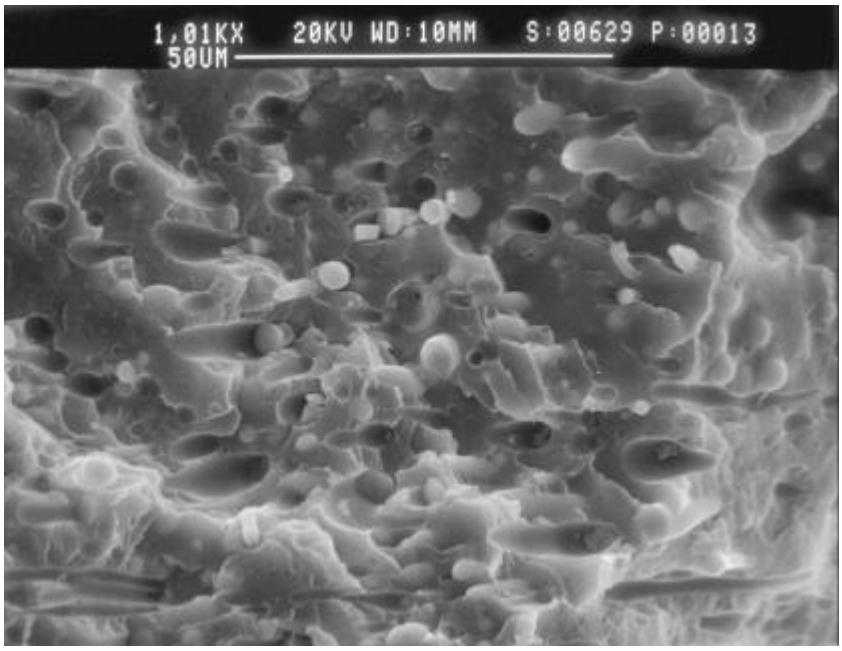

(a)

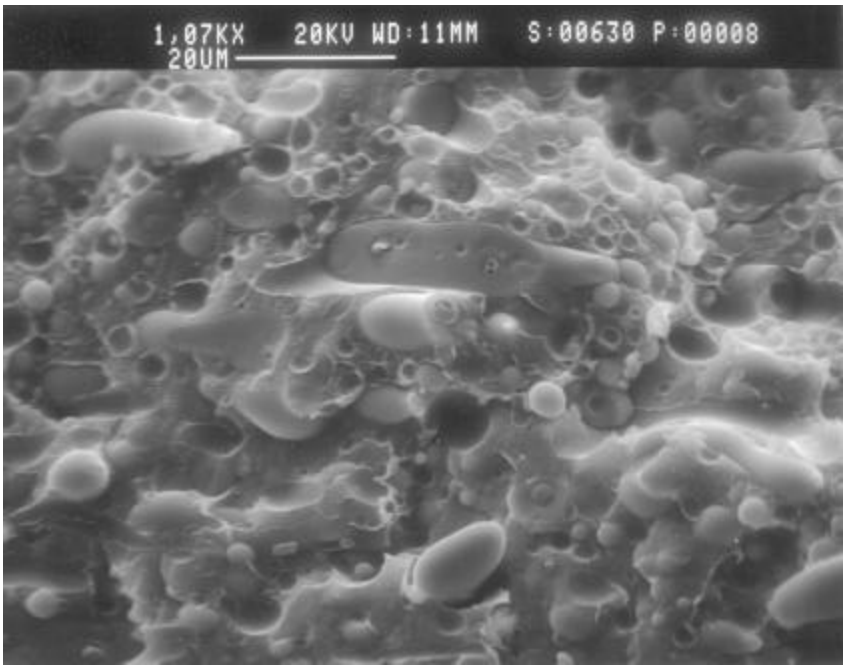

(b)

Figure 4.2: Scanning electron micrographs along the machine direction in the core region of injection molded samples. (a) 40 wt% P-glass (b) 60 wt% P-glass

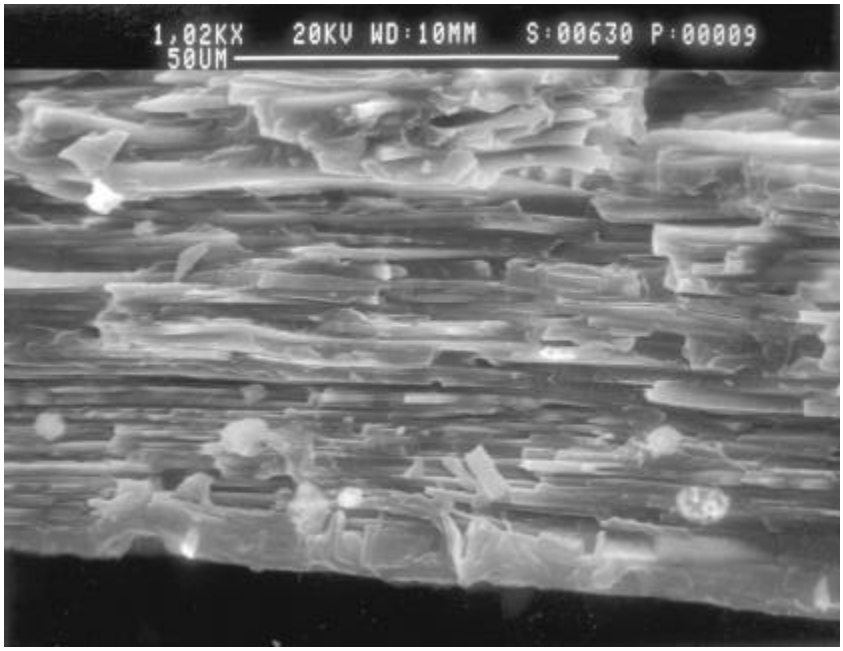

(a)

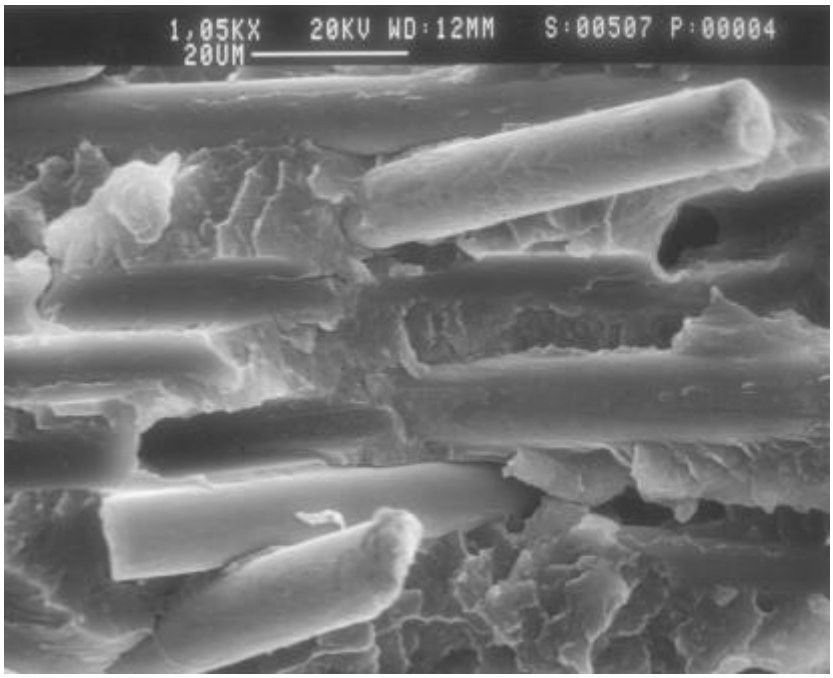

(b)

Figure 4.3: Scanning electron micrographs along the machine direction in the skin region of injection molded samples. (a) 60 wt% P-glass (b) 40 wt% E-glass

than the conventional E-glass reinforced material.

4.3.3 Composite Surface Roughness

Because it appeared that the small, high aspect ratio phosphate glass domains found in the skin region of injection molded samples may lead to smoother composite plaques, the surface roughness of the various materials were examined using surface profilometry. Common regions on the surface of injection molded plaques consisting of neat PPS and glass reinforced (P-glass & E-glass) composites were examined to determine if the surface roughness varied with the reinforcing materials. The arithmetic surface roughness (R_a) for the various materials is presented in Table 4.3. In the case of the phosphate glass reinforced materials, the addition of the glass led to no statistical deviation in the roughness when compared to the neat PPS except at the highest glass loading investigated (60 wt%). Neat PPS had an average roughness of 0.053 μm (± 0.015 μm) while a composite containing 60 wt% (44 vol%) phosphate glass had an average roughness of 0.093 μm (± 0.014 μm). Even though the addition of 60 wt% phosphate glass led to a rougher surface than the neat PPS, this composite blend was significantly smoother than a comparable E-glass fiber reinforced material. For a composite containing 40 wt% (26 vol%) E-glass fiber, the surface roughness was 0.202 μm (± 0.042 μm) almost twice that of the roughest phosphate glass reinforced composite. Similar trends were seen in the total indicator runout (TIR) which is the difference in height between the highest and lowest point within the 500 μm length scanned for each measurement. The E-glass filled composite showed greater variation over the scanned area displaying a TIR value of 1.224 μm (± 0.186 μm) as compared to 0.676 μm (± 0.178 μm) for the composite containing 60 wt% P-glass and 0.425 μm (± 0.077 μm) for the neat PPS.

4.3.4 Dynamic Mechanical Properties of Composite Blends

Along with the tensile and flexural mechanical properties, the dynamic mechanical response of the composite blends was also investigated both in solid and the melt state. The viscoelastic behavior of phosphate glass filled thermoplastics composites has been investigated only a limited basis and was shown to be useful tool in the characterization of these novel composite blends[6,12]. For the composites investigated in this study, dynamic mechanical thermal analysis (DMTA) was performed on strips cut from the injection molded specimens in order to establish the solid state response of the various composite blends over a wide temperature range. Dynamic mechanical testing was also performed in the melt state to evaluate the effects of factors such as temperature, glass loading, and glass type on the complex viscosity of the composite blends.

For the dynamic mechanical thermal analysis, temperature sweeps were performed on the neat PPS as well as the various glass reinforced composites. The storage modulus (G') versus temperature for the various materials is shown in Figure 4.4. The addition of

Table 4.3: Surface Properties of Various Glass Reinforced PPS Injection Molded Composites

Glass Loading (Weight %)	Arithmetic Roughness (R_a) (μm)	Total Indicator Runout (TIR) (μm)
Neat PPS	0.053 (0.015)	0.425 (0.077)
20% P-glass	0.060 (0.030)	0.428 (0.142)
40% P-glass	0.070 (0.020)	0.483 (0.166)
60% P-glass	0.093 (0.014)	0.676 (0.178)
40% E-glass	0.202 (0.042)	1.224 (0.186)

Note: Standard Deviations given in parentheses

$$R_a = \left(\frac{1}{N}\right)\sum_{i=1}^{N}|\xi_i|$$

where N = number of measurements

ξ = height above the mean line

TIR - Difference in height between the highest and lowest point within the sampling length

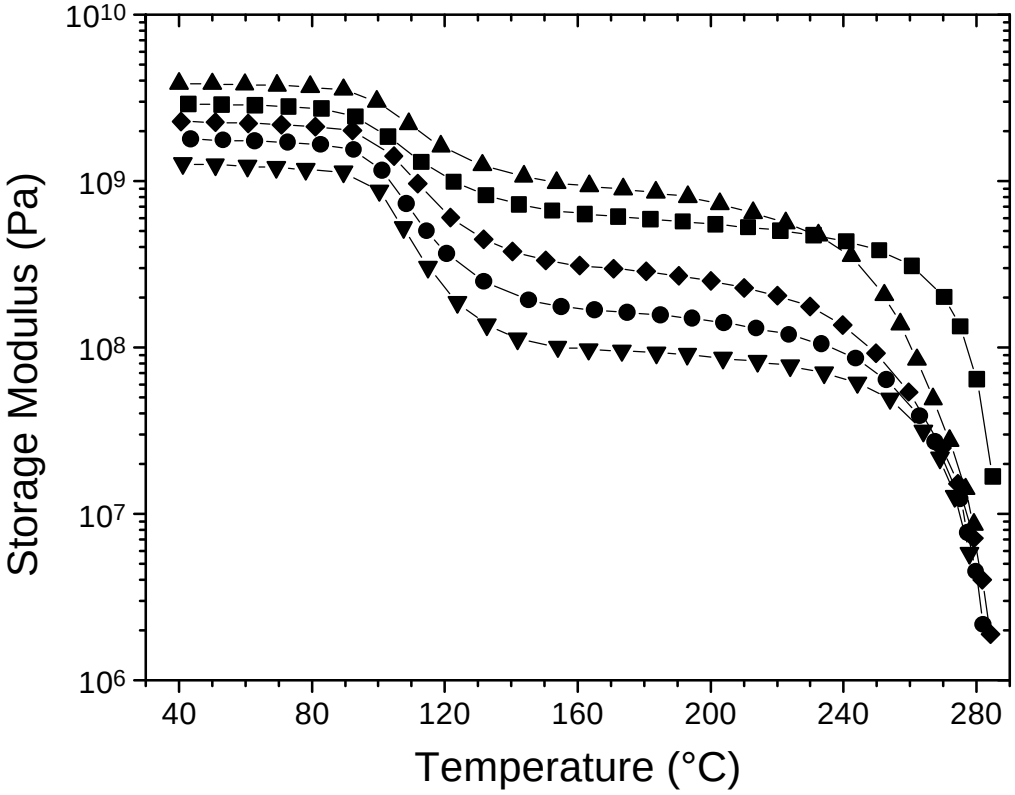

Figure 4.4: Storage modulus (G′) versus temperature of the neat PPS and various glass filled composites for a heating rate of 2.5 ± 0.1 °C/min. (▼) neat PPS, (●) 20 wt% P-glass, (◆) 40 wt% P-glass, (■) 40 wt% E-glass, and (▲) 60 wt% P-glass.

both the phosphate glass and E-glass led to storage moduli greater than that of the neat PPS. For the lower phosphate glass concentrations (<40 wt%), the storage modulus of the composite blends always fell below that of the composite containing 40 wt% E-glass. For the phosphate glass composite containing a higher glass loading (60 wt%), the storage modulus exceeded that of the E-glass filled composites up to a temperature of approximately 230°C. Above a temperature of 230°C, the storage modulus quickly fell approaching that of the neat PPS at a temperature of approximately 270°C. In the case of the phosphate glass reinforced composites, the drop in the storage modulus at the higher temperatures (>230°C) can be attributed to the increased mobility in the phosphate glass phase whose T_g was found to be approximately 234°C from DSC measurements. The lower viscosity of the phosphate glass phase allowed the incorporation of a higher loading of 60 wt% (44 vol%) glass which allowed the phosphate glass filled composite to exhibit higher storage moduli than a composite reinforced with only 26 vol% E-glass fiber.

Solid state dynamic analysis was also used to examine the thermal transitions of the composite components in order to determine if there may be any interactions between the various materials. The loss factor (tan δ) plotted versus temperature for the neat PPS and various glass reinforced composites is presented in Figure 4.5. Both the neat PPS and 40 wt% E-glass filled composites showed similar behavior in regards to the glass transition temperature of the PPS (peak at ≈ 110°C) and the increased mobility of the PPS at temperatures approaching the melting point of the resin. For the composites reinforced with the phosphate glass, the glass transition temperature for the PPS did not undergo a significant shift indicating a lack of interaction (i.e. miscibility) between the PPS and phosphate glass. At higher temperatures (>160°C), the loss factor for the phosphate glass filled composite rose to values much greater than the neat PPS due to the increased mobility of the phosphate glass phase within the composite blend.

The behavior of the various composite blends was also investigated in the melt state using small strain dynamic oscillatory testing. Initial rheological testing was first attempted at a temperature of 350°C, which was the temperature utilized for the manufacture of the phosphate glass filled composites. The various composites displayed limited thermal stability at the high temperatures and longer time scales (10-15 minutes) required for heating and testing the composite blends. At a temperatures of 350°C, the PPS/P-glass blends produced volatiles that displaced material from between the parallel plates resulting in erroneous estimates of the magnitude of the complex viscosity. Due to the limited thermal stability of the composite blends at the higher temperatures, rheological testing was performed at a lower temperature (300°C) commonly utilized for the processing of neat PPS and E-glass filled composites. Dynamic time sweeps performed at 300°C and an angular frequency of 1 rad/sec revealed that the complex viscosity of the neat PPS and composite blends was thermally stable showing no significant decline over a twenty minute period.

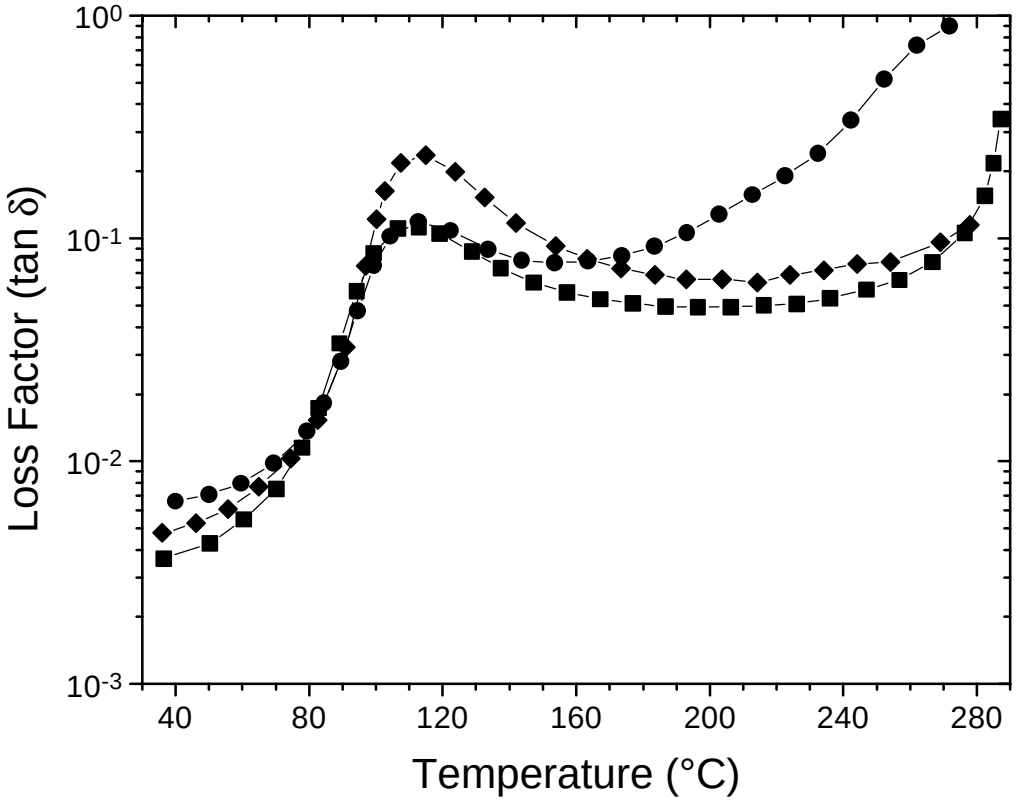

Figure 4.5: Loss factor (tan δ) versus temperature of the neat PPS and various glass filled composites for a heating rate of 2.5 ± 0.1 °C/min. (◆) neat PPS, (■) 40 wt% E-glass, and (●) 60 wt% P-glass.

The strain dependence of the dynamic properties of the composite blends was investigated to determine if the materials displayed a linear viscoelastic response at the conditions utilized for testing. The strain dependence of the dynamic shear moduli for select glass filled blends is presented in Figure 4.6. At the highest phosphate glass loadings 60 wt% (44 vol%), the moduli of the blend displayed a low sensitivity to the applied strain with the storage modulus only dropping approximately 20% for strains applied over a range of 0.1 - 2.5%. The E-glass fiber filled composite, containing a lower glass loading (26 vol%), displayed a greater strain dependence with the storage modulus showing almost a 80% drop over the same strain range. Though not shown here, the dynamic properties of the composites containing lower phosphate glass loadings (12 & 26 vol%) also showed much lower strain dependence than the E-glass filled material. Due to the highly nonlinear behavior of the E-glass filled composite, subsequent rheological testing was performed at the lowest strains that allowed adequate resolution of the transducer torque signal.

The complex viscosity versus angular frequency at 300°C for the neat materials (PPS and P-glass) and various composite blends is presented in Figure 4.7. With the addition of 20 wt% (12 vol%) phosphate glass, the complex viscosity of the composite blend was found to display negative deviation falling below that of both the neat phosphate glass and PPS. At the higher P-glass concentrations (40 & 60 wt%), the viscosity of the blends fell between that of the neat glass and PPS. It was believed that the high viscosity of the phosphate glass phase at 300°C ($\approx 10^6$ Pa·s) helped lead to the significant increases in the complex viscosity of the blends at the higher phosphate glass loadings. For composites containing 40 wt% (26 vol%) glass, the phosphate glass filled material typically displayed a lower complex viscosity than the E-glass filled composite at the lower angular frequencies (< 1 rad/sec). At higher angular frequencies, the complex viscosity of the E-glass composite was found to fall below that of the P-glass reinforced blend possibly due to the nonlinear behavior of the composite blend. The differences in the frequency dependence of the complex viscosity of the E-glass and P-glass filled blends can be partially attributed to the reinforcing phase morphology and interfacial tension between the reinforcing phases and the PPS. The E-glass filled material contained large diameter (≈ 12 μm), higher aspect ratio glass fibers that have been treated with a sizing agent to help reduce the interfacial tension between the glass and PPS. The phosphate glass filled composites typically contained glass beads that appeared to display higher interfacial tension with PPS as indicated by the formation of the large glass domains and glass pullout seen with scanning electron microscopy. Additional experimentation would be required to ascertain the exact role of these parameters on the overall dynamic response of the various blends.

In an effort to determine how the phosphate glass viscosity would affect the viscoelastic response of the blends, the complex viscosity of the glass filled materials was examined as a function of temperature. Phosphate glasses utilized for reinforcing thermoplastics have been found to possess activation energies on the order of 70-90

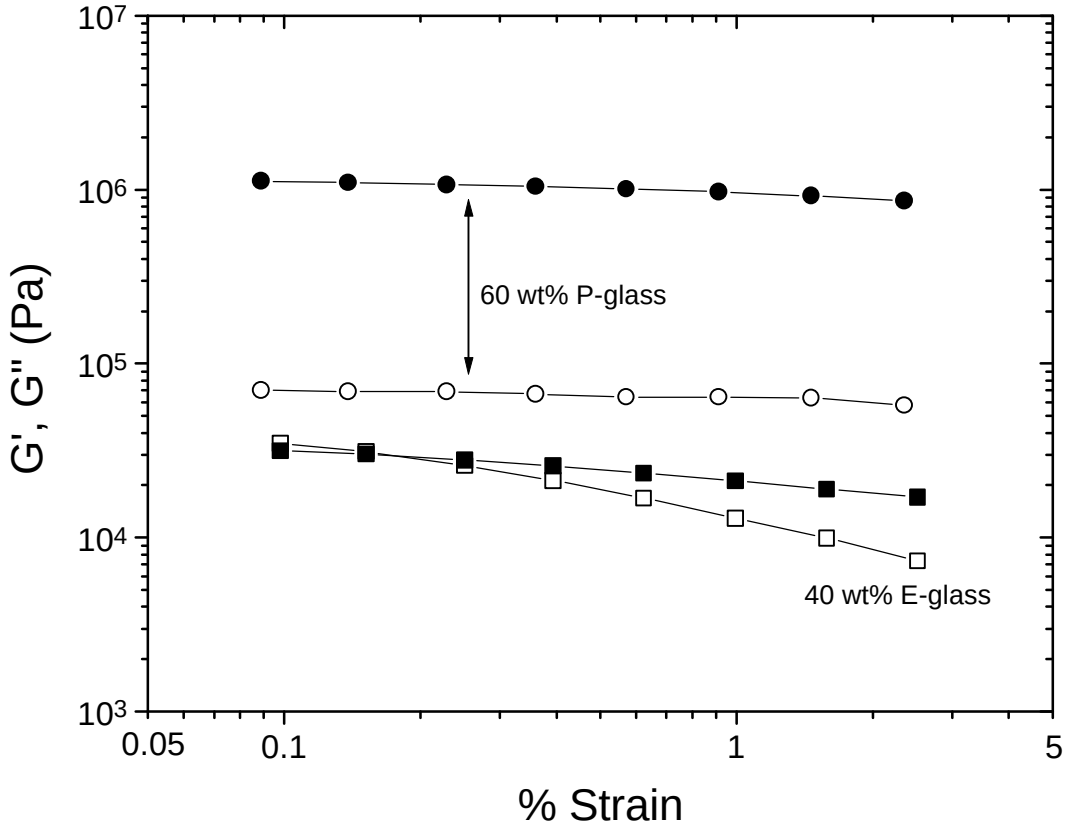

Figure 4.6: Storage Modulus (G′) and Loss Modulus (G″) versus applied strain at 10 rad/sec and 300.1 ± 0.1°C for glass filled PPS composites. (●) G″ and (○) G′ (60 wt% P-glass) ; (■) G″ and (□) G′ (40 wt% E-glass).

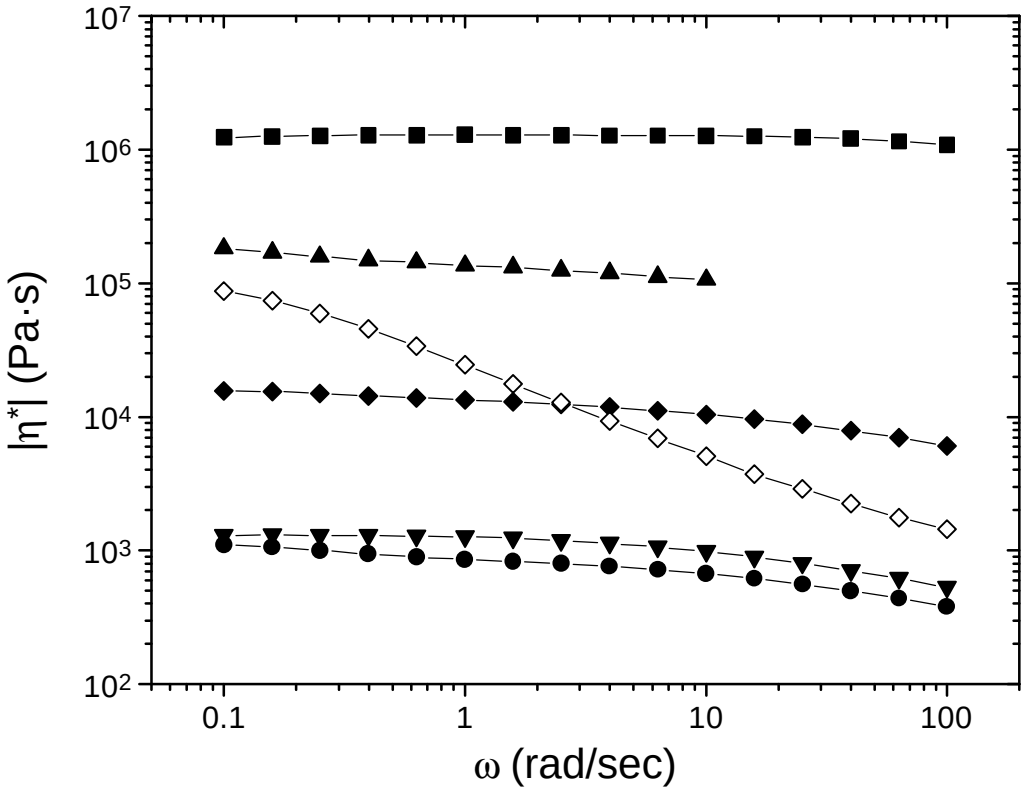

Figure 4.7: Complex viscosity (|η*|) versus angular frequency (ω) for neat PPS, neat P-glass, and various glass filled composites at 300.1 ± 0.1°C. (▼) neat PPS, (●) 20 wt% P-glass, (◆) 40 wt% P-glass, (▲) 60 wt% P-glass, (■) neat P-glass, and (◇) 40 wt% E-glass fiber.

kCal/mol which can serve to lower the glass viscosity an order of magnitude for every 20-30°C [14,17]. Due to the limited thermal stability of the blends at the higher temperatures, the complex viscosity of the various samples was measured at an angular frequency of 1 radian/second as the materials were heated rapidly from 300°C at a rate of approximately 5°C/min. The complex viscosity versus temperature for the neat PPS and various glass filled composites is shown in Figure 4.8. For the neat PPS and composite blend containing 40 wt% E-glass, only the viscosity of the PPS was lowered upon heating which resulted in the similar activation energies displayed by the materials. For the composite containing 60 wt% phosphate glass, the complex viscosity of the blend displayed a much greater decline with increasing temperature. The large decline in the complex viscosity of the composite blend was attributed to the large activation energy of the phosphate glass which was found to be on the order of 87.9 ± 1.1 kCal/mol [14]. The large activation energy of the phosphate glass resulted in the complex viscosity falling from 1.5×10^6 Pa·s at 300°C to a value of approximately 3000 Pa·s for a temperature of 350°C [14]. The large drop in the phosphate glass viscosity allowed the complex viscosity of the blend to fall by almost two orders of magnitude resulting in a viscosity only slightly greater than that of the neat resin. The fluidity of the phosphate glass at the temperatures used to process the thermoplastic resin offers a large advantage in that the viscosity of the composite blend can easily be adjusted to the desired magnitude by simply varying the processing temperature.

4.4 Conclusions

The addition of phosphate glass to PPS was found to be an effective method for producing injection molded composites that exhibited greater stiffness than the neat resin. Even at very low loadings (12 vol%), the addition of the phosphate glass was found to elevate the machine direction moduli by 1-2 GPa. Composites containing up to 44 vol% phosphate glass were easily injection molded yielding materials that possessed machine direction tensile and flexural moduli almost 4 times those of the neat PPS. Machine direction moduli comparable to conventional E-glass fiber filled composite (40 wt%) could be achieved by utilizing higher phosphate glass loadings on the order of 60 wt%.

While the addition of the phosphate glass led to enhancements in the modulus of the composite blend, the strength of the materials often fell with increasing glass concentration. For all the glass concentrations investigated, the tensile strengths of the composite blends were found to fall below those of the neat resin. The transverse direction flexural strength displayed a similar loss while the flexural strength along the machine direction was found to be insensitive to glass loading, showing a slight improvement (≈ 15%) over the neat resin. The strength of the phosphate glass reinforced composite was found to be approximately 2-3 times lower than a composite reinforced with a similar loading of E-glass fiber.

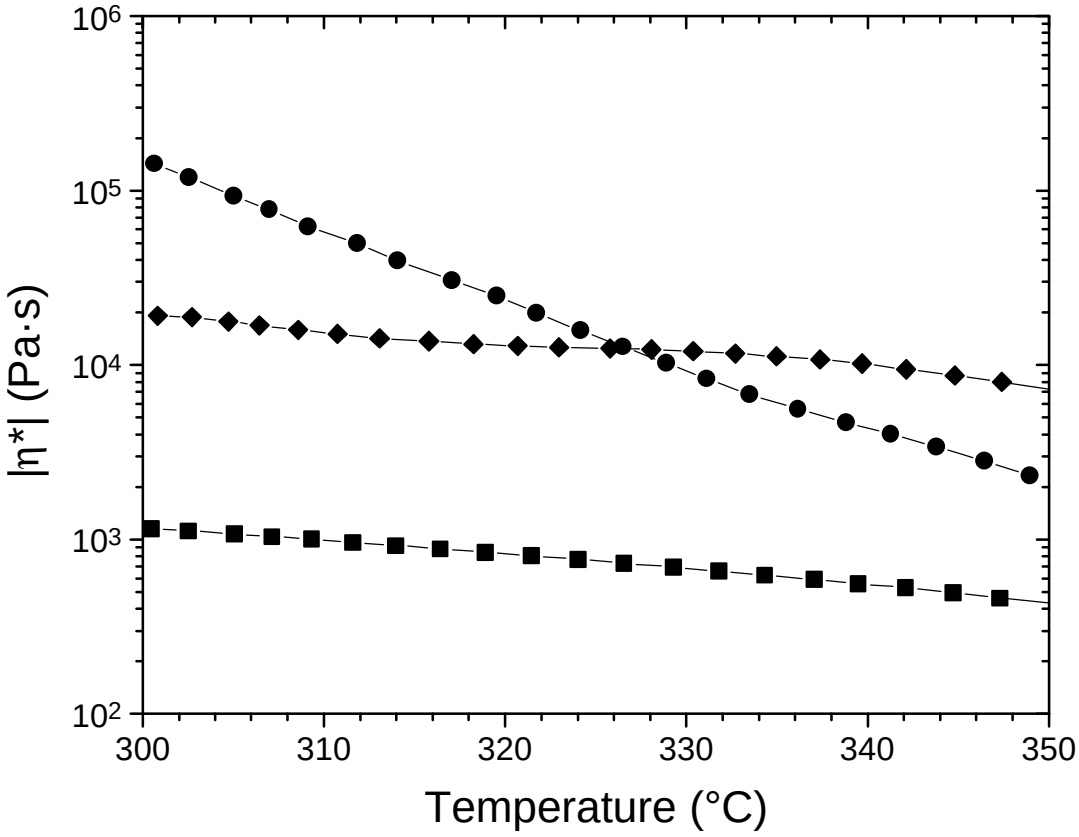

Figure 4.8: Complex viscosity (|η*|) versus temperature for neat PPS and various glass filled composites for a heating rate of 4.6 ± 0.1°C/min. (■) neat PPS, (◆) 40 wt% E-glass, and (●) 60 wt% P-glass.

Even though the phosphate glass reinforced composites offered lower strengths than neat PPS and an E-glass fiber filled material, these composites were found to offer certain advantages. For film-gated injection molded samples, all the phosphate glass reinforced composites investigated displayed much lower anisotropy in mechanical properties than an E-glass fiber filled material. The use of the phosphate glass also resulted in the formation of smaller reinforcing domains leading to composites which possessed smoother surfaces. The reduced viscosity of the phosphate glass during processing facilitated the injection molding of higher glass loadings than were possible with a conventional solid glass fiber reinforced material.

4.5 Acknowledgments

The authors would like to gratefully recognize the financial support of the NSF Science and Technology Center for High Performance Polymeric Adhesives and Composites at Virginia Tech (Grant No. DMR-8809174 AMD 1) and the Army Research Office (Grant No. DAAH04-94-G-0282). Also, we would like to thank Phillips Chemical Company and Hoechst Celanese for supplying the PPS and Corning Inc. for producing the phosphate glass utilized in this study. Appreciation is also extended to Dr. Garth Wilkes for allowing use of the scanning electron microscope, Dr. Norm Eiss for his assistance in the surface profilometry measurements, and to Dr. Mike McLeod for his assistance in obtaining the SEM images.

4.6 References

1 Schweizer and Winterman, *Thermoplastic Polymer Additives: Theory and Practice*, ed. J.T. Lutz Jr., Marcel Dekker, New York 1989.

2 S. Kessler, in *Plastics Additives and Modifiers Handbook* (Chapter 48), ed. J. Edenbaum, Van Nostrand Reinhold, New York 1992.

3 G. Kiss, *Polym. Eng, Sci.*, 27, 410 (1987)

4 N.H. Ray and F.R. Sherliker, U.S. Patent 3,732,191 (1973).

5 W.A. Bahn, G.H. Beall, J. Ference, B.C. Monahan, C.J. Quinn, and P.S. Roussel, U.S. Patent 5,043,369 (1991).

6 C.J. Quinn, P. Frayer, and G.H. Beall, in *Polymeric Materials Encyclopedia* (vol. 4), ed. J.C. Salamone, 2766 (1996).

7 C.J. Quinn and G.H. Beall, in *Chem. Process. Adv. Mater*., ed L. Hench, 799 (1992).

8 G.H. Beall and C.J. Quinn, U.S. Patent 4,940,677 (1990).

9 G.H. Beall and J.E. Pierson, U.S. Patent 5,328,874 (1994).

10 B.G. Aitken, G.H. Beall, and J.E. Dickenson, Jr., U.S. Patent 5,529,961 (1996).

11 W.A. Bahn and C.J. Quinn, *SPE ANTEC Proc*., 2370 (1991).

12 J.U. Otaigbe, C.J. Quinn, and G.H. Beall, *Polym. Comp*., 19 (1), 18 (1998)

13 J. Geibel and J. Leland, in *Encyclopedia of Chemical Technology*, 4 (19), 904 (1996).

14 R.T. Young, *PhD Dissertation*, Virginia Polytechnic Institute and State University (1999).

15 P.K. Mallick, *Fiber Reinforced Composites*, Marcel Dekker, New York 1988.

16 PPG Industries, Inc., in *Modern Plastics Encyclopedia '92*, McGraw-Hill, New York 1992.

17 R.L. Sammler, J.U. Otaigbe, M.L. Lapham, N.L. Bradley, B.C. Monahan, and C.J. Quinn, *J. Rheol*., 40 (2), 285 (1996).

Chapter 5:
Processing Effects and Molded Properties

Preface

This chapter is focused on the first and third objectives of the research. Specifically, the effects of the rheological and interfacial properties of the blend components on the properties of injection molded composites was examined. This chapter is organized as a manuscript for future publication.

Processing and Properties of Injection Molded Thermoplastic Composites Reinforced with Melt Processable Glasses

R.T. Young and D.G. Baird

Department of Chemical Engineering and
NSF Science and Technology Center for High Performance
Polymeric Adhesives and Composites

Virginia Polytechnic Institute and State University
Blacksburg, VA 24061-0211

(ABSTRACT)

This work was concerned with evaluating the properties of injection molded composites comprised of polyetherimide (PEI) and polyetheretherketone (PEEK) reinforced with various lower T_g melt processable phosphate glasses. Composites were produced utilizing a variety of glass and resin combinations in order to ascertain the effects of factors such as glass concentration and viscosity of the components on the mechanical properties of the composite blends. Changes in the rheological and interfacial properties of the blends obtained by varying the resins and phosphate glasses used during processing resulted in a variety of reinforcing morphologies consisting of glass beads, ribbons, and an interpenetrating network structure. The large variations in the glass phase morphologies obtained during injection molding led to composites that displayed a wide range of properties. Generally, it was found that the use of resin/glass combinations that minimized the viscosity difference between the components resulted in composites displaying the best overall properties. The stiffness of the composites were found to increase with glass concentration with loadings up to 45 vol% glass leading to moduli 3-4 times greater than those of the neat resins. While the addition of the phosphate glasses produced significant enhancements in the stiffness of the composite blends, the strength often fell to values 2-3 times lower than the neat resins.

5.1 Introduction

The addition of high aspect ratio inorganic reinforcement, such as glass fiber, to thermoplastics has allowed the production of composite systems that possess moduli and strengths significantly greater than those of neat matrices. While the addition of solid reinforcement often results in significant enhancements in the mechanical properties, it can

also lead to numerous problems in an process such as injection molding. During injection molding the presence of solid fibers can result in wear on various parts such as the screw, barrel, and mold. The complex interactions between the fibers and flow field seen during molding can result in molded products that suffer from a variety of problems such as anisotropy in properties, weld line formation, and poor surface appearance [1,2].

Due to the processing difficulties created by the addition of solid reinforcement, work has been performed on the development of alternative composite systems that overcome many of the problems associated with conventional short fiber reinforced thermoplastics [3-11]. One such method referred to as in situ composite manufacturing relies on the formation of the reinforcing phase morphology during processing [3,5,7]. During processing operations, both the thermoplastic matrix and reinforcing phase are fluid, thereby alleviating many of the problems seen with conventional solid reinforced systems. The final reinforcing phase morphology can be developed from deformation applied through a variety of processing techniques such as injection molding, fiber spinning, and film casting.

One of the materials that has shown great promise for in situ composite generation techniques are melt processable glasses [8-11]. These inorganic glasses have low glass transition temperatures (200-350°C) allowing them to be combined with thermoplastic resins for use in conventional polymer processing techniques. The lower thermal transition temperatures for these materials are obtained by utilizing P_2O_5 instead of SiO_2 as the primary glass former. Additional materials such as alkali and alkaline earth oxides are added in order to help control the thermal transitions and chemical durability of the glasses [10]. Due to their structure, phosphate based glasses typically display lower mechanical properties than borosilicate glasses commonly utilized in the reinforcement of thermoplastics. The use of phosphate glasses in engineering applications has been limited due to the poor chemical durability of the glass. Present research is being focused on formulating melt processable glasses with lower transition temperatures and improved chemical durability [12-14]. The development of more durable glasses with lower transition temperatures could make these materials a viable alternative reinforcing phase for a variety of composite fabrication techniques.

Investigations using phosphate glasses as a reinforcement for thermoplastics have mainly concentrated on injection molding applications [8-11]. Much of the work has involved the blending of a variety of thermoplastics with a number of glasses in order to ascertain the properties that could be achieved. In recent years, the development of glasses with lower transition temperatures and increased chemical durability have shown great promise for the process of injection molding. For example Bahn, Quinn and co-workers [9-11] injection molded composites consisting of higher transition glasses (225°C $< T_g <$ 350°C) blended with higher processing temperature thermoplastics such as polyetherimide (PEI), polyethersulfone (PES), polyetheretherketone (PEEK), polyetherketone (PEK), and thermotropic liquid crystalline polymers (TLCPs). Much of

the work focused on higher glass loadings (50-70 vol%) because P-glass composites manufactured with conventional glass loadings (up to 40 vol%) appeared to offer only modest increases in mechanical properties relative to those obtained with E-glass. Composites reinforced with high loadings of phosphate glass typically had tensile moduli 4-10 times greater than that of the neat resins. For example, an injection molded PEK composite containing 70 vol% phosphate glass had a tensile modulus of approximately 30 GPa while the neat thermoplastic resin only had a modulus of 4 GPa. In addition to greater stiffness, phosphate glass reinforced composites were shown to offer other advantages such as low mechanical anisotropy, finer molding tolerances, greater resistance to creep and stress relaxation, and lower thermal expansion coefficients [10,11]. One of the drawbacks found with utilizing such high inorganic loadings was that the tensile strengths of the composite blends were found to fall below that of the neat resins.

While a number of thermoplastics reinforced with phosphate glasses have been investigated under injection molding, limited studies have been conducted on the effects of processing parameters on the morphology and properties of P-glass reinforced composites. Work performed by Bahn and Quinn [15] investigated the role of parameters such as glass concentration and the glass and matrix viscosity on the morphology of extruded composites consisting of polyaryletherketones (PAEK) reinforced with a phosphate glass. At low glass loadings (10-40 vol%), limited dispersion of the glass was obtained within a twin screw extruder resulting in a glass microstructure consisting of large glass particles (>100 μm) interdispersed with fine glass spheres on the order of 2-3 μm. Increasing the glass loading to 40-65 vol% resulted in a glass microstructure consisting of well dispersed spherical particles (2-3 μm). The formation of the well-dispersed morphology was attributed to increased glass particle interactions which led to the elongation of the glass phase into strands which eventually reached a critical diameter and broke into spherical particles. It was also found that lower viscosity ratios ($\eta_{glass}/\eta_{matrix}$) typically resulted in smaller dispersed glass phases. The lower viscosity ratios between the glass and polymer matrices were achieved through a variety of techniques including the utilization of higher processing temperatures and higher viscosity thermoplastic resins. Composite blends containing high glass loadings (>65 vol%) were found to undergo phase inversion with the polymer resin being present as dispersed droplets. The phase inversion also appeared to be linked to factors such as the glass loading and the viscosity differences between the glass and thermoplastic resin.

The reinforcing glass phase morphology generated during processing has also been found to have a large effect on the mechanical properties of the composites blends as shown by Quinn and coworkers [10] who investigated the injection molding of a thermotropic liquid crystalline polymer (Xydar) reinforced with a zinc alkali phosphate glass. A variety of reinforcing morphologies consisting of small glass beads, fibers, and ribbons were produced using a high speed injection molding unit capable of screw forward speeds up to approximately 1000 mm/sec. High speed injection molding was utilized due to the high thermal conductivity and rapid solidification of the composite blends which

contained up to 62 vol% phosphate glass. The transition of the glass morphology from beads to elongated ribbons led to significant increases in the composite's mechanical properties. For a blend containing 62 vol% glass, a morphology consisting of small glass beads yielded a tensile modulus of 17 GPa while a morphology consisting of glass ribbons resulted in tensile modulus of 28 GPa. Similar enhancements in the strength were observed with the transition in morphology elevating the tensile strength from 52 MPa to 72 MPa. Even though a variety of data were presented on the effects of the various morphologies on the properties of the composites, no correlations were made between the formation of the composite morphology and processing conditions utilized.

For other in situ composite systems, the formation of the reinforcing phase morphology during molding has been shown to be dependent on a complex interaction between both material and processing parameters [16-21]. Material parameters such as the viscosity ratio and interfacial tension between the various phases have been shown to play key roles in the formation of the reinforcing phase morphology [18-20]. Factors such as the stress fields and heat transfer have also been found to affect the mechanical properties of in situ composites which used TLCPs as the reinforcing phase [17,18]. For example, O'Donnell [18] studied the effects of mold thickness, viscosity ratio, melt temperature and mold fill rate on the properties of a polypropylene/maleic anhydride grafted polypropylene blend reinforced with 30 wt% of a TLCP (LC3000, a copolyester of polyethylene terephthalate and hydrobenzoic acid). The highest mechanical properties were obtained when a fibrillar reinforcing morphology was generated within the skin regions of the molded samples. This was promoted when the PP/TLCP viscosity ratio was approximately one and the storage and loss moduli of the TLCP melt were approximately equal. It was also found that variations in the stresses and heat transfer could lead to composites displaying a wide range of properties. Processing conditions which generated higher stresses and prolonged the deformation of the reinforcing phase during mold filling were generally found to produce composites with the highest level of reinforcement. It was also believed that processing conditions which allowed the elongated TLCP fibrils to solidify before they had a chance to breakup due to interfacial instabilities maximized the reinforcement attained with the addition of the TLCP.

Theories developed for droplet deformation and breakup for Newtonian fluids have often been applied to the formation of the reinforcing phase morphology within in situ composites. Work performed with Newtonian fluids established that a dispersed droplet can be elongated into a higher aspect ratio thread when exposed to either shear or elongational flow under certain conditions [22-27]. Deformation of the suspended droplet typically occurs when the disruptive hydrodynamic force is great enough to overcome the cohesive interfacial force between the components. The magnitude of the hydrodynamic force (stress) will depend strongly on the applied deformation rates as well as the rheological properties of the components. The viscosity ratio between the components (ratio of droplet to matrix viscosity) has also been found to have a large effect on the ability of the suspended phase to undergo deformation. Within simple shear flow,

viscosity ratios between 0.1 and 3.5 have been shown to lead to conditions favorable to the deformation and eventual breakup of suspended droplets. Meanwhile, shearfree or extensional flows provide conditions favorable to the deformation of the suspended phase over a much wider range of viscosity ratios. Trends similar to those seen with Newtonian fluids have been qualitatively observed in regards to the formation of the reinforcing morphology within in situ injection molded composites[4,16-21]. The extensional flow field generated from the advancing front during mold filling has been found to lead to the formation of elongated fibrillar morphologies over a broad range of viscosity ratios. Regions within the molded injection specimens where shear flow was predominant often contained lower aspect ratio domains due to the inability of the flow field to adequately deform the reinforcing phase.

The purpose of this paper was to evaluate the effects of glass concentration and the viscosity of the components (resin and glass) on the morphology and properties of various composite blends. In particular, a polyetherimide (PEI) and polyetheretherketones (PEEK) of varying molecular weight were injection molded with a lower T_g phosphate glass to ascertain the influence of the resins on the properties of the composite blends. The use of the two different resins (PEI and PEEK) served to vary both the interfacial and rheological properties of the blend while the utilization of the various grades of PEEK allowed the influence of the resin viscosity to be investigated. The two different grades of PEEK were also blended with a higher T_g phosphate glass to investigate the effects of changing the rheological and interfacial properties of the phosphate glass. The properties of the various resin/glass combinations were examined through a variety of methods including mechanical testing, scanning electron microscopy, and dynamic mechanical thermal analysis (DMTA).

5.2 Experimental

5.2.1 Materials

The melt processable phosphate glasses used in this study were experimental materials produced by Corning, Inc. (Corning, NY). The lower T_g phosphate glass investigated was comprised of P_2O_5 (33 mol%), $ZnCl_2$ (26 mol%), B_2O_3 (4 mol%), and M_2O (37 mol%) where M consisted of various alkali metals. The glass transition temperature for the glass was found to be 233.7 ± 2.2°C from differential scanning calorimetry (DSC) measurements performed at a heating rate of 10°C/min. The density of the glass was determined to be 2.62 ± 0.01 g/cm^3 from measurements made on as received glass samples utilizing a pyconometer (Micrometrics Accupyc, Model 1330). A higher T_g zinc sulfophosphate glass having a transition temperature of 281.8 ± 1.7°C and a density of 3.44 ± 0.03 g/cm^3 was also investigated. The sulfophosphate glass was comprised of P_2O_5 (25 mol%), ZnO (35 mol%), SO_3 (18 mol%), and various metal oxides (22 mol%).

Both of the glasses are considered non-durable in that the materials suffer from a loss in weight and mechanical properties when exposed to hot water. The glass samples were received as large shards that were crushed and sorted to yield particles ranging from 1-2 mm for use in injection molding. For rheological studies, the glass shards were ground to yield 25 or 7.9 mm diameter disks with thicknesses ranging from 1-2 mm.

Polyetherimide (PEI) and polyetheretherketone (PEEK) were used as the matrix resins for the injection molded phosphate glass reinforced composites. The grade of PEI used was designated as Ultem 1000 which was produced and supplied by General Electric. Ultem 1000 is a high temperature, amorphous thermoplastic having a glass transition temperature of 217°C and a density of 1.27 g/cm^3. An injection molding grade of PEI reinforced with 30 wt% E-glass fiber (Ultem 2300) was also processed to facilitate comparisons between the two types of glass reinforced composites. Phosphate glass reinforced composites were also manufactured with the high temperature, semi-crystalline engineering resin PEEK (Victrex USA Inc.). Two grades were used, a low viscosity injection molding grade of PEEK designated as 150G and a general purpose extrusion/injection molding grade designated as 450G. Both grades of PEEK possess a glass transition temperature of approximately 160°C, a melting point of 340°C, and a density of 1.30 g/cm^3.

5.2.2 Rheological Characterization

Rheological characterization of the neat thermoplastic and glass samples was performed using parallel plate fixtures attached to a Rheometrics Mechanical Spectrometer (Model RMS-800). Dynamic oscillatory measurements were carried out under a variety of conditions depending on the materials being investigated. The complex viscosity ($|\eta^*|$) of the resins was determined from test specimens consisting of pellets of the neat resin loaded between 25 mm diameter plates. For the glass samples, test specimens consisted of pre-ground disks having thicknesses ranging from 1-2 mm and a diameter of either 7.9 or 25 mm. Smaller diameter plates (7.9 mm) were utilized with the glass under certain conditions in order to generate lower strains and help insure measurements did not exceed the compliance of the instrument. Each sample was brought to the desired temperature and allowed to equilibrate for a least three minutes before the start of testing. The sample temperature was monitored by a thermocouple in contact with the lower plate fixture. The temperature was maintained by blanketing the sample with heated nitrogen in order to minimize degradation. Before rheological testing, samples were dried for at least 24 hours in a vacuum oven maintained at 150°C.

The complex viscosity of the various materials was determined by varying the angular frequency (ω) while holding the sample temperature constant. Angular frequency sweeps for the neat thermoplastic resins were performed using strains that ranged from 3-20%. For the neat glass samples, angular frequency sweeps were performed at the lowest

possible strains (0.1-5%) that allowed adequate resolution of the transducer torque signal ($\geq$ 0.2 gm·cm). The lowest possible strains were used in anticipation the glass would show the lowest strain dependence at these conditions allowing testing to occur in the linear viscoelastic region.

In order to study the processing behavior of the materials under nonisothermal conditions similar to those seen during mold filling, the complex viscosity was monitored as samples were cooled from a specified temperature. Samples were held at the desired temperature for a brief period ($\approx$ 3 minutes) and then cooled at a rate of approximately 2.5°C/min. while the complex viscosity was monitored at an angular frequency of one radian/second. The strain applied during testing was reduced as the sample viscosity rose to help insure the testing occurred within the linear viscoelastic region. The neat resin measurements were performed with 25 mm diameter plates while 7.9 mm plates were utilized with the phosphate glass in order to facilitate the application of lower strains.

5.2.3 Injection Molding

Composite blends were produced using an Arburg Allrounder, model 221-55-250, injection molding unit. The molder has a 22 mm screw with a check ring non-return valve and was fitted with a general purpose nozzle having a 2 mm exit diameter. For this study, the injection molding unit was used for two main processing steps including preblending of the materials and actual composite manufacture. All materials used during processing were dried for at least 24 hrs at 150°C under vacuum before being plasticated.

The first processing step involved using the injection molding unit as an extruder to preblend the glass with the resins. Due to the variety of blends to be studied and the limited availability of the phosphate glasses, the molding unit was seen as an effective way to preblend small batches of the composite materials. The initial dispersion of the glass within the thermoplastic matrix could be achieved rapidly while minimizing thermal degradation of the matrix resins at the higher processing temperatures.

For preblending, the barrel assembly frame was released from the mold assembly and modified to run as an extruder by adjusting the back pressure so the material would flow freely from the nozzle. A dry blend of the glass and polymer was passed through the screw operating at 200 rpm with the extrudate being collected, quenched, and granulated using a Cumberland Granulator (Model 6x8). This granulated material was then subsequently used as feed stock for the injection molding studies. For the composites manufactured with the lower T_g (234°C) glass, the barrel temperature profile progressing from the solids conveying zone to the nozzle consisted of 350°C, 370°C, 370°C, and 370°C. The temperatures of the zones were increased by 40°C to facilitate the processing of composites reinforced with the higher T_g (282°C) phosphate glass.

The second main processing step involved the fabrication of the composite blends into test specimens by injection molding. Composite plaques were produced by injecting the plasticated blend into a film-gated mold having dimensions of 75 mm by 80 mm by 1.6 mm. During molding operations, the injection pressure (5 MPa), holding pressure (10 MPa), screw speed (200 rpm), and cooling time (45 seconds) were all held constant. All the composites reinforced with the lower T_g glass were produced using an injection rate of approximately 10 cm^3/sec. with a mold temperature of 160°C. Due to the rapid solidification of the higher T_g glass reinforced composites, a higher injection rate (≈ 35 cm^3/sec.) and mold temperature (200°C) were used to help insure the material completely filled out the mold.

5.2.4 Mechanical Properties

The tensile and flexural properties of the various composite blends were measured using an Instron Mechanical Tester (Model 4204). Test specimens approximately 75 mm long by 8 mm wide were cut from the injection molded plaques along both the machine (flow) and transverse directions. Tensile properties were measured using a 5 kN load cell following ASTM standard B 638-87B. The crosshead speed was kept constant at 1.27 mm/min. with the strain imposed on the sample measured using an extensionmeter (Instron Model 2630-25). Flexural properties were measured using a three-point bending test following ASTM standard D 790M 86. All the mechanical properties reported are the average of at least five test specimens.

5.2.5 Dynamic Mechanical Thermal Analysis

In order to study how the addition of the various glasses affected the viscoelastic behavior of the composite blends, the dynamic response of the materials in the solid state was examined over a wide range of temperatures. Dynamic mechanical thermal analysis (DMTA) was performed in torsion using a Rheometrics RMS-800. Rectangular strips cut along the machine direction of the injection molded plaques were heated in air at a rate of approximately 2.5°C/min. while the viscoelastic properties of the materials were probed at an angular frequency (ω) of 10 rad/sec and a strain of 0.1%.

5.2.6 Morphology

The morphology of the injection molded composite plaques was examined using a Stereoscan S200 scanning electron microscope with an accelerating voltage of 20 kV. The surfaces examined were prepared by immersing the sample in liquid nitrogen for approximately 5 minutes before fracturing. The samples were subsequently attached to mounting studs and coated with a layer of gold using a sputter coater (Bal-Tec Model SCD 005) to enhance conductivity.

5.3 Results and Discussion

5.3.1 Rheological Characterization

Rheological characterization was performed on the neat resins as well as the phosphate glasses to help ascertain the effects of various thermal and deformation histories on the response of the materials. The rheological testing was seen as an effective way to determine the processing conditions that would facilitate the dispersion and deformation of the phosphate glass phase during processing.

The rheological response of the lower T_g phosphate glass (234°C) and various thermoplastic resins was examined by performing angular frequency sweeps under small strain dynamic oscillatory testing. The complex viscosity of the various materials was examined at a temperature of 370°C. The complex viscosity as a function of angular frequency for the PEI, phosphate glass, and various grades of PEEK is presented in Figure 5.1. At this temperature, the complex viscosity of the phosphate glass showed a strong dependence on angular frequency, falling by almost 50% over the angular frequencies investigated. The large variation in the complex viscosity at the lower angular frequencies (< 1 rad/sec) may be an indication of the formation of crystalline regions within the glass melt. An Arrhenius fit for the zero shear viscosity from rheological testing performed at lower temperatures (300-350°C) predicted the zero shear viscosity of the glass would fall in the range of 300 Pa·s, a value comparable to that observed at the higher angular frequencies [28]. It appears that the development of structure within the phosphate glass melt served to elevate the complex viscosity at the lower frequencies while having minimal effect on the response of the material at the higher frequencies. Similar behavior that was presumed to be caused by the formation of crystalline regions has also observed for a phosphate glass of another composition [29]. The complex viscosity of the neat glass was found to fall well below that of the neat PEI (Ultem 1000) and higher molecular weight grade of PEEK (Victrex 450G) over the angular frequencies investigated. At the lower frequencies, the Victrex 450G displayed a much higher complex viscosity than the Ultem 1000 with the materials displaying similar responses at the higher angular frequencies. The Victrex 150G, a lower molecular weight grade of PEEK, displayed complex viscosities comparable to the phosphate glass over the entire frequency range examined. Assuming the Cox-Merz rule [i.e. $|\eta^*(\omega)| \approx \eta(\dot{\gamma})$] applies for the materials investigated, the viscosity ratios ($\eta_{glass}/\eta_{resin}$) were all on the order of 0.1-1, which should be favorable for the dispersion and deformation of the glass phase at a processing temperature of 370°C.

A similar analysis of the complex viscosity versus angular frequency was performed for the higher T_g phosphate glass (282°C) and the two grades of PEEK. Rheological characterization of the neat phosphate glass revealed that temperatures

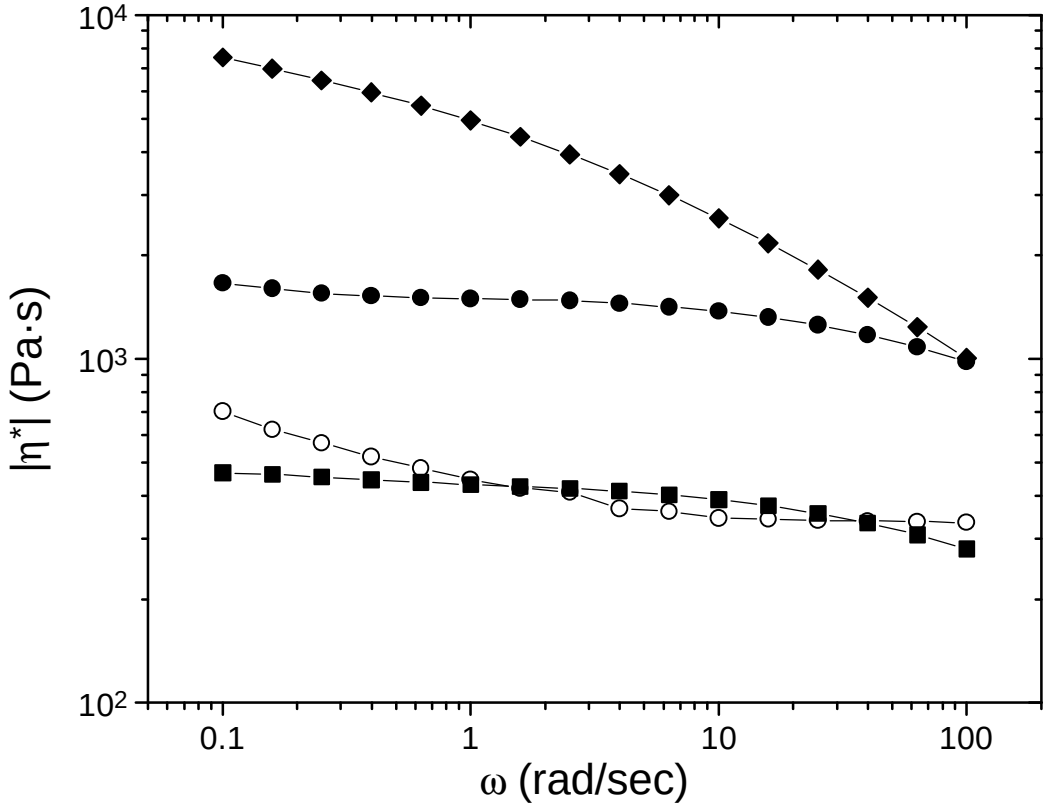

Figure 5.1: The complex viscosity (|η*|) versus angular frequency (ω) for various materials at 370.3 ± 0.5°C. (○) Phosphate glass (T_g - 234°C), (◆) PEEK (Victrex 450G), (●) PEI (Ultem 1000), and (■) PEEK (Victrex 150G)

greater than 400°C provided a lower glass complex viscosity that would facilitate processing with the PEEK [28]. The complex viscosity versus angular frequency for the various materials measured at a temperature of 410°C is presented in Figure 5.2. For the frequencies investigated, the phosphate glass displayed Newtonian behavior with the complex viscosity exceeding that of both grades of PEEK. For the higher viscosity grade of PEEK (450G), the complex viscosity approached that of the phosphate glass at the lower angular frequencies (0.1 rad/sec) while the complex viscosity of the glass exceeded that of the PEEK by almost an order of magnitude at the higher frequencies (100 rad/sec). The large drop in the 450G complex viscosity over the range of angular frequencies led to unfavorable viscosity ratios (η_{glass}/η_{PEEK}) ranging on the order of 1 to 5. The complex viscosity of the Victrex 150G also fell below that of the P-glass leading to even more unfavorable viscosity ratios of 10-20.

The nonisothermal response of the various materials was also investigated to provide some insight into how the temperature changes seen during mold filling would affect the viscosity of the materials. The neat components to be combined with the lower T_g phosphate glass were held at 370°C and then cooled at a rate of approximately 2.5°C/minute while monitoring the evolution of the complex viscosity. The complex viscosity versus temperature for the phosphate glass and various thermoplastics is shown in Figure 5.3. The phosphate glass displayed a rapid rise in viscosity upon cooling which is indicative of the large activation energies found with inorganic glasses of this type [28,29]. For the PEI, the complex viscosity was higher than that of the phosphate glass only over a small temperature range where the much larger activation energy of the glass resulted in a rapid divergence in the viscosity of the materials. For the angular frequency investigated, the higher molecular weight grade of PEEK (450G) appeared to offer a higher viscosity than the glass down to a temperature of approximately 330°C where the PEEK displayed the onset of solidification due to crystallization. While the higher molecular weight grade of PEEK appeared to offer a favorable viscosity ratio over a wide temperature range, the complex viscosity of the Victrex 150G quickly fell well below that of the phosphate glass. The lower viscosity seen with the 150G could serve to limit the deformation of the phosphate glass phase during the mold filling step.

The nonisothermal rheological response of the higher T_g phosphate glass (282°C) and two grades of PEEK cooled from a temperature of 410°C is presented in Figure 5.4. The complex viscosity of the glass rose rapidly upon cooling, always exceeding the viscosity of the two grades of PEEK investigated. The viscosity ratios (η_{glass}/η_{PEEK}) were always much greater than one at the angular frequency investigated with the higher molecular grade of PEEK (450G) showing a viscosity ratio almost an order of magnitude lower than the Victrex 150G. The rapid rise in the glass viscosity coupled with the lower viscosity of the PEEK appeared to result in conditions that would be unfavorable for achieving deformation of the phosphate glass into a higher aspect ratio reinforcing morphology.

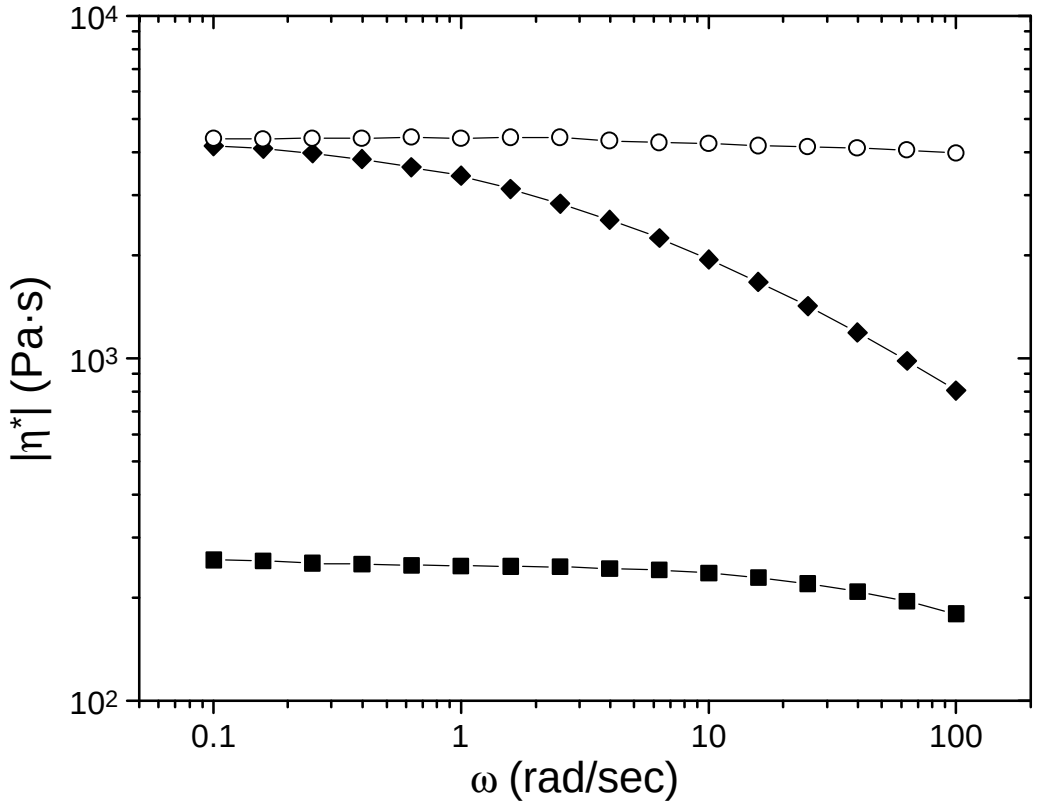

Figure 5.2: The complex viscosity (|η*|) versus angular frequency (ω) for various materials at 410.1 ± 0.1°C. (○) Phosphate glass (T_g - 282°C), (◆) PEEK (Victrex 450G), and (■) PEEK (Victrex 150G)

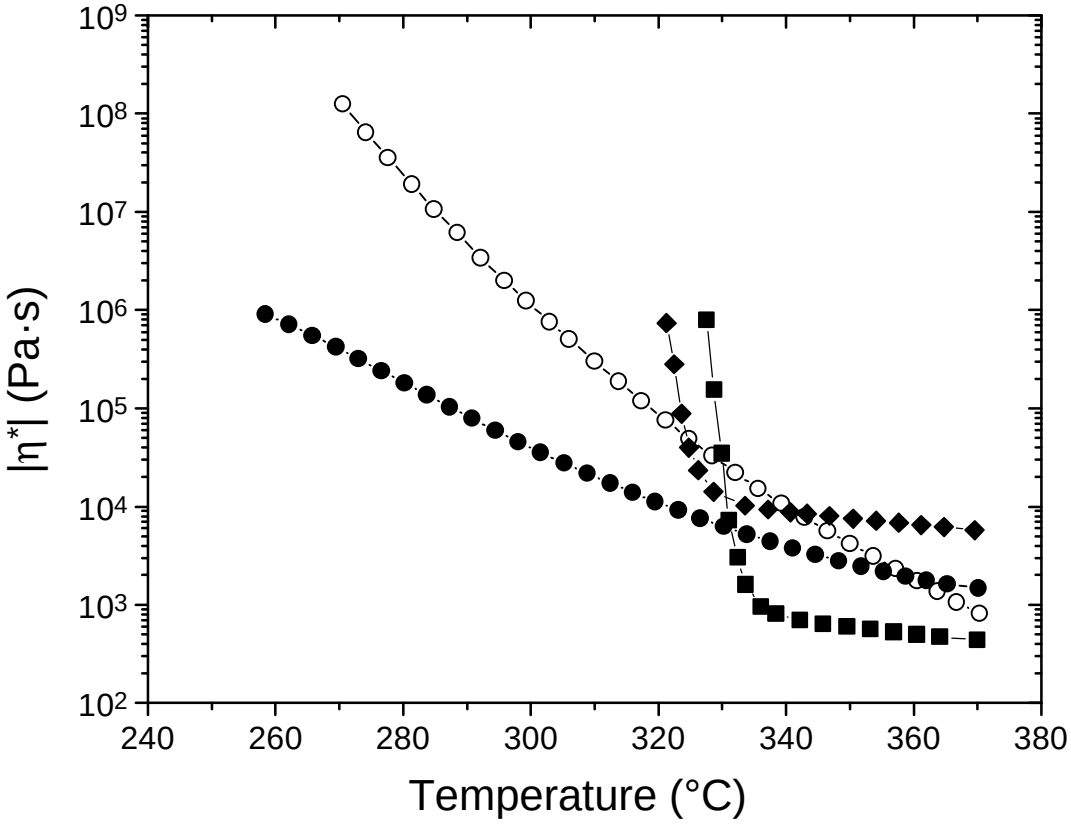

Figure 5.3: The complex viscosity (|η*|) versus temperature for various materials, cooling from 370°C using a rate of 2.4 ± 0.1 °C/min. (○) Phosphate glass (T_g - 234°C), (◆) PEEK (Victrex 450G), (●) PEI (Ultem 1000), and (■) PEEK (Victrex 150G)

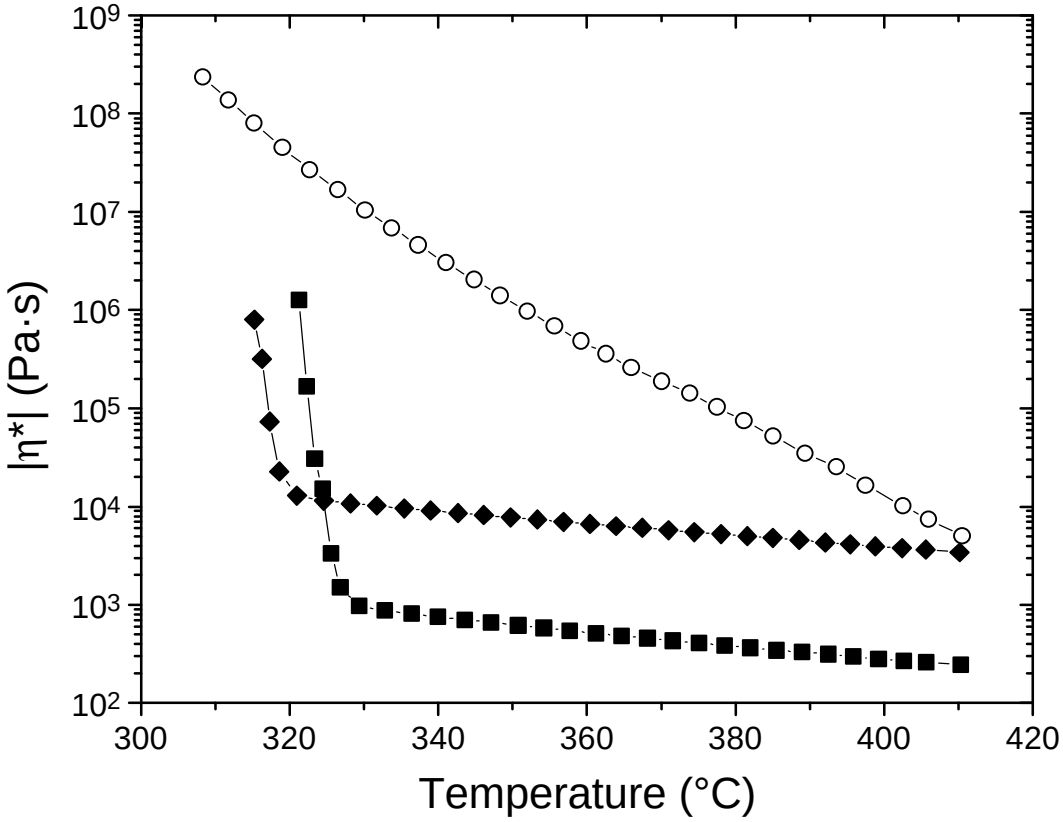

Figure 5.4: The complex viscosity (|η*|) versus temperature for various materials, cooling from 410°C using a rate of 2.4 ± 0.1 °C/min.
(○) Phosphate glass (T_g -282°C), (◆) PEEK (Victrex 450G), and (■) PEEK (Victrex 150G)

5.3.2 Composite Mechanical Properties

Blends consisting of polyetherimide and polyetheretherketone reinforced with phosphate glass were injection molded to determine the effects of varying the rheological and interfacial properties of the components on the composite's mechanical properties. The glass concentration, resin viscosity, and the glass/resin combination utilized were varied in an effort to achieve the highest level of reinforcement from the addition of the phosphate glasses.

Composites consisting of polyetherimide reinforced with various loadings of the lower T_g phosphate glass were injection molded under conditions found to produce composites with the best overall properties [28]. The tensile and flexural mechanical properties for the various phosphate glass filled PEI composites is presented in Table 5.1. Both the tensile and flexural moduli rose with phosphate glass concentration with the stiffest composites being obtained at the highest glass loading investigated. Neat PEI, processed under the same conditions, had machine direction tensile and flexural moduli of 2.85 GPa (± 0.13 GPa) and 3.40 GPa (± 0.05 GPa), respectively. The addition of 60 wt% (42 vol%) phosphate glass elevated the machine direction tensile modulus to 13.84 GPa (± 1.29 GPa) while the flexural modulus rose to a value of 15.51 GPa (± 0.66 GPa). The addition of 30-60 wt% phosphate glass also served to enhance the transverse direction stiffness of the composites leading to moduli that were 2-8 GPa greater than that of the neat PEI.

While the addition of the phosphate glass led to an enhancement in the stiffness of the injection molded samples, the strength of the composites often fell below that of the neat PEI (Table 5.1). The loss in strength was most pronounced in the tensile properties with the addition of 60 wt% glass resulting in a 50% loss in strength along the machine direction while the transverse direction fell by almost 75%. The lowering of the strength of the composite blends to values below that of the neat PEI was partially attributed to the addition of the lower strength phosphate glass. The tensile strength of phosphate glasses used to reinforce thermoplastics has been reported to be as low as approximately 20 MPa, a value well below the 100 MPa found for neat PEI [9]. Another factor that was believed to contribute to the lower strengths of the composite blends was a possible lack of adhesion between the PEI and glass phase. It should be noted that the addition of the phosphate glass was far less detrimental to the flexural strengths of the composite blends. For all the glass concentrations examined, the addition of the phosphate glass actually served to enhance the machine direction flexural strength to values exceeding those of the neat PEI. A similar trend was seen in the transverse direction flexural strength with only the composite containing 60 wt% P-glass exhibiting a strength less than the neat PEI.

The mechanical properties of the phosphate glass filled PEI were also compared to a E-glass fiber reinforced PEI (Table 5.1). Because both the phosphate glass and

Table 5.1: Mechanical Properties for injection molded PEI based composites reinforced with various loadings of P-glass (T_g - 234°C) and E-glass

Machine Direction					
Glass Loading (weight %)	**Tensile Properties**			**Flexural Properties**	
	Modulus (GPa)	**Strength (MPa)**	**% Elong.**	**Modulus (GPa)**	**Strength (MPa)**
Neat PEI	2.85 (0.13)	100.4 (1.0)	6.14 (0.32)	3.40 (0.05)	107.9 (1.0)
30% P-glass	6.49 (0.27)	90.5 (3.8)	1.89 (0.23)	7.81 (0.10)	179.3 (3.9)
45% P-glass	9.62 (0.26)	69.9 (4.7)	0.79 (0.07)	11.27 (0.36)	160.0 (9.9)
60% P-glass	13.84 (1.29)	44.8 (4.4)	0.37 (0.08)	15.51 (0.66)	122.6 (5.7)
30% E-glass	8.48 (0.26)	149.6 (7.1)	2.35 (0.21)	10.00 (0.17)	251.5 (4.3)
Transverse Direction					
Glass Loading (weight %)	**Tensile Properties**			**Flexural Properties**	
	Modulus (GPa)	**Strength (MPa)**	**% Elong.**	**Modulus (GPa)**	**Strength (MPa)**
Neat PEI	2.88 (0.07)	97.6 (0.6)	5.88 (0.13)	3.46 (0.06)	109.1 (1.8)
30% P-glass	5.00 (0.09)	68.3 (3.8)	1.82 (0.26)	5.43 (0.17)	119.7 (7.7)
45% P-glass	8.23 (0.33)	45.3 (3.0)	0.58 (0.04)	8.91 (0.29)	102.5 (9.8)
60% P-glass	10.89 (0.71)	27.7 (5.4)	0.27 (0.05)	12.13 (0.72)	79.8 (7.1)
30% E-glass (Ultem 2300)	4.99 (0.40)	95.2 (7.5)	2.56 (0.41)	5.09 (0.14)	128.6 (3.5)

Note: % Elong. = Elongation to break ; Standard deviations given in parentheses
For neat PEI, Elongation and strength based on yield values

borosilicate (Type E) glass have the same approximate density (≈ 2.6 g/cm^3), composites containing similar glass loadings can be compared directly on a volumetric basis. At 30 wt% glass, the phosphate glass reinforced material displayed machine direction moduli approximately 25% lower than the E-glass filled composite while the transverse direction stiffness of the materials were essentially the same. Due to the low viscosity of the phosphate glass, higher glass loadings (upwards of 60 wt%) were easily processed to produce composites that displayed moduli 1.5 to 2 times greater than a composite containing 30 wt% E-glass fiber. The phosphate glass filled composites were found to offer a key advantage in regards to the distribution of the mechanical properties within the molded part. For the both the tensile and flexural moduli, the phosphate glass filled materials typically displayed anisotropy ratios (machine/transverse direction properties) on the order of only 1.3 while the E-glass filled material possessed machine direction moduli more than twice that of the transverse direction. The high anisotropy in the E-glass filled material was attributed to the preferential orientation of the glass fibers along the machine direction due to the flow field in the film-gated mold. While the addition of the phosphate glass was found to be an effective way enhance the stiffness of the composites to values comparable to those found with E-glass fiber, these composites were often at a disadvantage in regards to strength. For example, the strength of the phosphate glass filled PEI composite was on the order of 10-30% lower than a composite containing the equivalent loading of E-glass fiber.

The differences in the mechanical properties of the phosphate and borosilicate glass filled composites were thought to be partially due to the variations in the properties of the glasses themselves. The tensile moduli of phosphate glasses used to reinforce thermoplastics have been reported to be in the range of 20-40 GPa while the strength has been reported to be as low 20 MPa [8,9]. These values are much lower than the modulus and strength of borosilicate glass (Type E) which have been reported to fall in the range of 70-80 GPa and 1500-2000 MPa, respectively [30,31]. The strength of the E-glass filled material was also enhanced due to the use of a sizing agent that served to promote adhesion between the glass and PEI phases. Variations in the size and shape of the glass reinforcing phase may also be partially responsible for the discrepancies in the mechanical properties found by utilizing the various glasses.

The properties of the composites produced with the lower T_g (234°C) P-glass compared favorably to other polyetherimide/phosphate glass blends that had been produced in an earlier investigation [9]. For this study, composites reinforced with 45-60 wt% of the lower T_g (234°C) P-glass were found to have machine direction tensile moduli and strengths ranging from 9-14 GPa and 70-45 MPa, respectively. Polyetherimide composites of similar glass loadings produced by Bahn and coworkers [9] were found to display a wide range of mechanical properties. A composite containing 50 wt% of a phosphate glass having a T_g of 226°C was found to have a tensile modulus and strength of only 4.1 GPa and 48 MPa, respectively. The utilization of a higher T_g glass (313°C) offered much improved properties with composites containing 60 wt% glass having a

tensile modulus of 11.9 GPa and strength of 68.3 MPa. It should be pointed out that discrepancies in the volumetric loading of the glasses coupled with the variations in the processing histories makes meaningful direct comparisons between the materials produced in the various investigations almost impossible.

Select composites reinforced with the lower T_g (234°C) phosphate glass were also produced utilizing the two different grades of PEEK to evaluate the effects of changing the interfacial and rheological properties of the resin on the properties of the composite blends. Composites containing 45 wt% (29 vol%) phosphate glass were injection molded at the same conditions used for the production of the PEI based composites. Two grades of PEEK were used to determine if variations in the resin viscosity had an effect on the mechanical properties of the injection molded composite blends (Table 5.2). The higher viscosity PEEK (450G), which led to more favorable viscosity ratios [i.e. $0.1 < (\eta_{glass}/\eta_{PEEK}) < 1$], yielded a composite offering only slight improvements (5-10%) in the machine direction moduli when compared to a composite manufactured with the lower viscosity Victrex 150G. While the machine direction moduli were unaffected by resin, the use of the higher viscosity 450G was found to lead to significant enhancements in the transverse direction stiffness. For example, the transverse direction flexural modulus for a composite produced with the 150G was 6.48 GPa (± 0.31 GPa) while the use of the 450G increased this value by almost 50% resulting in a modulus of 9.35 GPa (± 0.64 GPa). While the use of the higher viscosity 450G elevated the transverse direction moduli, the overall strength of the blend was found to fall approximately 30-40% below that obtained by utilizing the lower viscosity resin.

A comparison between the composites produced with the PEI and PEEK was made to determine if any one of the resins offered a substantial advantage in regards to the mechanical properties that could be obtained with the addition of 45 wt% (≈ 29 vol%) of the lower T_g phosphate glass. The machine direction moduli obtained were generally found to be insensitive to the resin utilized (Tables 5.1 and 5.2) with all the composites displaying a tensile modulus on the order of 9-10 GPa with a flexural modulus of approximately 11 GPa. The use of the various resins was found to have the greatest impact on the transverse direction moduli, with the higher viscosity resins (PEI and PEEK 450G) offering the greatest enhancements in the stiffness of the composite blends along this direction. This improvement in the transverse direction moduli served to help lower the mechanical anisotropy found within the composite blends. Composites produced with the PEI and PEEK (450G) had flexural moduli anisotropy ratios of only 1.26 ± 0.06 and 1.22 ± 0.09, respectively. The use of the lower viscosity PEEK (150G) led to much greater anisotropy (1.67 ± 0.10) in regards to the flexural modulus, indicating the presence of a glass reinforcing morphology elongated mainly along the machine direction within the skin region of the molded sample. The strength of the composite blends also showed great variation with resin which was attributed to a variety of factors including the properties of the neat resins, glass phase morphology, and adhesion between the glass and resin.

Table 5.2: Mechanical Properties for injection molded PEEK based composites reinforced with 45 wt% (29 vol%) P-glass (T_g - 234°C)

Machine Direction					
Grade of PEEK	**Tensile Properties**			**Flexural Properties**	
	Modulus (GPa)	**Strength (MPa)**	**% Elong.**	**Modulus (GPa)**	**Strength (MPa)**
Victrex 150G	8.60 (0.55)	74.2 (5.7)	0.91 (0.11)	10.79 (0.37)	161.0 (6.5)
Victrex 450G	9.39 (0.42)	50.4 (5.7)	0.59 (0.04)	11.44 (0.20)	135.0 (4.1)
Transverse Direction					
Resin (Grade)	**Tensile Properties**			**Flexural Properties**	
	Modulus (GPa)	**Strength (MPa)**	**% Elong.**	**Modulus (GPa)**	**Strength (MPa)**
Victrex 150G	6.22 (0.36)	52.2 (5.3)	0.91 (0.12)	6.48 (0.31)	96.8 (4.0)
Victrex 450G	7.50 (0.30)	33.5 (1.7)	0.49 (0.02)	9.35 (0.64)	86.5 (9.8)

Note: % Elong. = Elongation to break; Standard deviations given in parentheses

The interfacial and rheological properties of the composite blends were also varied by blending the two grades with PEEK with the higher T_g (282°C) phosphate glass. A limited study was performed to determine if variations in the viscosity of the resin had a substantial effect on the properties of the composite blends. The mechanical properties of the composites produced with the two grades of PEEK reinforced with 51 wt% (28 vol%) glass are presented in Table 5.3. The higher molecular weight grade of PEEK (450G) led to the formation of a composite that showed a slight improvement in properties when compared to the composite manufactured with the when compared to the composite manufactured with the Victrex 150G. The improvement was most pronounced in the machine direction tensile properties with the use of the 450G raising the modulus and strength by 1.07 ± 0.32 GPa and 18.1 ± 4.4 MPa, respectively. The Victrex 450G displayed a complex viscosity almost an order of magnitude greater than the 150G (Figures 5.2 and 5.4) which appeared to offer a limited improvement in the dispersion and deformation of the phosphate glass during processing. The composite manufactured with the higher viscosity PEEK was also found to display tensile properties comparable to those found with the lower molecular PEEK (150G) reinforced with the same volume fraction of the lower T_g (234°C) phosphate glass (Table 5.2). While the tensile properties of the composites reinforced with the various glasses were similar, the flexural properties were quite varied indicating a possible difference in the reinforcing morphology found within the skin region of the injection molded samples.

The glass concentration within the polyetheretherketone based composites was increased to a higher loading (43 vol%) to facilitate comparisons between the various composite blends. The mechanical properties for the various highly loaded PEEK/phosphate glass injection molded blends is presented in Table 5.4. The addition of the phosphate glasses was found to increase the stiffness of the composite blends to values 2-4 times greater than that of the neat resin. The lower T_g (234°C) phosphate glass reinforced composite offered the greatest stiffness and strength along the machine direction but was highly anisotropic with the machine direction moduli being almost 1.5 times greater than the transverse direction. This higher degree of anisotropy appeared to indicate the formation of a reinforcing phase morphology oriented predominately along the machine direction. The composite reinforced with the higher T_g (282°C) phosphate glass generally displayed lower machine direction properties while the transverse direction properties were found to exceed those of the lower T_g glass reinforced composite. The composite reinforced with the higher T_g phosphate glass was also found to be generally isotropic in regards to the mechanical properties, possibly indicating the presence of a lower aspect ratio reinforcing phase morphology. While the addition of the phosphate glasses was found to elevate the stiffness to values greater than the neat PEEK, the strengths of both composites were generally found to be lower than that of the neat resin. The strengths of the blends followed the same trends seen in regards to the modulus, with the composites reinforced with the lower T_g glass offering higher machine direction values with a higher degree of anisotropy than that seen by utilizing the higher T_g glass. It should be noted that the mechanical properties for these blends were found to be somewhat lower

Table 5.3: Mechanical Properties for injection molded PEEK based composites reinforced with 51 wt% (28 vol%) P-glass (Tg - 282°C)

Machine Direction					
	Tensile Properties			**Flexural Properties**	
PEEK Grade	**Modulus (GPa)**	**Strength (MPa)**	**% Elong.**	**Modulus (GPa)**	**Strength (MPa)**
Victrex 150G	6.58 (0.14)	51.0 (2.6)	0.82 (0.05)	8.26 (0.30)	115.2 (1.6)
Victrex 450G	7.65 (0.29)	69.1 (3.5)	1.03 (0.09)	8.54 (0.49)	123.3 (1.8)
Transverse Direction					
	Tensile Properties			**Flexural Properties**	
PEEK Grade	**Modulus (GPa)**	**Strength (MPa)**	**% Elong.**	**Modulus (GPa)**	**Strength (MPa)**
Victrex 150G	6.41 (0.35)	49.9 (3.4)	0.81 (0.05)	8.33 (0.17)	112.2 (4.2)
Victrex 450G	6.70 (0.57)	54.2 (6.0)	0.87 (0.12)	8.66 (0.51)	115.5 (3.1)

Note: % Elong. = Elongation to break; Standard deviations given in parentheses

Table 5.4: Mechanical Properties for injection molded PEEK based composites reinforced with approximately 43 vol% P-glass

Machine Direction					
	Tensile Properties			**Flexural Properties**	
P-glass (T_g) Resin	**Modulus (GPa)**	**Strength (MPa)**	**% Elong.**	**Modulus (GPa)**	**Strength (MPa)**
(234°C) Victrex 150G	12.10 (0.63)	63.8 (3.6)	0.55 (0.03)	14.24 (0.51)	132.7 (3.4)
(282°C) Victrex 450G	11.21 (0.40)	52.8 (5.0)	0.50 (0.06)	11.95 (0.21)	90.4 (2.6)
Neat Victrex 450G	3.54 (0.07)	88.7 (1.1)	5.15 (0.23)	4.35 (0.17)	119.0 (2.3)
Transverse Direction					
	Tensile Properties			**Flexural Properties**	
P-glass (Tg) Resin	**Modulus (GPa)**	**Strength (MPa)**	**% Elong.**	**Modulus (GPa)**	**Strength (MPa)**
(234°C) Victrex 150G	7.98 (0.34)	36.7 (3.5)	0.48 (0.05)	9.22 (0.51)	78.6 (5.2)
(282°C) Victrex 450G	11.37 (0.47)	41.3 (5.5)	0.39 (0.07)	11.21 (0.25)	82.7 (2.2)
Neat Victrex 450G	3.34 (0.16)	96.1 (1.6)	4.08 (0.21)	3.97 (0.11)	119.2 (4.0)

Note: % Elong. = Elongation to break; Standard deviations given in parentheses
Composites contain 60 wt% (234°C) and 66 wt% (282°C) P-glass

than those reported by Bahn and coworkers [9] for other composite blends consisting of PEEK reinforced with phosphate glasses of varying compositions. Injection molded composites reinforced with 50-80 wt% glass were found to yield tensile moduli ranging from 8-27 GPa with strengths ranging from 40-90 MPa. The lower mechanical properties achieved in this study are thought to be due to the variations in the glass compositions coupled with the processing conditions utilized. In the work performed by Bahn et. al. [9], the composite blends were preblended in a twin-screw extruder and subsequently injected into a mold of an unspecified configuration utilizing what appeared to be a high speed injection molding unit (screw forwards speeds up to 1000 mm/sec.). Improvements in the dispersion and deformation of the glass during processing coupled with favorable mechanical, rheological, and interfacial properties of the glass are thought to have led to the elevated properties of the composite blends.

A comparison between the mechanical properties obtained by using the polyetherimide versus polyetheretherketone for composites reinforced with a higher loading of 43 vol% of the lower T_g phosphate glass can be seen in Tables 5.1 and 5.4. The composite blends were found to offer comparable stiffness along the machine direction with the tensile and flexural moduli ranging from 12-14 GPa and 14-16 GPa, respectively. The transverse direction moduli of the PEI based composite was typically 30-40% higher than PEEK based composite. While the elevated transverse direction stiffness of the PEI based blends served to create blends with lower mechanical anisotropy, the tensile strength of the blends was found to suffer falling 30-40% below the values obtained for the PEEK based composites.

5.3.3 Composite Morphologies

The various composite blends were examined with scanning electron microscopy to ascertain the reinforcing morphologies that were developed during injection molding. The resin/glass combinations investigated were found to yield a wide range of mechanical properties partially due to the reinforcing glass phase morphology generated during the injection molding. An examination of these morphologies provided some insight into how parameters such as the viscosity of the components and glass concentration affected the ultimate properties of the phosphate glass reinforced materials.

The morphology typically found in the polyetherimide based composites reinforced with the lower T_g (234°C) phosphate glass can be seen in Figures 5.5 and 5.6. The skin region contained an interpenetrating network structure consisting of areas of continuous glass which were found to increase in size with glass concentration (Figure 5.5). The formation of the interpenetrating structure was attributed to the large stresses generated from the elongational flow at the advancing front coupled with the strong shear gradients found near the mold wall. Within the core regions of the molded samples, the glass was present as droplets interdispersed with elongated glass regions at the lower

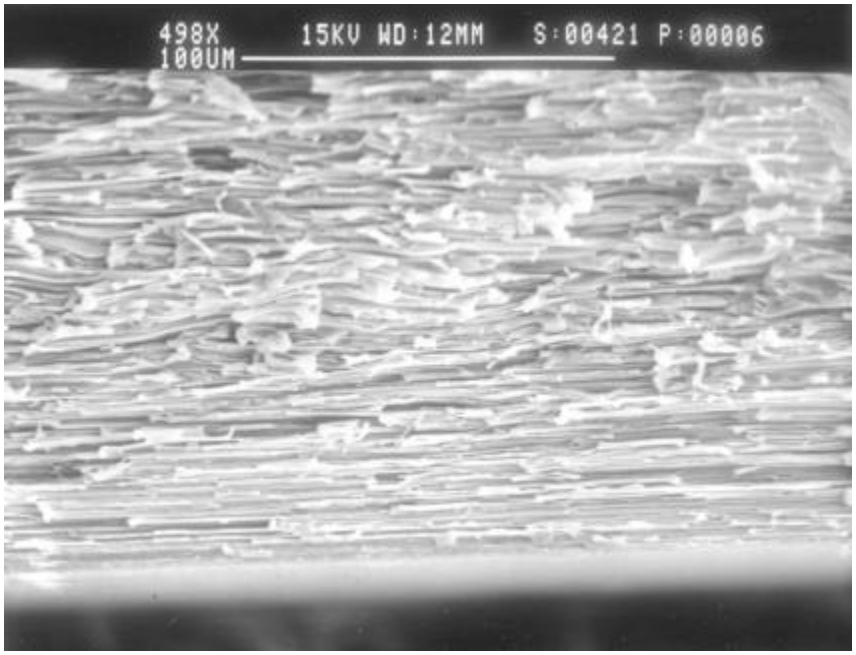

(a)

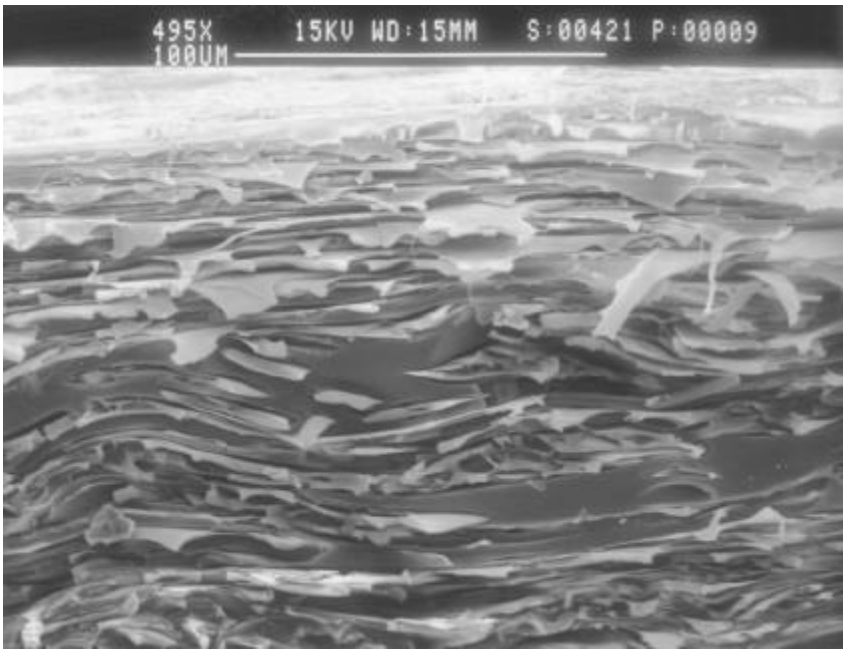

(b)

Figure 5.5: Scanning electron micrographs along the machine direction in the skin region of injection molded PEI composites reinforced with P-glass (T_g - 234°C). (a) 30 wt% P-glass (b) 45 wt% P-glass

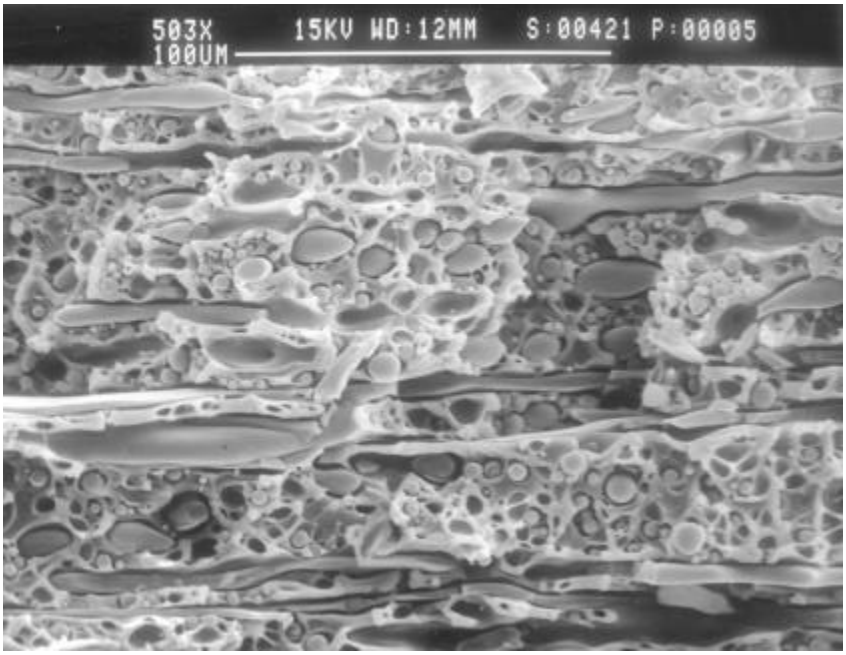

(a)

(b)

Figure 5.6: Scanning electron micrographs along the machine direction in the core region of injection molded PEI composites reinforced with P-glass (T_g - 234°C). (a) 30 wt% P-glass (b) 45 wt% P-glass

concentration (30 wt%) while a structure similar to that found in the skin region was obtained at the higher glass concentrations (Figure 5.6). The higher viscosity of the polyetherimide appeared to lead to a favorable viscosity ratio with phosphate glass while also facilitating the generation of higher stresses which served to elongate the glass regions across the entire thickness of the sample. The larger glass domains found at the higher loadings were believed to be the result of coalescence due to increased glass-glass particle interactions. The formation of these larger domains coupled with a lack of adhesion between the glass and PEI, as indicated by the glass pullout observed with microscopy, help offer an explanation for the large losses in the composite strength. The presence of the interpenetrating glass phase morphology also explains the lower degree of mechanical anisotropy found within the composite blends.

The composites consisting of the two grades of PEEK reinforced with 45 wt% of the lower T_g phosphate glass were found to display substantial differences in mechanical properties (Table 5.2) which were consistent with the observed morphologies (Figures 5.7 and 5.8). The composite generated with the lower molecular weight grade of PEEK (150G) contained high aspect ratio glass ribbons within the skin region of the injection molded sample near the mold wall (Figure 5.7a) which helps account for the high anisotropy seen in the flexural properties. The formation of the high aspect ratio glass phase within the skin region at the unfavorable viscosity ratios ($\eta_{glass}/\eta_{PEEK} >1$) was facilitated by the rapid solidification of the material after being exposed to strong extensional deformation. Work performed with immiscible fluid blends has shown that extensional or shearfree flows lead to conditions more favorable to droplet deformation over a wide range of viscosity ratios [24-27]. The higher viscosity of Victrex 450G produced a morphology within the skin region consisting of an interpenetrating network structure (Figure 5.7b) similar to that seen in the PEI based composites (Figure 5.5). The differences in the viscosity of the two grades of PEEK also led to major shifts in the morphology within the core region of the injection molded samples (Figure 5.8). For the composite produced with the lower viscosity 150G, the core region was comprised of small, glass droplets having diameters less than 5 μm. The formation of the glass droplets within this region was attributed to the unfavorable viscosity ratios with the PEEK, which served to limit the deformation of the glass in the shear flow field found within the core region. The more favorable viscosity ratios coupled with higher stresses obtained by using the Victrex 450G resulted in greater deformation of the glass phase within the core region (Figure 5.8b), which led to the formation of an interpenetrating network morphology similar to that seen within the skin region. While this interlocking morphology across the entire thickness of the sample led to significant enhancements in modulus, the overall strength of the composite system was found to suffer. Lack of adhesion between the materials, as shown by glass pullout, coupled with the large surface area of the glass ribbons resulted in composites with substantially lower strengths.

The use of the two different phosphate glasses to reinforce the PEEK was found to lead to significant variations in the distribution of the mechanical properties (Table 5.4).

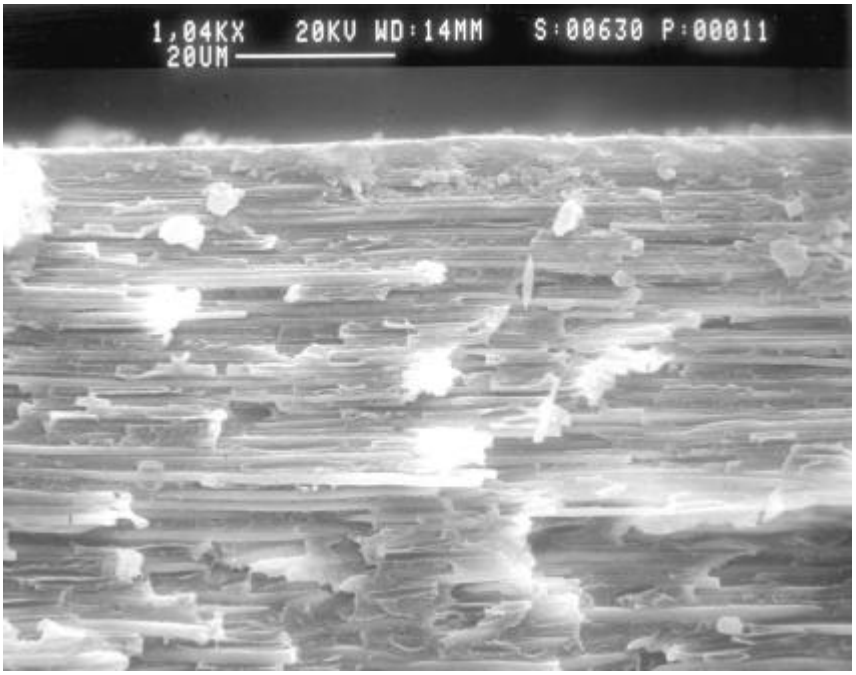

(a)

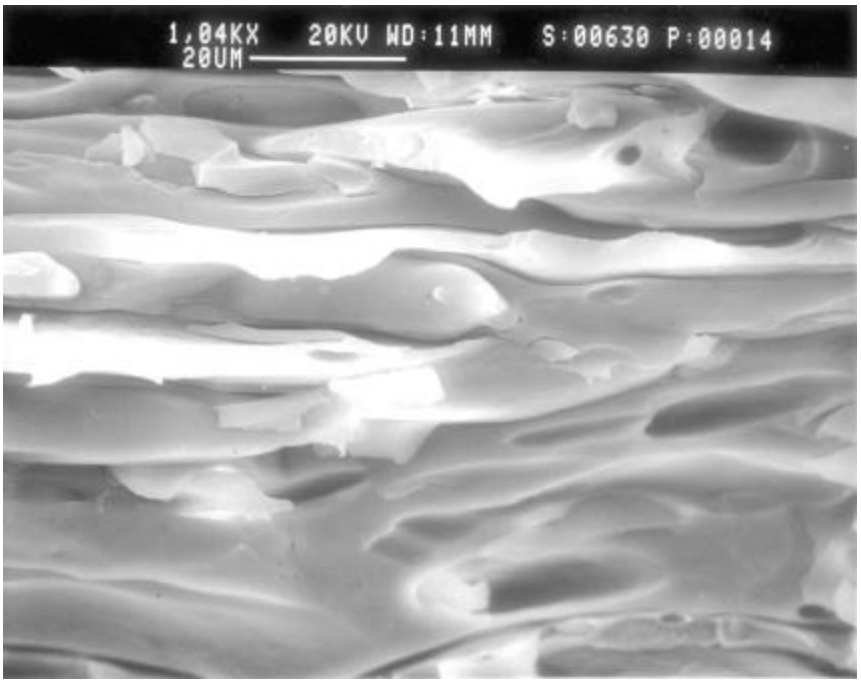

(b)

Figure 5.7: Scanning electron micrographs along the machine direction in the skin region of injection molded PEEK composites reinforced with 45 wt% P-glass (T_g - 234°C). (a) Victrex 150G (b) Victrex 450G

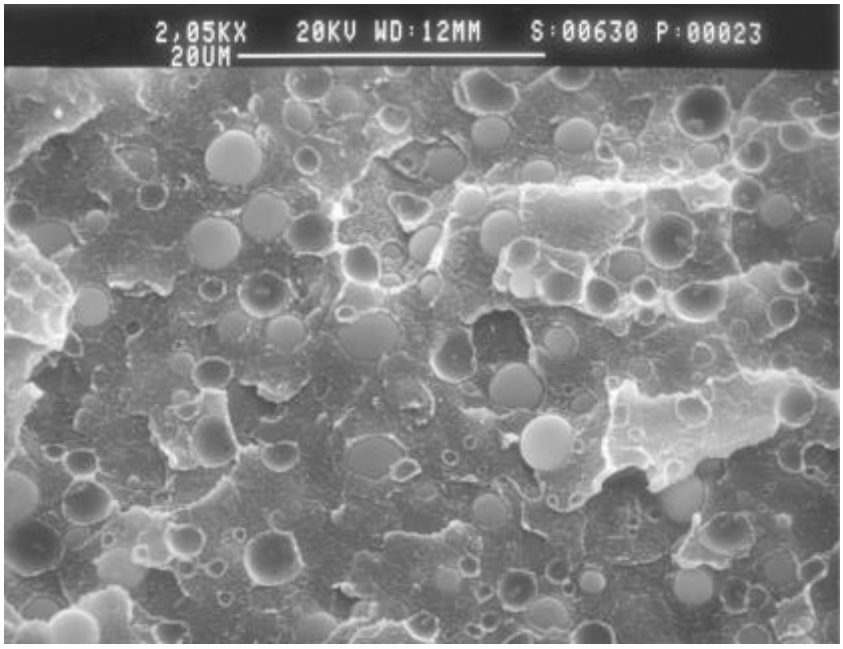

(a)

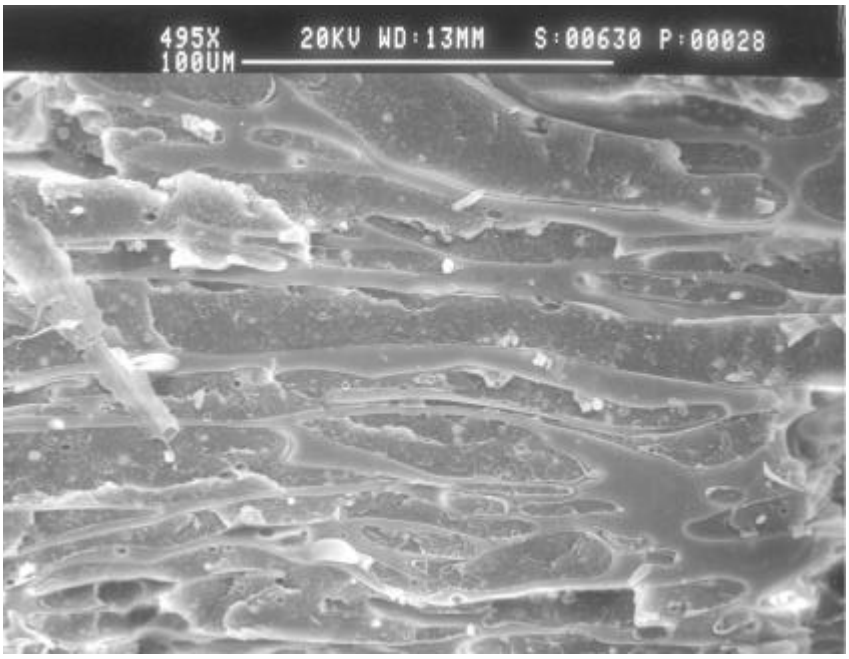

(b)

Figure 5.8: Scanning electron micrographs transverse to the flow direction in the core region of injection molded PEEK composites reinforced with 45 wt% P-glass (T_g - 234°C). (a) Victrex 150G (b) Victrex 450G

This was attributed to the large differences in the morphology developed within the composites (Figure 5.9). For the composite reinforced with the lower T_g phosphate glass, the skin region contained many small, high aspect ratio, glass ribbons oriented along the machine direction (Figure 5.9a) while the core region contained glass droplets similar to those found at the lower glass concentrations (Figure 5.8a). The formation of these higher aspect ratio glass domains within the skin region led to the high degree of mechanical anisotropy found within these composites. The composite containing the higher T_g phosphate glass was found to display little variation in the reinforcing morphology across the thickness of the injection molded sample with the glass being present as small diameter (< 2 μm) droplets (Figure 5.9b). It appeared that the interfacial and rheological properties of the PEEK and higher T_g glass resulted in limited deformation of the glass phase within both the extensional and shear flow fields generated during the filling of the mold. The presence of these small glass beads across the entire thickness of the sample explains the low degree of mechanical anisotropy found for both the tensile and flexural properties.

5.3.4 Dynamic Mechanical Response

Along with the tensile and flexural mechanical properties, the dynamic mechanical response of the composite blends was also examined in the solid state. Dynamic mechanical thermal analysis (DMTA) was performed on strips cut from the injection molded specimens in order to evaluate the viscoelastic properties of the various composite blends over a wide range of temperatures. Dynamic thermal analysis was seen as an effective way to investigate the effects of the resin/glass combination utilized on the overall response of the composite blends.

The storage modulus (G') versus temperature for neat PEI and the composites reinforced with the two types of glasses is shown in Figure 5.10. The addition of the phosphate glass and E-glass were both found to lead to storage moduli greater than that of the neat PEI. Composites reinforced with 30 wt% (17 vol%) of the phosphate and borosilicate glass displayed similar responses up to a temperature of 160°C where the storage modulus of the P-glass reinforced material fell slightly below that of the E-glass filled PEI, possibly due to the increased mobility of the phosphate glass at temperatures approaching the glass T_g of 234°C. All the glass filled materials retained high storage moduli up to a temperature of approximately 220°C, where the modulus fell rapidly due to the increased mobility in the polyetherimide. Composites reinforced with the higher phosphate glass loadings (45 & 60 wt%) displayed moduli well above those of the neat PEI and E-glass (30 wt%) filled composite due to the higher volumetric loadings of glass and reinforcing morphology obtained within the composites. The interpenetrating network morphology found across the entire thickness of the samples at the higher P-glass loadings appeared to facilitate the retention of the composite modulus at temperatures well above the glass transition temperature for the polyetherimide.

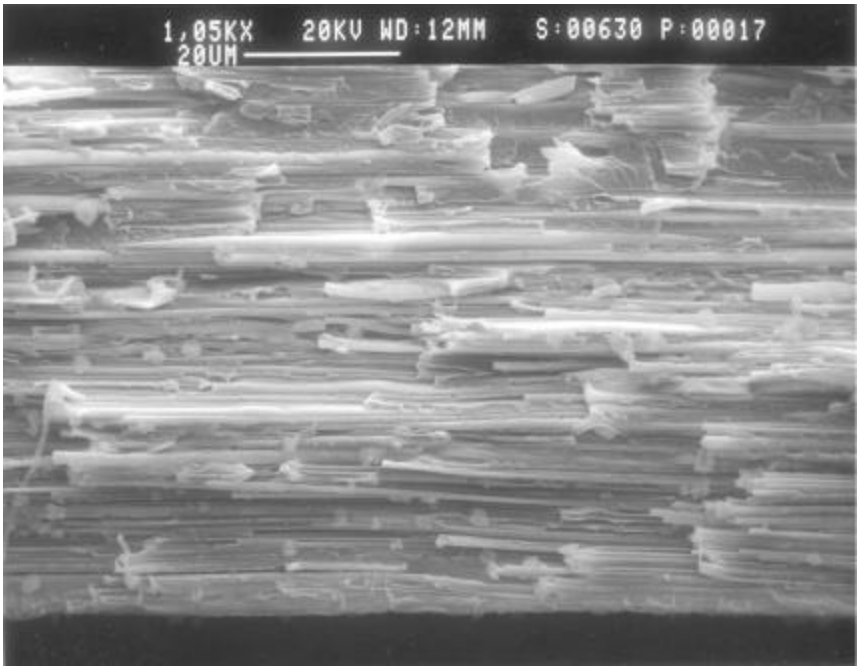

(a)

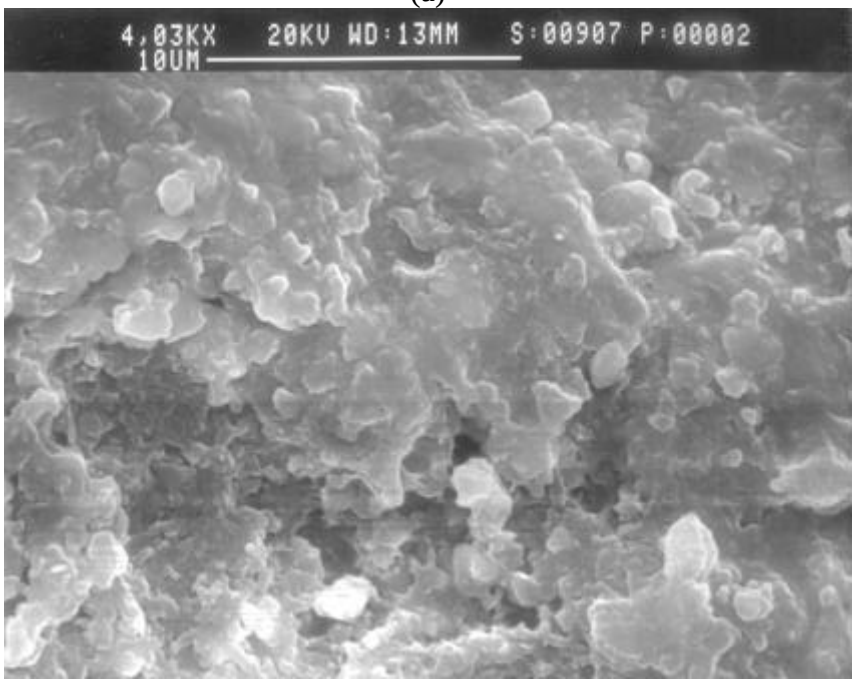

(b)

Figure 5.9: Scanning electron micrographs along the machine direction within the skin region of injection molded PEEK composites reinforced with 43 vol% P-glass. (a) Victrex 150G with 60 wt% P-glass (T_g - 234°C) (b) Victrex 450G with 66 wt% P-glass (T_g - 282°C)

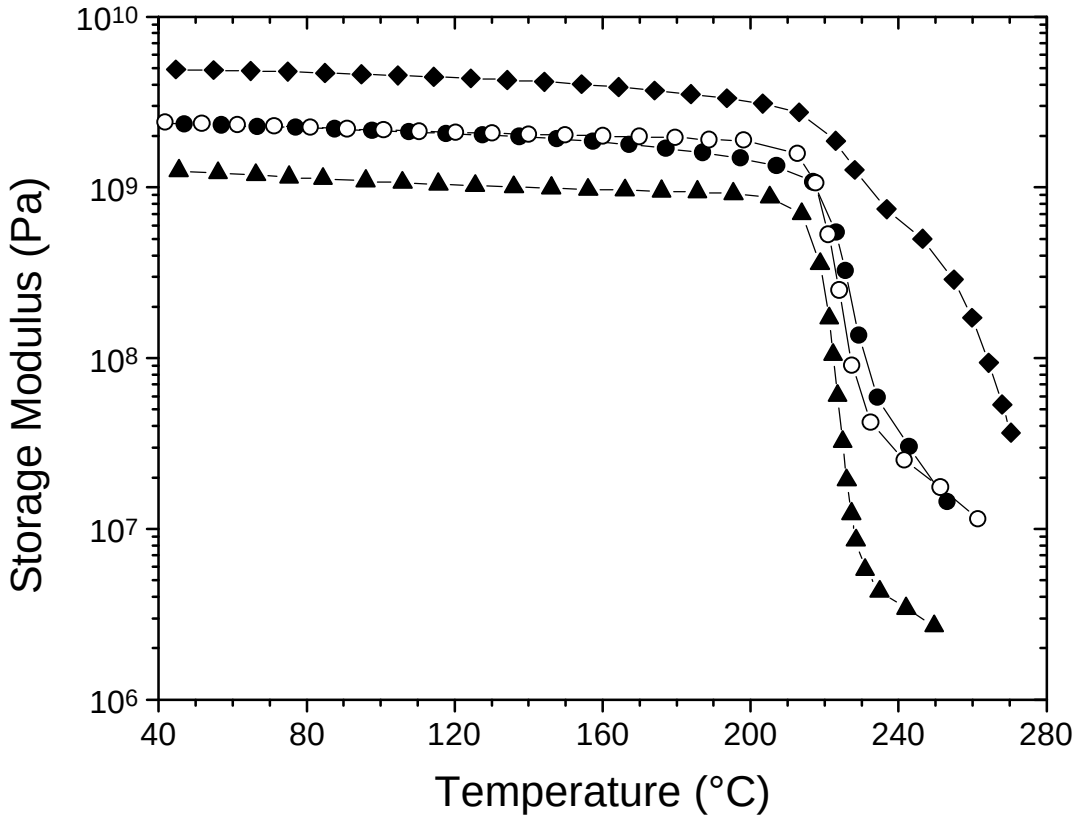

Figure 5.10: Storage modulus (G′) versus temperature for neat PEI and various glass {E-glass & P-glass (T_g - 234°C)} filled composites using a heating rate of 2.5 ± 0.1 °C/min. (▲) neat PEI, (●) 30 wt% P-glass, (○) 30 wt% E-glass, and (◆) 60 wt% P-glass.

The effects of utilizing the two different phosphate glasses was investigated by examining the dynamic response of the PEEK composites reinforced with 43 vol% glass (Figure 5.11). The addition of the phosphate glasses led to storage moduli greater than that of the neat PEEK with the two composite blends displaying equivalent moduli up to a temperature of approximately 240°C. Above a temperature of 240°C, the storage modulus of the composite blend reinforced with the lower T_g phosphate glass dropped rapidly, approaching that of the neat PEEK at the higher temperatures (280°C). The increased mobility of the lower T_g phosphate glass above 240°C resulted in the large loss in the storage modulus while the higher T_g (282°C) of the other phosphate glass allowed the storage modulus of the composite blend to exceed that of the neat resin up to the melting point of the PEEK (≈ 360°C).

Solid state dynamic mechanical thermal analysis was also used to examine the thermal transitions of the composite components in order to determine if there may be any interactions between the various materials. The loss factor (tan δ) versus temperature for neat PEI and composites reinforced with various glasses can be seen in Figure 5.12. The addition of the various glasses led to no significant shifts in the glass transition temperature of the PEI (peak at ≈ 230°C) indicating a lack of interaction (i.e. miscibility) between the PEI and phosphate glass. For the phosphate glass filled materials, the loss factor showed a broad, constant rise with temperature that was thought to be due to the increased mobility of the glass phase. The thermal transitions for the PEEK based composites reinforced with the two phosphate glasses were also examined using dynamic mechanical thermal analysis (Figure 5.13). For the composite manufactured with the higher T_g phosphate glass, the glass transition peak for the polyetheretherketone (≈ 160°C) dropped slightly as compared to the neat PEEK and composite manufactured with the lower T_g phosphate glass. The slight drop in the glass transition temperature may be due to a variety of causes such as slight degradation of the PEEK from the use of the higher processing temperatures (410°C) or variations in the degree of crystallinity within the molded samples. For both composite blends, the loss factor was found to rise significantly at temperatures greater than 200°C due to increased mobility of the glass reinforcing phases. The glass transition temperature for the lower T_g phosphate glass was found to be approximately 270°C as indicated by the peak in the loss factor. The composite produced with the higher T_g (282°C from DSC) phosphate glass did not show a distinct peak in the loss factor but rose steadily at temperatures greater than 200°C.

5.4 Conclusions

The addition of phosphate glass to the neat thermoplastic resins was found to be an effective method to produce injection moldable composites. The stiffness of the blends was found to increase with glass loading with composites containing up to 45 vol% glass exhibiting machine direction tensile and flexural moduli almost 3-5 times greater than that of the neat thermoplastics. A phosphate glass reinforced PEI based composite was found

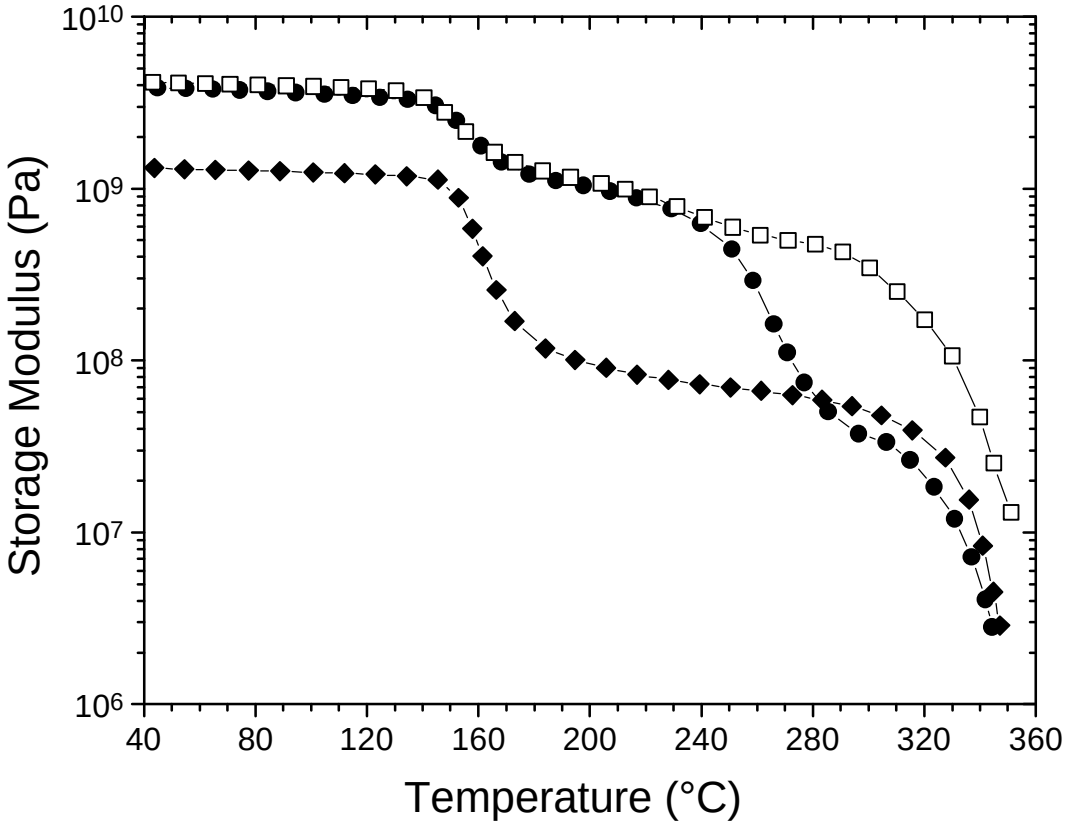

Figure 5.11: Storage modulus (G′) versus temperature for neat PEEK and composites reinforced with 43 vol% of various phosphate glasses using a heating rate of 2.5 ± 0.1 °C/min. (◆) neat PEEK (450G), (●) 60 wt% P-glass (T_g - 234°C), and (□) 66 wt% P-glass (T_g - 282°C).

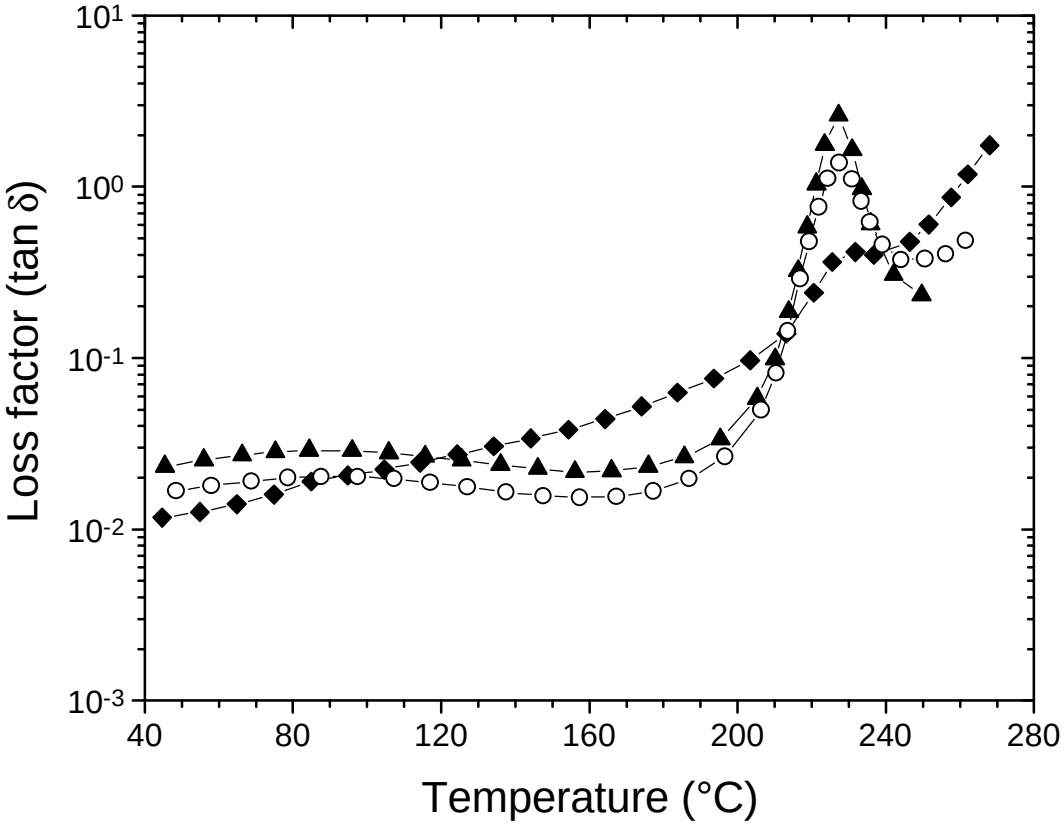

Figure 5.12: Loss factor (tan δ) versus temperature of the neat PEI and various glass filled composites using a heating rate of 2.5 ± 0.1 °C/min. (▲) neat PEI, (○) 30 wt% E-glass, and (◆) 60 wt% P-glass (T_g - 234°C).

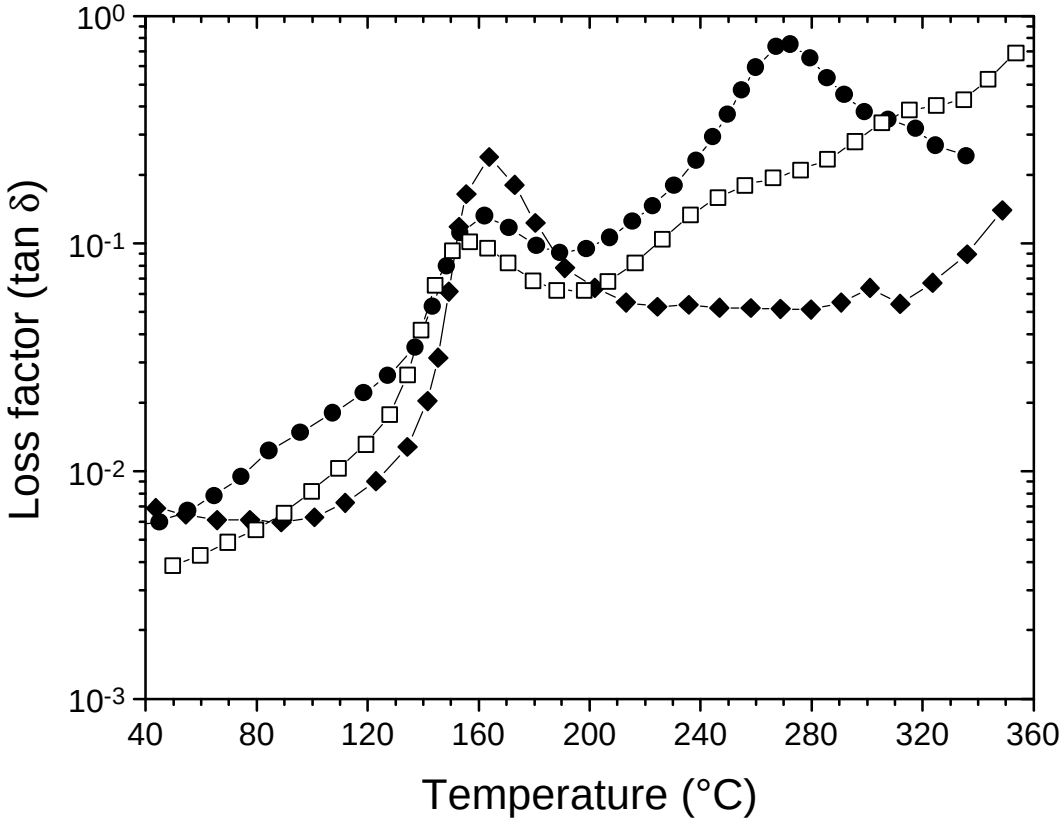

Figure 5.13: Loss factor (tan δ) versus temperature for PEEK reinforced with 43 vol% of various phosphate glasses using a heating rate of 2.5 ± 0.1 °C/min. (◆) neat PEEK (450G), (●) 60 wt% P-glass (T_g - 234°C), and (□) 66 wt% P-glass (T_g - 282°C).

to possess machine direction moduli that were approximately 25% lower than those of a composite reinforced with a comparable loading of E-glass fiber. The lower viscosity of the phosphate glass during processing did, however, allow the production of highly loaded composites that were stiffer and less anisotropic than a conventional E-glass fiber reinforced material.

While the inclusion of phosphate glasses led to an enhancement in the modulus of the composite blend, the strength of the materials often fell with increasing glass concentration. The addition of the phosphate glass was found to have the greatest impact on the tensile strengths of the blends, which were found to fall below that of the neat resins. The phosphate glass had a lesser effect on the flexural strength with certain resin/glass combinations producing composites with flexural strengths greater than that of the neat resins. When compared to a material reinforced with a comparable loading of E-glass fiber, a phosphate glass filled composite was found to offer strengths that were approximately 10-30% lower.

The properties of the injection molded phosphate glass filled composites were found to show great variation with the resin/glass combinations utilized. Material combinations that served to minimize the viscosity difference between the thermoplastic resin and phosphate glass typically resulted in composites that displayed the greatest enhancement in moduli. The lower viscosity mismatch between the resins and glasses appeared to facilitate greater deformation of the phosphate glass phase which often led to an enhancement in the machine direction properties of the film-gated injection molded samples. A variety of glass phase reinforcing morphologies including droplets, ribbons, and an interpenetrating network structure were produced through the utilization of the various resin/glass combinations. These large variations in the reinforcing morphologies were found to produce composites with a wide range of mechanical properties.

5.5 Acknowledgments

The authors would like gratefully recognize the financial support of the NSF Science and Technology Center for High Performance Polymeric Adhesives and Composites at Virginia Tech (Grant No. DMR-8809174 AMD 1) and the Army Research Office (Grant No. DAAHA04-94-G-0171) . Also, we would like to thank GE Plastics for supplying the PEI and Corning Inc. for producing the phosphate glass utilized in this study. Appreciation is also extended to Dr. Garth Wilkes for allowing use of the scanning electron microscope and to Dr. Mike McLeod for his assistance in obtaining the SEM images.

5.6 References

1 Schweizer and Winterman, *Thermoplastic Polymer Additives: Theory and Practice*, ed. J.T. Lutz Jr., Marcel Dekker, New York 1989.

2 S. Kessler, in *Plastics Additives and Modifiers Handbook* (Chapter 48), ed. J. Edenbaum, Van Nostrand Reinhold, New York 1992.

3 G. Kiss, *Polym. Eng, Sci.*, 27, 410 (1987)

4 D.G. Baird, in *Polymeric Materials Encyclopedia* (vol. 5), e.d. J.C. Salamone, 3207 (1996).

5 A.A. Handlos and D.G. Baird, *J. Macromol. Sci., Rev. Macromol. Chem. Phys*., C35, 183 (1985).

6 F.P. La Mantia, G. Timanlio, and A. Valenzia, in *Thermotropic Liquid Crystalline Polymer Blends (Chap. 5*), ed. F.P. La Mantia. Technomic, Lancaster PA 1993.

7 D.G. Baird and M.A. McLeod, in *Polymer Blends: Formulation and Performance (Chap. 32*), ed. D.R. Paul and C. Bucknall (In Press).

8 N.H. Ray and F.R Sherliker, U.S. Patent 3,732,191 (1973).

9 W.A. Bahn, G.H. Beall, J. Ference, B.C. Monahan, C.J. Quinn, and P.S. Roussel, U.S. Patent 5,043,369 (1991).

10 C.J. Quinn, P. Frayer, and G.H. Beall, in *Polymeric Materials Encyclopedia* (vol. 4), ed. J.C. Salamone, 2766 (1996).

11 C.J. Quinn and G.H. Beall, in *Chem. Process. Adv. Mater*., ed L. Hench, 799 (1992).

12 G.H. Beall and C.J. Quinn, U.S. Patent 4,940,677 (1990).

13 G.H. Beall and J.E. Pierson, U.S. Patent 5,328,874 (1994).

14 B.G. Aitken, G.H. Beall, and J.E. Dickenson, Jr., U.S. Patent 5,529,961 (1996).

15 W.A. Bahn and C.J. Quinn, *SPE ANTEC Proc*., 2370 (1991).

16 A.I. Isayev and M. Modic, *Polym. Comp*., 8(3), 158 (1987)

17 H.J. O'Donnell and D.G. Baird, *Intl. Polym. Proc*., 11(3), 257 (1996).

18 H.J. O'Donnell and D.G. Baird, *Polym. Eng. Sci*., 36(7), 963 (1996).

19 H.J. O'Donnell and D.G. Baird, *Polymer*, 36 (2), 259 (1995).

20 J.P. de Souza and D.G. Baird, *Polymer*, 37 (10), 1985 (1996).

21 R.J. Krishnaswamy, S.E. Bin Wadud, and D.G. Baird, Polymer, 40, 701 (1998).

22 G. Crevecoeur, *PhD Dissertation*, Catholic University of Leuven (1991).

23 F.D. Rumsheidt and S. Mason, *J. Coll. Inerf. Sci*., 16, 238 (1961).

24 G.I. Taylor, *Proc. Roy. Soc*., A138, 41 (1932).

25 G.I. Taylor, *Proc. Roy. Soc*., A146, 501 (1932).

26 G.I. Taylor, *Proc. Roy. Soc*., A226, 289 (1954).

27 H.P. Grace, *Chem. Eng. Commun*., 14, 225 (1982).

28 R.T. Young, *PhD Dissertation*, Virginia Polytechnic Institute and State University, (1999).

29 R.L. Sammler, J.U. Otaigbe, M.L. Lapham, N.L. Bradley, B.C. Monahan, and C.J. Quinn, *J. Rheo*., 40 (2), 286 (1996).

30 P.K. Mallick, *Fiber Reinforced Composites*, Marcel Dekker, New York 1988.

31 PPG Industries, Inc., in *Modern Plastics Encyclopedia '92*, McGraw-Hill, New York 1992.

Chapter 6:
Forming and Shaping Behavior

Preface

This chapter concerns work performed in regards to addressing the second objective of this research. The processing behavior of phosphate glass reinforced materials was examined at the temperatures commonly used for shaping and forming operations. In particular, the composite blends were exposed to various extensional deformations to evaluate the effects on the mechanical properties of the materials. This chapter is organized as a manuscript for future publication.

Extensional Processing Behavior of Thermoplastics Reinforced with a Melt Processable Glass

R.T. Young, M.A. McLeod, and D.G. Baird

Department of Chemical Engineering and
NSF Science and Technology Center for High Performance
Polymeric Adhesives and Composites
Virginia Polytechnic Institute and State University
Blacksburg, VA 24061-0211

(ABSTRACT)

The purpose of this paper was to investigate the processing behavior of thermoplastics reinforced with a melt processable phosphate glass under extensional flows at temperatures used for forming and shaping operations. Injection molded blends consisting of polyetherimide (PEI) and polyphenylene sulfide (PPS) reinforced with 30-60 wt% phosphate glass were exposed to uniaxial and planar deformation at temperatures above the T_g of the phosphate glass (234°C) to evaluate the effects of shearfree deformation on the morphology and mechanical properties of the composites. Tensile testing at elevated temperatures (250-300°C) was used to evaluate the forming behavior and ascertain the conditions most suited for the deformation of the composite blends. A temperature of approximately 268°C was found to offer conditions most conducive to the deformation of the PEI/P-glass blends, leading to minimal changes in the morphology and mechanical properties after exposure to both uniaxial and planar shearfree deformation. A polyetherimide composite reinforced with 30 wt% conventional E-glass fiber was found to offer inferior performance at the higher temperatures (250-285°C), showing lower properties during tensile testing and substantial losses in mechanical properties after the application of deformation. Performance differences between the various glass filled polyetherimide composites were also evident during thermoforming. The P-glass reinforced materials produced parts with smoother surfaces and even material distribution while an E-glass reinforced composite led to a part with a rough, broken surface. For PPS reinforced with phosphate glass, the application of planar shearfree deformation near the melting point of the PPS (≈ 283°C) was found to elongate the phosphate glass phase. The increased aspect ratio of the glass reinforcing phase led to enhanced stiffness of the composite blends along the principal deformation direction. For a PPS composite blend containing 60 wt% phosphate glass, the application of a strain of 0.50 was found to elevate the composite tensile modulus by approximately 25% to a value of approximately 15 GPa.

6.1 Introduction

The addition of high aspect ratio inorganic reinforcement, such as glass fiber, has allowed the production of composite systems that possess moduli and strengths significantly greater than those of neat thermoplastics. While the addition of solid reinforcement typically results in significant enhancements in mechanical properties, it often adversely affects the dynamic performance of the material in a variety of fabrication techniques. In processes such as injection molding, the complex interactions between the fibers and flow field seen during molding often results in molded products that suffer from a variety of problems such as anisotropy in properties, weld line formation, and poor surface appearance [1,2]. In shaping and forming operations, the extensibility of the composite blends are often limited because of the inability of the reinforcement to undergo deformation. The lack of deformability of the reinforcing fibers and weakened interfacial adhesion between the reinforcement and matrix can lead to problems such as fiber buckling and breakage, formation of cracks or voids, and uneven deformation within the sample which results in finished products with undesirable appearances or properties [3-6].

Due to the processing difficulties created by the addition of solid reinforcement, work has been performed on the development of alternative composite systems that overcome many of the problems associated with conventional solid fiber reinforced materials. One such method referred to as in situ composite manufacturing relies on the formation of the reinforcing phase morphology during processing [7]. During processing operations, both the polymeric matrix and reinforcing phase are deformable, alleviating many of the problems seen with conventional solid reinforced systems. The final reinforcing phase morphology within the composite can be developed from deformation applied through a variety of polymer processing techniques such as injection molding, fiber spinning, film casting, and thermoforming.

One of the materials that has shown great promise for in situ composite generation techniques are melt processable glasses [8-11]. These inorganic glasses have low glass transition temperatures (200-350°C) allowing them to be combined with thermoplastic resins for use in conventional polymer processing techniques. The lower thermal transition temperatures for these materials are obtained by utilizing P_2O_5 instead of SiO_2 as the primary glass former. Additional materials such as alkali and alkaline earth oxides are added in order to help control the thermal transitions and chemical durability of the glasses [10]. Due to their structure, phosphate based glasses typically display lower mechanical properties than borosilicate glasses commonly used in the reinforcement of thermoplastics. The use of these phosphate glasses in engineering applications has been limited due to the poor chemical durability of the glass. Present research is being focused on formulating melt processable glasses with lower transition temperatures and improved chemical durability [12-14]. The development of more durable glasses with lower transition

temperatures could make these materials a viable alternative reinforcing phase for a variety of composite fabrication techniques.

Investigations of phosphate glasses as a reinforcement for thermoplastics have mainly concentrated on injection molding applications [8-11,15]. Much of the work has involved the blending of a variety of thermoplastics with a number of glasses in order to ascertain the properties that could be achieved. In recent years, the development of glasses with lower transition temperatures and increased chemical durability have shown great promise for the process of injection molding. For example, Bahn, Quinn and co-workers [9-11] injection molded composites consisting of glasses with higher glass transitions ($225°C < T_g < 350°C$) blended with higher performance thermoplastics such as polyetherimide (PEI), polyethersulfone (PES), polyetheretherketone (PEEK), polyetherketone (PEK), and thermotropic liquid crystalline polymers (TLCPs). Much of the work focused on higher glass loadings (50-70 vol%) because P-glass composites manufactured with conventional glass loadings (up to 40 vol%) appeared to offer only modest increases in mechanical properties relative to those obtained with E-glass. Composites reinforced with high loadings of phosphate glass typically had tensile moduli 4-10 times greater than those of the neat resins. For example, an injection molded PEK composite containing 70 vol% phosphate glass had a tensile modulus of approximately 30 GPa while the neat thermoplastic resin only had a modulus of 4 GPa. In addition to greater stiffness, phosphate glass reinforced composites were shown to offer other advantages such as low anisotropy, finer molding tolerances, greater resistance to creep and stress relaxation, and lower thermal expansion coefficients [10,11]. One of the drawbacks found with utilizing such high inorganic loadings was that the tensile strengths of the composite blends were found to fall below that of the neat resins.

The reinforcing glass phase morphology generated during processing has been shown to have a large effect on the mechanical properties of composite blends [8-10,15] . For example, Quinn and coworkers [10] found that the phosphate glass phase reinforcing morphology within a thermotropic liquid crystalline polymer (Xydar) had a significant effect on the mechanical properties of the composite. By varying the injection molding conditions, a variety of reinforcing morphologies consisting of small glass beads, fibers, and ribbons were produced within the composite blends. The transition of the glass morphology from low aspect ratio beads to elongated ribbons was found to result in significant increases in the composite's mechanical properties. For a blend containing 62 vol% glass, a morphology consisting of small glass beads yielded a tensile modulus of 17 GPa while a morphology consisting of high aspect ratio glass ribbons resulted in tensile modulus of 28 GPa. Similar enhancements in the strength were observed with the transition in morphology elevating the tensile strength from 52 MPa to 72 MPa.

The formation of the reinforcing morphology within in situ composites has been shown to be dependent on a number of factors such as the interfacial and rheological properties of the components, the stresses generated during processing, and the loading

of the various components [15-19]. Theories developed for droplet deformation and breakup for Newtonian fluids have often been applied to the formation of the reinforcing phase morphology within in situ composites. Work performed with Newtonian fluids established that a dispersed droplet can be elongated into a higher aspect ratio thread when exposed to either shear or elongational flow under certain conditions [20-24]. Deformation of the suspended droplet typically occurs when the disruptive hydrodynamic force is great enough to overcome the cohesive interfacial force between the components. The magnitude of the hydrodynamic force (stress) will depend strongly on the applied deformation rates as well as the rheological properties of the components. The viscosity ratio between the components (ratio of droplet to matrix viscosity) has also been found to have a large effect on the ability of the suspended phase to undergo deformation. Within simple shear flow, viscosity ratios between 0.1 and 3.5 have been shown to lead to conditions favorable to the deformation and eventual breakup of suspended droplets. Meanwhile, shearfree or extensional flows provide conditions favorable to the deformation of the suspended phase over a much wider range of viscosity ratios. Trends similar to those seen with Newtonian fluids have been qualitatively observed in regards to the formation of the reinforcing morphology within in situ injection molded composites [15,17-19,25]. The extensional flow field generated from the advancing front during mold filling has been found to lead to the formation of elongated fibrillar morphologies over a broad range of viscosity ratios. Regions within the molded injection specimens where shear flow was predominant often contained lower aspect ratio domains due to the inability of the flow field to adequately deform the reinforcing phase.

While composites reinforced with deformable reinforcing phases have shown great promise in injection molding applications, these materials may offer their greatest advantage in forming or shaping operations. At temperatures well below those required for injection molding, it may be possible to deform both the matrix resin and reinforcing phase in a process such as compression molding or thermoforming. The ability of both components to undergo deformation enhances the extensibility of the material and may serve to elevate the mechanical properties of the composite due to changes in the reinforcing phase morphology. For example, the shearfree flow field generated in the thermoforming process has been shown to lead to an enhancement in the properties of composite blends containing thermotropic liquid crystalline polymers (TLCPs) as the deformable reinforcing phase [26,27]. In contrast, the limited deformability of conventional solid fiber reinforced composites often leads to the formation of shaped products that suffer from reduced mechanical properties and poorer surface appearances [3-6]. Shearfree deformation generated by other techniques, such as tensile stretching at elevated temperatures (uniaxial deformation) and lubricated compression molding (planar and biaxial deformation), has been shown to affect the mechanical properties of in situ composites reinforced with TLCPs [26,28]. For example, de Souza and Baird [28] evaluated the effects of shearfree deformation on the properties of injection molded composites consisting of polyetherimide (PEI) reinforced with various TLCPs. Various types of shearfree deformation were applied to the composite blends in an effort to deform

the reinforcing phase to a greater degree and lower the mechanical anisotropy within the composites. Uniaxial deformation was found to transform TLCP droplets into fibrils which resulted in significant increases in mechanical properties along the stretching direction. The application of planar deformation resulted in the formation of ribbon-like structures that served to enhance the mechanical properties primarily along the stretching direction. Disc-like structures were found to be the result of the application of biaxial deformation which typically led to the formation of composites that displayed lower mechanical anisotropy.

The purpose of this paper is to evaluate the processing behavior of phosphate glass filled blends at temperatures commonly used for forming and shaping operations such as thermoforming or compression molding. In particular, injection molded composite blends consisting of polyetherimide and polyphenylene sulfide reinforced with a melt processable phosphate glass were exposed to shearfree deformations at temperatures above the T_g of the glass. Tensile testing was performed on composites reinforced with either phosphate or borosilicate glass at temperatures above the T_g of the P-glass in an effort to determine how the deformability of the glass phase affected the forming behavior of the composite blends. Injection molded composites were exposed to various imposed strains under both uniaxial and planar shearfree flows to determine the effects of the deformation on the reinforcing morphology and mechanical properties of the composite blends. The forming and shaping behavior of the glass reinforced polyetherimide composite blends was also examined with plug assisted matched die thermoforming.

6.2 Experimental

6.2.1 Materials

The reinforcing phase used in this work consisted of an experimental melt processable phosphate glass produced by Corning, Inc. (Corning, NY). This particular phosphate glass is composed of P_2O_5 (33 mol%), $ZnCl_2$ (26 mol%), B_2O_3 (4 mol%), and M_2O (37 mol%) where M consists of various alkali metals. The glass utilized is considered non-durable in that the material suffers from a loss in weight and mechanical properties when exposed to water. The glass was received as large shards that were crushed and sorted to yield particles ranging from 1-2 mm for blending with the thermoplastic resins. The glass transition temperature of the glass was found to be 233.7 ± 2.2°C based on differential scanning calorimetry (DSC) measurements performed at a heating rate of 10°C/min. The density of the glass was determined to be 2.62 ± 0.01 g/cm^3 based on measurements made on as received glass samples utilizing a pyconometer (Micrometrics Accupyc, Model 1330).

Polyphenylene sulfide (PPS) and polyetherimide (PEI) were utilized as the matrix resins for the injection molded phosphate glass reinforced composites. Polyphenylene

sulfide is a semi-crystalline engineering thermoplastic that has good mechanical properties, excellent chemical resistance, high temperature thermal stability, and inherent flame resistance[29]. An extrusion grade of PPS, designated as Ryton PR09 (Phillips Chemical Company), having a glass transition temperature of 91°C, a melting point of 279°C, and a density of 1.40 g/cm^3 was used to produce composites of various P-glass loadings. A general purpose grade of polyetherimide (Ultem 1000, GE Plastics) was also used to produce the phosphate glass reinforced composites. The Ultem 1000 is a commercially available amorphous polymer having a glass transition temperature of 217°C and a density of 1.27 g/cm^3. A commercially available grade PEI (Ultem 2300, GE Plastics) containing 30 wt% borosilicate (Type E) glass fiber was also evaluated in order to facilitate comparisons between the deformability of composite systems reinforced with phosphate glass and E-glass.

6.2.2 Composite Blend Preparation

The samples used for the deformation studies consisted of injection molded composite plaques produced with an Arburg Allrounder model 221-55-250. The molding unit was utilized in two main processing steps including the preblending of the materials and fabrication of the test specimens. All the materials were dried for at least 24 hours at 150°C under vacuum before being plasticated to form blends that contained a range of phosphate glass loadings (30-60 wt%).

The first processing step involved utilizing the injection molding unit as an extruder to preblend the glass with the thermoplastics resins. Due to the variety of blends to be studied and the limited availability of the phosphate glass, the molding unit was seen as an effective way to achieve the initial dispersion of the glass within small batches of composite material. Dry blends of the glass and resins were passed through the molder screw operating at 200 rpm with the extrudate being collected, quenched, and granulated using a Cumberland Granulator (Model 6x8). For the PPS based composites, the molder barrel temperature profile consisted of 330°C, 350°C, 350°C and 350°C, progressing from the solid conveying zone to the nozzle. The zone temperatures were increased by 20°C to facilitate the blending of the phosphate glass with the polyetherimide.

Test specimens for the deformation studies were generated by feeding the granulated material back into the injection molding unit operating at the same temperature profiles used in the blending step. Composite plaques were produced by injecting the plasticated blend into a film-gated mold having dimensions of 75 mm by 80 mm by 1.6 mm. For all the composites, the mold fill rate (≈10 cm^3/sec), injection pressure (5 MPa), holding pressure (10 MPa), screw speed (200 rpm), and cooling time (45 seconds) were all held constant. Mold temperatures consisting of 140°C for the PPS and 160°C for the PEI were utilized to help facilitate the deformation of the glass during the filling of the mold.

6.2.3 Composite Tensile Mechanical Properties

The tensile properties of the various composite blends before and after deformation were measured at room temperature using an Instron Mechanical Tester (Model 4204). Test specimens approximately 75 mm long by 8 mm wide were cut from both injection molded plaques and samples exposed to the shearfree deformation. Tensile properties were measured along the machine (stretching) and transverse directions using a 5 kN load cell following ASTM standard B 638-87B. The crosshead speed was kept constant at 1.27 mm/min with the strain imposed on the sample measured using an extensionmeter (Instron Model 2630-25). All the mechanical properties reported are the average of at least five test samples.

In order to examine the forming potential of the various composite blends, the tensile properties of the materials were evaluated at temperatures above the T_g of the phosphate glass (250-300°C). The higher temperatures were achieved by fitting an Instron Mechanical Tester (Model 4204) with a forced convection oven manufactured by Russells Technical Products (Model RB-2-340). An accurate determination of the sample temperature was obtained by mounting a small thermocouple within the center of undeformed composite blends that were clamped to crossheads grip situated within the oven. After being loaded within the preheated oven, the sample temperature was found to rise to a value approximately 15°C below the oven setpoint showing little variation (±1°C) after a period of approximately 10 minutes. Rectangular test specimens (75 mm x 8 mm), cut along the machine direction of the injection molded plaques, were clamped within the grips and preheated for a period of 12 minutes before the onset of tensile testing. Samples of an initial gauge length (L_0) of 40 mm were deformed at a constant stretching velocity (V) of 250 mm/min. in order to evaluate the response of the composite blends under rapid, large scale deformation. The high crosshead speeds allowed the generation of an initial strain rate ($\dot{\varepsilon}_0 = V/L_0$) of approximately 0.10 sec^{-1} which was similar to the instantaneous strain rates (0.1-10 sec^{-1}) commonly seen in forming operations such as thermoforming [30]. The tensile properties of the blends including the modulus and toughness (area under the stress-strain curve) were to be used as a quantitative way to evaluate the effects of factors such as temperature and glass loading on the deformability of the materials. All the values reported for the tensile testing at the elevated temperatures are an average of measurements made on a least five test specimens.

6.2.4 Morphology

The morphology of the injection molded plaques and deformed samples was examined using a Stereoscan S200 scanning electron microscope with an accelerating voltage of 20 kV. The surfaces examined were prepared by immersing the sample in liquid nitrogen for approximately 5 minutes before fracturing. The samples were

subsequently attached to mounting studs and coated with a layer of gold using a sputter coater (Bal-Tec Model SCD 005) to enhance conductivity.

6.2.5 Deformation of Composite Blends

Uniaxial deformation of the composite blends was obtained by stretching the injection molded samples parallel to the machine direction with the configuration utilized for the tensile testing at the elevated temperatures. Entire injection molded plaques were stretched to various lengths (L) by controlling the displacement of the movable crosshead within the oven. In an effort to accurately control the deformation of the blends, a lower stretching velocity (V) of 50 mm/min. was applied to the samples. The use of a constant stretching velocity resulted in a strain rate that varied during testing with the highest strain rate ($\dot{\varepsilon}_0$) of 0.02 seconds^{-1} being achieved at the onset of deformation. Stretching in this manner led to necking of the sample which limited the formation of homogeneous, uniaxial deformation to the center region of the specimen. Due to the necking and constrained deformation of the material located near the grips, the actual strain exerted on the sample was evaluated by two different methods which were found to offer comparable results. The first involved using the change in the thickness of the sample blend within the deformed regions to calculate the total strain exerted on the sample. The other method involved measuring the change in dimensions of a square (25.4 mm x 25.4 mm) drawn in the center of the undeformed sample. From the two methods, the total amount of deformation experienced by the samples was characterized by the Hencky strain (ε) along the principal deformation direction which can defined as $\varepsilon = \ln(L/L_0)$.

The composite blends were exposed to planar deformation by means of lubricated compression molding with a picture frame mold. The mold assembly was preheated between the platens of a hot press before the injection molded specimen was placed within the mold so the material was constrained on the sides perpendicular to the principal deformation (machine) direction. A thermocouple in contact with the sample was used to monitor the composite temperature and once the desired conditions were achieved, a compressive force was applied. For the polyphenylene sulfide based composites, a force of approximately 10 kN was applied while the lower temperatures utilized with the polyetherimide composites required the application of higher forces in the range of 15-40 kN. Various extents of deformation or Hencky strain (ε) were achieved by allowing samples of varying initial length (L_0) to flow down the rectangular mold channel until the material reached a length (L) that completely filled the picture frame. After the deformation, the mold assembly was then transferred to a water chilled press where the sample was cooled at a rate of approximately 50°C/minute. The total amount deformation seen by the material was verified by calculating the applied strain from the change in the sample thickness. The amount of shear experienced during deformation was minimized by sandwiching the sample between sheets of polyimide film treated with a high temperature

silicone release agent. It should be pointed out that due to the manual operation of the hot press, the strain rates experienced during the compression molding could not be estimated.

6.2.6 Thermoforming of Composite Blends

The shaping behavior of select composites reinforced with P-glass and E-glass was evaluated using plug assisted matched die forming via a Hydrotrim (Model 1620) Thermoformer. Rectangular injection molded blanks (75 mm x 80 mm x 1.6 mm) of the polyetherimide based composite blends were shaped using a shallow rectangular mold heated to a temperature of 180°C. The gap between the bottom female mold half (50.8 mm x 25.4 mm x 12.7 mm) and the plug was 1.4 mm. The mold configuration utilized resulted in a maximum linear draw ratio of two (0.70 maximum strain) and an areal draw ratio (A/A_0) of 2.5. The heating conditions (infrared oven temperature and residence time) were varied in order to obtain shaped articles that displayed the best surface appearance and material distribution.

6.3 Results and Discussion

6.3.1 Forming Properties of Composite Blends

For a process such as thermoforming, the properties of the material often serve to place limitations on the fabrication conditions utilized to obtain the finished part. For example, the material sheet has be rigid enough to support its own weight during pre-heating but still remain pliable enough to be shaped into the final product. The properties of the material can serve to limit processing parameters such as the sheet temperature, deformation rates, and total extent of deformation experienced during forming. Tensile testing at elevated temperatures has shown great promise as a method to gauge the formability of various materials [6,30-32]. The tensile stress versus elongation response of a material at elevated temperatures can be used to obtain important data such as the modulus, strength, elongation to yield, and toughness of the material which can be related to certain processing characteristics. The tensile modulus can be used to gauge the ability of the material to resist sheet sag during heating while the toughness (area under the stress-strain curve) can be used to estimate the ability of the material to undergo deformation. Other data, such as the elongations where the load levels off to a minimum value (viscous flow) can be used to establish the limits in deformation that would minimize localized thinning and variations in thickness within the formed article.

In an effort to evaluate the formability and optimum temperatures required to obtain deformation of the phosphate glass phase, tensile testing at elevated temperatures was performed for a variety blends. The first composites investigated consisted of polyetherimide reinforced with either phosphate or borosilicate glass. Temperatures well above the T_g of the PEI (217°C) and the phosphate glass (234°C) were utilized to

determine if the deformable reinforcing phase offered any performance advantages over conventional solid fiber reinforcement. The response of the composites was obtained using a high crosshead speed (250 mm/min.) in an effort to emulate the instantaneous high deformation rates commonly seen in a process such as thermoforming. Because of inhomogenous deformation within the samples due to the shape of the test specimens and the clamping configuration, the mechanical properties obtained by the method were qualified as being apparent values.

The apparent tensile modulus (initial slope of stress-strain curve) versus temperature for the various PEI/glass blends is presented in Figure 6.1. The phosphate glass filled blends showed higher tensile moduli than the E-glass fiber filled material up to temperature of about 280°C. The greater stiffness exhibited by the phosphate glass filled materials was attributed to the reinforcing morphology generated within the injection molded composites. For both the composites reinforced with the phosphate glass, a high aspect ratio or interlocking network morphology was found across the entire thickness of the injection molded specimen while the E-glass filled composite contained shorter, larger diameter fibers (Figure 6.2). This interpenetrating morphology within the phosphate glass reinforced materials appeared to help these composites exhibit a high degree of stiffness over a wide temperature range. The higher tensile moduli also indicate that these materials should be able to resist sheet sag more readily than the E-glass filled composite. The increased deformability of the phosphate glass at the higher temperatures was evident by the large drop in the modulus of the blends with increasing temperature. For composite blends containing the same weight (30%) and volumetric loading of glass, the stiffness of the phosphate glass filled material showed a much greater sensitivity to temperature. For example, raising the temperature by 30°C resulted in an exponential drop in the modulus of the phosphate glass filled material from a value 154.6 ± 9.5 MPa to only 11.1 ± 1.0 MPa. The large drop in the modulus was believed to be partially due to a substantial lowering of the phosphate glass viscosity whose activation energy was found to be on the order of 87.9 ± 1.1 kCal/mol [15]. Over the same temperature range, the E-glass filled material showed a less dramatic, linear decline in modulus, only falling from 47.3 ± 1.3 MPa to 13.4 ± 1.1 MPa due to the increased fluidity of only the polyetherimide phase.

Another parameter obtained from the tensile testing found useful in evaluating the formability of the materials was the apparent tensile toughness which was taken as the area under the stress-strain curve. In Figure 6.3, the apparent toughness versus temperature for a variety glass filled polyetherimide based composites is presented. For the E-glass filled material, the toughness shows a slight decline with temperature which was attributed to the increased fluidity of the polyetherimide which led to the formation of lower tensile stresses within the material. The limited elongation that could be obtained before the material broke due to catastrophic failure (<100%) also served to lower the toughness values for the E-glass filled material. For the phosphate glass reinforced composites, the toughness was found to increase with temperature with maximum values being obtained at

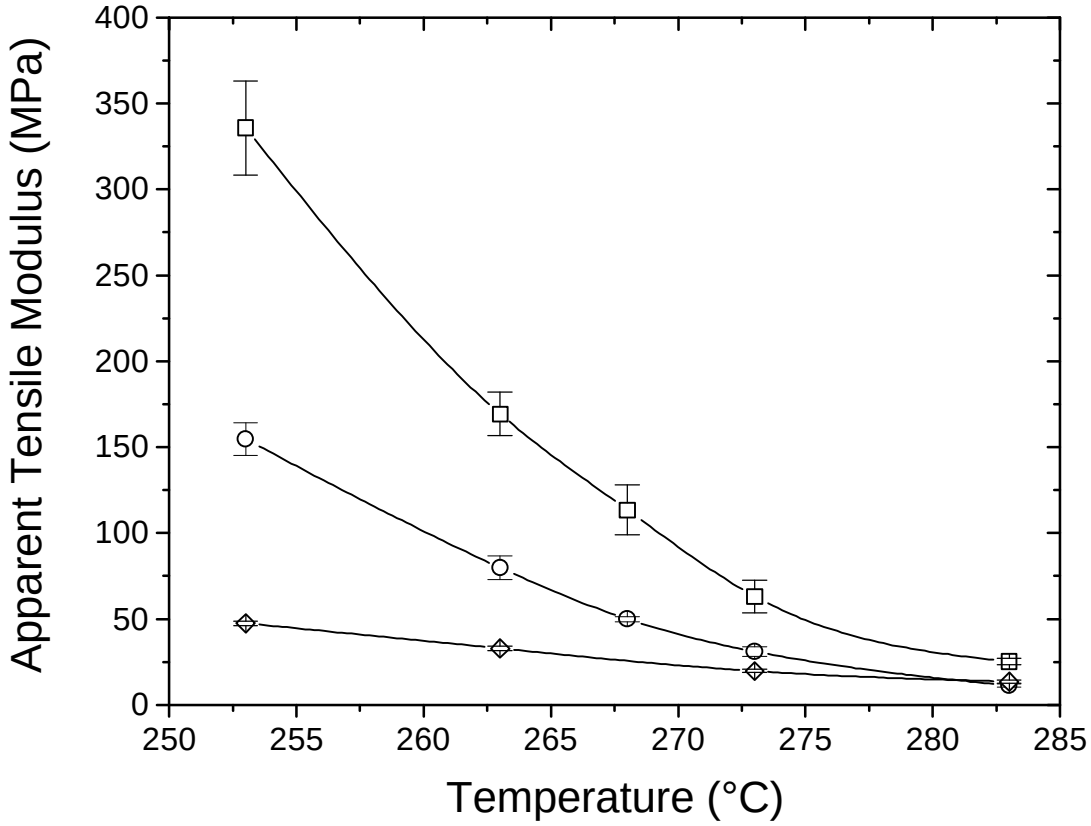

Figure 6.1: Apparent tensile modulus versus temperature for polyetherimide reinforced with various glasses. (◇) 30 wt% E-glass, (○) 30 wt% P-glass, and (□) 45 wt% P-glass.

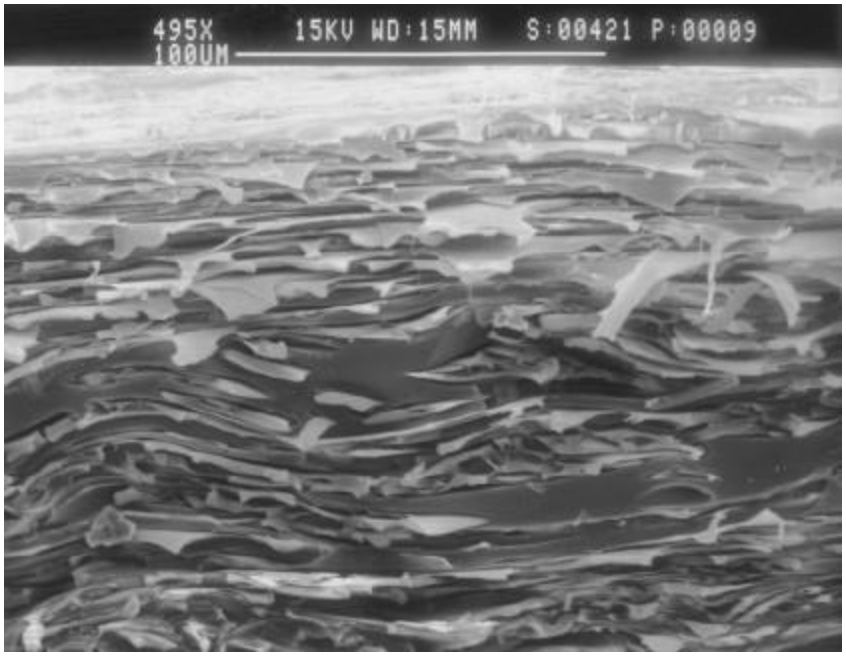

(a)

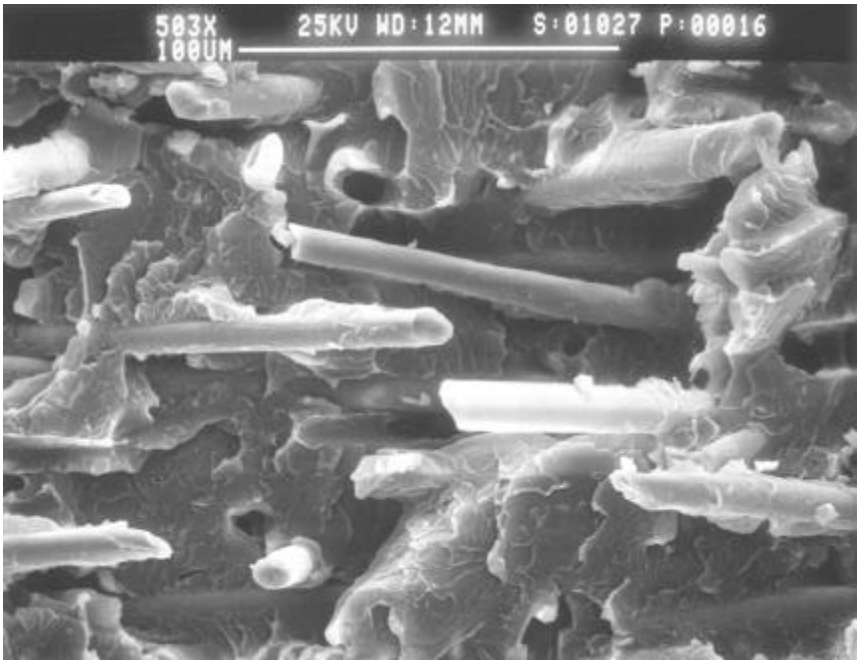

(b)

Figure 6.2: Scanning electron micrographs from the skin region of polyetherimide injection molded composites along the machine direction. (a) 45 wt% P-glass (b) 30 wt% E-glass fiber

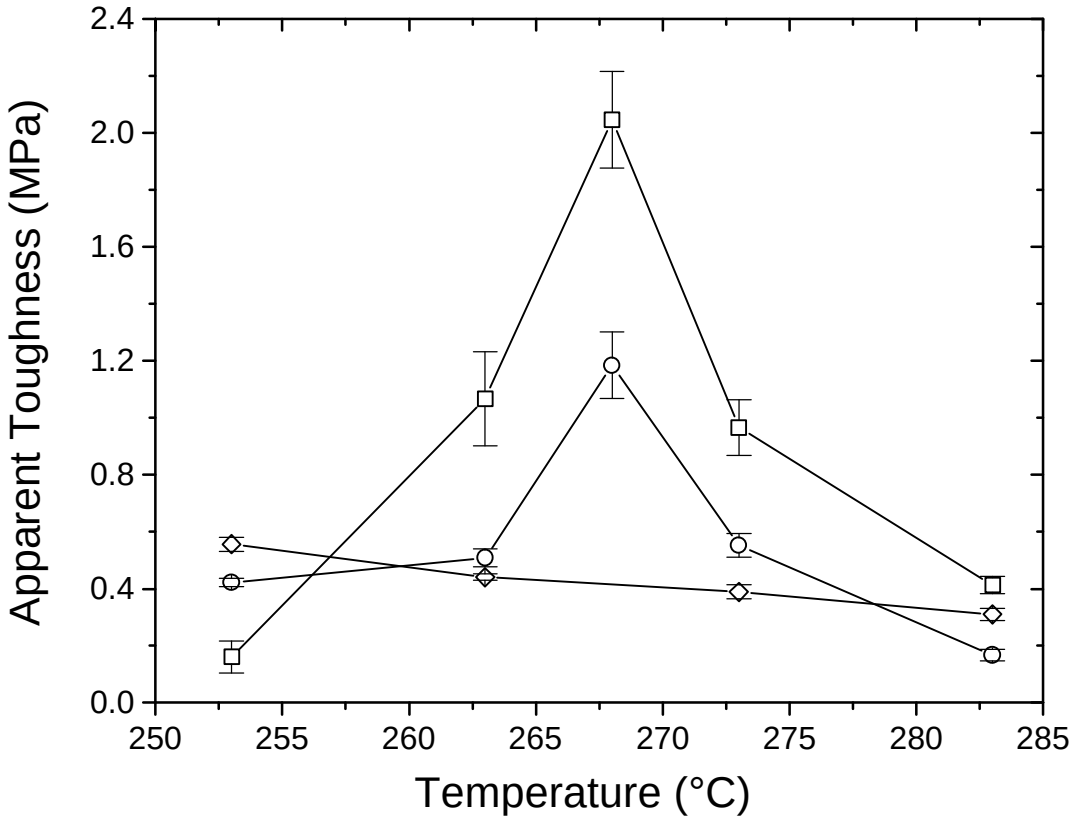

Figure 6.3: Apparent tensile toughness versus temperature for polyetherimide reinforced with various glasses. (◇) 30 wt% E-glass, (○) 30 wt% P-glass, and (□) 45 wt% P-glass.

a temperature of approximately 268°C. Below this temperature, the phosphate glass filled blends failed at very low elongations (< 35%) in a manner very similar to that seen with the E-glass filled composite. At the higher temperatures (≥ 268°C), it was possible to extend both of the phosphate glass reinforced composites to the maximum extent allowed within the testing limits of the oven (≈ 400% elongation). The large transition in the toughness of the phosphate glass filled composites over a temperature range of 263-273°C can be seen by examining the stress-strain response curve for a composite reinforced with 45 wt% P-glass (Figure 6.4). At a temperature of 263°C, the material displayed limited deformation undergoing catastrophic failure at very low applied strains. By raising the temperature by 5°C, the composite blend could be extended to the maximum extent within the testing oven suggesting the phosphate glass phase readily deformed. The high degree of extensibility of the composite blend at this condition led to a toughness value almost double that obtained at 263°C. Increasing the temperature by another 5°C to 273°C still allowed the blend to be elongated to the maximum extent within the oven but a substantial drop in the toughness was observed due to a number of possible phenomena including the increased fluidity of the phosphate glass or possible break up of the glass phase reinforcing morphology. It should be pointed out that samples elongated at temperatures ≥ 268°C were found to offer an even material distribution and smooth surfaces indicating fairly homogenous deformation of the composite blend. For both the phosphate and borosilicate glass reinforced composites, the region after yielding was found to make the greatest contribution to the overall toughness of the blends. Because forming usually occurs in the region of plastic flow after yield, the conditions that maximize the toughness should be most suited for the deformation of the composite blends.

Tensile testing at elevated temperatures was also performed for the composite blends consisting of polyphenylene sulfide reinforced with phosphate glass. The tensile properties of a PPS composite reinforced with 40 wt% phosphate glass were examined near the melting point of the PPS for temperatures ranging from 270°C to 295°C. The apparent tensile modulus followed a trend similar to that seen for the PEI based composites with the modulus falling exponentially to lower values near the melting point of the PPS. The apparent toughness (≈ 0.2 MPa) showed little variation with temperature and was found to be much lower than the values found for the polyetherimide based blends. The composite blends consisting of the polyphenylene sulfide also exhibited much lower strengths and elongations to break than the composites generated with the amorphous PEI. For the polyphenylene sulfide composite, three phases were present including the phosphate glass and both amorphous and crystalline PPS. At the lower temperatures investigated, these crystalline regions would serve to act in manner similar to physical crosslinks which would serve to severely limit the extensibility of the material. The presence of these rigid crystalline regions coupled with a possible lack of interfacial adhesion between the P-glass and PPS may help account for the catastrophic failure of the composite blend at lower imposed strains during the free surface deformation for the tensile testing at elevated temperatures. While creating problems in a tensile stretching

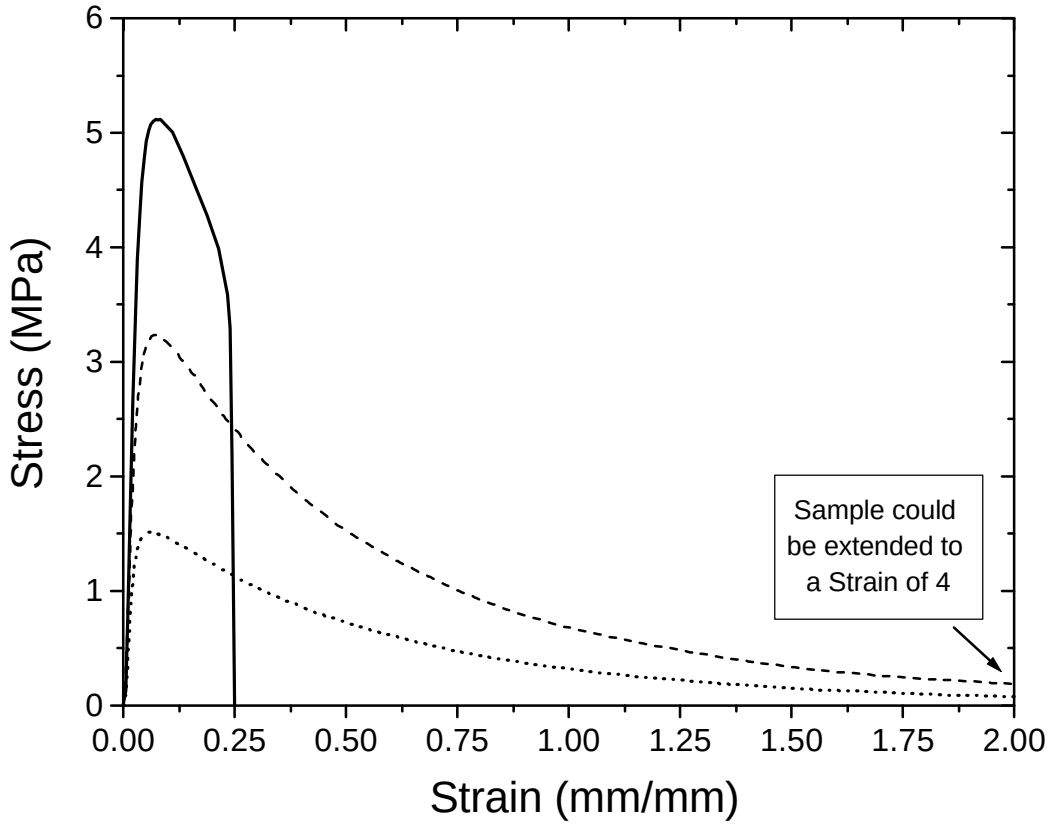

Figure 6.4: Stress-strain curves for polyetherimide reinforced with 45 wt% phosphate glass as function of temperature. (——) 263°C, (– – –) 268°C, and (- - - -) 273°C.

type process, the presence of these crystalline regions should serve to elevate the viscosity of the PPS which may be advantageous in a constrained type of deformation, such as compression molding, where melt strength is no longer an issue.

6.3.2 Uniaxial Deformation of the Composite Blends

While tensile testing at elevated temperatures showed it was possible to elongate the polyetherimide/phosphate glass blends to a large extent under uniaxial elongation, the effects of this deformation on the morphology and properties of the blends had yet to be determined. From the tensile testing, a temperature of 268°C appeared to be the most conducive for the deformation of the composite blends as indicated by the maximized apparent toughness and high degree of extensibility (> 400% elongation). The effects of uniaxial deformation applied at this temperature were analyzed by stretching whole injection molded plaques to various extents within the Instron/oven configuration. After stretching, the composite blends were cooled and the effects of deformation examined through mechanical testing and scanning electron microscopy. A composite reinforced with 30 wt% borosilicate glass fiber was also deformed under the same conditions to facilitate a comparison between the different types of reinforcing material.

The effects of uniaxial deformation on the stretching direction mechanical properties of the glass filled polyetherimide composites are presented in Table 6.1. The deformation was applied along the machine direction of the injection molded composites in an effort to further elongate the phosphate glass reinforcing phase. For the phosphate glass filled blends (30 and 45 wt%), the deformation appeared to have no significant effect on the stretching direction stiffness and strength. In fact, it was possible to expose the blends to high extents of deformation ($\varepsilon \approx 1.1$ or 200% elongation) without significant losses in the stretching direction properties. It appears that the applied deformation may have served to further elongate the glass phase, but due to the high initial aspect ratio and interpenetrating morphology found within the original molded composites, no significant enhancement in the mechanical properties could be achieved. A very different trend was seen for the 30 wt% E-glass fiber reinforced composite. Both the tensile modulus and strength along the stretching direction were lowered with the application of deformation resulting in substantial losses in the mechanical properties. For example, an injection molded blend containing 30 wt% E-glass fiber had a tensile modulus and strength of 8.17 ± 0.31 GPa and 151.4 ± 6.0 MPa, respectively, while exposing the composite to 200% elongation lowered the modulus to 6.72 ± 0.44 GPa while the strength fell to 83.3 ± 17.4 MPa. The significant difference between the trends seen with the phosphate and E-glass filled materials was partially attributed to the size and lack of deformability of the E-glass reinforcing phase. This lack of deformability was evident looking at the surfaces of composites blends (Figure 6.5) containing the same weight (30%) and volumetric loading of the various glasses exposed to the same extent of deformation ($\varepsilon \approx 0.75$ or 112% elongation). For the E-glass filled material, the surface was rough and broken indicating

Table 6.1: Tensile Properties for injection molded PEI composites reinforced various loadings of glass stretched uniaxially along the machine direction at 268°C and 50 mm/min (Initial strain rate = 0.02 sec^{-1})

Machine (Stretching) Direction						
	30 wt% P-glass		**45 wt% P-glass**		**30 wt% E-glass**	
Uniaxial Strain	**Modulus (GPa)**	**Strength (MPa)**	**Modulus (GPa)**	**Strength (MPa)**	**Modulus (GPa)**	**Strength (MPa)**
As Molded	6.09 (0.26)	86.6 (2.3)	9.43 (0.33)	72.3 (4.5)	8.17 (0.31)	151.4 (6.0)
0.36 (0.07)	6.37 (0.44)	80.2 (3.7)	9.41 (0.20)	66.2 (3.2)	8.00 (0.31)	150.4 (5.1)
0.74 (0.04)	6.12 (0.22)	85.9 (1.8)	8.25 (0.30)	66.4 (4.1)	7.55 (0.34)	129.0 (6.4)
1.09 (0.06)	5.80 (0.17)	76.8 (2.8)	8.65 (0.50)	65.6 (5.0)	6.72 (0.44)	83.3 (17.4)
Transverse Direction						
	30 wt% P-glass		**45 wt% P-glass**		**30 wt% E-glass**	
As Molded	4.77 (0.07)	56.2 (3.4)	8.34 (0.38	44.5 (3.5)	4.95 (0.32)	91.7 (2.4)
0.74 (0.04)	4.19 (0.14)	56.3 (3.7)	6.95 (0.29)	35.6 (2.1)	3.59 (0.17)	71.5 (5.1)

Note: Standard deviations given in parentheses

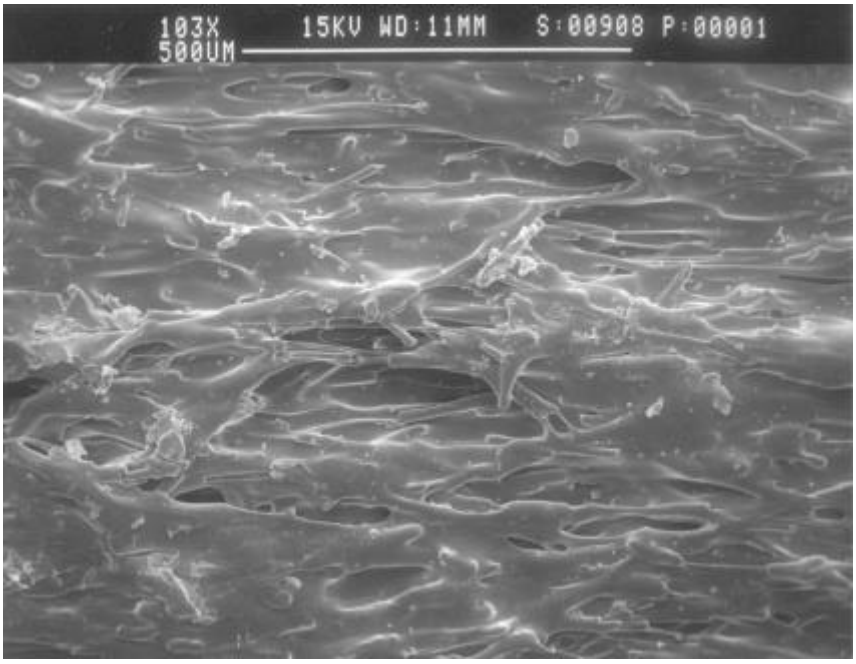

(a)

(b)

Figure 6.5: Scanning electron micrographs of the surface of injection molded polyetherimide composites stretched uniaxially. (a) 30 wt% E-glass fiber (b) 30 wt% P-glass (T = 268°C, $\varepsilon \approx 0.75$, $\dot{\varepsilon}_0 = 0.02\ sec^{-1}$)

that only the polyetherimide was only able to undergo deformation while possibly being constrained by glass fibers. This limited deformation of the composite blend led to an uneven material distribution with the formation of voids within the composite which served to lower the overall mechanical properties and promote premature failure of the composite during testing. In the case of the phosphate glass filled material, the surface of the composite blend was much smoother possibly due to deformation of both the PEI and P-glass within the composite.

While the phosphate glass filled materials retained most of their machine direction properties after stretching, the deformation appeared to have a detrimental effect on the transverse direction properties (Table 6.1). Composite blends stretched to approximately strain units typically displayed a 10-30% loss in both the transverse direction modulus and strength when compared to the as molded composites. Examination of the composites by scanning electron microscopy revealed the higher aspect ratio phosphate glass reinforcing morphology remained intact during deformation but was accompanied by the formation of voids within the composite blends (Figure 6.6). For the composite blend containing 30 wt% phosphate glass, these voids were limited to core region of the specimen while for the composite containing 45 wt% P-glass, the voids were more numerous and dispersed across the entire thickness of the sample. It was believed that a lack of adhesion between the polyetherimide and phosphate glass coupled with the stresses generated during the stretching helped pull the materials apart leading to the formation of the voids within the composites.

6.3.3 Planar Deformation of the Composite Blends

The effects of planar shearfree deformation on the properties of the composite blends were also investigated by lubricated compression molding. The lubricated mold configuration allowed deformation to be applied to the polyphenylene sulfide (PPS) based composites which did not have the melt strength for the free surface uniaxial deformation. In the case of the polyetherimide based composites, the compression molding was performed at the same temperatures investigated in the uniaxial stretching experiments. For the PPS based composites, compression molding was performed at temperatures of 282-283°C which were experimentally determined to be the lowest temperatures at which deformation of the PPS within the mold was possible. The lower temperatures were utilized in an effort to preserve the crystalline regions within the PPS which should serve to elevate the viscosity and help minimize the viscosity difference between the phosphate glass and PPS.

The mechanical properties of the polyetherimide based composites exposed to planar deformation are presented in Table 6.2. As with the uniaxial stretching, the deformation appeared to offer no significant improvement in the machine direction mechanical properties of the phosphate glass reinforced composite blends. The utilization of the planar deformation generated by a squeezing flow was found to offer slightly better

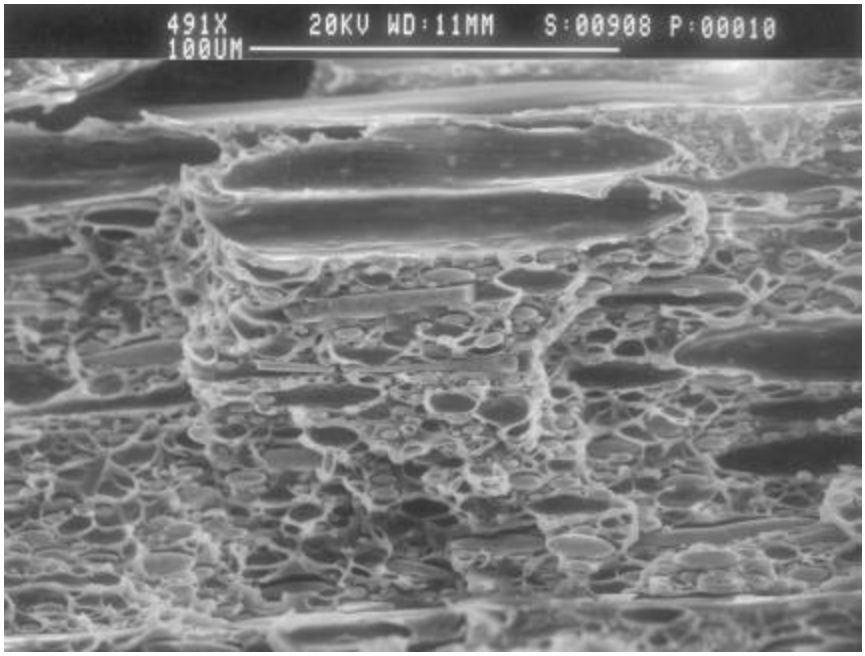

(a)

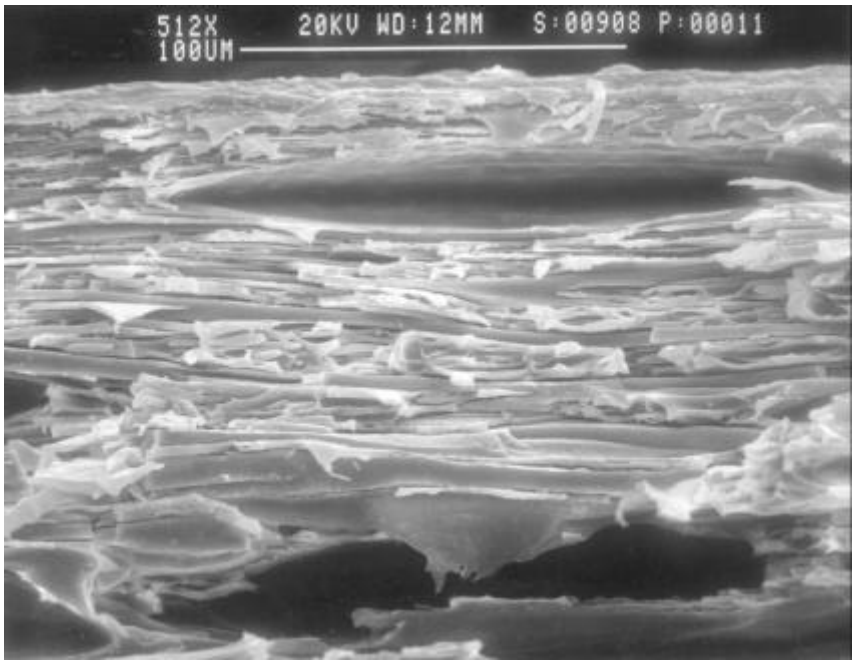

(b)

Figure 6.6: Scanning electron micrographs parallel to the deformation direction for polyetherimide injection molded specimens stretched uniaxially. (a) 30 wt% P-glass, core region (b) 45 wt% P-glass , skin region (T = 268°C, $\varepsilon \approx 0.75$, $\dot{\varepsilon}_0 = 0.02\ \text{sec}^{-1}$).

Table 6.2: Tensile Properties for injection molded PEI composites reinforced various loadings exposed to planar deformation along the machine direction at 268°C

Machine (Stretching) Direction						
	30 wt% P-glass		**45 wt% P-glass**		**30 wt% E-glass**	
Planar Strain	**Modulus (GPa)**	**Strength (MPa)**	**Modulus (GPa)**	**Strength (MPa)**	**Modulus (GPa)**	**Strength (MPa)**
As Molded	6.09 (0.26)	86.6 (2.3)	9.43 (0.33)	72.3 (4.5)	8.17 (0.31)	151.4 (6.0)
0.25	5.91 (0.25)	81.9 (2.8)	10.17 (0.50)	73.7 (2.5)	-	-
0.50	5.99 (0.34)	82.5 (2.8)	10.05 (0.26)	71.7 (2.6)	-	-
0.75	6.34 (0.50)	73.2 (1.3)	9.49 (0.59)	69.0 (2.3)	8.54 (0.54)	103.5 (6.8)
Transverse Direction						
	30 wt% P-glass		**45 wt% P-glass**		**30 wt% E-glass**	
As Molded	4.77 (0.07)	56.2 (3.4)	8.34 (0.38	44.5 (3.5)	4.95 (0.32)	91.7 (2.4)
0.75	4.22 (0.14)	64.2 (1.6)	7.72 (0.51)	45.9 (5.3)	4.32 (0.15)	79.9 (3.7)

Note: Standard deviations given in parentheses

transverse direction properties than comparable composites exposed to uniaxial deformation. Scanning electron micrographs for the composites exposed to planar deformation (Figure 6.7) revealed an absence of voids unlike the composites exposed to the uniaxial deformation (Figure 6.6). The force applied during the compression molding appeared to keep the glass and PEI in intimate contacting during deformation minimizing the formation of voids which possibly resulted in enhanced stress transfer between the various materials. Composites reinforced with 30 wt% borosilicate glass fiber were also exposed to deformation under the same conditions. It should be pointed out that pressures more than double that required for the deformation of the phosphate glass had to be used due to increased viscosity caused by the presence of the solid reinforcing phase. As with the phosphate glass filled material, the deformation had little effect on the machine direction modulus while the transverse direction stiffness dropped slightly possibly due to the orientation of the glass fibers along the flow direction. Unlike the phosphate glass filled composites, the deformation led to significant losses (10-30%) in both the machine and transverse direction tensile strength possibly due to breakage of the glass fibers.

Polyphenylene sulfide based phosphate glass reinforced composites were also exposed to planar shearfree flow to evaluate the deformability of the blends. The reduced viscosity of the phosphate glass at temperatures near the melting point of the PPS (≈ 280°C) should result in a composite blend that displays better overall deformability than a conventional solid reinforced material. Shearfree deformation similar to that which would be seen during a forming operation was applied to the blends in effort to determine how the ability of the reinforcing phase to undergo deformation affected the morphology and mechanical properties of the composites.

The effects of deformation on the machine (stretching) direction properties of the PPS composites reinforced with 40 and 60 wt% phosphate glass are shown in Table 6.3. For the composite containing 40 wt% P-glass, the modulus of the composite along the deformation direction was found to generally increase with the amount of deformation imparted on the sample. For example, the modulus of the as-molded sample was found to be 6.94 ± 0.20 GPa while the application of a Hencky strain of 0.75 (112% elongation) at 283°C was found to elevate this value to 8.31 ± 0.37 GPa. The composite containing 60 wt% glass was found to follow a similar trend with the maximum properties being achieved at an elongation of 65% or 0.50 strain units. The applied planar deformation was found to enhance the modulus by approximately 25% from a value of 12.44 ± 0.57 GPa to 15.41 ± 1.00 GPa. At a higher extent of deformation ($\varepsilon = 0.75$), the modulus was found to fall back down to a value comparable to the original injection molded specimen. While it was possible to increase the modulus of the composites by applying shearfree deformation, the strength of the composite blends often fell after the compression molding step. The loss in strength was attributed to changes in the crystalline nature of the PPS due to the thermal history experienced during the deformation step. During the compression molding, the composite blends were only heated to a temperature of approximately 283°C which would facilitate the retention of crystalline regions of PPS.

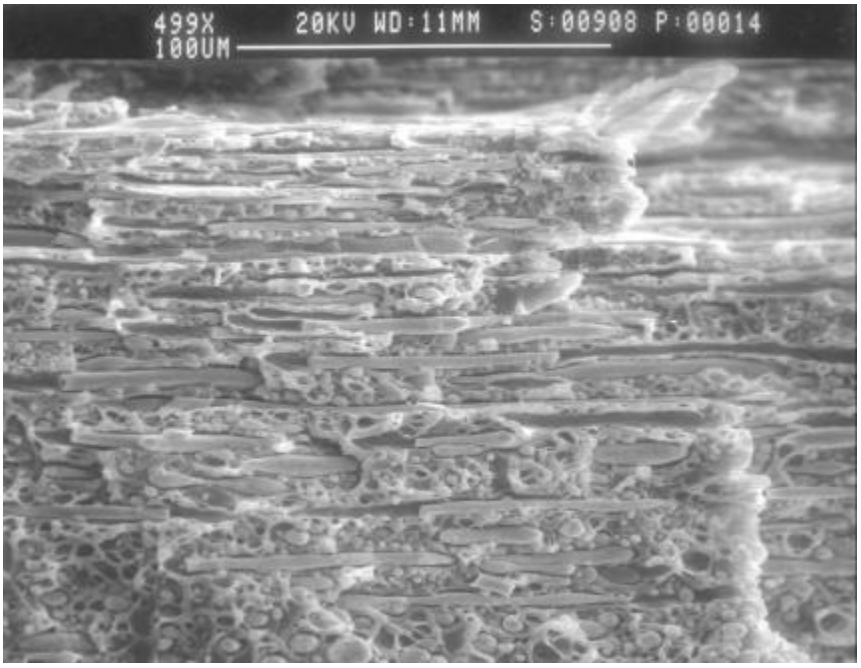

(a)

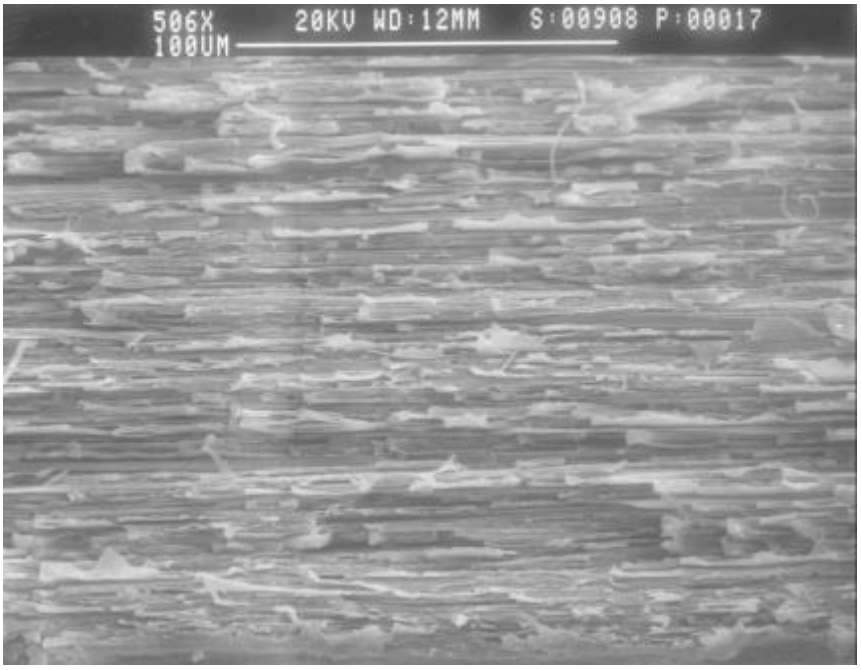

(b)

Figure 6.7: Scanning electron micrographs parallel to the deformation direction for polyetherimide injection molded specimens exposed to planar deformation. (a) 30 wt% P-glass, core region (b) 45 wt% P-glass , skin region ($T = 268°C$, $\varepsilon \approx 0.75$)

Table 6.3: Tensile Properties for injection molded PPS composites reinforced with phosphate glass exposed to planar deformation along the machine direction at 282-283°C

	40 wt% P-glass			60 wt% P-glass		
Planar Strain	**Modulus (GPa)**	**Strength (MPa)**	**% Elong.**	**Modulus (GPa)**	**Strength (MPa)**	**% Elong.**
As Molded	6.94 (0.20)	51.6 (3.2)	0.76 (0.06)	12.44 (0.57)	47.1 (6.0)	0.38 (0.06)
* None	7.38 (0.11)	35.1 (2.8)	0.48 (0.04)	12.37 (0.71)	21.0 (3.3)	0.17 (0.02)
0.25	7.82 (0.21)	45.9 (5.5)	0.59 (0.07)	13.18 (0.65)	21.8 (3.6)	0.16 (0.03)
0.50	7.51 (0.14)	33.6 (4.9)	0.46 (0.06)	15.41 (1.00)	19.6 (5.2)	0.13 (0.05)
0.75	8.31 (0.37)	41.2 (1.8)	0.51 (0.05)	12.13 (1.42)	19.8 (3.2)	0.18 (0.03)

Note: Standard deviations given in parentheses
* None- material exposed to same thermal history without the application of deformation

After deformation within the hot press, the heated mold assembly was removed and transferred to a water cooled press at another location. During this transferring process (≈1 minute), the residual crystallites combined with the slower cooling rates appeared to lead to a change in the polyphenylene sulfide. This change in the nature of the PPS coupled with a lack of adhesion between the PPS and glass, as indicated by glass pullout from the micrographs, could lead to premature failure of the composites resulting in the lower strengths. It should be pointed out that composite blends exposed to the compression molding thermal history without the application of deformation displayed a similar loss in strength and offered an elevated storage modulus (G′) after crossing the T_g of the PPS (Figure 6.8) giving a good indication of a change in the crystalline nature of the polyphenylene sulfide.

Scanning electron microscopy was used to evaluate the changes in the composite reinforcing morphology due to exposure to the planar deformation. The original injection molded composites contained elongated glass domains within the skin region of the samples due to the extensional deformation generated at the advancing front while only slightly elongated glass drops were obtained within the core region (Figure 6.9). The effects of the deformation were found to be most discernable in the center (core) regions of the deformed samples. For the composite blend containing 40 wt% phosphate glass, the application of deformation was found to elongate the glass regions within the core yielding the morphology found in Figure 6.10. The increased aspect ratio of the glass phase within this region helps account qualitatively for the almost 1 GPa increase in the tensile modulus along the deformation direction. The composite blend containing 60 wt% phosphate glass was found to display the maximum tensile modulus after the application of a Hencky strain of 0.50 which can be partially attributed to the transition in the glass reinforcing morphology within the core region (Figures 6.9b and 6.11a). It appeared that the applied deformation led to significant elongation of the glass droplets which may have eventually impinged on one another to due to the high volume fraction (43%) of glass present. This deformation and possible coalescence of the glass led to the formation of the high aspect ratio almost continuous reinforcing morphology with the core region (Figure 6.11a). Further elongation of the composite blend to a Hencky strain of 0.75 led to the breakup of elongated morphology (Figure 6.11b) which is consistent with the loss in modulus for the composite blend. The breakup of the elongated glass phases at the higher imposed strains and glass concentrations was attributed to the applied stress and the interfacial tension between the phases as evidenced by the pinching of the deformed glass into numerous smaller droplets. For the composite reinforced with 60 wt% phosphate glass, the deformed glass phases were found to breakup at lower applied strains which may be partially explained by theory developed for droplet deformation and breakup for Newtonian fluids. Taking the interfacial tension and viscosity ratio between the PPS and P-glass to be constant for both the glass concentrations investigated, theory developed by Taylor [22-24] predicts that the critical elongational stress at which fiber breakup occurs would be inversely proportional to the glass domain size. Therefore, larger domains within the composite reinforced with 60 wt% glass (Figures 6.9b and 6.11a) would have a

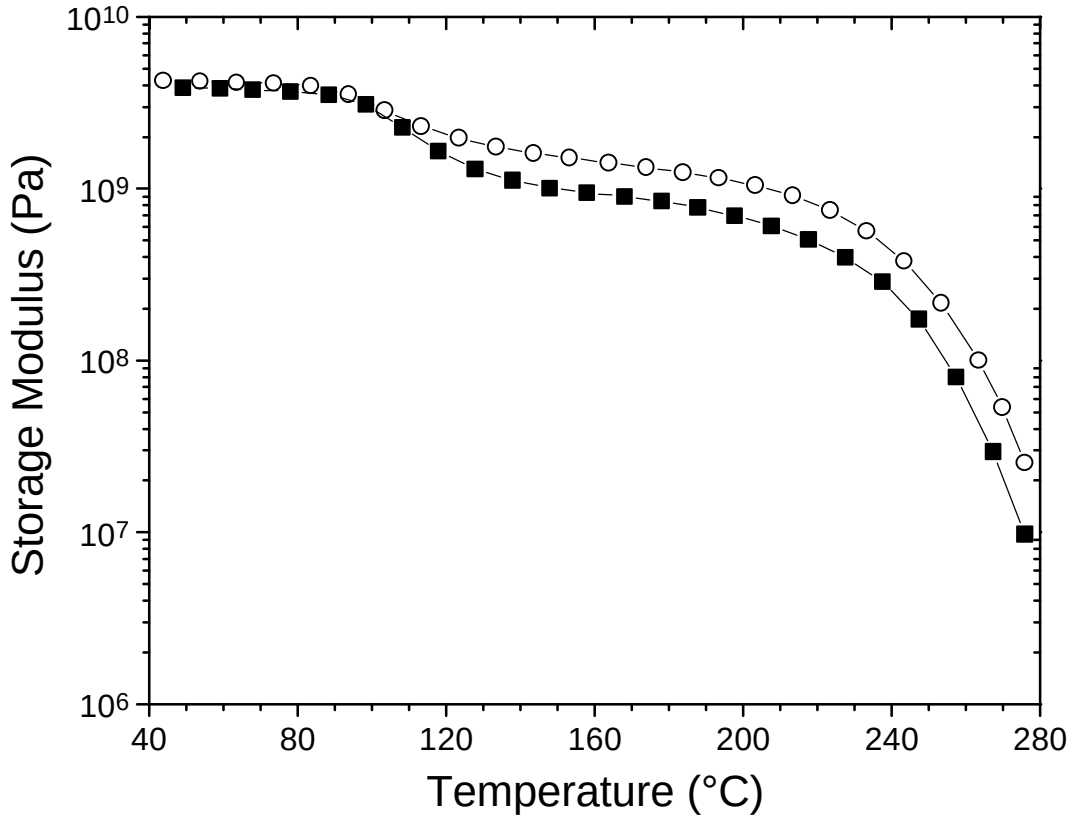

Figure 6.8: Storage Modulus (G′) versus temperature for PPS reinforced with 60 wt% phosphate glass measured at 2.4 ± 0.1°C/min., 10ω, and 0.1% strain. (○) As molded and (■) Compression molded (no applied deformation)

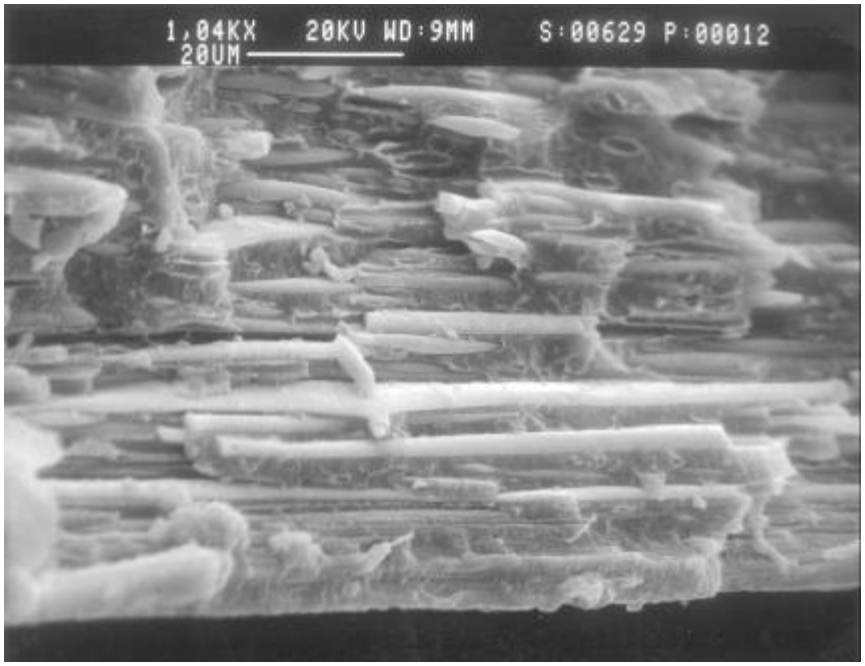

(a)

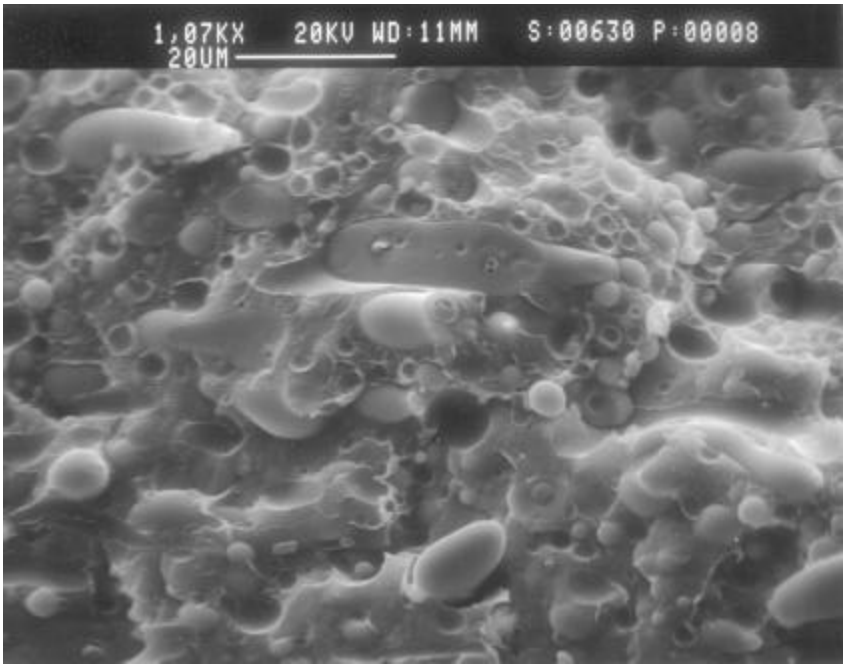

(b)

Figure 6.9: Scanning electron micrographs parallel to the machine direction for polyphenylene sulfide injection molded composites. (a) 40 wt% P-glass, skin region (b) 60 wt% P-glass, core region.

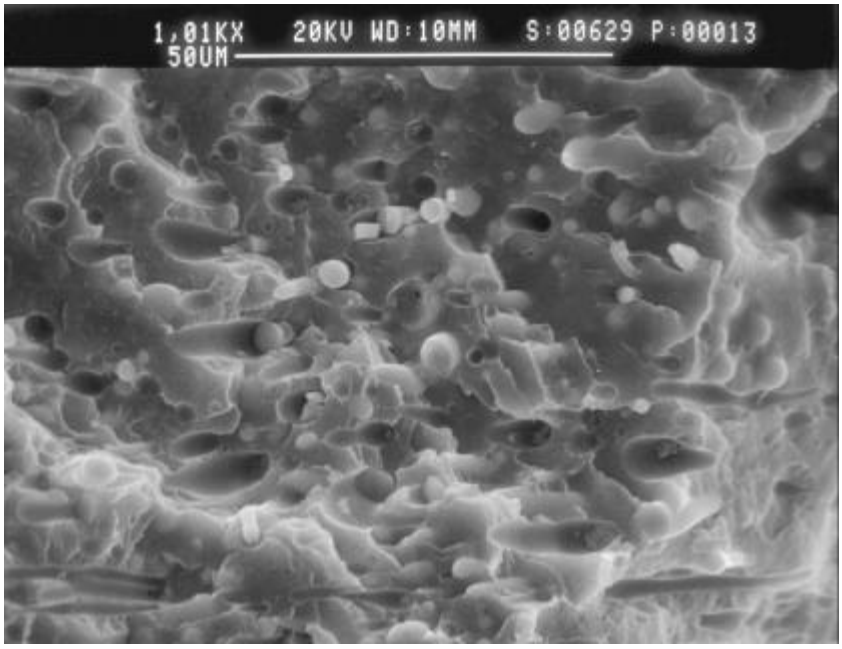

(a)

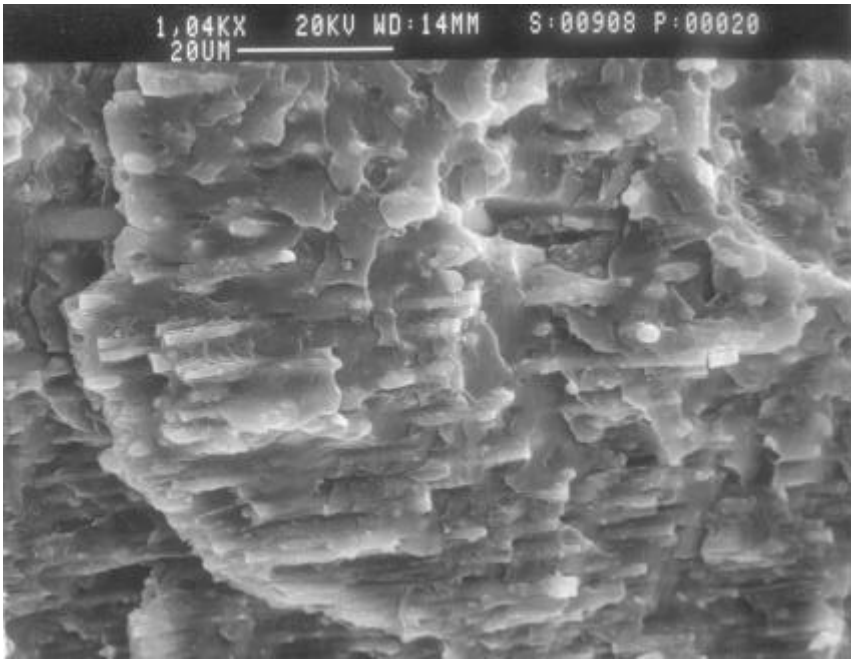

(b)

Figure 6.10: Scanning electron micrographs parallel to the deformation direction for polyphenylene sulfide injection molded composites reinforced with 40 wt% phosphate glass exposed to planar deformation at 282°C. (a) Core region, as molded (b) Core region, $\varepsilon \approx 0.75$.

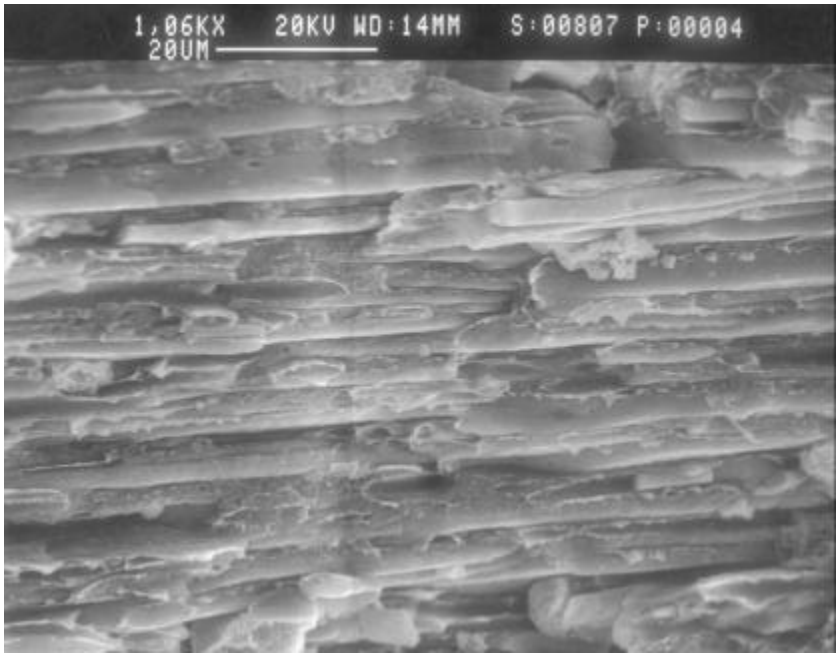

(a)

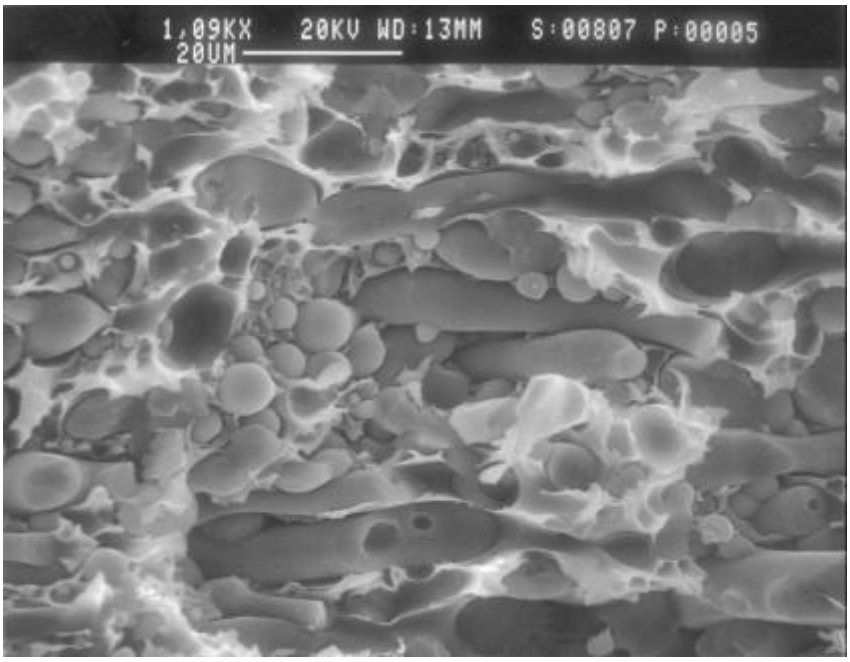

(b)

Figure 6.11: Scanning electron micrographs parallel to the deformation direction for polyphenylene sulfide injection molded composites reinforced with 60 wt% phosphate glass exposed to planar deformation at 283°C. (a) Core region, $\varepsilon \approx 0.5$ (b) Core region, $\varepsilon \approx 0.75$.

tendency to rupture a lower applied stresses which was consistent with the experimental observations.

The planar deformation experiments performed with the polyphenylene sulfide based composites, revealed that temperatures of approximately 283°C served to elongate the glass reinforcing phase within the composites. The effect of higher temperatures (268-283°C) on the mechanical properties of the polyetherimide based composites was also investigated by exposing the blends to a Hencky strain of approximately 0.75 using both uniaxial and planar shearfree deformation. For both the phosphate glass filled blends (30 & 45 wt%), the stretching direction moduli for the deformed materials was generally found to decline with increasing temperature. For example, the utilization of a deformation temperature of 283°C on a composite reinforced with 30 wt% P-glass led to a stretching direction tensile modulus of 4.99 ± 0.12 GPa (uniaxial deformation) and 5.19 ± 0.40 GPa (planar deformation), values less than the 6.09 ± 0.26 GPa found for the undeformed injection molded specimen. A similar trend was seen with the composite containing 45 wt% P-glass where the tensile moduli dropped approximately 10-15% when compared to the as-molded specimens. An examination of the morphology revealed the formation of voids and breakup of the higher aspect ratio reinforcing morphology with the use of the higher deformation temperatures. Changes in both the viscous and interfacial forces within the blend due to the use of the higher temperatures appeared to facilitate the breakup of the elongated regions. The development of interfacial tension-driven instabilities (Rayleigh or capillary instabilities) have been shown to lead to the breakup of highly elongated threads under both flow and quiescent conditions [33-36]. It was believed that the enhanced formation of these interfacial instabilities at the higher temperatures facilitated the breakup of the elongated glass phase during the deformation process. Determination of the exact causes for the breakup of the reinforcing morphology would require further investigation and is beyond the scope of this work.

6.3.4 Thermoforming of Composite Blends

Previous experimentation indicated that the phosphate glass reinforced polyetherimide composites appeared to offer properties conducive to a process such as thermoforming. Tensile testing at elevated temperatures indicated that these materials should offer greater resistance to sheet sag and better extensibility than an E-glass fiber reinforced composite. After exposure to uniaxial and planar deformation similar to what would be seen during forming, the P-glass reinforced composites were also generally found to retain a large degree of their original mechanical properties.

For thermoforming operations, one of the key parameters to obtaining a part of a good quality is the selection of the preheating conditions. The material has to be heated to a point where it is pliable enough to be shaped while supporting its own weight during the heating process. It is also desirable to minimize the temperature gradients across the thickness of the sample which is facilitated by the use of longer pre-heating times coupled

with lower oven temperatures. With this in mind, the preheating times for the composite blanks (injection molded plaques) were held constant at 90 seconds while the radiant infrared oven temperature was varied to find the lowest temperature which would allow adequate deformation of the blend during forming. For the phosphate glass filled blends, a radiant oven operating temperature of 343°C (650°F) was found to lead to the formation of quality parts with minimal sheet sag during preheating. A thermocouple placed within a sample blank indicated temperatures in the range of 270-280°C at the onset of forming which corresponded to the optimum deformation conditions determined from the tensile testing at elevated temperatures. A composite consisting of PEI reinforced 30 wt% short E-glass fiber was also thermoformed under the same conditions to facilitate comparisons between the forming behavior of the phosphate and E-glass filled materials.

Micrographs of thermoformed polyetherimide samples reinforced with phosphate glass and E-glass fibers are presented in Figure 6.12. The high degree of extensibility for the phosphate glass filled blends led to the formation of thermoformed parts that displayed a much better overall appearance than the composite reinforced with E-glass fiber. A direct comparison between composites reinforced with equivalent weight (30%) and volumetric loadings of glass found the phosphate glass filled material to offer a much smoother surface after deformation indicative of what was observed with the uniaxial stretching studies (Figure 6.5). The P-glass reinforced blends were also found to undergo more uniform deformation during shaping due the increased extensibility of the blends which eliminated the problems of uneven material distribution and strain whitening observed within the E-glass filled material.

Although it was not possible to measure the mechanical properties of the small thermoformed articles, it was believed that the phosphate glass filled materials offered an advantage in terms of the retention of properties after forming. For the mold configuration investigated, the material was exposed to maximum linear draw ratio of two which would lead to a Hencky strain of 0.70, a value comparable to those investigated in the deformation studies. For temperatures ranging from 268-283°C, uniaxial and planar deformation applied to approximately 0.75 strain units led to maximum losses in the moduli and strengths of approximately 15% for the phosphate glass reinforced materials. Exposing the E-glass filled material to the equivalent deformation was also detrimental, typically leading to losses in tensile properties (especially strength) on the order of 30%. While the deformation appeared to lead to a slight decline in mechanical properties of the phosphate glass reinforced composites, these materials still displayed tensile moduli ranging from 4-6 GPa (30 wt% P-glass) and 7-10 GPa (45wt% P-glass) which were greater than the 3 GPa found for neat polyetherimide [15]. Hence, it was expected that a similar situation would exist for the thermoformed samples.

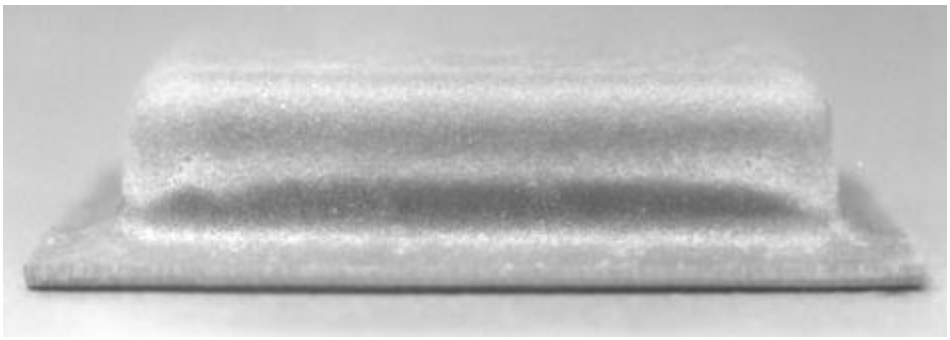

(a)

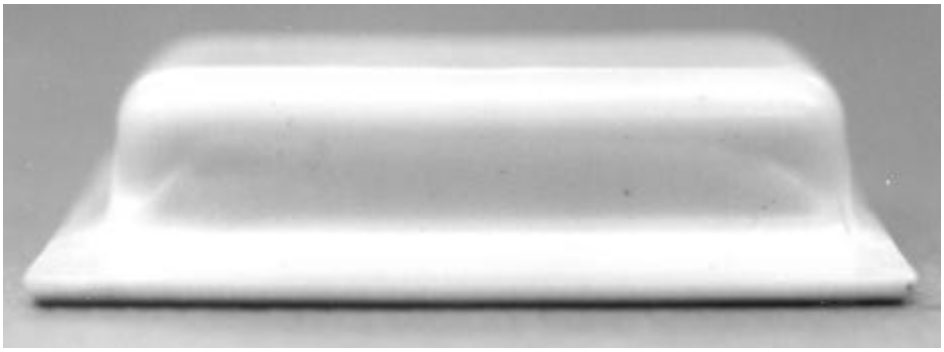

(b)

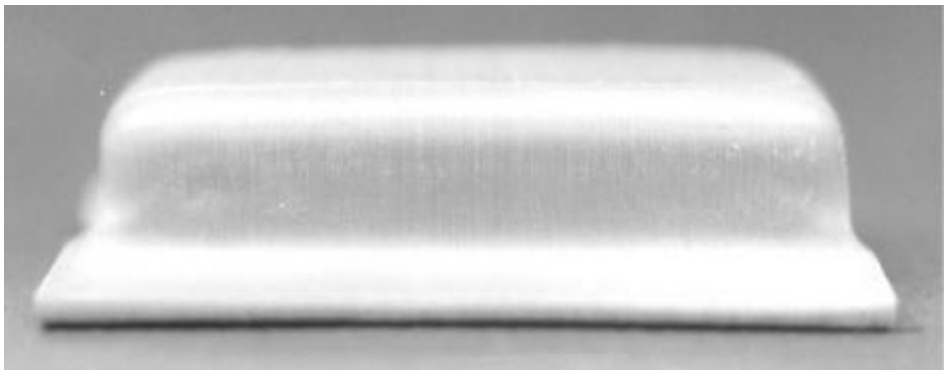

(c)

Figure 6.12: Thermoformed polyetherimide based composites reinforced with various glasses. (a) 30 wt% E-glass, (b) 30 wt% P-glass, (c) 45 wt% P-glass.

6.4 Conclusions

Polyetherimide composites reinforced with a melt processable phosphate glass were found to offer properties more conducive for shaping and forming operations when compared to a material reinforced with E-glass fiber. Tensile testing at elevated temperatures revealed that the phosphate glass reinforced composites were at an advantage in regards to the modulus, toughness, and extensibility of the materials. These improved properties at the elevated temperatures translated into enhanced performance of the phosphate glass filled materials during the process of thermoforming. Small thermoformed trays produced from injection molded phosphate glass filled blends were found to offer smoother surfaces and better material distribution when compared to an article produced with a comparable loading of E-glass fiber.

Polyetherimide composites reinforced with phosphate glass were also found to offer an advantage in regards to the retention of properties after exposure to deformation. From the optimum deformation conditions determined from tensile testing at elevated temperatures, it was possible to deform the phosphate glass filled polyetherimide composite blends to high extents (≈ 110% elongation) using both uniaxial stretching and planar squeezing flows. Deformation applied at a temperature of 268°C was found to have little effect on the mechanical properties of the phosphate glass filled blends while comparable deformation applied to an E-glass fiber reinforced composite often resulted in significant losses (≈ 30%) in the mechanical properties. Deformation applied at higher temperatures (>268°C) led to a slight decline (≈ 15%) in the properties of the phosphate glass filled composites due to the breakup of the elongated glass domains.

The application of planar shearfree deformation was found to enhance the stiffness of injection molded polyphenylene sulfide composites reinforced with a melt processable glass. With the application of planar deformation near the melting point of the PPS (≈ 283°C), it was possible to elongate lower aspect ratio glass domains within the core region of the injection molded specimens. For a composite containing 60 wt% phosphate glass, the generation of the higher aspect ratio glass phase led to a 25% increase in stiffness yielding a composite that had a tensile modulus of approximately 15 GPa. The phosphate glass concentration and applied strain were found to have a large influence on the reinforcing morphology and enhancement in mechanical properties obtained from the applied deformation.

In summary, the use of a melt processable glass as the reinforcing phase in thermoplastic resins was found to offer certain advantages at the temperatures used for processing operations such as compression molding and thermoforming. The ability of the lower T_g phosphate glass reinforcing phase to undergo deformation resulted in composite blends that displayed greater extensibility than a solid E-glass fiber reinforced material. For the materials investigated, it was determined that shearfree deformation applied at

temperatures 30-50°C above the T_g of the phosphate glass can serve to elongate the glass reinforcing phase leading to an enhancement in the mechanical properties of the composite blends.

6.5 Acknowledgments

The authors would like to gratefully recognize the financial support of the NSF Science and Technology Center for High Performance Polymeric Adhesives and Composites at Virginia Tech (Grant No. DMR-8809174 AMD 1) and the Army Research Office (Grant No. DAAH04-94-G-0171). Also, we would like to thank Phillips Chemical Company and GE Plastics for supplying the thermoplastic resins and Corning Inc. for producing the phosphate glass utilized in this study. Appreciation is also extended to Dr. Garth Wilkes for allowing use of the scanning electron microscope.

6.6 References

1 Schweizer and Winterman, *Thermoplastic Polymer Additives: Theory and Practice*, ed. J.T. Lutz Jr., Marcel Dekker, New York 1989.

2 S. Kessler, in *Plastics Additives and Modifiers Handbook* (Chapter 48), ed. J. Edenbaum, Van Nostrand Reinhold, New York 1992.

3 J. Schuster and K. Friedrich, *Appl. Comp. Mat.*, 1, 55 (1994).

4 H.F. Giles and D.L. Reinhard, *Comp. Polym.*, 5(2), 90 (1991).

5 M. Hou, K. Friedrich and R. Sherer, *Comp. Struct.*, 27, 157 (1994).

6 R.K. Okine, D.H. Edison, and N.K. Little, *32nd International SAMPE Symposium*, 1417 (1987).

7 G. Kiss, *Polym. Eng, Sci.*, 27, 410 (1987)

8 N.H. Ray and F.R. Sherliker, U.S. Patent 3,732,191 (1973).

9 W.A. Bahn, G.H. Beall, J. Ference, B.C. Monahan, C.J. Quinn, and P.S. Roussel, U.S. Patent 5,043,369 (1991).

10 C.J. Quinn, P. Frayer, and G.H. Beall, in *Polymeric Materials Encyclopedia* (vol. 4), ed. J.C. Salamone, 2766 (1996).

11 C.J. Quinn and G.H. Beall, in *Chem. Process. Adv. Mater.*, ed L. Hench, 799 (1992).

12 G.H. Beall and C.J. Quinn, U.S. Patent 4,940,677 (1990).

13 G.H. Beall and J.E. Pierson, U.S. Patent 5,328,874 (1994).

14 B.G. Aitken, G.H. Beall, and J.E. Dickenson, Jr., U.S. Patent 5,529,961 (1996).

15 R.T. Young, *PhD Dissertation*, Virginia Polytechnic Institute and State University (1999).

16 W.A. Bahn and C.J. Quinn, *SPE ANTEC Proc*., 2370 (1991).

17 A.I. Isayev and M. Modic, *Polym. Comp*., 8(3), 158 (1987).

18 H.J. O'Donnell and D.G. Baird, *Intl. Polym. Proc*., 11(3), 257 (1996).

19 J.P. de Souza and D.G. Baird, *Polyme*r, 37(10), 1985 (1996).

20 G. Crevecoeur, *PhD Dissertation*, Catholic University of Leuven (1991).

21 F.D. Rumsheidt and S. Mason, *J. Coll. Interf. Sci*., 16, 238 (1961).

22 G.I. Taylor, *Proc. Roy. Soc*., A138, 41 (1932).

23 G.I. Taylor, *Proc. Roy. Soc*., A146, 501 (1934).

24 G.I. Taylor, *Proc. Roy. Soc*., A226, 289 (1954).

25 D.G. Baird, in *Polymeric Materials Encyclopedia* (vol. 5), ed. J.C. Salamone, 3207 (1996).

26 J.P. de Souza, *PhD Dissertation*, Virginia Polytechnic Institute and Statue University, (1994).

27 T. Sun, A. Datta, J.P. de Souza, and D.G. Baird, *SPE ANTEC Proc*., 933 (1991).

28 J.P. de Souza and D.G. Baird, *Polym. Comp*., 17(4), 578 (1996).

29 J. Geibel and J. Leland, in *Encyclopedia of Chemical Technology*, 4 (19), 904 (1996).

30 J.L. Throne, *Thermoforming*, Hanser Publishers, New York, 1987.

31 R.L. Harris and P.F. Bruins, in *Basic Principles of Thermoforming*, ed. P.F. Bruin, 103 (1973).

32 V.E. Malpass and J.T. Kempthorn, *SPE ANTEC Proc*., 63 (1986).

33 H.P. Grace, *Chem. Eng. Commun*., 14, 255 (1982).

34 S. Tomotika, *Proc. Roy. Soc. Lond., A.* 150, 322 (1935).

35 H.A. Stone and G.L. Leal, *J. Fluid Mech*., 198, 399 (1989).

36 J.J. Elmendorp, in *Polymer Processing (Chap. 2)*, ed. C. Raudewendaal, Marcel Dekker, New York 1991.

Chapter 7: Recommendations

7.0 Recommendations

1) Because the PPS based composites showed some success, additional research utilizing PPS as a matrix resin may be desirable. In particular, the properties of the neat PPS could easily be varied by solid state curing the resin to different extents before combining it with the glass. Curing the PPS before processing would serve to elevate the viscosity and lead to changes in the interfacial properties of the resin that may prove beneficial for the production of the phosphate glass filled composites.

2) A process such as coinjection molding may be a viable way to improve the chemical durability of phosphate glass filled composites. A material could be selectively placed at the surface of a molded product in order to create a protective layer for the phosphate glass rich regions. For example, the resin polyetheretherketone could be used to encapsulate a composite blend consisting of polyetherimide and a phosphate glass. The semi-crystalline PEEK would provide excellent protection for the composite blend while also displaying miscibility with the polyetherimide.

3) From the deformation studies, it appeared that extensional flows were effective in elongating the phosphate glass within the composite blends. These composite materials have the potential to be viable in processing applications where elongational flows are predominant such as fiber spinning, blow molding, and vacuum forming. Investigations of these materials in the aforementioned processes would help lead to the establishment of correlations between the flow kinematics and the reinforcing morphology obtained during processing.

4) The higher surface energy of the phosphate glasses as compared to the polymeric materials would typically lead to interfacial tensions greater than those typically seen with polymer-polymer blends. Considering the important role of interfacial tension in the formation of the composite morphology, fundamental investigations examining the interfacial interactions between phosphate glasses and thermoplastic resins in the melt would be useful. Evaluation of the interfacial tension through dynamic methods such as thread breakup, fiber retraction, and dynamic shear measurements should help offer insight into the formation of the reinforcing morphology within phosphate glass filled thermoplastics.

5) The addition of phosphate glasses have been found to result in significant losses in the strength of the composite blends. Improving the interfacial adhesion between the thermoplastic resin and phosphate glass would serve to elevate the strength of the composite blend as well as improve the chemical durability by limiting the degradation of the polymer/glass interface. The development of phosphate glass compositions or possible additives that promote interactions between the polymer and glass would

serve to increase the viability of the phosphate glasses as a reinforcing material for composite applications.

Appendix A:

Phosphate Glass Rheological Data

Table A.1: Complex viscosity (|η*|) versus angular frequency (ω) for a phosphate glass (T_g - 234°C)

	Temperature					
	300°C	**320°C**	**325°C**	**330°C**	**335°C**	**340°C**
Frequency (rad/sec)	**|η*| (Pa·s)**	**|η*| (Pa·s)**	**|η*| (Pa·s)**	**|η*| (Pa·s)**	**|η*| (Pa·s)**	**|η*| (Pa·s)**
0.1	1.2371E6	91338	52227	34632	15245	8743
0.1585	1.2522E6	97698	55495	34970	15957	8606
0.2512	1.2666E6	102020	55610	34783	16341	8506
0.3981	1.2795E6	103610	56154	34681	16479	8509
0.6310	1.2831E6	105050	56669	34388	16600	8588
1	1.2887E6	106290	56656	34308	16510	8661
1.585	1.2866E6	106010	57242	34483	16539	8741
2.512	1.283E6	105420	57237	34033	16704	8700
3.981	1.2759E6	105220	56446	34314	16521	8686
6.310	1.2758E6	104980	56631	34205	16418	8809
10.00	1.2675E6	103910	56597	34211	16472	8778
15.85	1.2607E6	102690	56290	34075	16450	8816
25.12	1.2410E6	99679	55414	33799	16328	8843
39.81	1.2062E6	-	53631	33108	16296	8948
63.10	1.1564E6	-	-	31601	16020	9060
100	1.0888E6	-	-	-	15388	9201

Table A.1: Complex viscosity (|η*|) versus angular frequency (ω) for a phosphate glass (T_g - 234°C) (*Continued*)

	345°C	350°C	360°C	370°C	315°C	
Frequency (rad/sec)	**|η*| (Pa·s)**	**|η*| (Pa·s)**	**|η*| (Pa·s)**	**|η*| (Pa·s)**	**Frequency (rad/sec)**	**|η*| (Pa·s)**
0.1	4918	3512	1599	703	0.05	190850
0.1585	4869	3335	1346	623	0.0792	196980
0.2512	4900	3201	1202	570	0.1256	194480
0.3981	4893	3127	1110	520	0.1991	200450
0.6310	4873	3041	1027	482	0.3155	204780
1	4905	2908	948	446	0.5	204260
1.585	4869	2858	882	420	0.7925	202740
2.512	4611	2883	829	410	1.256	201360
3.981	4872	2750	804	368	1.991	201330
6.310	4843	2730	775	361	3.155	201530
10.00	4930	2705	769	344	5.000	199340
15.85	4825	2703	759	342	7.925	198430
25.12	4845	2686	763	339	-	-
39.81	4833	2674	757	338	-	-
63.10	4799	2658	753	336	-	-
100	4725	2628	749	334	-	-

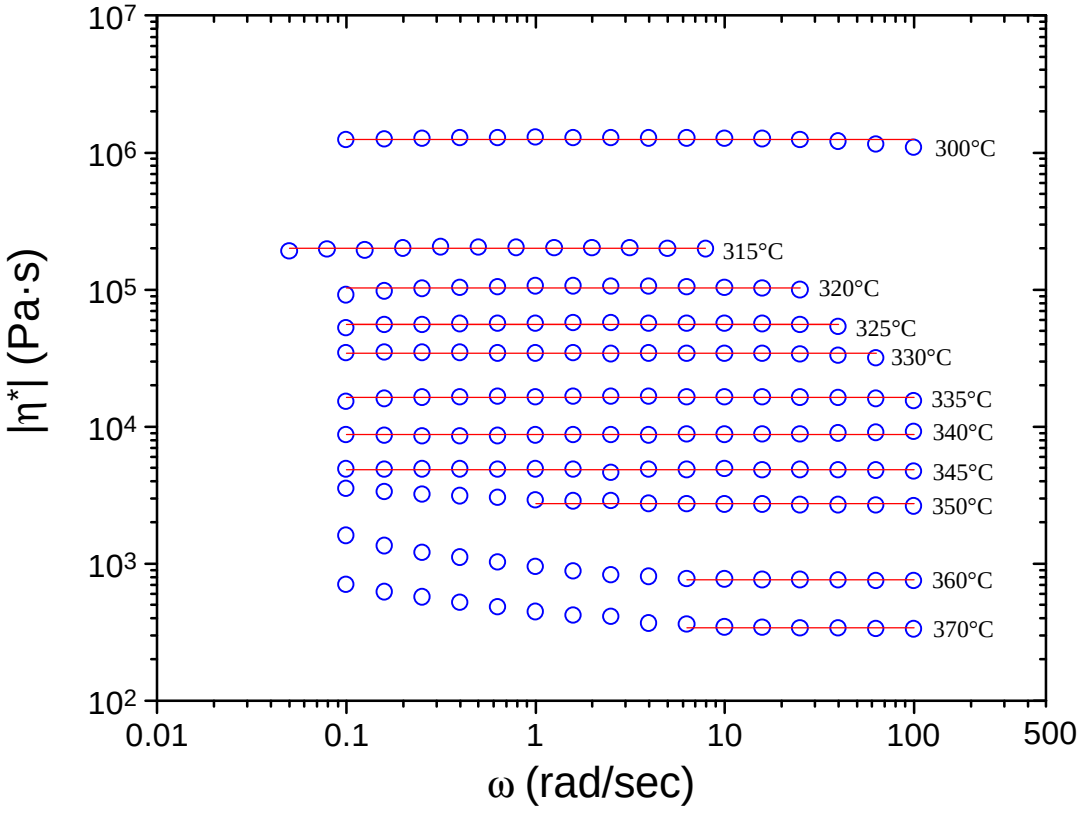

Figure A.1: Complex viscosity (|η*|) versus angular frequency (ω) with Newtonian viscosity fits for a phosphate glass (T_g - 234°C).

Table A.2: Newtonian (Zero shear) viscosity versus temperature for a phosphate glass (T_g - 234°C)

Temperature (°C)	**Newtonian Viscosity (Pa·s)**	**Error (Pa·s)**
300	1.2468E6	13600
315	199710	1167
320	102610	1172
325	55879	374
330	34106	213
335	16267	105
340	8762	47
345	4844	20
350	2744	29
360	761	3.4
370	342	3.3

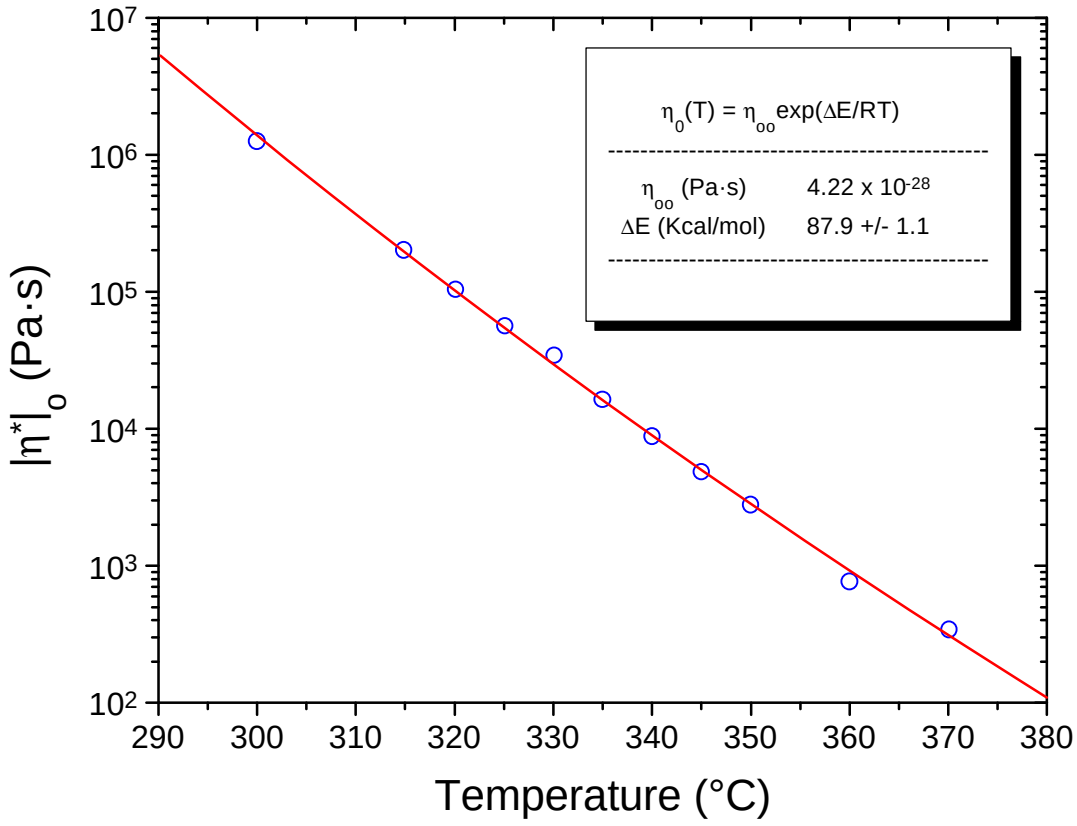

Figure A.2: Zero shear viscosity ($|\eta^*|_0$) versus temperature with an Arrhenius fit for a phosphate glass (T_g - 234°C).

Table A.3: Complex viscosity ($|\eta^*|$) at 1 radian/second versus temperature for a phosphate glass (T_g - 234°C)

Starting Temperature = 350°C Cooling Rate 2.4 ± 0.1 °C/min		**Starting Temperature = 370°C Cooling Rate 2.4 ± 0.1 °C/min**	
Temperature (°C)	**$\|\eta^*\|$ (Pa·s)**	**Temperature (°C)**	**$\|\eta^*\|$ (Pa·s)**
350.4	3052	370.4	818
347.2	4324	366.7	1060
344.2	6185	363.7	1370
340.8	9530	360.6	1759
337.3	15311	357.1	2337
333.7	24919	353.6	3119
330.1	41664	350.0	4164
326.5	66382	346.5	5671
322.9	108870	342.9	7755
320.0	156500	339.3	10768
317.1	242920	335.6	15296
313.4	411260	332.1	22171
310.3	630580	328.4	32948
306.5	1.0762E6	324.8	49096
303.6	1.6166E6	321.1	75609
300.1	2.6418E6	317.3	118750
296.4	4.4032E6	313.8	187570
292.7	7.5694E6	310.0	301010
289.1	1.3249E7	306.0	505610
285.5	2.1694E7	302.9	756600
281.9	3.7078E7	299.3	1.2487E6
278.3	6.4421E7	295.9	2.0003E6
274.7	1.1333E8	292.2	3.4156E6
271.0	1.9670E8	288.5	6.1415E6
		284.9	1.0667E7
		281.4	1.9025E7
		277.6	3.5518E7
		274.2	6.4371E7
		270.6	1.2483E8

Table A.4: Complex viscosity ($|\eta^*|$) at 1 radian/second versus time for a phosphate glass (T_g - 234°C)

time (seconds)	330°C	350°C	370°C
6	33114	2853	531
96	32779	2617	505
186	32449	2644	492
276	32246	2709	460
366	33297	2731	415
456	34192	2732	370
546	34994	2708	332
636	35452	2647	318
726	35778	2595	299
816	36348	2552	298
906	37296	2517	287
996	37383	2458	280
1086	37872	2409	280
1176	38141	2360	282
1266	38707	2320	280
1356	39427	2285	283
1446	40242	2229	285
1536	40838	2175	278
1626	41377	2116	276
1716	42152	2067	290
1806	43032	2067	295

Table A.5: Complex viscosity ($|\eta^*|$) versus angular frequency (ω) for a phosphate glass (T_g - 282°C)

	Temperature			
	340°C	**350°C**	**360°C**	**370°C**
Frequency (rad/sec)	$\|\eta^*\|$ **(Pa·s)**	$\|\eta^*\|$ **(Pa·s)**	$\|\eta^*\|$ **(Pa·s)**	$\|\eta^*\|$ **(Pa·s)**
0.1	2.4454E6	766350	270890	109000
0.1585	2.4400E6	759610	274970	110250
0.2512	2.4849E6	759700	275690	108590
0.3981	2.4467E6	752180	274990	107370
0.6310	2.4338E6	756240	278750	107070
1	2.4256E6	756050	275560	106080
1.585	2.4036E6	748060	274210	105620
2.512	2.3888E6	747050	273850	105330
3.981	2.3743E6	743480	275250	103780
6.310	2.3119E6	739290	272080	102590
10.00	2.2413E6	729850	268150	103270
15.85	2.2110E6	726020	270280	103110
25.12	2.1695E6	722590	268100	101940
39.81	2.1153E6	716030	267210	101890
63.10	1.9980E6	704170	264030	101380
100	-	685040	260970	100570

Table A.5: Complex viscosity ($|\eta^*|$) versus angular frequency (ω) for a phosphate glass (T_g - 282°C) (*Continued*)

	Temperature			
	380°C	**390°C**	**400°C**	**410°C**
Frequency (rad/sec)	**$\|\eta^*\|$ (Pa·s)**	**$\|\eta^*\|$ (Pa·s)**	**$\|\eta^*\|$ (Pa·s)**	**$\|\eta^*\|$ (Pa·s)**
0.1	54137	21474	9552	4378
0.1585	53293	21413	9652	4370
0.2512	53429	21435	9675	4390
0.3981	52907	21623	9701	4388
0.6310	52420	21599	9639	4422
1	51423	21500	9534	4391
1.585	50578	21474	9422	4409
2.512	56571	21313	9482	4409
3.981	51224	21241	9269	4314
6.310	49508	21171	9162	4261
10.00	47383	21146	9048	4230
15.85	47546	21020	8950	4174
25.12	46417	20820	8842	4148
39.81	46821	20516	8745	4101
63.10	46326	19800	8564	4055
100	45742	18397	8310	3976

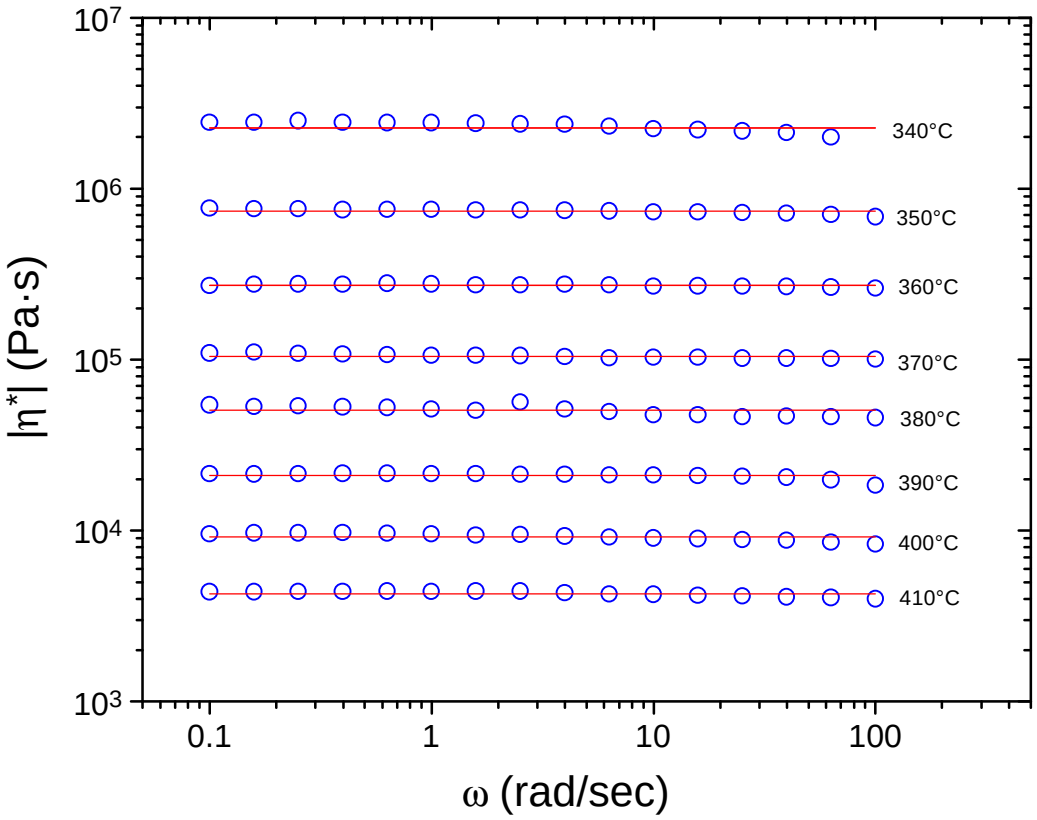

Figure A.3: Complex viscosity (|η*|) versus angular frequency (ω) with Newtonian viscosity fits for a phosphate glass (T_g - 282°C).

Table A.6: Newtonian (Zero shear) viscosity versus temperature for a phosphate glass (T_g - 282°C)

Temperature (°C)	**Newtonian Viscosity (Pa·s)**	**Error (Pa·s)**
340	2.2724E6	64130
350	738230	5662
360	271560	1204
370	104870	745
380	50358	833
390	20996	209
400	9222	109
410	4276	36

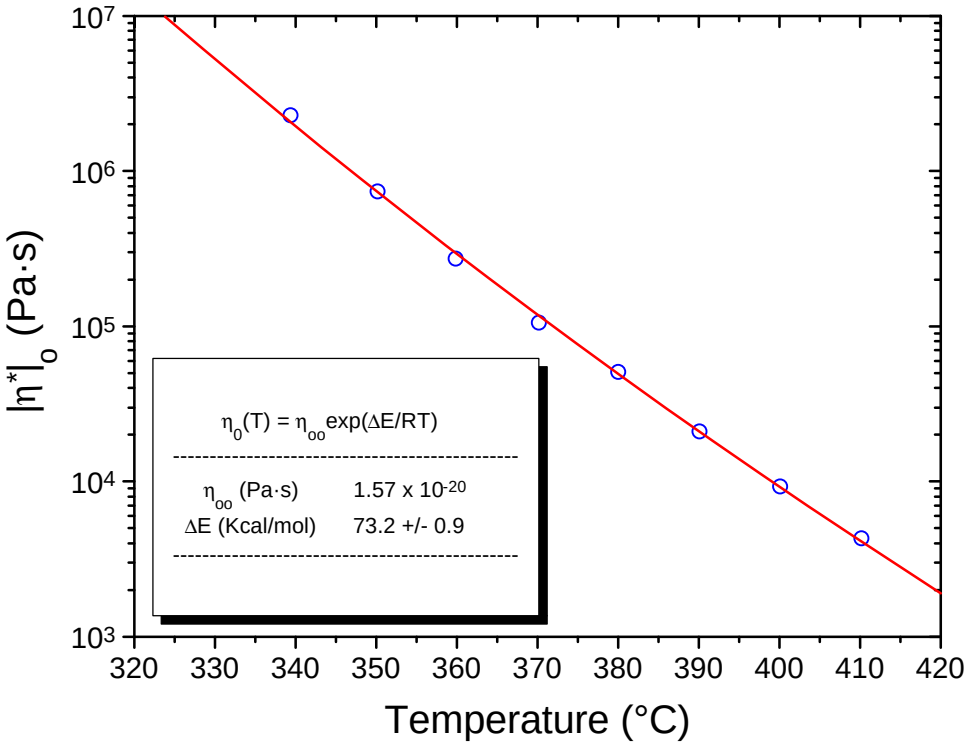

Figure A.4: Zero shear viscosity ($|\eta^*|_0$) versus temperature with an Arrhenius fit for a phosphate glass (T_g - 282°C).

Table A.7: Complex viscosity (|η*|) at 1 radian/second versus temperature for a phosphate glass (T_g - 282°C)

Starting Temperature = 410°C Cooling Rate 2.4 ± 0.1 °C/min	
Temperature (°C)	**|η*| (Pa·s)**
410.5	5005
406.0	7426
402.6	10141
397.5	16363
393.6	25210
389.4	34591
385.1	52208
381.2	74531
377.5	102870
373.8	142750
370.1	187560
366.0	258790
362.6	359040
359.2	481670
355.7	682530
352.0	967880
348.3	1.3975E6
344.9	2.0408E6
341.1	3.0304E6
337.3	4.5990E6
333.8	6.8147E6
330.2	1.0401E7
326.5	1.6799E7
322.7	2.6641E7
319.0	4.5265E7
315.2	7.9859E7
311.8	1.3709E8
308.4	2.3647E8

Table A.8: Complex viscosity ($|\eta^*|$) at 1 radian/second versus time for a phosphate glass (T_g - 282°C)

time (seconds)	390°C	410°C
6	16675	3171
96	16233	3568
186	16448	4046
276	16310	4247
366	16384	4565
456	16592	4855
546	16746	5167
636	17139	5372
726	17527	5629
816	17892	5755
906	18241	5917
996	18372	6223
1086	18584	6352
1176	18772	6398
1266	18998	6564
1356	19185	6765
1446	19369	6993
1536	19544	7249
1626	19687	7428
1716	19834	7735
1806	20146	7862

Appendix B:

Durability of Glass Reinforced Composites

Because phosphate glasses are known to show a loss in both weight and mechanical properties when exposed to aqueous environments, the phosphate glass reinforced composites were exposed to hot water (>50°C) to determine the effects on the properties of the materials. The composite blends were aged in hot water for a period of 24 hours after which the samples were dried in a vacuum oven for a period of 24 hours before undergoing tensile testing.

The effects of exposing the polyphenylene sulfide composites to hot water for a period of 24 hrs is presented in Table B.1. For composites containing both a low and high loading of the lower T_g P-glass, exposure to boiling water resulted in the modulus falling to values comparable to that of the neat PPS. After exposure to the boiling water, the tensile strength of the blends was also found to decline while the elongation break increased significantly. The large changes in the strength and elongation to break were partially attributed to a loss of adhesion between the polymer/glass phases due to a degradation of the interface. In an effort to enhance the durability of the composite blends, the materials were placed in a forced convection oven at operating at 230°C for a period of 24 hours in order to facilitate the crystallization and solid state curing of the PPS. Samples exposed to the conditioning step were found to retain a higher degree of stiffness after exposure to boiling water due to the added protection gained from the curing and crystallization of the PPS. Composite blends exposed to lower water temperatures (50°C) showed much improved durability which was attributed to the lower dissolution rates of the glass at this temperature. It was also believed that the limited mobility of the PPS at 50°C ($T_g \approx 90$°C) may have helped limit the ability of the water to attack the phosphate glass interface.

Similar boiling experiments were performed with the composites consisting of polyetherimide and polyetheretherketone reinforced with the low T_g glass and PEEK reinforced with the higher T_g glass (Table B.2). For the composites reinforced with the lower T_g glass, trends similar to those found with the PPS were observed. The composite blends suffered from both a loss in modulus and strength that became more pronounced at the higher glass loadings. For the PEI based composite, the interpenetrating network structure at the higher glass loadings failed at the PEI/glass interface which resulted in delamination of the composite blend. In the case of the PEEK composites, the blend reinforced with the higher T_g glass retained a larger percentage of the original properties but still displayed almost a 50% loss in properties after boiling. The increased durability of the higher transition phosphate glass possibly coupled with the size and shape of the reinforcing morphologies were believed to lead to the higher retention of properties.

The large change in the properties of the composites were thought to be due to a number of causes. Water is known to attack phosphate glasses through two mechanisms consisting of hydrolysis of the phosphate groups and hydration of the modifier cations which would serve to disrupt the ionic bonds between the chains. This hydrolysis combined with a loss of the modifier cations would serve to disrupt the glass network

Table B.1: Accelerated Aging of Polyphenylene Sulfide Composites Reinforced with P-glass (T_g - 234°C) and E-glass.

			Machine Direction		
Post Processing Conditioning	**Aging**	**Loading wt% (vol%)**	**Tensile Modulus (GPa)**	**Tensile Strength (MPa)**	**% Elong.**
None	**As Molded**	20 (12)	4.65 (0.28)	61.5 (3.1)	1.42 (0.14)
None	**Boiled (24 hrs)**	20 (12)	3.07 (0.12)	50.8 (3.6)	1.99 (0.24)
Cured 230°C (24 hrs)	**Boiled (24 hrs)**	20 (12)	3.72 (0.35)	50.3 (2.1)	1.59 (0.18)
Cured 230°C (24 hrs)	**50°C (24 hrs)**	20 (12)	4.75 (0.18)	59.1 (4.6)	1.34 (0.14)
None	**As Molded**	60 (44)	12.44 (0.57)	47.1 (6.0)	0.38 (0.06)
None	**Boiled (24 hrs)**	60 (44)	3.84 (0.27)	27.6 (3.8)	1.04 (0.20)
Vacuum 230°C (24 hrs)	**Boiled (24 hrs)**	60 (44)	4.91 (0.60)	31.7 (3.2)	0.82 (0.11)
Cured 230°C (24 hrs)	**Boiled (24 hrs)**	60 (44)	5.65 (0.45)	28.2 (2.5)	0.57 (0.08)
Cured 230°C (24 hrs)	**50°C (24 hrs)**	60 (44)	9.21 (1.35)	40.3 (5.0)	0.47 (0.05)
None (E-glass)	**As Molded**	40 (26)	13.2 (0.91)	140.5 (5.3)	1.30 (0.05
None (E-glass)	**Boiled (24 hrs)**	40 (26)	12.3 (0.81)	138.9 (7.2)	1.37 (0.04)

Note: Prior to testing after aging, samples dried 24 hrs at 100°C under vacuum
Standard deviations given in parentheses

Table B.2: Accelerated Aging of Polyetherimide and Polyetheretherketone Composites Reinforced with Phosphate glasses

			Machine Direction		
Resin/Glass Combination	**Aging**	**Loading wt% (vol%)**	**Tensile Modulus (GPa)**	**Tensile Strength (MPa)**	**% Elong.**
PEI/P-glass (T_g - 234°C)	**As Molded**	30 (17)	6.49 (0.20)	90.5 (3.8)	1.89 (0.23
	Boiled (24 hrs)	30 (17)	3.74 (0.26)	62.3 (2.7)	4.03 (0.27)
	As molded	60 (42)	13.84 (1.29)	53.8 (4.8)	0.46 (0.04)
	Boiled (24 hrs)	60 (42)	Unable to test (Delamination)		
PEEK/P-glass (T_g - 234°C)	**As Molded**	60 (43)	12.10 (0.63)	63.8 (3.6)	0.55 (0.03)
	Boiled (24 hrs)	60 (43)	3.89 (0.48)	35.1 (1.4)	2.16 (0.36)
PEEK/P-glass (T_g - 282°C)	**As Molded**	66 (42)	11.21 (0.40)	52.8 (5.0)	0.50 (0.06)
	Boiled (24 hrs)	66 (42)	6.16 (0.31)	32.3 (2.6)	0.53 (0.08)

Note: Prior to testing after aging, samples dried 24 hrs at 100°C under vacuum
Standard deviations given in parentheses

structure thereby lowering the mechanical properties of the glass. An examination of thermal transitions before and after boiling, as determined by dynamic mechanical thermal analysis, indicated a large shift in the transition temperature for the lower T_g phosphate glass (Figure B.1). This lends support to the idea that the water was able to breakdown the structure of the phosphate glass thus leading to the lower glass transition temperature.

For the composite reinforced with the higher T_g phosphate glass, it was difficult to establish if any changes in the transitions for the glass had occurred. The drop in the composite mechanical properties was also attributed to a loss of adhesion between the polymer and glass due the presence of the water. The weak interfacial adhesion between the polymers and phosphate glasses allowed water to penetrate the interface and disrupt the bonding between the components which would lead to a lower strength for the composite blend.

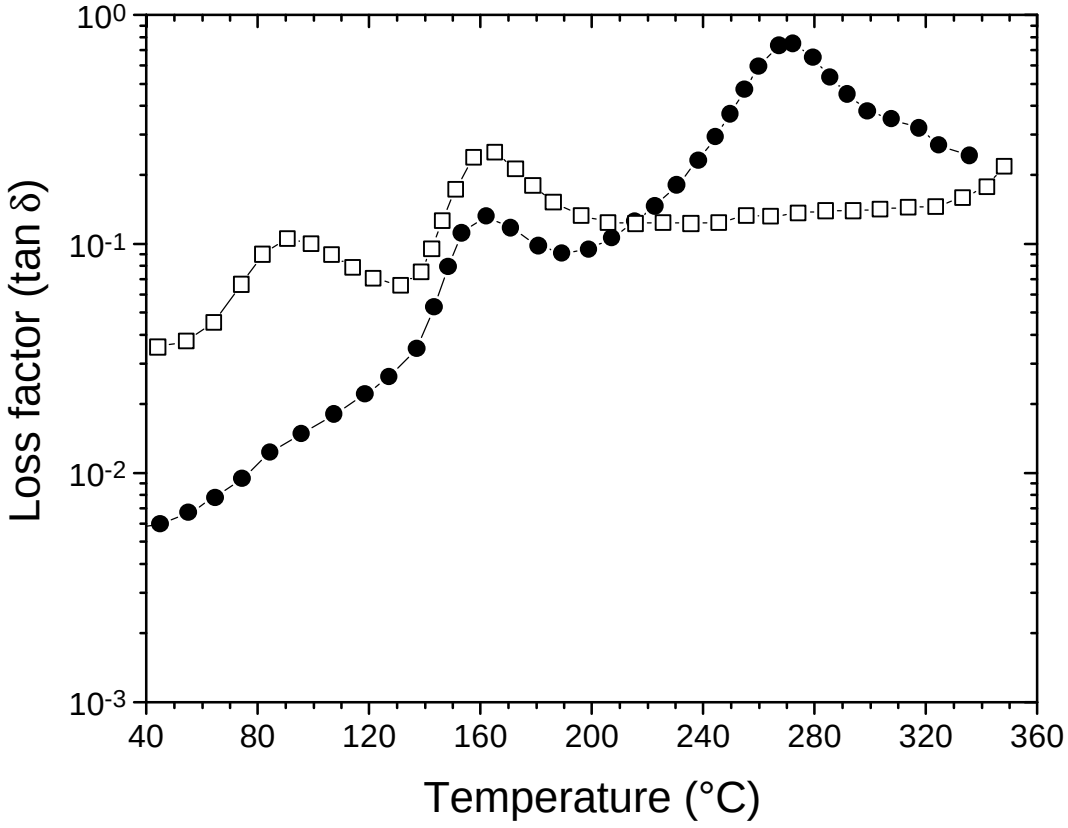

Figure B.1: Loss factor (tan δ) versus temperature for PEEK reinforced with 60 wt% P-glass (T_g - 234°C). (●) As molded (□) Boiled 24 hrs

Appendix C:

Effect of Processing Conditions on Mechanical Properties of PEI Reinforced with a P-glass

Table C.1: Effect of Injection rate on mechanical properties of PEI reinforced with 30 wt% phosphate glass (T_g -234°C) processed at 370°C

Machine Direction					
Injection Rate (cm^3/sec)	**Tensile Properties**			**Flexural Properties**	
	Modulus (GPa)	**Strength (MPa)**	**% Elong.**	**Modulus (GPa)**	**Strength (MPa)**
6	6.64 (0.20)	90.6 (2.8)	2.03 (0.35)	8.03 (0.18)	184.2 (6.2)
9	6.49 (0.27)	90.4 (3.8)	1.89 (0.23)	7.81 (0.10)	179.3 (3.9)
17	6.01 (0.17)	87.6 (4.1)	1.91 (0.24)	7.88 (0.10)	179.0 (4.2)
30	6.12 (0.29)	86.6 (4.0)	1.91 (0.31)	7.62 (0.15)	174.9 (5.5)
Transverse Direction					
Injection Rate (cm^3/sec)	**Tensile Properties**			**Flexural Properties**	
	Modulus (GPa)	**Strength (MPa)**	**% Elong.**	**Modulus (GPa)**	**Strength (MPa)**
6	4.80 (0.22)	65.4 (1.8)	1.84 (0.06)	5.66 (0.13)	125.3 (5.7)
9	5.00 (0.09)	68.3 (3.8)	1.82 (0.26)	5.43 (0.17)	119.7 (7.7)
17	4.75 (0.27)	67.1 (4.8)	1.79 (0.36)	5.75 (0.16)	125.3 (5.1)
30	4.93 (0.22)	69.6 (3.3)	1.75 (0.17)	5.88 (0.32)	128.8 (1.7)

Note: % Elong. = Elongation to break; Standard deviations given in parentheses

Table C.2: Effect of Injection Rate on mechanical properties of PEI reinforced with 60 wt% phosphate glass (T_g -234°C) processed at 370°C

Machine Direction					
Injection Rate (cm^3/sec)	**Tensile Properties**			**Flexural Properties**	
	Modulus (GPa)	**Strength (MPa)**	**% Elong.**	**Modulus (GPa)**	**Strength (MPa)**
6	12.86 (0.26)	53.8 (4.8)	0.46 (0.04)	15.39 (0.42)	128.7 (3.4)
9	13.84 (1.29)	44.8 (4.4)	0.37 (0.08)	15.51 (0.66)	122.6 (5.7)
17	13.89 (0.47)	48.0 (3.4)	0.38 (0.03)	16.34 (0.36)	119.6 (3.9)
30	13.12 (0.37)	43.8 (3.8)	0.37 (0.04)	15.56 (0.54)	113.8 (3.1)
Transverse Direction					
Injection Rate (cm^3/sec)	**Tensile Properties**			**Flexural Properties**	
	Modulus (GPa)	**Strength (MPa)**	**% Elong.**	**Modulus (GPa)**	**Strength (MPa)**
6	11.25 (0.81)	33.3 (3.6)	0.31 (0.02)	12.01 (0.54)	72.4 (3.5)
9	10.89 (0.71)	26.7 (5.4)	0.27 (0.05)	12.13 (0.72)	79.8 (7.1)
17	11.11 (0.75)	27.1 (4.1)	0.28 (0.03)	12.92 (0.77)	82.9 (7.2)
30	12.44 (0.64)	23.7 (1.8)	0.21 (0.04)	13.02 (0.17)	88.5 (2.0)

Note: % Elong. = Elongation to break; Standard deviations given in parentheses

Appendix D:

Tensile Properties for Composite Blends at Elevated Temperatures

Table D.1: Tensile Properties for Polyetherimide Composites reinforced with P-glass (T_g - 234°C) and E-glass evaluated at 250 mm/min (Initial strain rate of 0.10 sec^{-1})

	Testing Temp. (°C)	Tensile Modulus (MPa)	Tensile Strength (MPa)	Tensile Toughness (MPa)	% Elong. to yield	% Elong. to break
Neat PEI	253	3.75 (0.49)	0.54 (0.06)	0.782 (0.054)	49.3 (3.4)	261 (38)
	263	2.44 (0.17)	0.22 (0.04)	0.242 (0.079)	36.7 (2.9)	235 (52)
	273	1.68 (0.19)	0.11 (0.01)	0.131 (0.025)	26.2 (2.6)	277 (29)
30 wt% E-glass	253	47.34 (1.33)	2.22 (0.07)	0.557 (0.025)	12.5 (0.3)	34.6 (3.7)
	263	32.81 (1.51)	1.44 (0.05)	0.441 (0.012)	12.2 (0.3)	41.1 (2.7)
	273	19.67 (0.94)	0.85 (0.04)	0.389 (0.025)	12.8 (0.6)	69.2 (7.0)
	283	13.37 (1.05)	0.51 (0.01)	0.310 (0.020)	11.3 (0.4)	114.3 (10.1)
30 wt% P-glass	253	154.6 (9.5)	3.02 (0.15)	0.422 (0.015)	5.0 (0.1)	21.6 (3.5)
	263	79.75 (6.89)	2.08 (0.18)	0.508 (0.032)	7.7 (0.2)	36.0 (3.8)
	268	49.96 (1.44)	1.38 (0.10)	1.184 (0.116)	10.0 (0.4)	> 400
	273	30.93 (2.65)	0.71 (0.05)	0.552 (0.042)	8.0 (0.3)	> 400
	283	11.08 (1.02)	0.25 (0.02)	0.167 (0.021)	7.6 (0.1)	> 400
45 wt% P-glass	253	335.8 (27.3)	6.82 (0.49)	0.161 (0.056)	2.9 (0.3)	4.7 (0.7)
	263	169.2 (12.6)	4.62 (0.35)	1.067 (0.165)	7.7 (0.5)	29.6 (5.1)
	268	113.5 (14.6)	3.00 (0.30)	2.045 (0.170)	6.8 (0.2)	> 400
	273	63.1 (9.5)	1.44 (0.12)	0.966 (0.098)	6.0 (0.6)	> 400
	283	25.2 (1.9)	0.57 (0.03)	0.413 (0.030)	5.7 (0.7)	> 400

Table D.2: Tensile Properties for Polyphenylene Sulfide Composites reinforced with P-glass (T_g - 234°C) and E-glass evaluated at 250 mm/min (Initial strain rate of 0.10 sec^{-1})

	Testing Temp. (°C)	Tensile Modulus (MPa)	Tensile Strength (MPa)	Tensile Toughness (MPa)	% Elong. to yield	% Elong. to break
40 wt% E-glass	273	342 (49)	6.15 (0.72)	0.108 (0.011)	2.9 (0.2)	5.3 (0.4)
	278	257 (37)	5.02 (0.25)	0.101 (0.011)	3.0 (0.2)	5.6 (1.3)
	283	184 (19)	3.65 (0.16)	0.091 (0.010)	3.0 (0.3)	5.9 (0.9)
	288	87 (10)	1.96 (0.13)	0.082 (0.006)	3.5 (0.3)	8.7 (2.3)
	293	6.3 (0.9)	0.24 (0.04)	0.061 (0.002)	7.0 (0.8)	33.5 (5.1)
40 wt% P-glass	273	127 (13)	3.45 (0.12)	0.233 (0.080)	7.8 (0.8)	12.0 (2.8)
	278	65.0 (9.0)	2.15 (0.07)	0.305 (0.031)	10.7 (1.0)	20.0 (1.4)
	283	25.8 (1.7)	1.08 (0.07)	0.230 (0.032)	12.3 (0.5)	28.3 (3.7)
	288	8.8 (0.8)	0.32 (0.02)	0.125 (0.005)	11.8 (1.4)	56.4 (8.2)
	293	3.0 (0.3)	0.06 (0.01)	0.019 (0.006)	4.94 (0.8)	- -

Appendix E:

Rheological Properties of Neat Thermoplastics and Composite Blends

Table E.1: Complex viscosity (|η*|) versus angular frequency (ω) for various grades of neat PPS

	Ryton PR09		Fortron 0320	
	330°C	**350°C**	**330°C**	**350°C**
Frequency (rad/sec)	**|η*| (Pa·s)**	**|η*| (Pa·s)**	**|η*| (Pa·s)**	**|η*| (Pa·s)**
0.1	695	449	350	255
0.1585	677	427	351	247
0.2512	662	404	350	239
0.3981	648	387	349	234
0.6310	637	375	348	230
1	627	367	347	228
1.585	614	361	346	226
2.512	600	353	348	224
3.981	575	344	344	224
6.310	544	331	345	223
10.00	509	315	342	224
15.85	469	294	340	222
25.12	426	272	336	220
39.81	381	247	329	216
63.10	335	221	320	213
100	291	194	305	205

Note - Tests performed on unprocessed pellets

Table E.2: Complex viscosity (|η*|) versus angular frequency (ω) for a various grades neat of PEEK and PEI

	PEEK Victrex 150G		**PEEK Victrex 450G**		**PEI Ultem 1000**
	370°C	**410°C**	**370°C**	**410°C**	**370°C**
Frequency (rad/sec)	**|η*| (Pa·s)**	**|η*| (Pa·s)**	**|η*| (Pa·s)**	**|η*| (Pa·s)**	**|η*| (Pa·s)**
0.1	467	258	7540	4164	1664
0.1585	462	257	6993	4092	1605
0.2512	454	252	6469	3969	1553
0.3981	445	251	5963	3813	1527
0.6310	438	249	5457	3616	1507
1	431	247	4942	3409	1497
1.585	425	247	4434	3125	1489
2.512	421	247	3937	2828	1480
3.981	412	243	3452	2534	1451
6.310	403	241	2993	2244	1417
10.00	390	236	2565	1943	1378
15.85	374	229	2171	1672	1323
25.12	355	220	1819	1421	1257
39.81	333	209	1509	1189	1176
63.10	308	195	1239	983	1083
100	280	180	1008	806	981

Note - Tests performed on unprocessed pellets

Table E.3: Complex viscosity (|η*|) at 1 radian/second versus temperature for various grades of neat PPS, cooling from 350°C

Cooling Rate of 2.4 ± 0.1 °C/min.							
Ryton PR09				Fortron 0320			
Temp. (°C)	|η*| (Pa·s)	Temp. (°C)	|η*| (Pa·s)	Temp. (°C)	|η*| (Pa·s)	Temp. (°C)	|η*| (Pa·s)
350.1	319	252.6	2183	350.1	217	254.2	1083
346.0	322	249.4	2355	346.0	211	250.9	1177
343.0	330	246.1	2565	343.1	213	247.7	1267
339.8	345	242.8	2831	340.1	217	244.4	1397
336.6	361	239.6	3214	337.0	223	241.2	1567
333.4	379	237.2	3804	333.8	231	237.9	1953
330.2	402	234.7	5711	330.7	240	236.2	2692
326.8	426	234.0	7800	327.5	251	235.5	4006
323.7	454	233.1	14991	324.4	263	234.7	15427
320.5	484	232.3	140380	321.2	278	233.9	326400
317.2	512	231.2	691400	318.0	293	232.6	1.84E6
313.9	550	230.4	2.35E6	314.8	308		
310.8	587			311.7	326		
307.4	628			308.5	345		
304.3	674			305.4	366		
301.1	726			302.1	388		
297.9	778			298.9	411		
294.7	832			295.7	439		
291.5	888			292.6	467		
288.3	958			289.5	500		
285.1	1028			286.3	533		
281.9	1102			283.0	567		
278.6	1185			279.9	606		
275.3	1280			276.7	646		
272.2	1378			273.6	692		
269.0	1493			270.4	747		
265.7	1590			267.1	801		
262.3	1729			263.9	860		
259.1	1865			260.7	928		
255.9	2018			257.4	999		

Note - Tests performed on unprocessed pellets

Table E.4: Complex viscosity (|η*|) at 1 radian/second versus temperature for various neat thermoplastics, cooling from 370°C

Cooling Rate of 2.4 ± 0.1 °C/min.					
PEEK Victrex 150		**PEEK Victrex 450G**		**PEI Ultem 1000**	
Temp. (°C)	**|η*| (Pa·s)**	**Temp. (°C)**	**|η*| (Pa·s)**	**Temp. (°C)**	**|η*| (Pa·s)**
369.9	441	369.5	5783	370.1	1476
364.1	472	364.7	6221	365.3	1632
360.4	502	361.2	6480	362.0	1771
356.8	532	357.6	6846	358.7	1942
353.2	566	354.1	7176	355.3	2173
349.5	603	350.5	7538	351.8	2443
345.8	645	346.8	8019	348.3	2800
342.1	700	343.3	8436	344.6	3247
338.4	810	340.7	8746	341.1	3773
336.1	970	337.2	9309	337.5	4429
333.6	1617	333.6	10238	333.9	5222
332.4	3044	328.6	14101	330.3	6272
331.0	7302	326.2	23531	326.5	7600
329.9	34871	324.8	40111	323.1	9175
328.7	156240	323.6	88042	319.5	11252
327.5	799700	322.5	281280	316.0	13902
		321.3	734940	312.4	17314
				308.8	21732
				305.2	27712
				301.5	35706
				298.0	45757
				294.5	59631
				290.8	78719
				287.3	103380
				283.7	136890
				280.2	181690
				276.6	240060
				273.0	319720
				269.5	423630
				265.8	547950
				262.1	715710
				258.4	908840

Note - Tests performed on unprocessed pellets

Table E.5: Complex viscosity (|η*|) versus 1 radian/second temperature for various grades of neat PEEK, cooling from 410°C

Cooling Rate of 2.4 ± 0.1°C/min.			
Victrex 150G		**Victrex 450G**	
Temp. (°C)	**|η*| (Pa·s)**	**Temp. (°C)**	**|η*| (Pa·s)**
410.3	245	410.2	3423
405.7	262	405.6	3662
402.6	269	402.4	3781
399.2	283	398.8	3935
395.9	297	395.4	4139
392.5	314	392.0	4325
389.0	330	388.6	4559
385.5	345	385.0	4787
382.0	367	381.6	5006
378.5	386	378.0	5244
375.1	409	374.5	5497
371.6	432	371.0	5763
368.2	457	367.5	6078
364.7	483	363.9	6330
361.3	514	360.4	6639
357.7	545	356.9	6973
354.2	581	353.3	7372
350.8	619	349.8	7765
347.1	664	346.2	8153
343.6	704	342.7	8592
340.0	756	339.0	9083
336.4	809	335.5	9583
332.8	874	331.7	10212
329.3	977	328.2	10740
326.8	1498	324.6	11472
325.6	3353	321.0	12940
324.5	15221	318.6	22628
323.4	30533	317.4	73340
322.3	168370	316.3	319680
321.3	1.2769E6	315.2	804530

Note - Tests performed on unprocessed pellets

Table E.6: Strain sweeps performed at 10 radians/second and 300°C for PPS composite blends reinforced with P-glass (T_g - 234°C) and E-glass

20 wt% P-glass			40 wt% P-glass		
Applied Strain(%)	**G′ (Pa)**	**G″ (Pa)**	**Applied Strain(%)**	**G′ (Pa)**	**G″ (Pa)**
0.095	2284	7165	0.099	19951	95097
0.155	1866	7486	0.153	20514	95294
0.250	1885	7408	0.251	20608	95620
0.392	1885	7143	0.394	20460	95611
0.628	1908	7217	0.624	20216	95533
1.004	1950	7171	0.993	20007	95167
1.591	1951	7121	1.579	19871	94184
2.513	1939	7120	2.504	19475	92226
3.997	1960	7088	3.970	18702	88909
6.320	1958	7086	6.289	17624	83809
9.999	1951	7076			

60 wt% P-glass			40 wt% E-glass		
Applied Strain(%)	**G′ (Pa)**	**G″ (Pa)**	**Applied Strain(%)**	**G′ (Pa)**	**G″ (Pa)**
0.089	70419	1.1233E6	0.098	34874	31586
0.139	69108	1.1001E6	0.152	31186	30167
0.229	69150	1.0701E6	0.251	25986	27928
0.359	66657	1.0417E6	0.393	21290	25818
0.571	64438	1.0102E6	0.623	16841	23463
0.913	64240	972300	0.993	12943	21149
1.462	63748	923880	1.582	9975	19022
2.345	57586	861200	2.512	7337	17078
			3.986	5431	15374
			6.317	4223	14018
			9.992	3395	12849

Note - Tests performed on specimens cut from injection molded plaques

Table E.7: Complex viscosity (|η*|) versus angular frequency (ω) at 300°C for various PPS composite blends reinforced with P-glass (T_g - 234°C) and E-glass

	Neat PPS	**20 wt% P-glass**	**40 wt% P-glass**	**60 wt% P-glass**	**40 wt% E-glass**
Frequency (rad/sec)	**|η*| (Pa·s)**	**|η*| (Pa·s)**	**|η*| (Pa·s)**	**|η*| (Pa·s)**	**|η*| (Pa·s)**
0.1	1297	1099	15573	182160	87487
0.1585	1308	1059	15507	169170	74314
0.2512	1302	999	14970	158140	59631
0.3981	1298	941	14403	149200	45315
0.6310	1286	893	13891	143180	33768
1	1266	860	13426	135680	24440
1.585	1236	829	12924	131030	17555
2.512	1191	800	12381	124350	12776
3.981	1133	761	11789	118460	9291
6.310	1061	720	11130	112180	6868
10.00	982	671	10394	105890	5087
15.85	893	617	9622	-	3717
25.12	801	559	8780	-	2897
39.81	709	499	7910	-	2239
63.10	617	439	6991	-	1770
100	530	381	6056	-	1434

Note - Tests performed on specimens cut from injection molded plaques

Table E.8: Complex viscosity (|η*|) at 1 radian/second versus temperature for various PPS composite blends reinforced with P-glass (T_g - 234°C) and E-glass, heating from 300°C

Heating Rate of 4.6 ± 0.1 °C/min.					
Neat PPS (Ryton PR09)		**60 wt% P-glass (Ryton PR09)**		**40 wt% E-glass (Fortron 1140)**	
Temp. (°C)	**|η*| (Pa·s)**	**Temp. (°C)**	**|η*| (Pa·s)**	**Temp. (°C)**	**|η*| (Pa·s)**
300.5	1154	300.7	142532	300.8	19199
302.5	1123	302.6	119256	302.7	18780
305.1	1077	305.0	92975	304.7	17768
307.1	1039	307.0	77643	306.5	16843
309.3	1003	309.1	62136	308.6	15945
311.6	964	311.8	49857	310.8	15063
314.0	923	314.1	39540	313.1	14239
316.4	885	317.1	30576	315.8	13694
318.9	844	319.6	24888	318.3	13195
321.5	808	321.7	19767	320.7	12831
324.0	770	324.1	15809	323.0	12647
326.6	731	326.5	12743	325.8	12457
329.3	695	328.9	10228	328.1	12281
331.8	658	331.1	8363	330.4	11955
334.3	625	333.5	6789	332.7	11657
337.0	591	336.2	5591	335.0	11221
339.5	559	338.8	4712	337.4	10762
342.1	529	341.3	4024	339.7	10193
344.7	496	343.8	3395	342.1	9429
347.3	462	346.5	2824	344.8	8732
350.1	431	349.0	2329	347.4	8018
				350.0	7232

Note - Tests performed on specimens cut from injection molded plaques

Appendix F:

Dynamic Mechanical Thermal Analysis Data

Table F.1: Storage Modulus (G′) at 10 radians/second versus temperature for PPS composite blends reinforced with P-glass (T_g - 234°C) and E-glass

Heating Rate of 2.5 ± 0.1 °C/min.					
Neat PPS		**20 wt% P-glass**		**40 wt% P-glass**	
Temp. (°C)	**G′ (Pa)**	**Temp. (°C)**	**G′ (Pa)**	**Temp. (°C)**	**G′ (Pa)**
41.0	1.2670E9	43.5	1.7848E9	40.6	2.2847E9
50.9	1.2482E9	53.2	1.7610E9	50.9	2.2540E9
60.6	1.2267E9	62.8	1.7334E9	60.8	2.2200E9
69.3	1.2037E9	72.7	1.6990E9	70.8	2.1769E9
78.0	1.1772E9	82.6	1.6557E9	81.0	2.1243E9
89.5	1.1307E9	92.6	1.5386E9	92.2	2.0109E9
100.3	8.7067E8	101.1	1.1510E9	104.6	1.4169E9
107.5	5.2551E8	108.4	7.3049E8	111.8	9.6159E8
114.9	3.0362E8	114.5	4.9897E8	121.7	6.0587E8
123.7	1.8626E8	120.6	3.6510E8	131.7	4.4633E8
132.6	1.3712E8	131.7	2.4927E8	140.4	3.7641E8
141.9	1.1260E8	145.2	1.9294E8	150.4	3.3192E8
153.9	1.0070E8	155.1	1.7535E8	160.6	3.1011E8
163.3	9.7338E7	165.1	1.6743E8	170.7	2.9765E8
173.3	9.5248E7	175.0	1.6160E8	180.5	2.8531E8
183.6	9.2620E7	184.8	1.5645E8	190.4	2.7037E8
193.1	9.1112E7	194.4	1.4981E8	200.2	2.5086E8
203.7	8.6063E7	204.1	1.4082E8	210.1	2.2868E8
214.1	8.2338E7	213.7	1.3076E8	220.0	2.0488E8
224.0	7.7519E7	223.5	1.1916E8	229.8	1.7561E8
234.1	7.0278E7	233.4	1.0462E8	239.7	1.3646E8
244.1	6.1442E7	243.7	8.5801E7	249.7	9.2412E7
254.0	4.9137E7	253.0	6.3621E7	259.7	5.3828E7
264.0	3.1393E7	263.0	3.8740E7	269.6	2.4757E7
269.0	2.1667E7	267.6	2.7119E7	274.4	1.5216E7
273.5	1.2716E7	275.1	1.2326E7	279.3	7.1162E6
278.0	5.7602E6	277.5	7.6916E6	281.8	4.0283E6
		279.8	4.5090E6	284.3	1.8935E6
		282.1	2.1547E6		

Table F.1: Storage Modulus (G′) at 10 radians/second versus temperature for PPS composite blends reinforced with P-glass (T_g - 234°C) and E-glass (*Continued*)

Heating rate of 2.5 ± 0.1°C/min.			
60 wt% P-glass		40 wt% E-glass	
Temp. (°C)	G′ (Pa)	Temp. (°C)	G′ (Pa)
40.0	3.8526E9	42.8	2.9140E9
50.0	3.8248E9	52.8	2.8833E9
59.7	3.7888E9	62.8	2.8495E9
69.5	3.7427E9	72.9	2.8053E9
79.4	3.6793E9	82.8	2.7212E9
89.5	3.5287E9	93.0	2.4391E9
99.4	3.0136E9	102.9	1.8418E9
109.0	2.2035E9	112.8	1.3031E9
118.8	1.6166E9	122.7	9.9061E8
131.3	1.2431E9	132.4	8.2302E8
143.7	1.0617E9	142.3	7.2439E8
153.6	9.7666E8	152.3	6.6570E8
163.6	9.3018E8	162.1	6.3296E8
173.7	8.9244E8	172.1	6.0904E8
183.4	8.5137E8	181.8	5.8940E8
193.1	7.9891E8	191.6	5.7044E8
202.8	7.2835E8	201.4	5.5057E8
212.7	6.4296E8	211.2	5.2792E8
222.5	5.5774E8	221.0	5.0220E8
232.4	4.6973E8	231.0	4.7156E8
242.3	3.5322E8	240.8	4.3385E8
252.3	2.0551E8	250.7	3.8333E8
257.1	1.3759E8	260.5	3.1026E8
262.1	8.4431E7	270.3	2.0085E8
267.0	4.8798E7	275.1	1.3351E8
271.8	2.7543E7	280.1	6.4452E7
276.7	1.4061E7	284.9	1.6773E7
279.2	8.6151E6		

Table F.2: Storage Modulus (G′) at 10 radians/second versus temperature for PEI composite blends reinforced with P-glass (T_g - 234°C) and E-glass

Heating Rate of 2.5 ± 0.1 °C/min.					
Neat PEI		**30 wt% P-glass**		**45 wt% P-glass**	
Temp. (°C)	**G′ (Pa)**	**Temp. (°C)**	**G′ (Pa)**	**Temp. (°C)**	**G′ (Pa)**
45.4	1.2494E9	46.9	2.3466E9	42.0	3.4891E9
56.0	1.2155E9	57.0	2.3120E9	52.1	3.4439E9
66.3	1.1804E9	66.7	2.2781E9	62.1	3.3945E9
75.3	1.1499E9	77.1	2.2416E9	72.0	3.3417E9
84.4	1.1229E9	87.6	2.1993E9	82.1	3.2777E9
95.9	1.0916E9	97.7	2.1563E9	92.1	3.2036E9
105.9	1.0657E9	107.6	2.1147E9	102.1	3.1314E9
115.6	1.0439E9	117.7	2.0722E9	111.8	3.0604E9
125.5	1.0242E9	127.5	2.0292E9	121.8	2.9904E9
136.0	1.0047E9	137.5	1.9820E9	131.7	2.9206E9
146.1	9.8860E8	147.6	1.9277E9	141.6	2.8488E9
156.1	9.7398E8	157.4	1.8623E9	151.6	2.7748E9
166.0	9.6153E8	167.2	1.7827E9	161.7	2.6975E9
176.0	9.4980E8	177.1	1.6966E9	171.6	2.6149E9
185.6	9.3806E8	187.1	1.6028E9	181.6	2.5249E9
195.3	9.1974E8	197.3	1.4807E9	191.3	2.4257E9
205.2	8.7373E8	207.0	1.3364E9	201.1	2.2887E9
213.8	6.9583E8	217.0	1.0752E9	211.1	2.0735E9
218.7	3.5724E8	223.1	5.4476E8	218.4	1.7263E9
221.2	1.7104E8	225.6	3.2486E8	223.3	1.1867E9
222.3	1.0476E8	229.2	1.3635E8	228.3	6.2424E8
223.5	6.0282E7	234.3	5.8746E7	233.1	3.1298E8
224.8	3.2312E7	242.9	3.0214E7	240.7	1.8599E8
226.0	1.9219E7	253.2	1.4414E7	251.8	1.1572E8
227.3	1.2245E7			261.9	5.3275E7
228.4	8.5529E6				
230.9	5.7563E6				
234.8	4.2995E6				
242.1	3.4273E6				
249.6	2.7037E6				

Table F.2: Storage Modulus (G′) at 10 radians/second versus temperature for PEI composite blends reinforced with P-glass (T_g - 234°C) and E-glass (*Continued*)

Heating Rate of 2.5 ± 0.1°C/min.			
60 wt% P-glass		**30 wt% E-glass**	
Temp. (°C)	**G′ (Pa)**	**Temp. (°C)**	**G′ (Pa)**
44.7	4.9077E9	41.8	2.4092E9
54.8	4.8619E9	51.7	2.3707E9
64.9	4.8151E9	61.3	2.3298E9
74.9	4.7620E9	71.2	2.2855E9
85.0	4.6849E9	81.1	2.2410E9
94.9	4.5988E9	91.0	2.1996E9
104.7	4.5204E9	100.8	2.1631E9
114.3	4.4424E9	110.5	2.1301E9
124.4	4.3566E9	120.3	2.1002E9
134.2	4.2637E9	130.2	2.0732E9
144.2	4.1554E9	140.0	2.0485E9
154.4	4.0257E9	149.9	2.0253E9
164.3	3.8682E9	160.1	2.0035E9
174.1	3.6912E9	169.9	1.9813E9
183.8	3.5117E9	179.6	1.9585E9
193.7	3.3261E9	188.9	1.9000E9
203.3	3.1004E9	198.1	1.8920E9
213.2	2.7518E9	212.7	1.5738E9
223.0	1.8675E9	217.6	1.0599E9
228.1	1.2696E9	221.0	5.3000E8
236.8	7.4472E8	224.0	2.5000E8
246.5	5.0049E8	227.5	9.0947E7
255.0	2.8840E8	232.5	4.2044E7
259.9	1.7274E8	241.6	2.5274E7
264.4	9.4006E7	251.3	1.7547E7
268.0	5.3343E7	261.5	1.1443E7
270.4	3.6515E7		

Table F.3: Storage Modulus (G′) versus temperature at 10 radians/second for various grades of PEEK reinforced with 45 wt% P-glass (T_g - 234°C)

Heating Rate of 2.5 ± 0.1 °C/min.			
Victrex 150G		Victrex 450G	
Temp. (°C)	G′ (Pa)	Temp. (°C)	G′ (Pa)
51.0	2.4773E9	51.4	3.4551E9
60.8	2.4571E9	60.9	3.4184E9
70.7	2.4348E9	70.5	3.3565E9
81.0	2.4087E9	81.5	3.2632E9
91.0	2.3773E9	91.4	3.1942E9
100.8	2.3421E9	101.6	3.1318E9
110.7	2.3039E9	111.3	3.0728E9
120.4	2.2633E9	121.1	3.0084E9
130.5	2.2133E9	131.0	2.9360E9
140.3	2.1286E9	141.1	2.8314E9
150.5	1.7366E9	151.1	2.4156E9
158.0	1.1270E9	161.1	1.6418E9
165.5	7.2175E8	169.9	1.3081E9
173.0	5.4064E8	179.8	1.1492E9
184.2	4.4040E8	189.4	1.0619E9
195.3	3.9676E8	199.3	9.8275E8
205.0	3.6695E8	209.1	8.9324E8
215.1	3.3680E8	219.0	7.8194E8
224.8	3.0708E8	228.7	6.5191E8
234.7	2.7200E8	238.7	5.1216E8
245.8	2.1294E8	247.5	3.6642E8
255.7	1.4438E8	253.5	2.5141E8
264.7	9.6332E7	261.0	1.3882E8
275.7	6.7272E7	265.9	9.5556E7
286.6	5.7514E7	272.0	6.6792E7
297.7	4.9558E7	279.1	5.0737E7
308.7	4.1060E7	289.1	3.9094E7
319.9	3.1302E7	298.7	3.1088E7
329.6	2.0974E7	308.4	2.4602E7
338.2	1.0457E7	318.1	1.8876E7
343.3	5.5900E6	325.4	1.3180E7
347.0	2.5243E6	331.7	8.3370E6
349.7	9.8443E5	337.7	4.4054E6
		342.6	2.1926E6
		347.6	8.9251E5

Table F.4: Storage Modulus (G′) versus temperature at 10 radians/second for various grades of PEEK reinforced with 43 vol% P-glass

Heating Rate of 2.5 ± 0.1 °C/min.					
Neat PEEK (Victrex 450G)		**60 wt% P-glass (T_g - 234°C)**		**66 wt% P-glass (T_g - 282°C)**	
Temp. (°C)	**G′ (Pa)**	**Temp. (°C)**	**G′ (Pa)**	**Temp. (°C)**	**G′ (Pa)**
43.7	1.3143E9	44.9	3.8433E9	43.2	4.1511E9
54.5	1.3004E9	55.2	3.8080E9	52.3	4.1158E9
65.7	1.2870E9	64.8	3.7710E9	62.1	4.0794E9
77.6	1.2728E9	74.4	3.7293E9	70.8	4.0470E9
88.9	1.2593E9	84.5	3.6724E9	80.9	4.0097E9
100.8	1.2434E9	94.5	3.6082E9	91.0	3.9703E9
111.9	1.2264E9	104.9	3.5398E9	100.9	3.9280E9
123.0	1.2063E9	114.9	3.4694E9	110.7	3.8785E9
134.3	1.1820E9	124.7	3.3943E9	120.6	3.8154E9
145.4	1.1234E9	134.8	3.2967E9	130.5	3.7096E9
152.8	8.8294E8	144.6	3.0410E9	140.4	3.3650E9
157.8	5.8448E8	152.2	2.4876E9	148.0	2.7688E9
161.5	4.0368E8	161.0	1.7652E9	155.6	2.1462E9
166.5	2.5712E8	168.4	1.4177E9	165.8	1.6229E9
172.9	1.6943E8	178.3	1.2094E9	173.2	1.4200E9
184.1	1.1768E8	187.8	1.1127E9	183.2	1.2662E9
194.7	1.0077E8	197.7	1.0386E9	193.0	1.1667E9
205.9	9.0604E7	207.3	9.6438E8	204.1	1.0697E9
216.9	8.2711E7	216.7	8.7934E8	212.7	9.8930E8
228.2	7.6951E7	229.3	7.5888E8	221.3	8.9756E8
239.4	7.2776E7	239.9	6.2528E8	231.2	7.8555E8
250.6	6.9705E7	251.0	4.4443E8	241.1	6.8069E8
261.5	6.6414E7	258.6	2.9038E8	251.2	5.9679E8
272.6	6.2919E7	266.1	1.6248E8	261.1	5.3800E8
283.3	5.9144E7	270.9	1.1080E8	271.1	5.0053E8
294.0	5.4230E7	277.0	7.4228E7	280.9	4.7525E8
304.5	4.8008E7	285.6	5.0332E7	290.6	4.2716E8
315.7	3.9290E7	296.6	3.7428E7	300.5	3.4528E8
327.5	2.7197E7	306.4	3.3391E7	310.2	2.5170E8
336.0	1.5470E7	314.9	2.6345E7	320.1	1.7277E8
341.0	8.3310E6	323.6	1.8370E7	330.0	1.0620E8
344.7	4.4992E6	331.0	1.1961E7	340.0	4.6768E7
347.2	2.8708E6	337.0	7.1815E6	344.9	2.5293E7
		341.9	4.0592E6	351.1	1.3035E7
		344.4	2.8075E6		

Appendix G:

Miscellaneous PPS Data

Table G.1: Effect of Processing Temperature on Injection molded Mechanical Properties of neat PPS (Ryton PR09).

Machine Direction					
Maximum Processing Temperature	**Tensile Properties**			**Flexural Properties**	
	Modulus (GPa)	**Strength (MPa)**	**% Elong.**	**Modulus (GPa)**	**Strength (MPa)**
*290°C	3.14 (0.07)	76.9 (1.3)	3.62 (0.45)	4.05 (0.11)	113.0 (3.3)
330°C	3.08 (0.17)	70.9 (4.1)	3.10 (0.54)	3.92 (0.03)	113.8 (2.1)
350°C	3.20 (0.21)	71.9 (2.3)	3.26 (0.36)	3.61 (0.10)	106.8 (2.3)
Transverse Direction					
Maximum Processing Temperature	**Tensile Properties**			**Flexural Properties**	
	Modulus (GPa)	**Strength (MPa)**	**% Elong.**	**Modulus (GPa)**	**Strength (MPa)**
*290°C	3.23 (0.16)	76.5 (2.3)	3.37 (0.53)	3.86 (0.08)	113.8 (1.3)
330°C	3.13 (0.10)	70.9 (3.3)	3.02 (0.55)	3.74 (0.10)	109.3 (1.8)
350°C	3.02 (0.05)	70.5 (4.38)	2.88 (0.35)	3.75 (0.03)	109.5 (2.2)

Note: % Elong. = Elongation to break; Standard deviations given in parentheses

(*) Directly molded, while remaining samples were passed through injection molder twice to emulate P-glass composite processing history

During both rheological testing and injection molding, it was observed that blends consisting of polyphenylene sulfide (Ryton PR09) and the lower T_g (234°C) phosphate produced volatiles in the melt, possibly indicating some type of interactions between the PPS and glass. It was also observed that the glass loading had an effect on the volatilization with the composites containing the lower glass loadings showing the greatest amount of off-gasing. In order to collaborate what was qualitatively observed during processing, the off-gasing of the various materials was analyzed in a custom built apparatus at Phillips Chemical Company. For this method, the amount of condensable species given off within the melt are related a dimensionless number known as the QCM value. These QCM numbers are only qualitative with a higher QCM value indicating the presence of a larger amount of condensable volatiles. Experimental QCM values obtained for both the neat PPS and phosphate glass as well as the composite blends is presented in Table G.1. At the temperature of 320°C investigated, the neat phosphate glass was found to give off essentially no condensable volatiles while the neat PPS that had undergone the same processing history as the composite blends yielded a QCM value of approximately 0.25. Composites reinforced with the lower glass loadings (20 & 40 wt%) were found to exhibit much higher QCM values of 0.52 and 0.33, respectively. The QCM values greater than that of the neat materials appeared to indicate some possible interactions between the PPS and phosphate glass which was sensitive to the loading of glass within the composite blends. It was believed that the ionic nature of the P-glass may have resulted in interactions with ionic endgroups present in the PPS. This an area that may warrant further investigation but was beyond the scope of this work.

Table G.2: QCM Off-gasing values for neat PPS, P-glass (T_g-234°C) and various composite blends

Material	QCM Value
Neat PPS (Ryton PR09)	0.249
Composite blend (20 wt% P-glass)	0.516
Composite blend (40 wt% P-glass)	0.330
Composite blend (60 wt% P-glass)	0.180
Neat P-glass (T_g-234°C)	-0.019 (Zero)

Robert T. Young

The author was born in Columbia, South Carolina on February 9, 1969. Shortly thereafter, his family moved to Greensboro, North Carolina where he spent the remainder of his childhood. Upon completing high school, he attended North Carolina State University and received a B.A. in Chemistry and a B.S. in Chemical Engineering in 1993. While obtaining his undergraduate degrees, he was fortunate enough to work in the area of polyester fiber spinning for DuPont. Interest in the area of rheology and polymer processing fostered while at DuPont led the author to Virginia Tech in the summer of 1993. Under the direction of Dr. D.G. Baird, he performed research on thermoplastic composites reinforced with melt processable phosphate glasses, from which he received a Ph.D. in Chemical Engineering in March of 1999. He was offered and accepted a research and development position with DuPont in Buffalo, NY.

Robert Thomas Young